HYDROXYL FUNCTIONALITIES OF MIDDLE RANK BRITISH COALS

VOLUME II

Harminder Singh Manak

A thesis submitted for the Degree of Doctor of Philosophy

The University of Aston in Birmingham

January 1996

LIST OF CONTENTS Page

6. METHYLATION

7. CONCLUSIONS

LIST OF TABLES

LIST OF FIGURES

ACETYLATION

4.1 INTRODUCTION

4.1.1 General Introduction

The low relative concentrations of thiols, and primary and secondary amines in middle rank coals results in the hydroxyl functionality being the principal reacting species on acetylation of the coals. The hydroxyl group is the main acidic group in middle rank coals and coal-derived liquids and acetylation of this functionality leads to a reduction in the intermolecular hydrogen-bonding of the coal molecules, which subsequently leads to an increase in solubility of the coal during hydroliquefaction processes. Spectroscopic investigations are also able to provide us with valuable data on the environment of these acetyl groups, and hence the hydroxyl groups, in the coal.

4.1.2 Literature review

Early work developing acetylation as a selective derivatising technique for the hydroxyl functionality in coals, was carried out by Blom et al[26] in 1957. The procedure Blom and his co-workers used involved acetylating the coal with an acetic anhydride : pyridine mixture at 80-90°C followed by washing to remove the unreacted acetic anhydride and acetic acid. The next stage involved hydrolysis of the acetylated coal with a base, then acidification of the solution and finally titration of the acetic acid released during the hydrolysis step. Blom's results correlated well with data from previous non-aqueous titration and silylation work.

Later in 1980 Patel et al[63] reported that the solubility* of solvent-refined coal and solvent-refined lignite increased from 25-60 wt% to 80-100 wt% in benzene and chloroform (greater solubility was observed in chloroform) solvents upon acetylation of the samples. The test samples, which were acetylated by reacting 1.0g of the sample with 5 cm^3 of a 1 : 3 mixture of acetic anhydride : pyridine for 24 hrs under argon at room temperature, consisted of 2 North Dakota lignite coals and Kentucky No.9 and No.14 bituminous coals. The determination of hydroxyl functionality by acetylation has since been used fairly routinely for coal hydrogenation products[64] and coals[26,65-66].

*The solubility was measured by mixing 1.0g sample in 10 cm^3 of the solvent at room temperature for 24 hrs. The mixture was then filtered through a 5 μm teflon filter and the resulting filtrate and residue were dried and weighed.

The use of acetylation and isotopic ^{14}C to acquire quantitative data on hydroxyl functional groups in preasphaltenes from coal hydrogenation has been investigated by Baltisberger et al[67], 1982. The purpose of this work was to look into the structure of preasphaltenes formed during coal liquefaction processes by first derivatising the samples (via acetylation) so that they were more soluble in solvents suitable for IR and nmr spectroscopic analysis. The acetylation reactions were carried out at various temperatures using a ^{14}C-labelled acetic anhydride : pyridine mixture under argon. This method differs from the previous acetylation reactions devised by Blom, in that radio-labelled ^{14}C acetic anhydride was used. The introduction of this isotope meant that the laborious hydrolysis and distillation steps were no longer necessary. This new technique for the quantitative acetylation of coals was first introduced by Given et al[66]. The procedure involved burning the washed and dried acetylated samples in oxygen followed by collection and counting of the ^{14}CO formed. Again, the data obtained showed good correlation with previous silylation and non-aqueous titration methods.

DeWalt and Glenn[64] have carried out a study on the steric effects encountered during the acetylation of coal-derived liquids by attempting to acetylate a number of hindered-phenols at 118°C. They found that with the less sterically-hindered phenols, such as 2-tert-butyl-4-methylphenol and 2,6-dimethylphenol, the reaction was complete in a relatively short time at room temperature - the former phenolic compound showed 100% reaction after only 1 hr. The more hindered phenolic compounds, however, required a prolonged reaction time (2,6-di-tert-butyl-4-methylphenol showed only 5% conversion after 2 hrs reaction time) and only 2,6-di-tert-butylphenol greatly resisted acetylation.

Snape et al[68] have suggested acetylation using ^{13}C-labelled acetic anhydride in pyridine to act as 'markers' for phenols and carboxylic acids in coals. Unfortunately when the acetylated coals were analysed by ^{1}H and ^{13}C nmr, the methyl resonances from the acetyl groups overlapped with similar signals from the coal itself. This, coupled with the low sensitivity of ^{13}C nmr, limits the usefulness of this technique and makes it impossible to estimate the hydroxyl content in the coals from the ^{13}C methyl resonances. However, the carbonyl (from the acetyl groups) ^{13}C resonances were well separated from the aromatic carbon resonances in the nmr spectra. This allowed for an estimation of the hydroxyl contents of the coals. The results showed good agreement with values obtained from silylation studies.

Halleux et al[69] has reviewed some of the acetylation procedures involving various reagents and reaction conditions and found that a trend is observed, whereby as the coal rank increases, the fraction of oxygen present as -OH increases to a maximum and then decreases. If a graph is plotted of %C daf / dmmf (abscissa) vs % O_{OH} / O_{total} (ordinate), the position of the maximum varies on the plot with respect to the carbon content of the coal and the amount of -OH present.

More recently, work has been carried out on the acetylation of coal using ketene and also acetylation using liquid reagents in the microwave oven. This was the first time microwave heating had been used in the acetylation of coals. Bailey et al[41,58] succeeded in acetylating a rank series of nine coals both in the microwave oven and on the bench top for comparison. They found that when the acetylating reagent was ketene, acetylation was much greater than when 'conventional' reagents were employed. The reason for these higher results is probably due to the fact that ketene is a very reactive, small gaseous molecule, which is able to diffuse easily into the microporous structure of the coal reacting quickly and efficiently with even the more sterically-hindered phenolic compounds (with which conventional liquid reagents find it more difficult to react). Blom et al[26] have postulated that acetylation of coals proceeds slowly because of steric-hindrance encountered by the acetylating reagent and long reaction times are required if the reaction is to go to completion. The hydrolysis step of the process is also time-consuming, with several days of refluxing with barium hydroxide solution usually required, before acidification, distillation and titration of the released acetic acid. Bailey et al have succeeded in accelerating these time-consuming reactions by heating the reagents with microwave energy. Coals are effectively transparent to microwave radiation and heating is effected via interaction of the microwave radiation with a microwave-receptor solvent or reagent. The four liquid acetylating reagents used in Bailey's study were :

1. acetic anhydride : pyridine
2. acetic anhydride : conc. H_2SO_4
3. acetic anhydride : trifluoroacetic anhydride
4. acetic acid : trifluoroacetic anhydride

For the middle rank coals, the acetic anhydride : pyridine mixture produced the largest value for the concentration of -OH, but this mixture was less effective with the higher rank coals. It was also found that microwave heating (in a 650W domestic microwave oven) helped reduce the acetylation time (from 5 hrs to 1 hr for the Creswell coal) and the time required for hydrolysis of the acetylated coal sample (from over 100 hrs to approximately 1 hr - the exception was Cortonwood, which needed 3 hrs for complete hydrolysis in the microwave oven). Overall, the results show that the O_{OH} / O_{total} value increased with rank to a maximum and then decreased with higher rank coals. The microwave method also gave greater values of O_{OH} / O_{total} compared to the analogous bench top method.

Based on these conclusions it was decided to acetylate the raw coals and coal macerals, used in this study, with a mixture of acetic anhydride and pyridine in the microwave oven. The ketene reagent was ruled out because a ketene 'generator' would be required and ketene is a very toxic gaseous molecule, which has a high explosion hazard associated with it.

4.1.3 Coal macerals

Coal is a chemically heterogeneous material consisting of a complex mixture of maceral groups, mineral matter and moisture (see sections 1.5.1, 2.4 and 2.5). The maceral groups are a microscopic mixture of components, which have their origin in the decay of the different substituents of the original plant matter. During the coalification stage not all the plant material decomposes at the same rate e.g cellulose decomposes readily, lignin less so and spores, resins and leaf cuticles least readily.

A visual examination of coals reveals distinguishable bands of material running through the coal. These are called "lithotypes" and there are 4 types :

1. Vitrain - a glossy black material that breaks in a circular fashion.
2. Clarain - a glossy black material that breaks horizontally.
3. Durain - a dull black material with a granular appearance.
4. Fusain - a material that resembles charcoal.

The type of lithotype formed is thought to depend upon the prevailing conditions which existed when the coal was deposited. Lithotypes are composed of macerals and there are 3 main maceral groups - exinite (also known as liptinite), vitrinite and inertinite. The different maceral groups may be distinguished via microscopic examination of the coal. The diverse molecular components of plants account for the different maceral groups and amount of each maceral present can give a good indication as to how the coal will behave. The study of these maceral groups is known as "petrology" and analysis of the macerals is called "petrographic analysis". The different macerals present in the various lithotypes are shown below :

1. Vitrain - this is composed mainly of vitrinite with lesser amounts, if they are present at all, of exinite and inertinite.
2. Clarain - this is thought to be an agglomerate of vitrain and durain.
3. Durain - this contains all 3 maceral groups in approximately equal amounts.
4. Fusain - this contains large amounts of inertinite, with lesser amounts of exinite and vitrinite.

The chemical and optical differences become less apparent as the coal rank increases (in anthracites the maceral groups are very difficult to distinguish). Macerals mainly consist of organic macromolecules with lesser amounts of smaller, more volatile molecules. The detailed chemical structures of these macromolecules are very difficult to obtain. It is the macerals which form the combustible part of coal and different maceral groups have different origins and subsequently differ in chemical composition. Table 4.01 shows the source materials of macerals.

Table 4.01 The source materials of macerals

Maceral group	Macerals	Source materials
EXINITE	Alginite	Algal remains
	Cutinite	Leaf cuticles
	Resinite	Plant resins and waxes
	Sporinite	Fungal and other spores
	Liptodetrinite[a]	
VITRINITE	Collinite	Humic gels
	Telinite	Wood, bark and cortical tissues
	Vitrodetrinite[a]	
INERTINITE	Macrinite[b]	Unspecified detritus, 10-100 μm
	Micrinite	Similar, but < 10 μm
	Fusinite	'Carbonised' woody tissues
	Semifusinite	Similar
	Sclerotinite	Fungal sclerotia and mycelia
	Inertodetrinite[a]	

[a]These terms are used when small entities must be assigned to this group because of their reflectivity, but cannot be unequivocally identified with any maceral within the group.

[b]This is sometimes also referred to as massive micrinite.

Retcofsky and Van der Hart[70] have studied the CP ^{13}C MASNMR spectra of the macerals of West Virginia bituminous coal (85.8% C) and their findings show that the aromaticity increases in the order exinite < vitrinite / micrinite < fusinite. The results appear to indicate that fusinite contains larger aromatic clusters compared to vitrinite and inertinite.

The exinite maceral group is derived from the decomposition of spores → sporinite, resins and waxes → resinite, leaf cuticles → cutinite and algae → alginite. The reactivities of the macerals within the exinite maceral group are different - the waxes usually exist as long carbon chains linked by ester functional groups, whereas the resins may contain several adjacent rings of carbon atoms and have less hydrogen relative to the carbon compared to this ratio in the waxy material. The wax and resin will not dissolve in the same solvent and their behaviour on heating will be different. The exinite maceral group has a relatively high hydrogen content with the H / C ratio highest in high volatile bituminous coals. Exinite is thought to be derived from non-woody tissues of plants, which probably accounts for its low aromaticity. This maceral group usually has a high volatile matter content and plasticity and low -OH content.

The vitrinite maceral group is derived from woody and cortical tissues in plants, which accounts for its greater aromaticity compared to the exinite maceral group. The vitrinite maceral is the most abundant and occurs most frequently in coals. It is the most important maceral group and its content in coal rarely falls below 50%. Vitrinite is mainly derived from lignin, which gave rigidity to the plant tissue. Lignin is a non-crystalline 3-dimensional cross-linked polymer consisting of various hydroxy- and methoxy-phenyl units having characteristic distribution of substituents (2,5-, 2,4,5- or 2,4,5,6-) around the benzene ring. Oxygenated propane side-chains are also common. The vitrinite maceral group is also made up of cellulose, fats and carbohydrates. The hydrogen content of vitrinite is similar to that of the bulk coal.

The inertinite maceral group is derived mainly from the decomposition of carbonised wood or charcoal during the coalification stage. Inertinite has a relatively low hydrogen content and hence the lowest H / C ratio of all the 3 maceral groups (in high volatile bituminous coals). Fusinite is a type of charcoal formed by natural pyrolysis in ancient forest fires. It usually has a high carbon content, high reflectance and zero plasticity. Semifusinite is wood charred at a lower temperature (probably charred by some hot inner layer more remote than the burning outer layer).

During distillation and pyrolysis processes, the weight losses are greatest for the macerals that are more heavily alkylated. During hydroliquefaction, exinite and vitrinite can be extracted fairly readily, but very little inertinite is taken into solution. The extraction yield correlates approximately with reactive maceral (exinite and vitrinite) content of the coal. Consequently coals with a high inertinite content are not favoured for direct liquefaction. Exinite and vitrinite seldom show plastic behaviour on heating when C < 80.5% or C > 91% (exinites are more fluid than vitrinites), whereas inertinite shows no plasticity at all on heating, irrespective of its carbon content. Table 4.02 shows some general trends of the 3 coal maceral groups.

Table 4.02 General trends of the 3 maceral groups found in coals

PROPERTY OR CHARACTERISTIC	GENERAL TREND
% Carbon (daf*)	Inertinite highest. Vitrinite and Exinite similar
% Hydrogen (daf)	Exinite highest. Vitrinite > Inertinite
% Oxygen (daf)	Vitrinite > Exinite > Inertinite
% Volatile matter	Exinite highest. Vitrinite > Inertinite
% Reflectance	Inertinite > Vitrinite > Exinite
O as phenolic -OH (g / 100g coal)	Vitrinite > Exinite > Inertinite
Plasticity	Exinite > Vitrinite. Inertinite has zero plasticity

*daf = dry, ash-free basis

4.2 EXPERIMENTAL

4.2.1 Separation of coal macerals

The coal samples were ground to ≤32 μm and the macerals were separated using a gravitational method. Because exinites are richer and inertinites poorer than vitrinite with respect to their hydrogen content, it would be expected that the true density of exinite will be lower and that of inertinite higher than that of vitrinite. It is these differences in density that allow us a technique for fractionating the macerals, by using liquids of varying specific gravity to effect separation i.e a float-and-sink method. Before separation it is important to grind down the coal in order to demineralise the sample as much as possible. The mineral matter is denser than most of the organic components in coal and, as such, the presence of just a small amount of mineral matter can affect the density and separation of the macerals. Grinding down the coal to small particle sizes helps to liberate some of the mineral matter, as well as the coal macerals. It should also be noted that, at higher rank (approximately 90% C and above), the densities of the coal maceral groups converge and the exinite maceral group has virtually disappeared. The procedure for the separation of the coal macerals is outlined in section 2.5.

4.2.2 Scanning electron microscope (SEM)

The coal samples were analysed using a Jeol 6100 Scanning electron microscope (SEM) coupled with a LINK AN 10 000 Energy Dispersive Analysis System. The samples were splutter coated with Ag (to aid imaging and prevent charging of the materials under investigation) and analysed under vacuum using a potential of 20 kV at x170 and x950 magnification.

4.2.3 Reflectance measurements

A quantitative petrographic analysis of the coal maceral concentrates was carried out using a Leitz Orthoplan Microscope attached to a vertical illuminator consisting of a 100W / 12V tungsten incandescent lamp. Oil immersion objectives in the x50 magnification range (incorporating "cargille" immersion oil) were used in conjunction with a x10 eye-piece on the microscope. An MPV Photometer was attached vertically above the microscope and the sample was placed on a MAC 4000 Stage Controller. A CCTV attached to a camera was located behind the microscope allowing the option of photographing the sample.

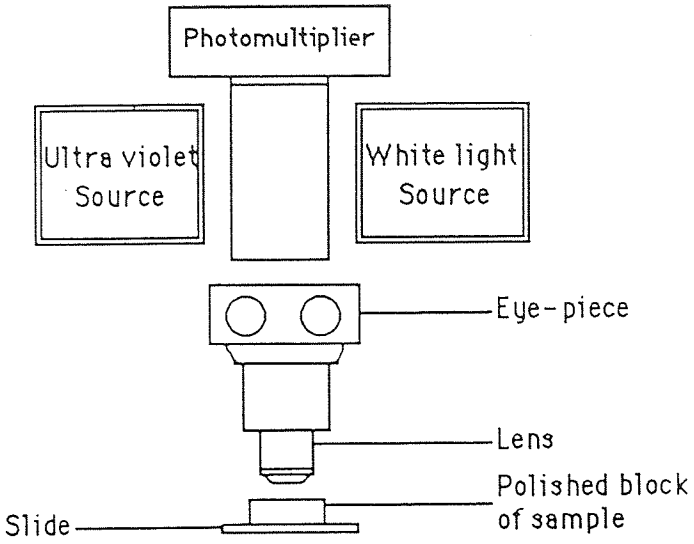

Fig4.01

Schematic representation of the apparatus used for coal reflectance measurements.

Petrographic analysis of a single coal sample is also able to provide information about the rank and microlithotype composition of the coal, as well as afford data on maceral concentrations. The reflectance of vitrinite is often seen as a superior measurement of coal rank, according to petrologists.

Reflectance involves a visual examination of the coal on a microscopic level. The various macerals are usually distinguishable by using reflected light microscopy. The reflectance is a function of the indices of refraction of the coal sample to be measured and the medium (immersion oil) in which it is measured, and the absorption index of the material.

Reflectance is a destructive technique which requires only small amounts of sample material. It is defined as the percentage of normally incident light that is reflected by a plane, polished surface of the sample under investigation e.g an oil reflectance of 1.00% for vitrinite indicates that only that proportion of the light incident on the coal surface is reflected under the conditions of measurement.

"Random" reflectance measurements were carried out on the raw coal and coal maceral samples i.e reflectance was determined in unpolarised light without rotation of the sample.

The sample for analysis was prepared as follows. A representative sample of the coal was air-dried and the particle size was checked to ensure an upper limit of 1.0 mm by passing the sample through a 1.0 mm wire-mesh sieve. Next, 30 cm^3 of the sample was mixed with epoxide resin and hardner and a mould was prepared by placing the mixture in a press and subjecting the sample to 8000-9000 psi for 3-5 second intervals - this was repeated 6 times. The mould was then subjected to a constant 5000 psi until it was cured (curing was complete when the temperature reached 96°C; the heating source employed was a scissor heating element). After curing the cylindrical block was polished using a Buehler Datamet Microprocessor grinding / polishing system - the sample was ground down using silicon carbide and diamond impregnated material and polished using a velvet disc. Copious amounts of water were used during and after each stage to remove particulate waste. When the surface of the specimen was clean, flat and scratch-free, it was ready for analysis.

Before the sample could be analysed, it was necessary to calibrate the light source. This was done by using 3 materials of known reflectance to obtain a linear plot, which should not deviate by more than ± 0.2%. The sample was then placed on the MAC 4000 Stage Controller, the immersion oil was placed on the surface of the block and the microscope was focused. The bottom-left and the top-right of the square area to be analysed were marked and the maceral directly under the 2 µm x 2 µm square to the left of the centre of the cross-hairs was noted. The stage then moved the sample to the next measuring point and the maceral under the measuring square was again noted, and so on, until the whole square area set out at the beginning of analysis, had been covered and 500 points had been counted. The optical properties of the coal were determined at a wavelength of 546 ± 5 nm (a 546 nm interference filter was used to concentrate the reflected beam of light from the sample to the photoelectric cells in the photomultiplier).

The different maceral groups show different reflectance - the exinite / liptinite maceral appears as a very dark material, whereas the vitrinite is observed as light-grey in colour and the inertinite appears as a light white colour. Pyrite (which appears as a very bright white material - highly oxidised inertinite can also appear to be very bright when viewed under the microscope. This should not be confused with pyrite), mineral matter and bi- and trimacerites were not counted in the analysis. The resin, exinite and mineral matter can all appear to be quite dark under the microscope and sometimes it is difficult to distinguish the exinite. When this is the case UV or blue light may be used to measure the exinite maceral concentration - this has the effect of making the exinite maceral group fluoresce, but has no effect on the mineral matter or the resin. Vitrinite and inertinite will not fluoresce with UV light.

The results were analysed by using CRE "in-house" petrographic data analysis software and reflectance histograms of the results were plotted.

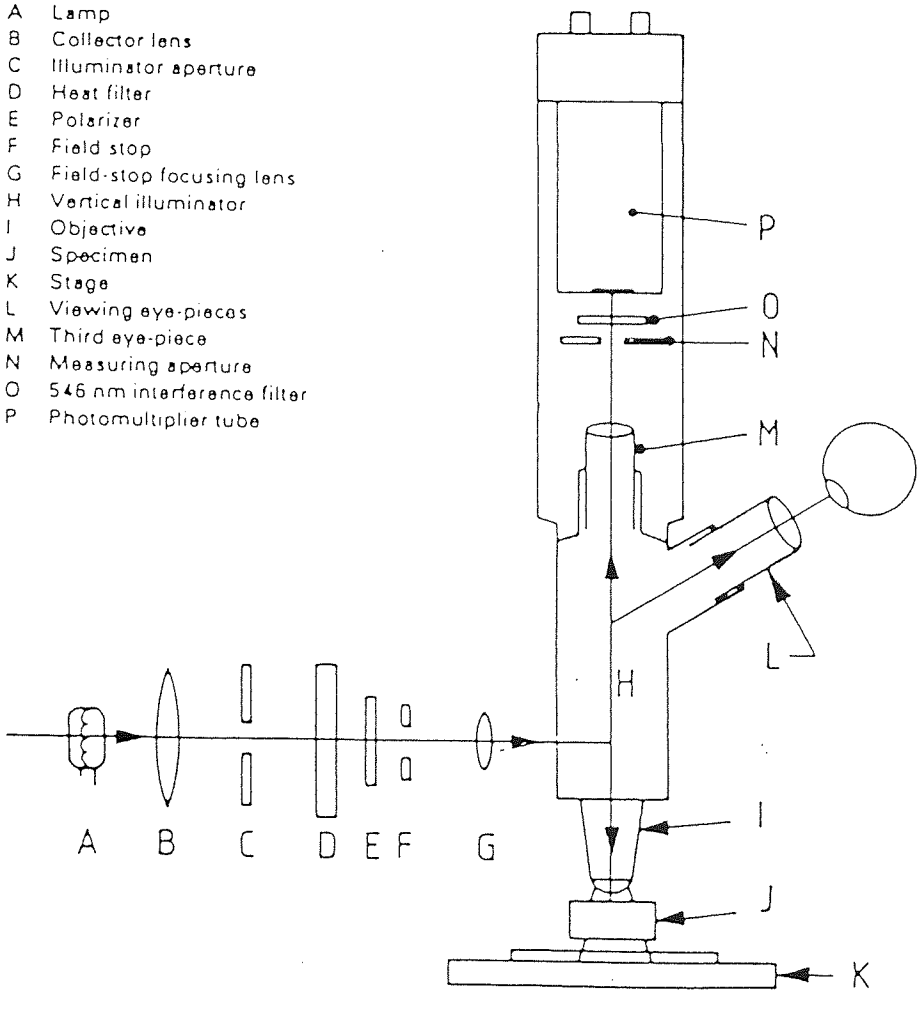

Fig4.02 Optical parts of a typical reflectance measuring microscope.

4.2.4 Acetylation of coals and coal macerals

The acetylation of the samples was carried out using both bench top (section 2.7.1) and microwave (section 2.7.2) techniques. In both cases the reaction involved the acetylation of the sample using an acetic anhydride / pyridine mixture for the appropriate reaction time. After reaction the mixture was poured onto distilled water and stirred to remove any excess acetic anhydride and acetic acid. The coal was then filtered, washed with water and dried overnight under dry N_2 at 110°C. The dried acetylated coal (0.10g) was then hydrolysed with 0.3M barium hydroxide solution and the reaction mixture cooled. Next the coal was filtered off and the filtrate was acidified with a few drops of concentrated phosphoric acid and distilled - 20 cm^3 aliquots of sample were titrated against 0.1015N NaOH using phenolpthalein indicator to determine how much acetic acid had been released. This procedure was repeated several times by adding 20 cm^3 distilled water to the filtrate and continuing the distillation until a constant titre (equal to the blank titre) was obtained. The respective titres were then added together to give the total titre, from which the acetyl content of the coal was calculated.

4.3 RESULTS AND DISCUSSION

4.3.1 Separation of coal macerals

(a) Creswell coal macerals

The Creswell coal sample was ground down to a particle size of ≤32 μm and the macerals were separated by a centrifugal technique, as outlined in section 2.5. In each run (on the Jouan CR4-22 centrifuge) 40g samples of Creswell coal were used and 3 runs were carried out in total. After filtering and drying, the like-macerals from each run were collected together and analysed. Table 4.03 shows the yields collected from each run.

Table 4.03 Yields from the density fractions of Creswell coal (≤32 μm)

Run No.	Specific gravity of solution					% Yield
	<1.25	1.25 -1.35	1.35 -1.45	1.45 -1.55	> 1.55	
Mass obtained from Run 1 (g)	1.5	28.0	6.4	0.3	0.2	91
Mass obtained from Run 2 (g)	1.6	28.7	6.8	0.3	0.4	95
Mass obtained from Run 3 (g)	1.3	33.2	3.0	0.3	0.3	95
Total mass (g)	4.4	89.9	16.2	0.9	0.9	94

As Table 4.03 shows the separations produced good yields of exinite (4.4g), vitrinite (89.9g) and inertinite (16.2g). The relatively low amounts of sample obtained at specific gravities higher than 1.45 gcm^{-3} is indicative of an efficient grinding process, whereby the bulk of the mineral matter has been liberated. The raw Creswell and Creswell macerals were analysed by petrographic analysis as outlined in section 4.2.3.

Fig 4.03 shows the reflectance histogram obtained for the raw Creswell coal. The exinite content is 7.6 vol%, the vitrinite content 80.4 vol% and the inertinite content 12.0 vol%. The major maceral component is vitrinite, as expected, with lesser amounts of inertinite and exinite. Fig 4.04 shows the reflectance histogram for the Creswell exinite maceral. Values for the exinite, vitrinite and inertinite maceral components are 53.0, 43.3 and 3.7 vol% respectively. The exinite maceral content has been concentrated from 7.6 vol% in the raw coal to 53.0 vol% in the maceral - this indicates a very good separation. Fig 4.05 shows the reflectance histogram for the Creswell vitrinite maceral. Values obtained for the exinite, vitrinite and inertinite maceral components are 5.4, 87.2 and 7.4 vol% respectively. The vitrinite maceral content has been concentrated from 80.4 vol% in the raw coal to 87.2 vol% in the maceral fraction. Although this may seem a small change in concentration, it is in fact still a very good separation when considering that the presence of small amounts of bimacerite and trimacerite components sets a limit as to how efficient a maceral separation can be. Fig 4.06 shows the reflectance histogram for the Creswell inertinite maceral. Values of 3.2, 39.6 and 57.2 vol% were obtained for the exinite, vitrinite and inertinite macerals respectively. In this instance the inertinite component of the Creswell coal has been concentrated from 12.0 vol% to 57.2 vol%. Again, this is a very good separation.

Because of the need to conserve as much of each maceral as possible (especially with respect to the exinite and inertinite macerals) for future experiments, only 0.4g (the minimum sample weight required for petrographic analysis) of the exinite and inertinite macerals was submitted for petrographic analysis and 0.6g for ultimate and proximate analysis.

The results from petrographic analysis indicate that very good separations for all 3 maceral groups have taken place. Table 4.04 gives a summary of the results.

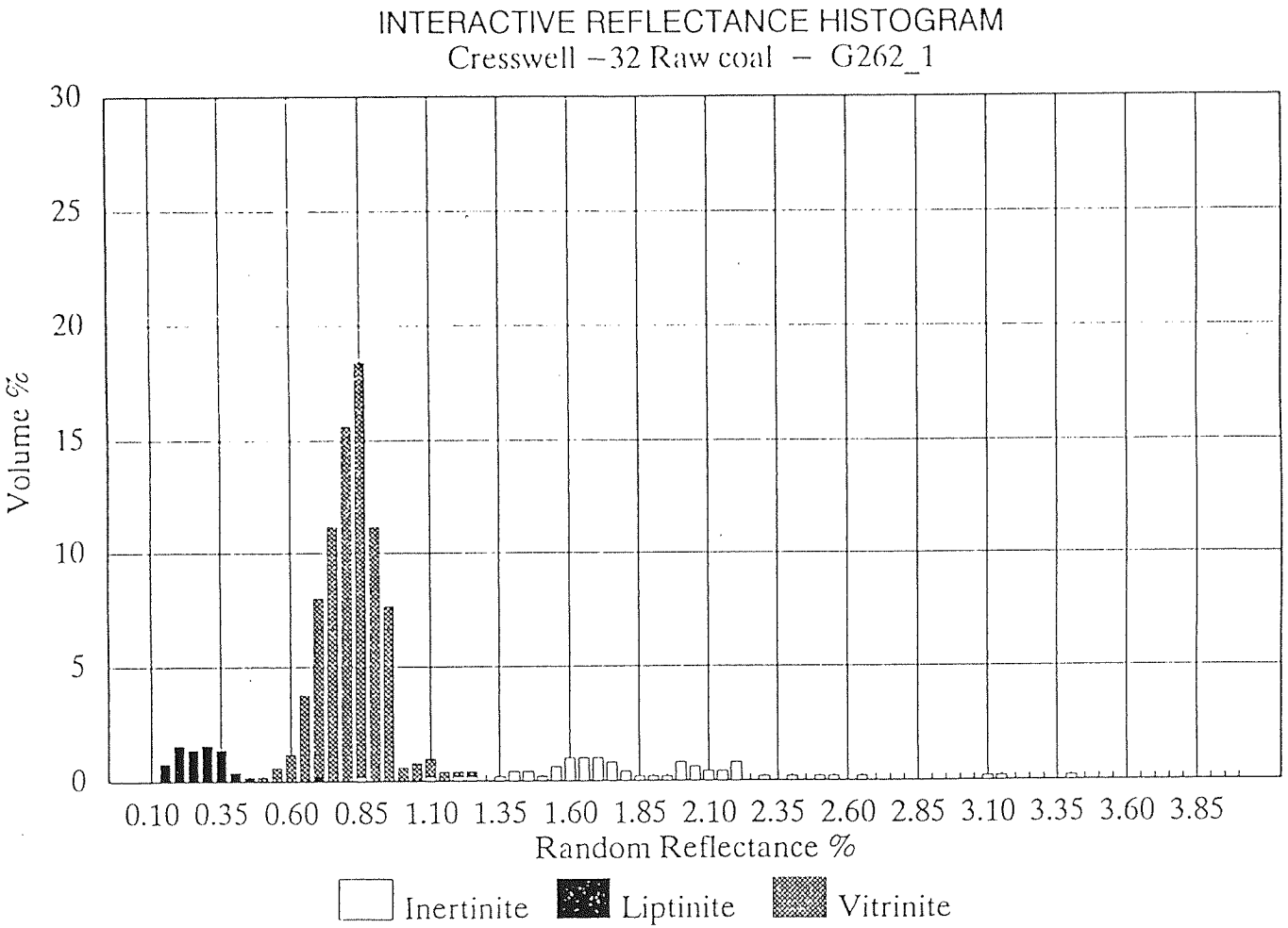

Fig4.03
Reflectance histogram of the raw Creswell coal

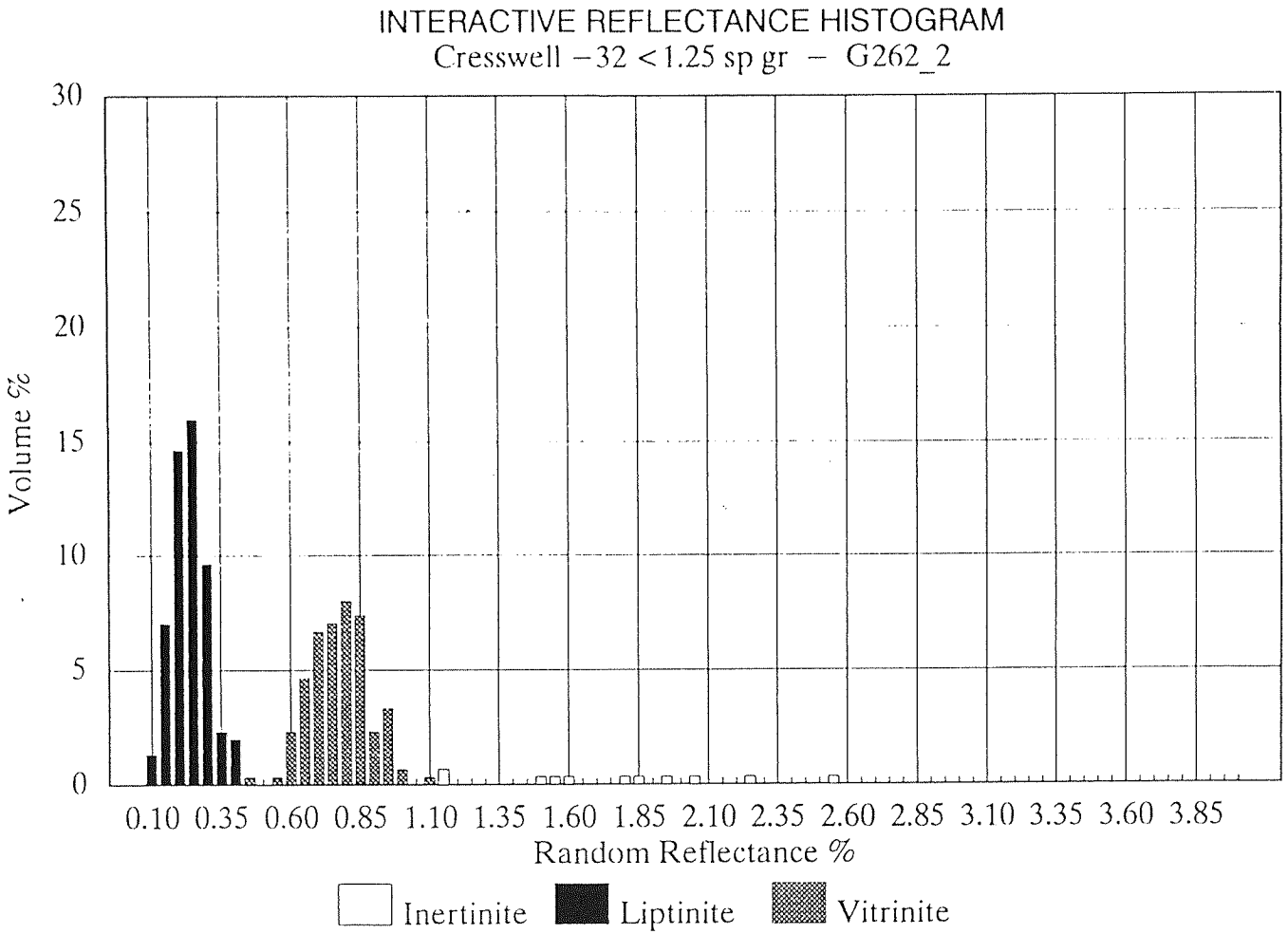

Fig4.04
Reflectance histogram of the Creswell exinite maceral

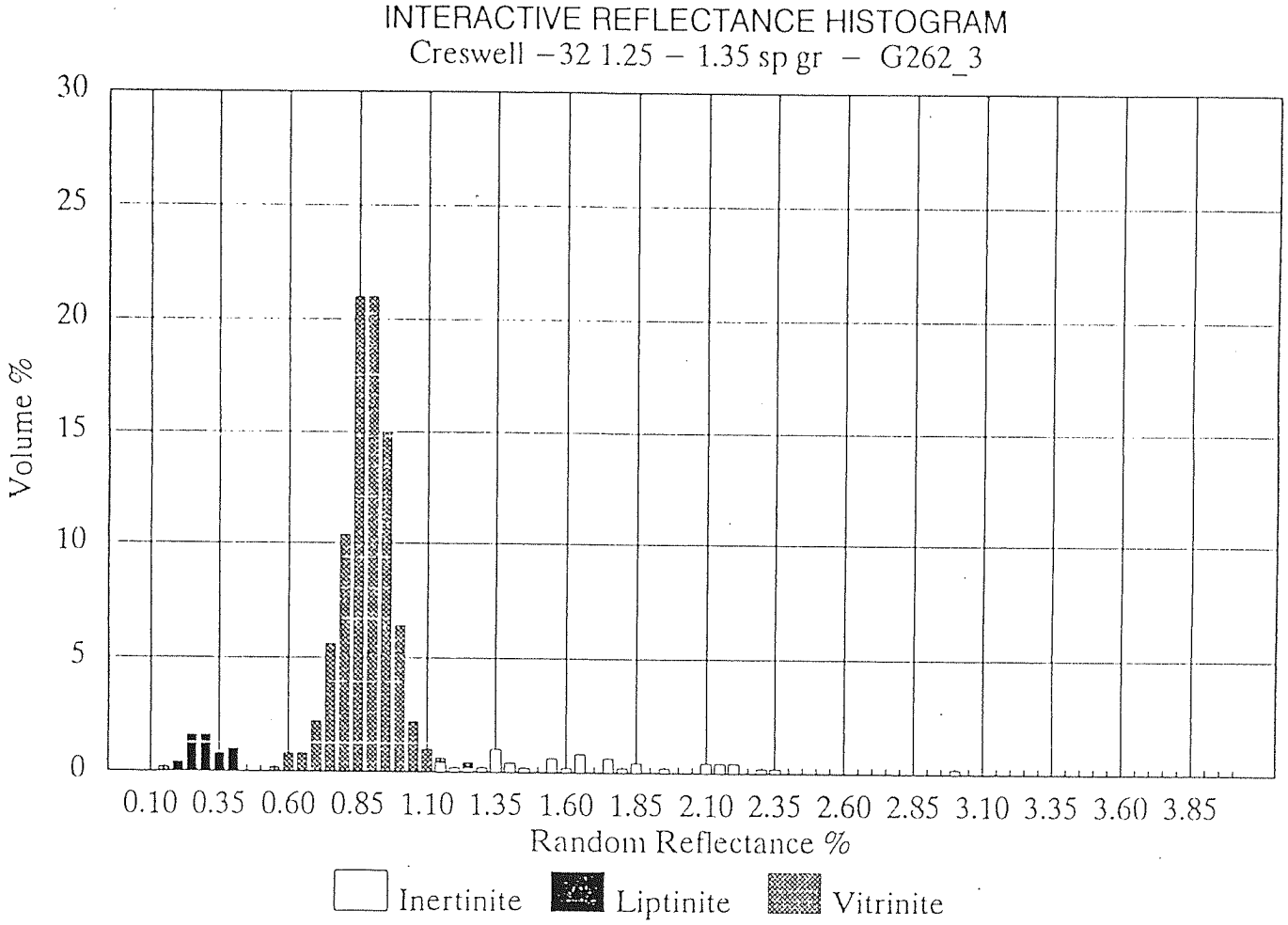

Fig4.05
Reflectance histogram of the Creswell vitrinite maceral

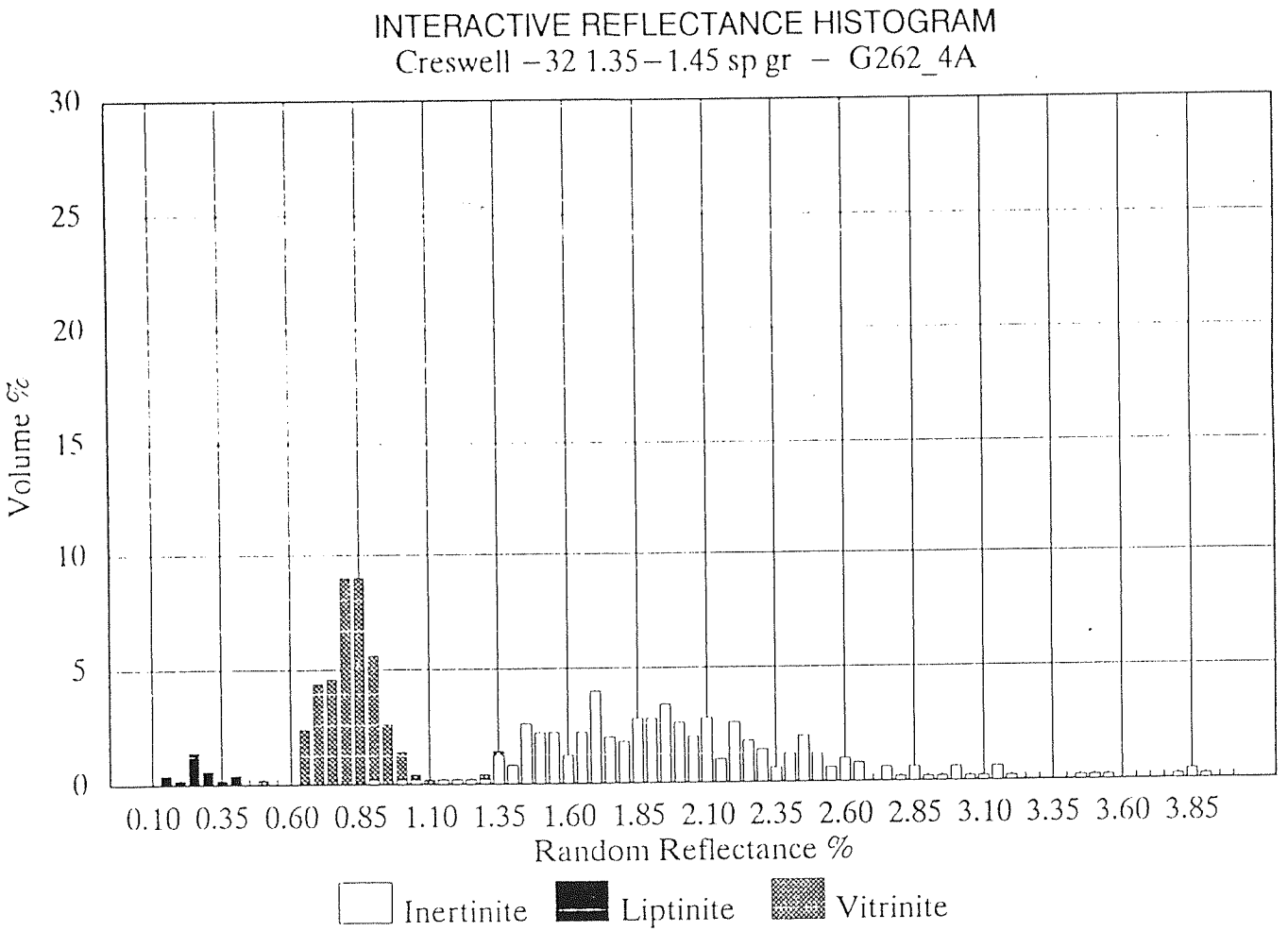

Fig4.06
Reflectance histogram of the Creswell inertinite maceral

Table 4.04

Reflectance measurements for Creswell coal and Creswell macerals

Creswell Component	Exinite (vol%)	Vitrinite (vol%)	Inertinite (vol%)
Creswell raw coal	7.6	80.4	12.0
Creswell exinite	53.0	43.3	3.7
Creswell vitrinite	5.4	87.2	7.4
Creswell inertinite	3.2	39.6	57.2

The Creswell coal macerals were also analysed by ultimate and proximate analysis at CRE (Coal Research Establishment).

Table 4.05 Ultimate analysis for the Creswell coal macerals

Coal Maceral	Carbon[a] (% ad)[b]	Hydrogen (% ad)	Nitrogen (% ad)	Sulfur (% ad)
Creswell exinite	81.4	6.1	1.7	1.1
Creswell vitrinite	81.6	5.3	1.8	0.9
Creswell inertinite	79.5	4.7	1.6	1.0

[a]The carbon results are not corrected for CO_2 i.e total carbon
[b]ad = as analysed

The apparatus used for the proximate analysis was a Stanton Redcroft STA 780 Thermal Analyser. The sample was heated from ambient to 815°C at a rate of 15°C min-1 in an atmosphere of nitrogen. The flow rate through the apparatus was 50 cm^3min^{-1}. The samples were kept at this stage until the weight loss was constant. At this point the atmosphere was changed to air with the same flow. Table 4.06 shows the proximate analysis for the Creswell coal macerals.

Table 4.06 Proximate analysis for the Creswell coal macerals

Coal Maceral	Moisture (%)	Volatile matter (%)	Fixed carbon (%)	Ash (%)
Creswell exinite	0.8	41.8	54.1	3.3
Creswell vitrinite	1.0	33.4	62.4	0.9
Creswell inertinite	2.3	30.2	64.6	2.9

In order to calculate the organic sulfur (S_{org}) we need to make the assumption that $S_{org} = S_{total}$. This is a reasonable assumption for the lighter fractions, but not so for fractions of specific gravity >1.55 gcm^{-3}.

The "Parr" formula is used to calculate the mineral matter from the ash content :

$$\mathbf{MM_{ad} = 1.08\ A_{ad} + 0.55\ S_{total,\ ad}}$$

where S_{total} = Sulfur content as analysed
A_{ad} = Ash content as analysed

The next step is to convert the C, H, N and S percentages obtained from the ultimate analysis (ad - as analysed) to a dry, mineral matter free (dmmf) basis. This is calculated by using the following equation from BS 1016 Part 16 :

$$\mathbf{dmmf = 100\ (C,\ H,\ N,\ S)_{ad} / [\ 100 - (M_{ad} + MM_{ad})]}$$

where M_{ad} = moisture content as analysed

The dry, mineral matter free (dmmf) oxygen (Odmmf) is then calculated by difference :

$$\% \ O_{dmmf} = 100 - (C + H + N + S_{org})_{dmmf}$$

Table 4.07

Calculation of Oxygen in the Creswell macerals on a dry, mineral matter free (dmmf) basis

Creswell Maceral	MM_{ad}	100 - (M_{ad}+MM_{ad})	C_{dmmf} (%)	H_{dmmf} (%)	N_{dmmf} (%)	S_{dmmf} (%)	O_{dmmf} (%)
Exinite	4.19	95.02	85.7	6.4	1.8	1.2	4.9
Vitrinite	1.47	97.53	83.7	5.4	1.8	0.9	8.2
Inertinite	3.69	94.01	84.6	5.0	1.7	1.1	7.6

As expected, the exinite maceral has the highest $\%H_{dmmf}$ content, followed by vitrinite and finally inertinite. The $\%N_{dmmf}$ content is fairly constant throughout and the $\%S_{dmmf}$ is highest in exinite - again, as expected.

(b) Cortonwood coal macerals

The Cortonwood coal was ground down to a particle size of ≤32 μm and separated using the centrifuge technique outlined in section 2.5. Table 4.08 shows the yields collected from each run on the centrifuge.

Table 4.08

Yields from the density fractions of Cortonwood coal (≤32 μm)

Run No.	Specific gravity of solution					% Yield
	<1.25	1.25 -1.35	1.35 -1.45	1.45 -1.55	> 1.55	
Mass obtained from Run 1 (g)	1.8	21.4	14.1	0.5	0.3	95
Mass obtained from Run 2 (g)	0.8	18.4	17.8	0.5	0.4	95
Mass obtained from Run 3 (g)	0.4	19.4	16.9	1.4	0.4	96
Total mass (g)	3.0	59.2	48.8	2.4	1.1	95

In this case there was a lower yield of Cortonwood exinite, but appreciable amounts of the other 2 maceral groups, compared to the Creswell separations. The reason for the low value of the Cortonwood exinite recovered during Run 3 is that there was some leakage from the flange of the Hartley funnel during filtration. This resulted in some of the Cortonwood exinite being lost. To compensate for this loss, an additional run was carried out, where only the Cortonwood exinite maceral fraction was separated and collected - this was then added to the exinite extracted from the other 3 runs. The mass of Cortonwood exinite obtained during this extra run was 0.90g - this brought the total mass of the Cortonwood exinite maceral up to 3.90g (of which 1.0g was submitted for analysis).

Fig 4.07 shows the reflectance histogram for the raw Cortonwood coal (particle size ≤32 μm). The exinite content is 5.0 vol%, the vitrinite content 77.0 vol% and the inertinite content 18.0 vol%. As expected, the major maceral component is vitrinite, followed by inertinite and finally the exinite maceral group. Fig 4.08 shows the reflectance histogram for the separated Cortonwood exinite fraction. Values for the exinite, vitrinite and inertinite maceral components are 86.2, 6.0 and 7.8 vol% respectively. The exinite maceral content has been concentrated from 5.0 vol% in the raw coal to 86.2 vol% in the maceral fraction - this indicates an excellent separation. Fig 4.09 shows the reflectance histogram for the Cortonwood vitrinite maceral group. Values obtained for the exinite, vitrinite and inertinite maceral components were 26.2, 48.8 and 25.0 vol%. The vitrinite maceral component was not concentrated at all during this separation - the maceral concentration went from 77.0 vol% in the raw coal to 48.8 vol% in the vitrinite concentrate. A possible explanation for this occurrence is that the distinct maceral groups are very sensitive to slight changes in density and only through a process of trial-and-error can the optimum density range of each maceral be determined. This, however, is a very long and laborious process, which is why in most cases, general density "cut-off" points are used for the separation of the macerals - as in this case. It is possible that, if further separations had been made in the density range of, say specific gravity 1.25 - 1.37, a greater proportion of the vitrinite maceral (lost in the inertinite fraction), could have been recovered. In this case, however, this procedure is not necessary, as the raw Cortonwood coal already has a fairly high concentration of the vitrinite maceral group and this may be used as a substitute for the Cortonwood vitrinite maceral. Fig 4.10 shows the reflectance histogram for the Cortonwood inertinite maceral fraction. Values of 3.8, 17.2 and 79.0 vol% were obtained for the exinite, vitrinite and inertinite maceral groups respectively. The inertinite component of the Cortonwood coal was concentrated from 18.0 vol% in the raw coal to 79.0 vol% in the maceral fraction. This is an excellent separation. Table 4.09 gives a summary of the results.

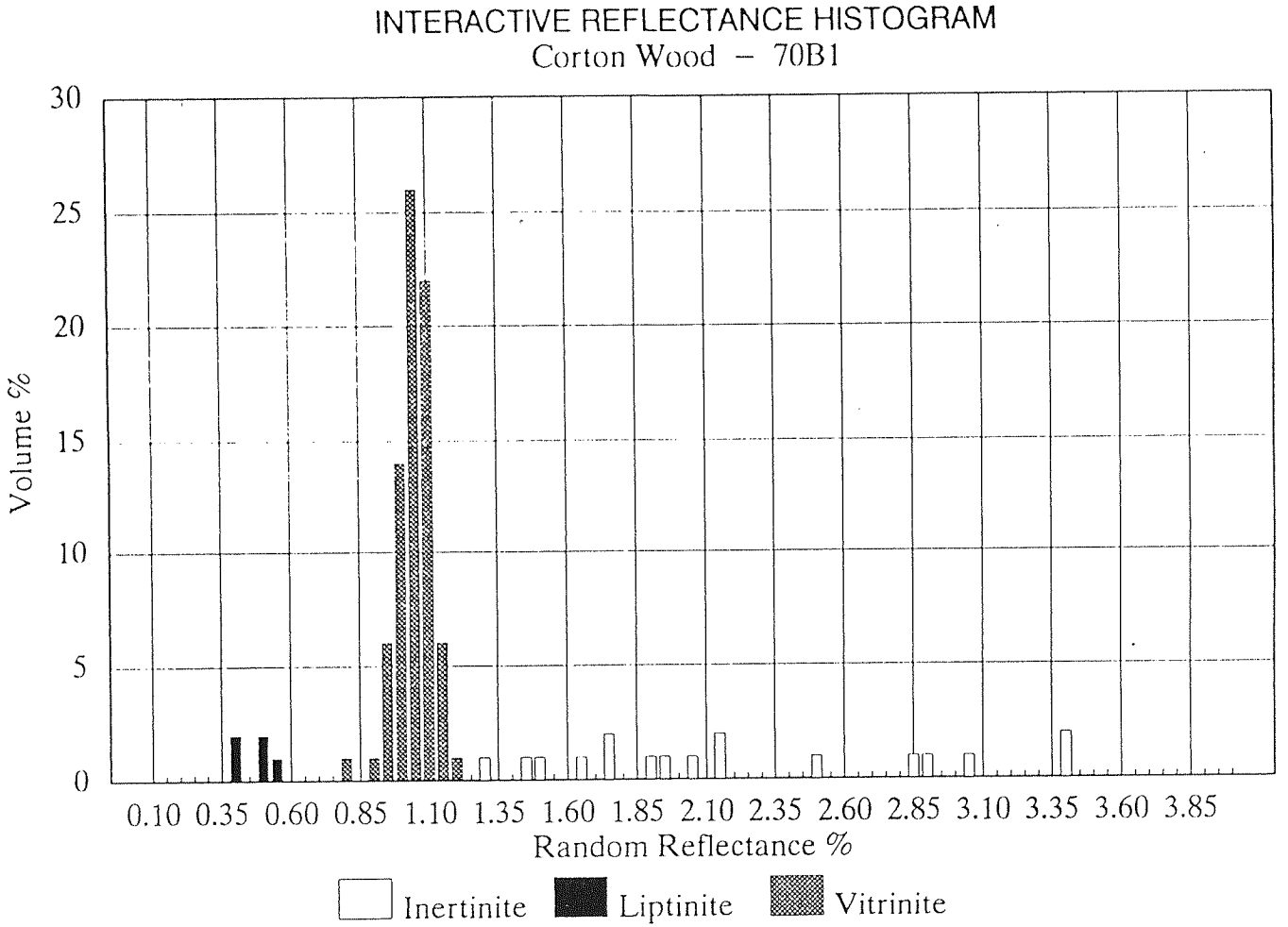

Fig4.07
Reflectance histogram of the raw Cortonwood coal

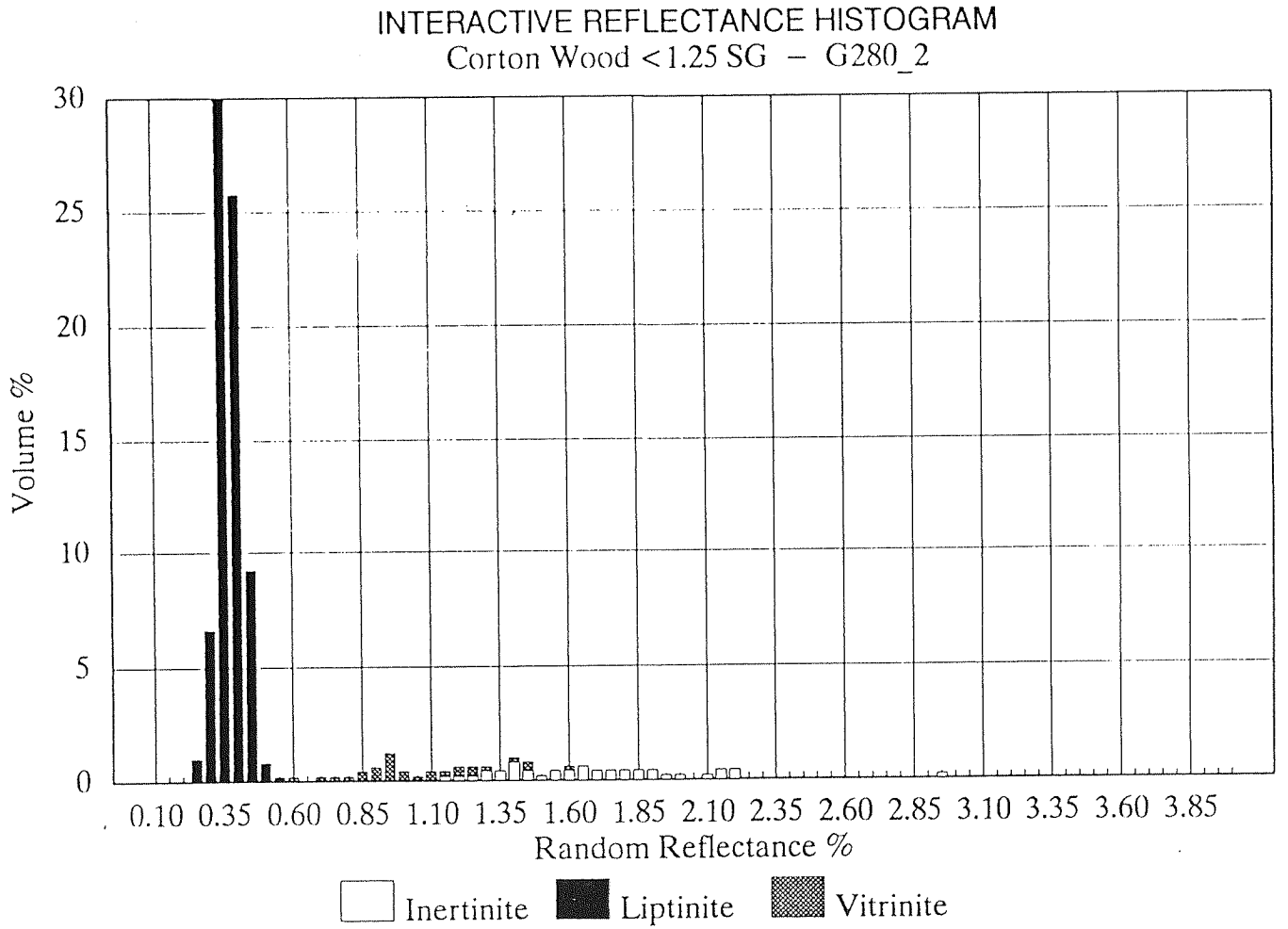

Fig4.08
Reflectance histogram of the Cortonwood exinite maceral

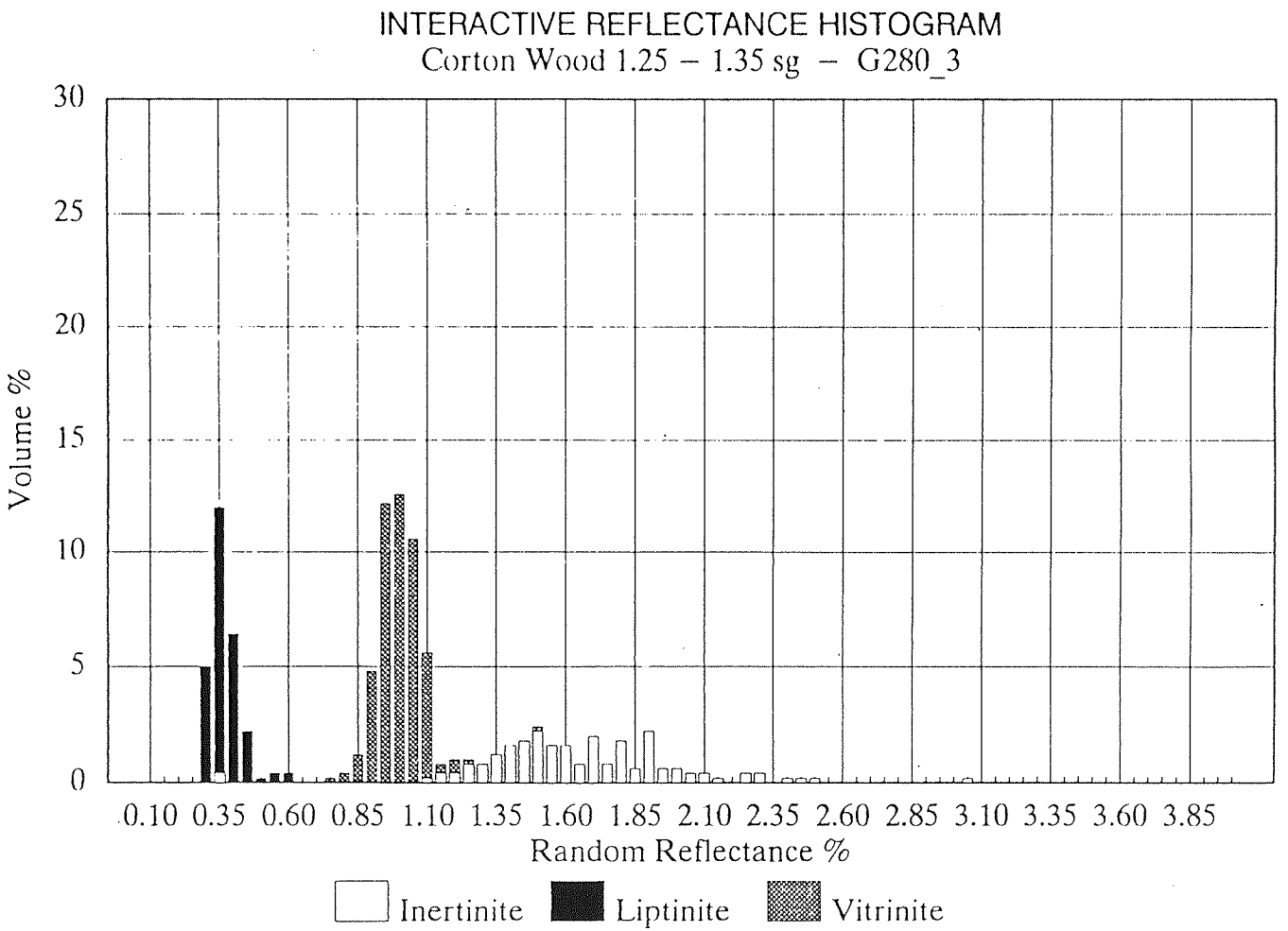

Fig4.09
Reflectance histogram of the Cortonwood vitrinite maceral

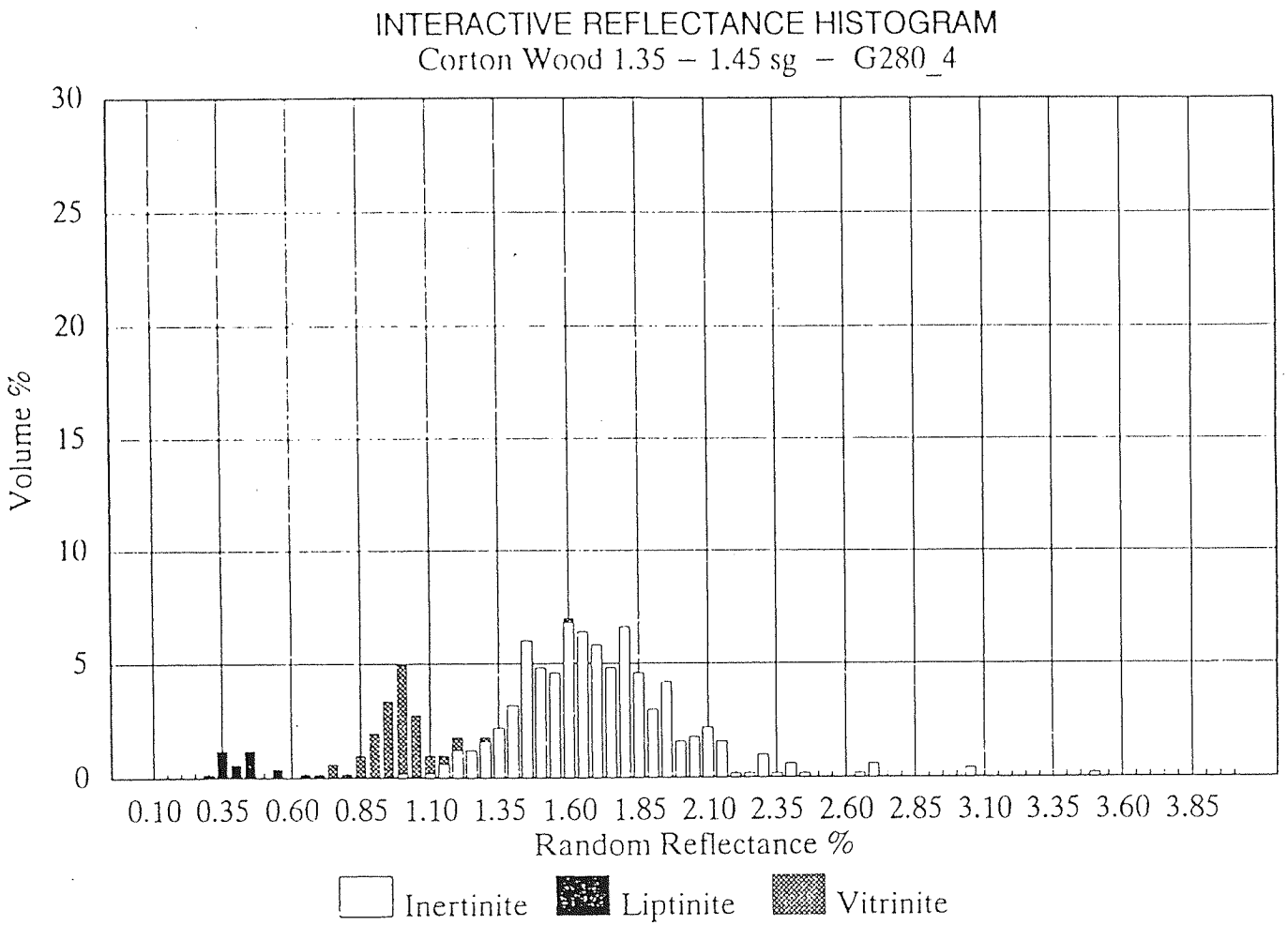

Fig4.10
Reflectance histogram of the Cortonwood inertinite maceral

Table 4.09

Reflectance measurements for Cortonwood coal and Cortonwood macerals

Cortonwood Component	Exinite (vol%)	Vitrinite (vol%)	Inertinite (vol%)
Cortonwood raw coal	5.0	77.0	18.0
Cortonwood exinite	86.2	6.0	7.8
Cortonwood vitrinite	26.2	48.8	25.0
Cortonwood inertinite	3.8	17.2	79.0

Fig 4.11 shows a photograph, taken through the microscope, of the raw Cortonwood coal (≤32 μm). Most of the particle sizes are <30 μm and the majority of the particles vary from fine to very fine grained particles evenly dispersed throughout the sample. The photograph shows that the raw Cortonwood coal consists mainly of vitrinite and inertinite macerals and slightly to the right-of-centre of the photograph a fairly large lump of trimacerite can be seen.

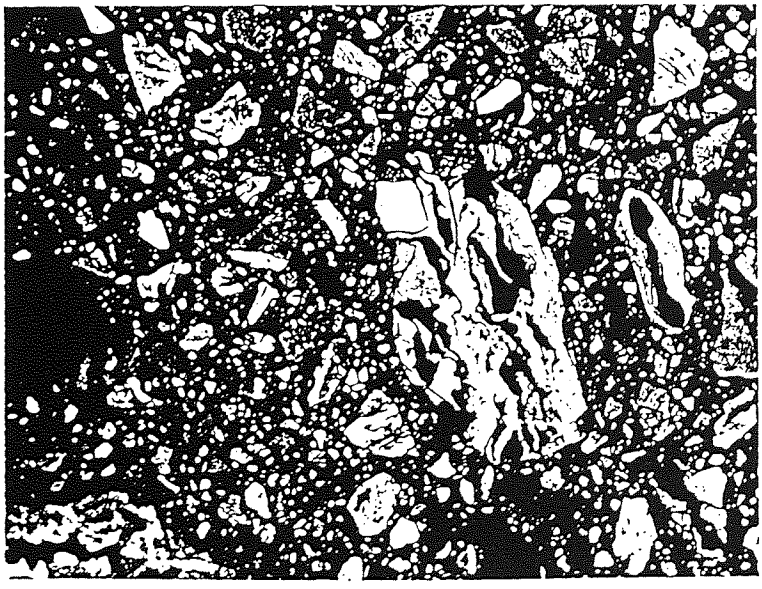

Fig4.11

Photograph of raw Cortonwood coal (x 437 magnification. 1cm = 23μm)

Fig 4.12 shows a photograph of the large well liberated vitrinite (sporinite) macerals found in the Cortonwood vitrinite fraction. There are also complex combinations of very fine inertinite, vitrinite and occasional exinite fragments.

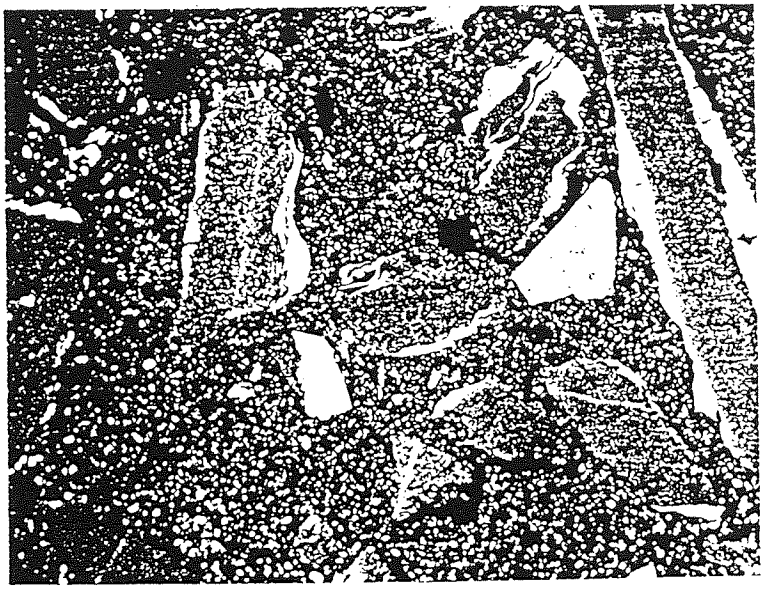

Fig4.12
Photograph of the separated Cortonwood vitrinite maceral fraction
(x 437 magnification. 1cm = 23μm)

Fig 4.13 shows a photograph of the Cortonwood inertinite concentrate. Between the larger size particles (consisting of all 3 maceral groups), there is a fine dispersion of very fine grained inertinite and vitrinite. Inertinite and vitrinite maceral groups appear to predominate in this sample.

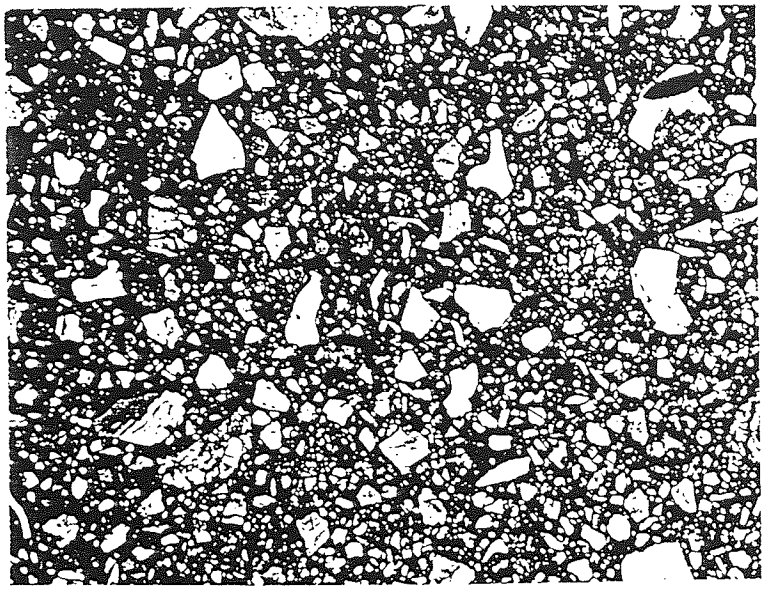

Fig4.13

Photograph of the separated Cortonwood inertinite maceral fraction (x 437 magnification. 1cm = 23μm)

The Cortonwood coal macerals were also analysed by ultimate and proximate analysis at CRE (Coal Research Establishment).

Table 4.10 Ultimate analysis for the Cortonwood coal macerals

Coal Maceral	Carbon[a] (% ad)[b]	Hydrogen (% ad)	Nitrogen (% ad)	Sulfur (% ad)
Cortonwood exinite	83.9	5.8	1.4	0.6
Cortonwood vitrinite	84.8	5.0	1.6	0.6
Cortonwood inertinite	84.9	4.5	1.6	0.5

[a]The carbon results are not corrected for CO_2 i.e total carbon
[b]ad = as analysed

Table 4.11 shows the proximate analysis for the Cortonwood coal macerals

Table 4.11 Proximate analysis for the Cortonwood coal macerals

Coal Maceral	Moisture (%)	Volatile matter (%)	Fixed carbon (%)	Ash (%)
Cortonwood exinite	0.8	50.1	46.5	2.5
Cortonwood vitrinite	1.4 (1.2)*	30.1 (34.5)	61.3 (62.0)	7.2 (2.3)
Cortonwood inertinite	1.6	27.9	70.1	0.5

*The figures in brackets for the Cortonwood vitrinite maceral are the values obtained on re-analysis of the sample.

The Cortonwood macerals show fairly low moisture contents. The exinite maceral group contains almost twice the volatile matter of the Cortonwood inertinite maceral. This correlates with what we would expect for exinite. The elemental carbon analyses from the ultimate analysis do not vary much, but there is a slight increase with density. Again, there is a decrease in the hydrogen content in going from exinite to inertinite. The only value which seems out of place is the high ash content for the Cortonwood vitrinite. It was decided to re-analyse this sample again and the results obtained are displayed in brackets in Table 4.11. The new analytical values appear to be more accurate than the first set of results and it was decided to use the former for future work and calculations.

Using the calculations outlined earlier in this section, the oxygen in each of the macerals was calculated on a dry, mineral matter free (dmmf) basis.

Table 4.12

Calculation of Oxygen in the Cortonwood macerals on a dry, mineral matter free (dmmf) basis

Cortonwood Maceral	MM_{ad}	100 - (M_{ad}+MM_{ad})	C_{dmmf} (%)	H_{dmmf} (%)	N_{dmmf} (%)	S_{dmmf} (%)	O_{dmmf} (%)
Exinite	3.04	96.16	87.3	6.0	1.5	0.6	4.6
Vitrinite	2.79	96.01	88.3	5.2	1.7	0.6	4.2
Inertinite	0.84	97.56	87.0	4.6	1.6	0.6	6.2

The carbon, nitrogen and sulfur values are all fairly constant, but the hydrogen value decreases in going from exinite to inertinite, as expected. The Cortonwood vitrinite maceral group appears to have an unusually low oxygen content compared to the other two macerals. This is probably due to the poor separation of this maceral and the presence, in appreciable amounts, of the other two maceral groups, in the vitrinite fraction.

(c) Kellingley coal macerals

The Kellingley coal was ground down to ≤32 μm and the maceral groups were separated by centrifuging. Table 4.13 shows the yields collected from each run on the centrifuge.

Table 4.13 Yields from the density fractions of Kellingley coal (≤32μm)

Run No.	Specific gravity of solution					% Yield
	<1.25	1.25 -1.35	1.35 -1.45	1.45 -1.55	> 1.55	
Mass obtained from Run 1 (g)	1.1	23.5	13.0	0.4	0.3	96
Mass obtained from Run 2 (g)	0.1	33.9	4.5	0.3	0.2	98
Mass obtained from Run 3*(g)	0.2	15.1	10.0	0.4	0.3	96
Total mass (g)	1.3	72.5	27.5	1.1	0.8	97

*Only 26.9g of Kellingley coal was available for this run.

The Kellingley coal samples were submitted to the Geology section at CRE for petrographic assessment and it was discovered that, although the samples were thought to represent a particle size of ≤32 μm, significant portions of the Kellingley coal contained particle sizes up to 50 μm. It was also found that particles greater than 25 μm commonly displayed bimacerite and trimacerite combinations. Fig 4.14 shows an SEM micrograph of the raw Kellingley coal - the oversize particles are clearly discernible. Fig 4.15 shows a micrograph where a single particle of the Kellingley raw coal is visible - the coal particle is approximately 70 μm long!

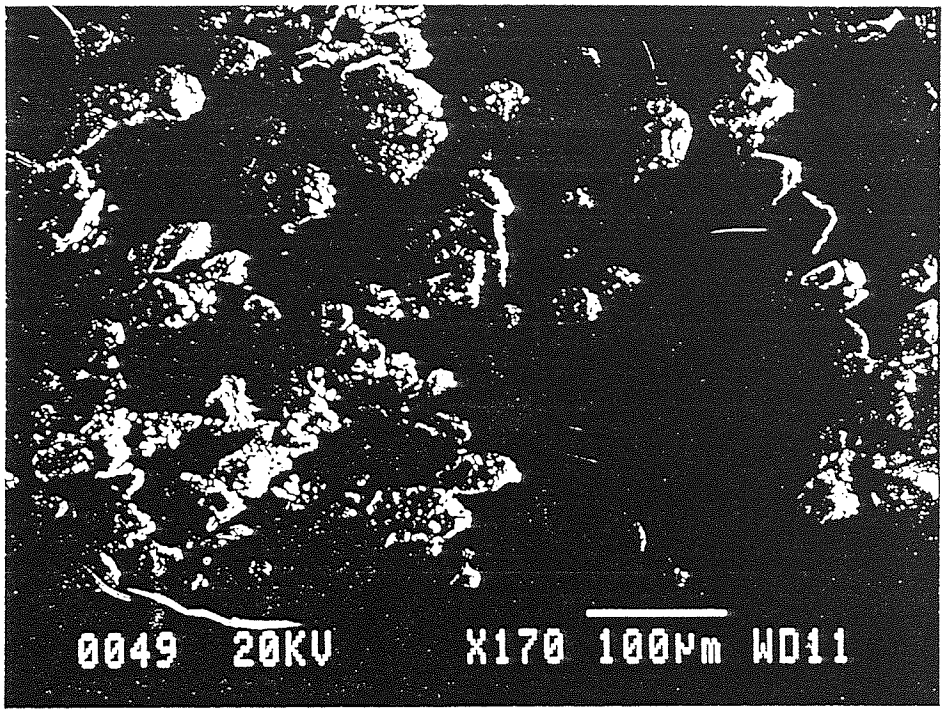

Fig4.14
Scanning electron microscope (SEM) micrograph of raw Kellingley coal

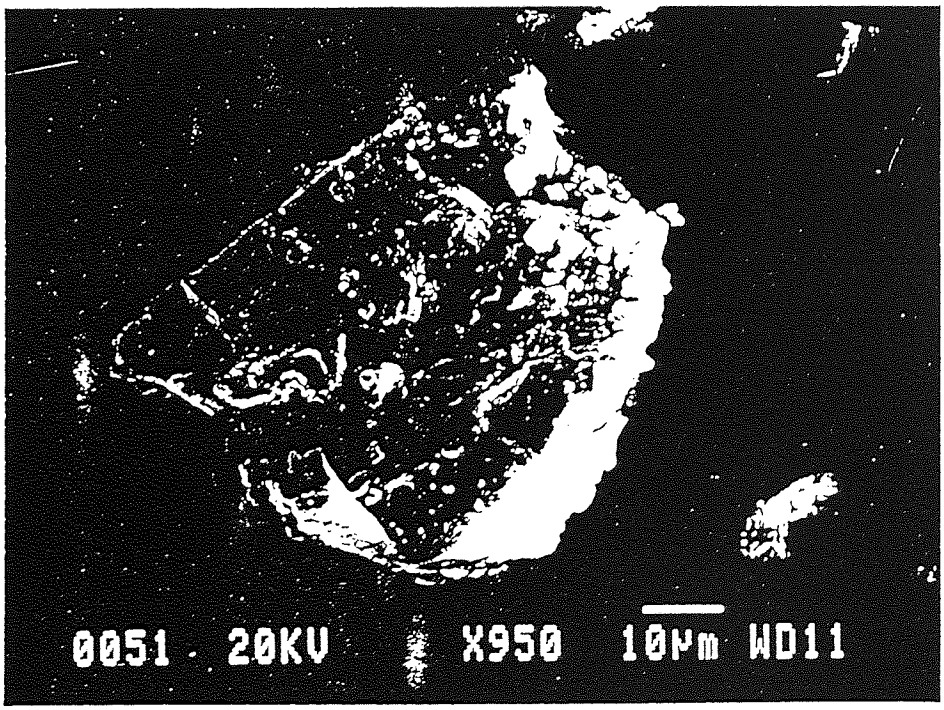

Fig4.15
Scanning electron microscope (SEM) micrograph of a single particle of Kellingley coal

(d) Gedling coal macerals

The Gedling coal was ground down to ≤32 μm and the maceral groups were separated by centrifuging. Table 4.14 shows the yields from the centrifuge runs.

Table 4.14 Yields from the density fractions of Gedling coal (≤32 μm)

Run No.	Specific gravity of solution					% Yield
	<1.25	1.25 -1.35	1.35 -1.45	1.45 -1.55	> 1.55	
Mass obtained from Run 1 (g)	0.1	19.8	15.8	0.8	0.1	92
Mass obtained from Run 2 (g)	0.1	23.5	12.1	0.6	0.1	91
Mass obtained from Run 3 (g)	0.1	20.5	16.0	0.4	0.1	93
Total mass (g)	0.3	63.8	43.9	1.8	0.3	92

The Gedling coal samples were also sent to the Geology section at CRE for petrographic assessment. It was found that the raw Gedling coal contained particles up 140 μm! Below 25 μm the particles showed reasonable maceral separation, but above this particle size bimacerites and trimacerites were present in significant amounts. Figs 4.16 and 4.17 show photographs of the Gedling raw coal and the Gedling vitrinite fraction respectively. The large lumps of bimacerite and trimacerite are clearly visible.

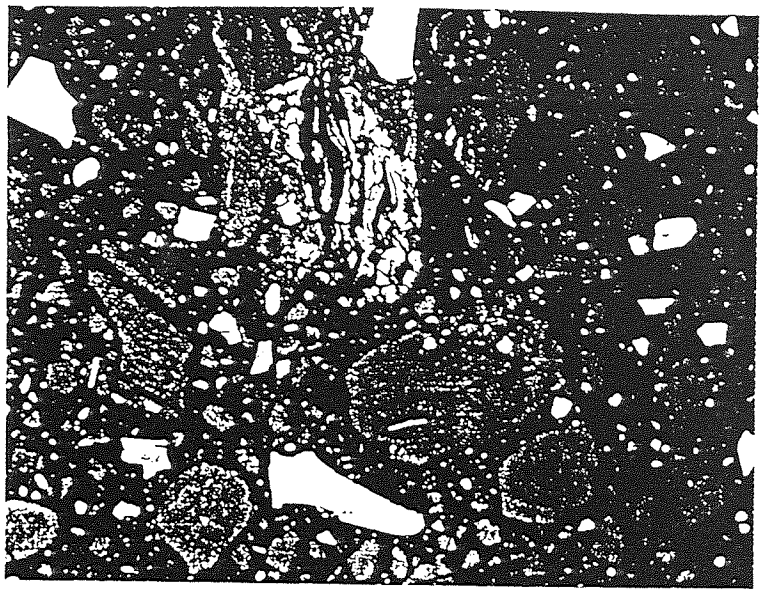

Fig4.16
Photograph showing the bimacerites and trimacerites in Gedling raw coal

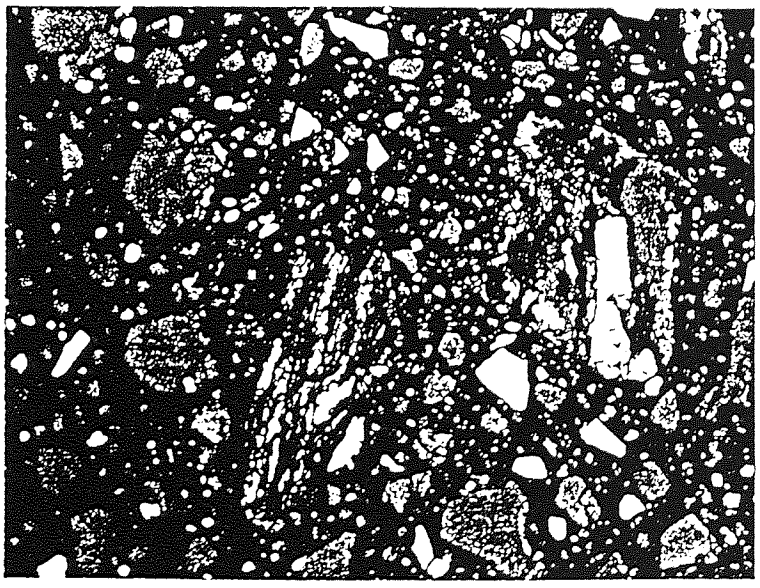

Fig4.17
Photograph showing the bimacerites and trimacerites in the Gedling vitrinite fraction

Because of the discrepancies in particle size, the low yields acquired for the exinite macerals and the high bimacerite and trimacerite concentrations in Kellingley and Gedling coals, it was decided to concentrate testing on the Creswell and Cortonwood macerals, which showed better particle size distribution and superior maceral separation.

4.3.2 Acetylation of Creswell and Creswell macerals

The acetylation reaction involves the conversion of the hydroxyl groups to acetyl groups. There are 4 main steps to the reaction :

1. Esterification of the hydroxyl group with acetic anhydride

$$2\ ROH + (CH_3CO)_2O \rightarrow 2\ CH_3COOR + H_2O$$

If thiols and primary and secondary amines are present, they may also react with the acetylating reagent :

$$2\ RSH + (CH_3CO)_2O \rightarrow 2\ CH_3COSR + H_2O$$

$$2\ RNH_2 + (CH_3CO)_2O \rightarrow 2\ CH_3CONHR + H_2O$$

$$2\ R_2NH + (CH_3CO)_2O \rightarrow 2\ CH_3CONR_2 + H_2O$$

Because the concentrations of organic thiol groups and primary and secondary amines (such as indoles and carbazoles) are quite low in the coals we are testing, their effect on the measured phenolic hydroxyl concentrations is likely to be small. It has also been shown that aromatic secondary amine groups do not react as readily as hydroxyl functional groups with acetic anhydride[67].

2. Saponification of the esterified coal

$$2\ CH_3COOR + Ba(OH)_2 \rightarrow 2\ ROH + Ba(OOCCH_3)_2$$

3. Acidification and release of the acetic acid

$$3\ Ba(OOCCH_3)_2 + 2\ H_3PO_4 \rightarrow Ba_3(PO_4)_2 + 6\ CH_3COOH$$

4. Titration of the released acetic acid with 0.1015N NaOH

$$CH_3COOH + NaOH \rightarrow Na(OOCCH_3) + H_2O$$

Assuming that the acetylatable oxygen present in the coal is in the form of hydroxyl groups, the percentage O_{OH} / O_{total} is calculated thus :

The acetyl content (A) in m.equiv.g^{-1} is given by :

$$A = \frac{(T-T_O)n}{m}$$

where
- T = total titre (in cm^3)
- T_O = total blank titre (in cm^3) = 0.04
- n = normality of NaOH = 0.1015
- m = mass of the acetylated coal = 0.10g

The hydroxyl content (H) in m.equiv.g^{-1} is given by :

$$H = \frac{A}{(1-0.042A)}$$

where A = acetyl content (in m.equiv.g^{-1})

Conversion of $\%O_{dmmf}$ to m.equiv.g^{-1} is carried out via the equation :

m.equiv.g^{-1} = (O_{dmmf} / 100) (100 / 0.1) 1 / 16

The percentage of O_{OH} / O_{total} is then given by :

$$\% \frac{O_{OH}}{O_{total}} = \frac{H}{O_{dmmf}} \times 100\%$$

In all 4 samples of Creswell coal were acetylated - the raw Creswell coal and the Creswell exinite, vitrinite and inertinite macerals. Table 4.15 gives some analytical data (obtained from CRE coal bank data) on the raw Creswell coal sample.

Table 4.15 Analytical data for the raw Creswell coal (≤32 μm)

ANALYSIS	DATA	
Ultimate analysis (%)	Carbon (dmmf)[a]	86.2
	Hydrogen (dmmf)	5.2
	Oxygen (dmmf)	5.6
	Nitrogen (dmmf)	1.91
	Organic sulfur (db)[b]	0.95
	Sulfate sulfur (db)	< 0.05
	Pyritic sulfur (db)	0.40
Proximate analysis (%)	Moisture (ad)[c]	2.5
	Ash (ad)	2.6
	Volatile matter (ad)	34.7
	Fixed carbon (ad)	60.2

[a]dmmf = dry, mineral matter free
[b]db = dry basis
[c]ad = as analysed

The Creswell macerals were acetylated for 30 mins in the Sharp Carousel II microwave oven. Hydrolysis for 30 mins with barium hydroxide was also carried out in the microwave oven. The titration results can be seen in Table 4.16.

Table 4.16

Titration results for the Creswell coal macerals using the microwave hydrolysis technique

Titre No.	Volume of 0.1015N NaOH (cm^3) Exinite maceral	Volume of 0.1015N NaOH (cm^3) Vitrinite maceral	Volume of 0.1015N NaOH (cm^3) Inertinite maceral
1	0.08	0.22	0.35
2	0.08	0.18	0.18
3	0.06	0.20	0.20
4	0.08	0.16	0.12
5	0.06	0.16	0.11
6	0.08	0.14	0.12
7	0.06	0.09	0.09
8	0.07	0.11	0.08
9	0.06	0.10	0.09
10	0.06	0.08	0.08
11	0.06	0.07	0.06
12	0.04	0.08	0.04
13	0.04	0.08	0.04
14	0.04	0.04	0.04
15	0.04	0.04	0.04
16	0.04	0.04	0.04

The "cut-off" point for the titrations is just before the blank titre value (0.04 cm^3) is reached. Hence for the Creswell exinite maceral the cut-off point is at titre No.11, for the vitrinite maceral at titre No.13 and for the inertinite maceral titre No.11. All the titration values, up to the blank titre value, were added together to give the total titration value for each maceral group. The total titration values obtained were 0.75, 1.67 and 1.48 cm^3 for the Creswell exinite, vitrinite and inertinite maceral groups respectively. During the hydrolysis step in the microwave oven, it was found that the barium hydroxide solution superheated very rapidly. This resulted in expansion of the teflon digestion vessel and subsequent venting after only very short time intervals (10-20 seconds). A consequence of this was that some barium hydroxide solution was lost from the containment vessel, effectively reducing the efficiency of the hydrolysis step. Another consequence of this rapid superheating was that the reaction needed to be stopped at fairly short intervals, in order that essential cooling of the reagents could take place. To overcome these obstacles, it was decided to carry out the hydrolysis step on the bench top via refluxing for 24 hrs. The initial acetylation step continued to be carried out in the microwave oven for a reaction time of 30 mins. Table 4.17 shows the titration values obtained for the Creswell macerals using this new adapted method.

Table 4.17

Titration results for the Creswell coal macerals using the reflux hydrolysis technique

Titre No.	Volume of 0.1015N NaOH (cm^3) (Exinite maceral)	Volume of 0.1015N NaOH (cm^3) (Vitrinite maceral)	Volume of 0.1015N NaOH (cm^3) (Inertinite maceral)
1	0.14	0.37	0.34
2	0.12	0.37	0.26
3	0.14	0.28	0.24
4	0.10	0.22	0.20
5	0.10	0.18	0.18
6	0.09	0.18	0.18
7	0.08	0.18	0.16
8	0.06	0.12	0.14
9	0.06	0.12	0.12
10	0.06	0.12	0.10
11	0.06	0.12	0.08
12	0.06	0.10	0.08
13	0.06	0.10	0.08
14	0.04	0.10	0.06
15	0.06	0.10	0.06
16	0.04	0.10	0.04
17	0.04	0.08	0.04
18	0.04	0.10	0.04
19	-	0.10	-
20	-	0.10	-
21	-	0.08	-
22	-	0.08	-
23	-	0.08	-
24	-	0.08	-
25	-	0.08	-
26	-	0.08	-
27	-	0.08	-
28	-	0.06	-
29	-	0.06	-
30	-	0.06	-
31	-	0.04	-
32	-	0.04	-
33	-	0.04	-

The results from Table 4.17 are displayed graphically in figs 4.18 - 4.20

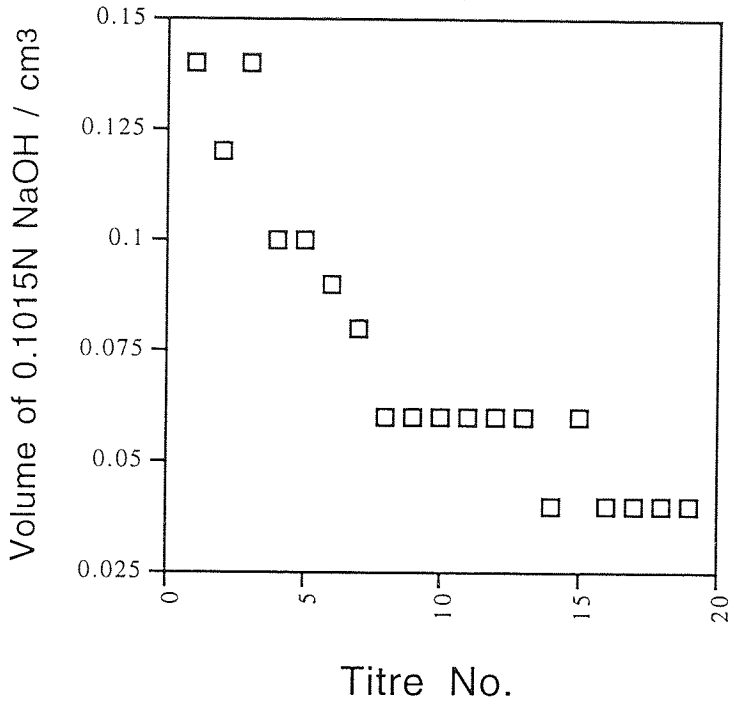

Fig4.18 Plot of the titration of liberated acetic acid with 0.1015N NaOH for the Creswell exinite maceral

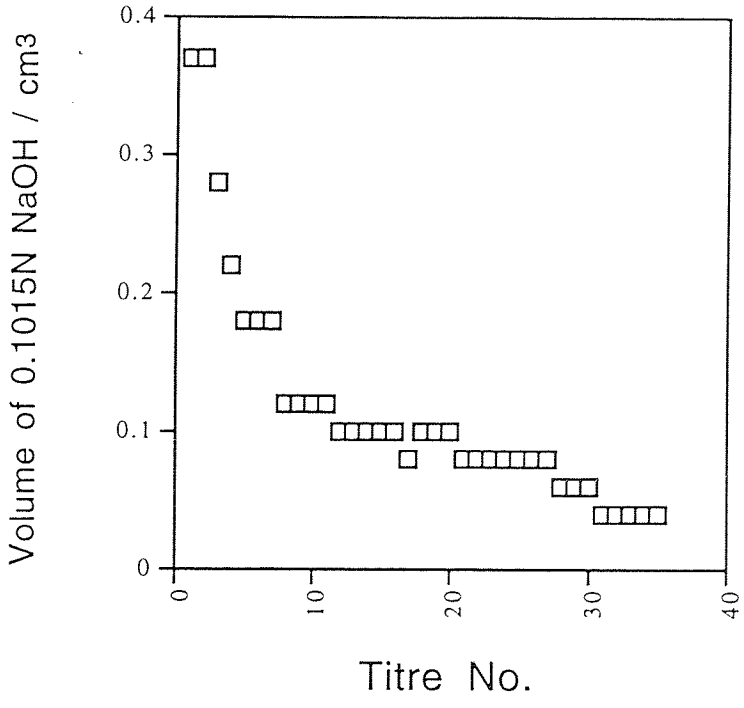

Fig4.19 Plot of the titration of liberated acetic acid with 0.1015N NaOH for the Creswell vitrinite maceral

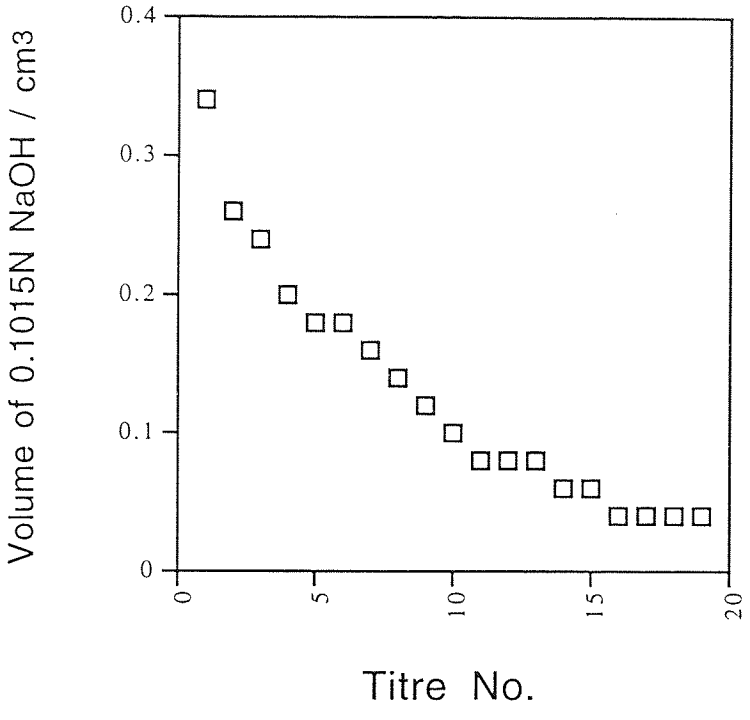

Fig4.20 Plot of the titration of liberated acetic acid with 0.1015N NaOH for the Creswell inertinite maceral

By using the microwave-acetylation and reflux-hydrolysis technique, total titration values of 1.23, 3.88 and 2.28 cm^3 were obtained for the exinite, vitrinite and inertinite macerals respectively. Table 4.18 shows a comparison of the results obtained by both techniques.

Table 4.18

Comparison of total titration values obtained using the microwave hydrolysis and reflux hydrolysis techniques for the Creswell macerals

TECHNIQUE	Total titration value for Creswell exinite maceral (cm^3)	Total titration value for Creswell vitrinite maceral (cm^3)	Total titration value for Creswell inertinite maceral (cm^3)
Microwave hydrolysis	0.75	1.67	1.48
Reflux hydrolysis	1.23	3.88	2.28

It can clearly be seen that there is a marked increase in reaction when the bench top hydrolysis technique is used. This is probably due to an incomplete reaction occurring in the microwave oven due to the loss of the saponificating agent. This occurred when high pressures built up rapidly (due to superheating of the barium hydroxide solution) in the digestion vessel resulting in subsequent opening of the relief valve and venting of the hot gases.

FT-IR showed that the Creswell macerals had reverted back to their original structure after 24 hrs refluxing and refluxing for periods longer than 24 hrs did not significantly improve the reaction and release of acetic acid. Acetylation of the raw Creswell coal yielded a total titration value of 1.51 cm^3. Table 4.19 and fig 4.21 show the titration values obtained for the raw Creswell coal in a tabulated and diagrammatic format respectively.

Table 4.19

Titration values for the acetylation of the raw Creswell coal

Titre No.	Volume of 0.1015N NaOH added (cm^3)
1	0.10
2	0.09
3	0.08
4	0.08
5	0.07
6	0.08
7	0.08
8	0.08
9	0.08
10	0.08
11	0.08
12	0.07
13	0.08
14	0.08
15	0.08
16	0.08
17	0.08
18	0.08
19	0.06
20	0.04
21	0.04
22	0.04

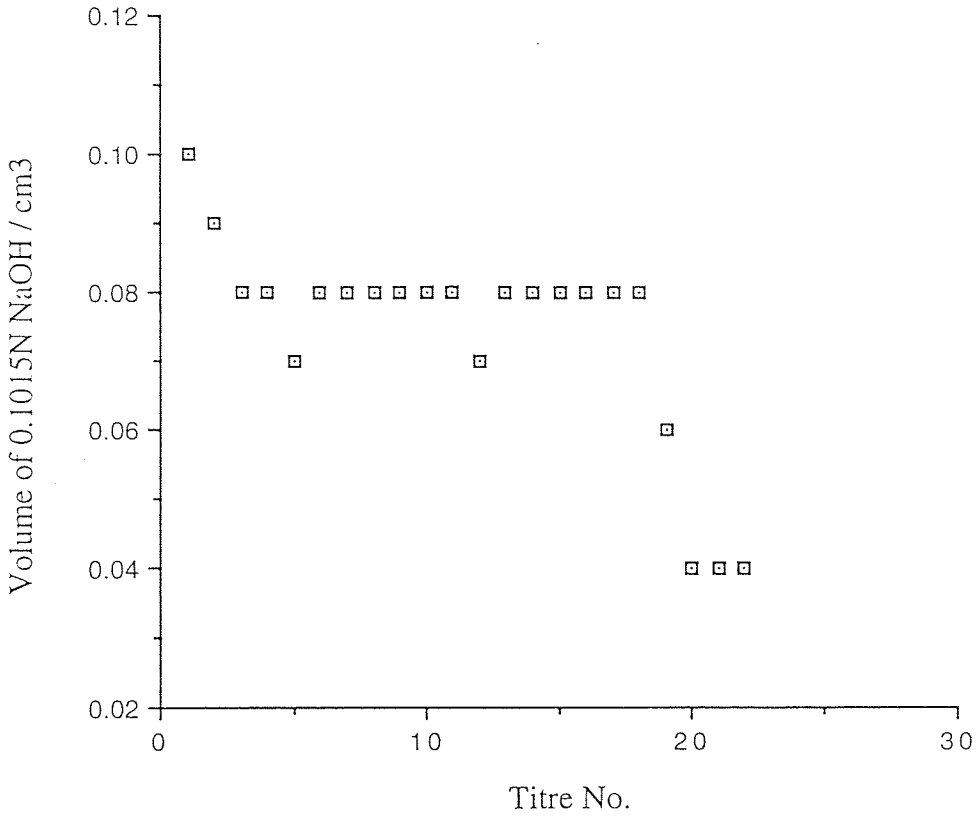

Fig4.21 Plot of the titration of liberated acetic acid with 0.1015N NaOH for the raw Creswell coal

A rapid assessment of the extent of acetylation was possible by the use of FT-IR spectrometry. Fig 4.22 shows the IR spectrum of the raw Creswell coal (≤32 μm). The hydrogen-bonded OH broad stretching frequency at 3436 cm^{-1} is clearly visible. Fig 4.23 shows the spectrum of the acetylated raw Creswell coal (reflux-hydrolysis method). The spectrum shows that there is a significant reduction in the OH stretching frequency on acetylation of the sample. There is also the appearance of a sharp band at 1763 cm^{-1} - this frequency is indicative of the C=O stretch found in phenolic acetates. Another major absorption appears at 1195 cm^{-1} - this is characteristic of C-O (also found in phenolic acetates). More evidence that acetylation has taken place is indicated by the stronger absorption of the peak at 1365 cm^{-1} - this corresponds to $C-CH_3$ symmetric deformations. There is also a slight shoulder at approximately 1655 cm^{-1} which can be assigned to a small amount of acetylated alkyl secondary amines. The major changes in structure can be seen more clearly in fig 4.24, which shows a comparison of the IR spectra of the raw Creswell coal and the acetylated raw Creswell coal.

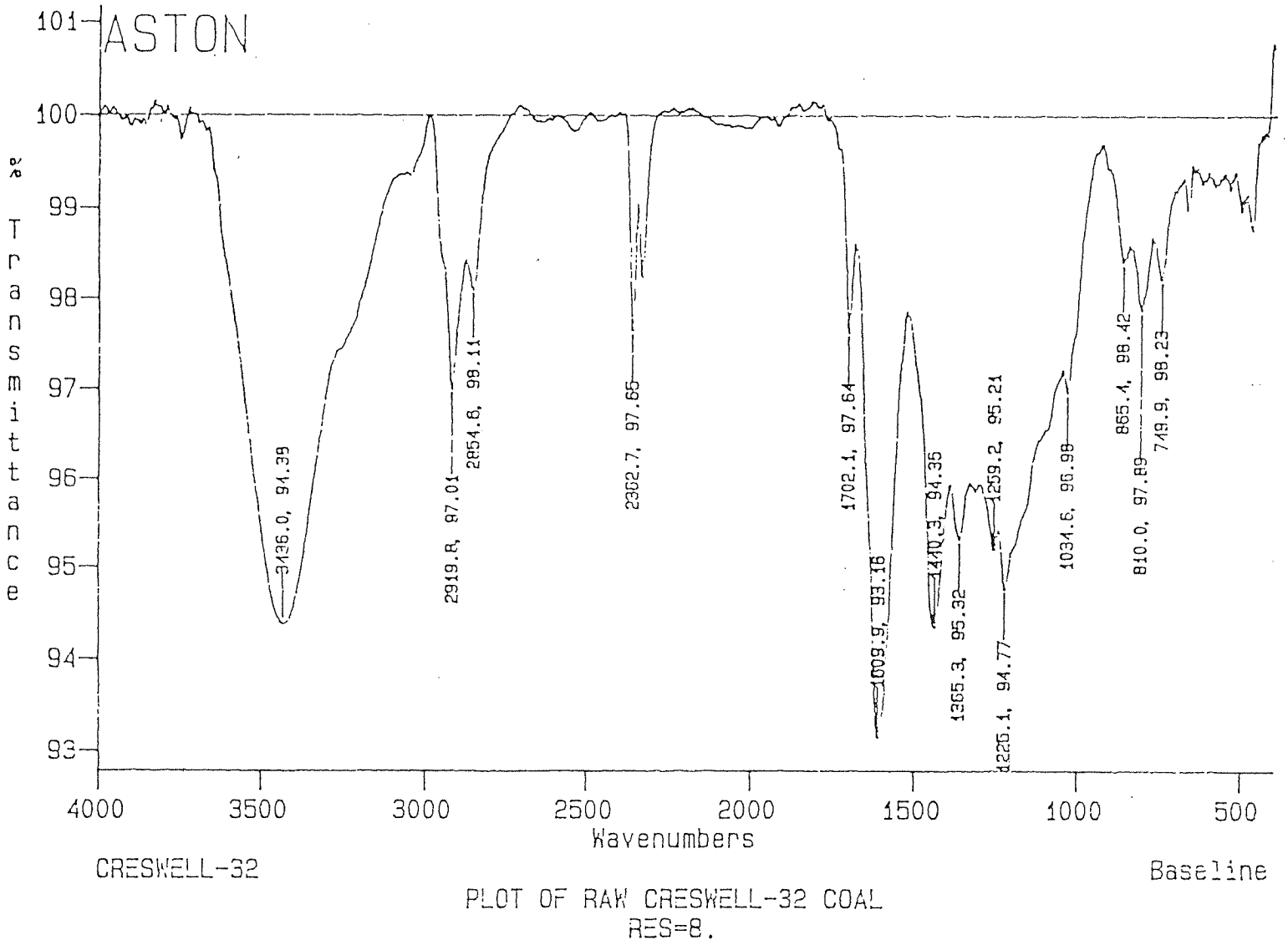

Fig4.22
IR of undried raw Creswell coal

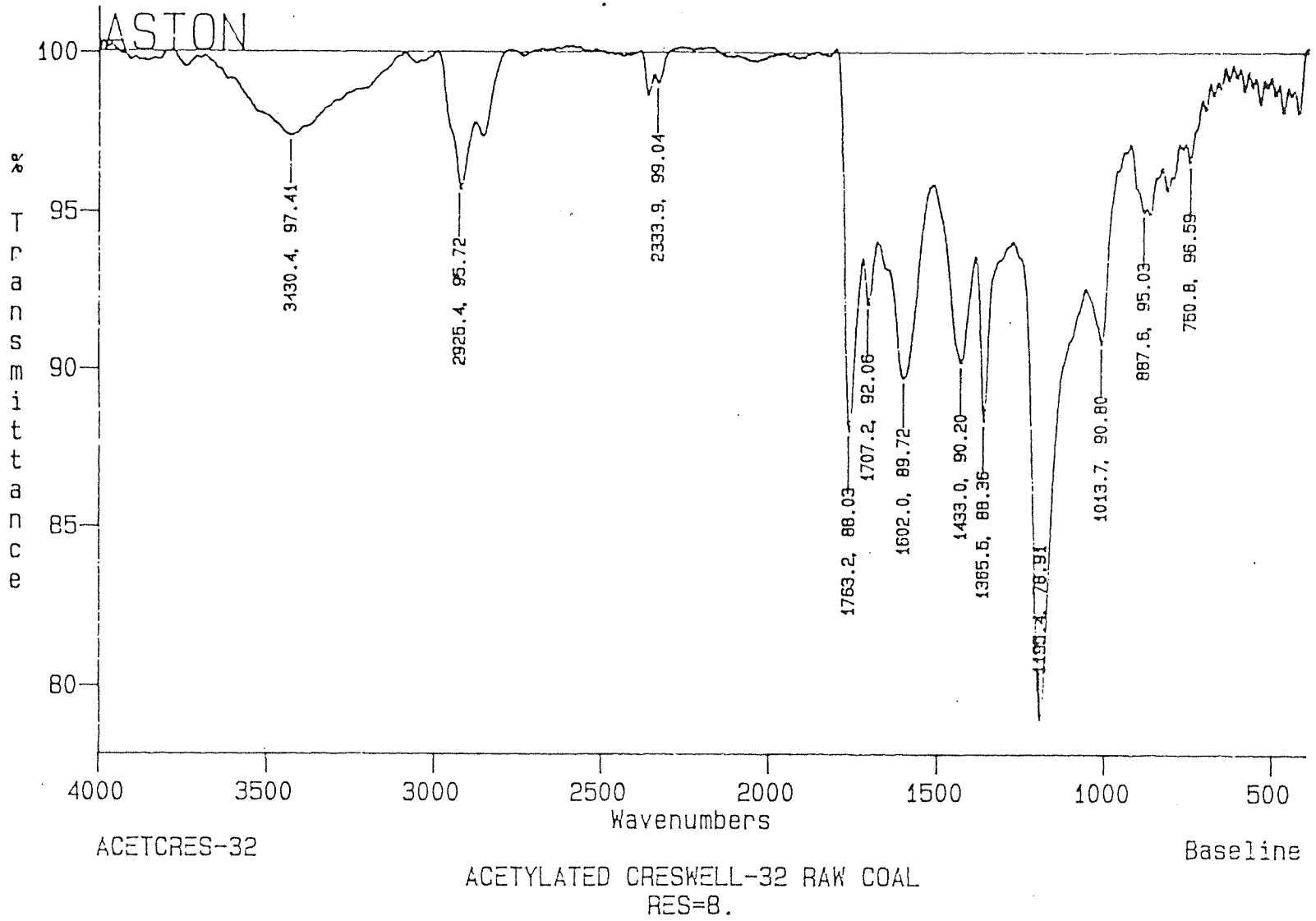

Fig4.23
IR of the acetylated raw Creswell coal

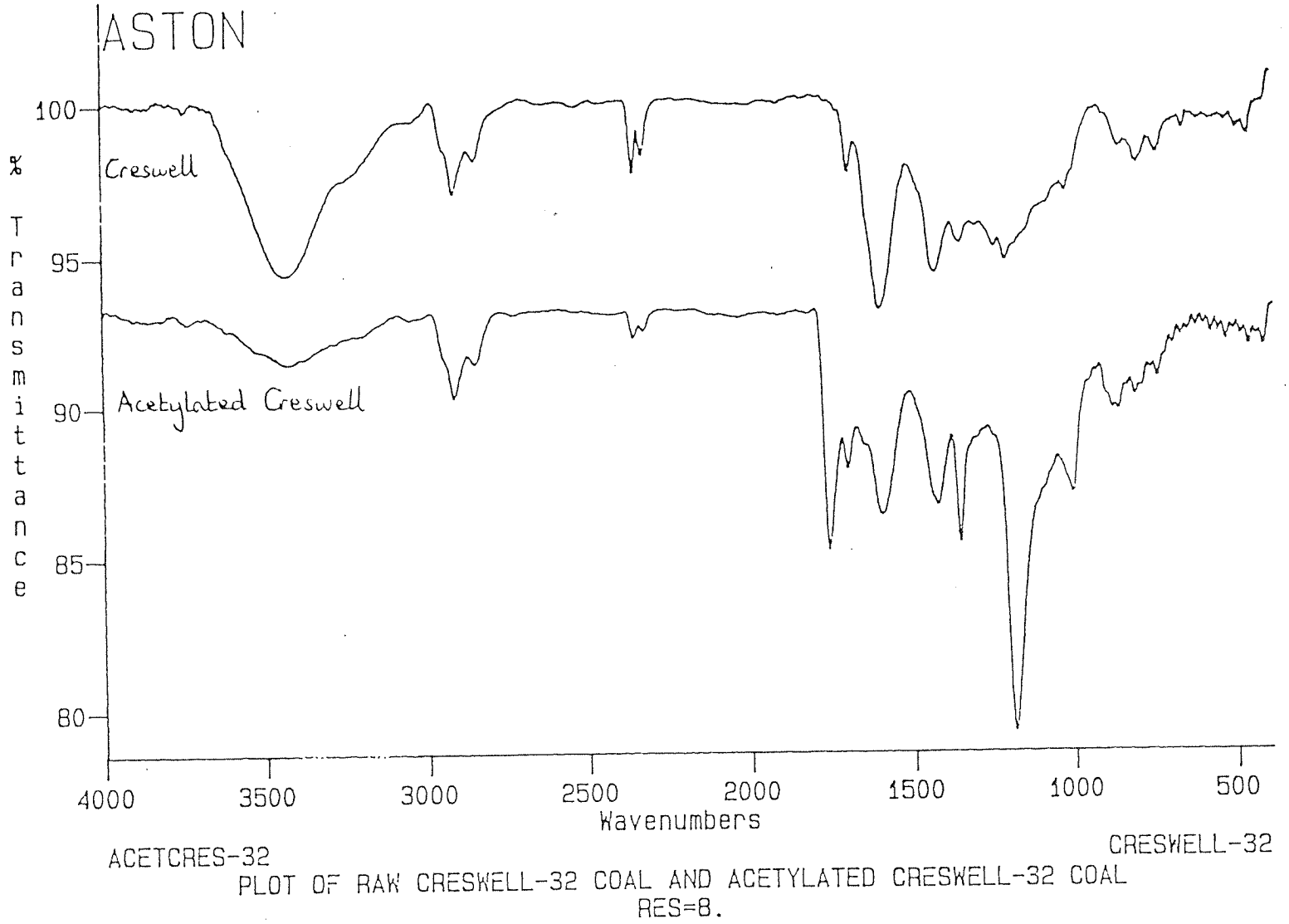

Fig4.24
IR comparison of the unreacted undried raw Creswell coal and acetylated raw Creswell coal

Fig 4.25 shows the IR spectrum of the acetylated Creswell exinite maceral (reflux-hydrolysis method). The characteristic peaks denoting acetylation are present at 1764 cm^{-1} (C=O), 1195 cm^{-1} (C-O) and 1366 cm^{-1} ($C-CH_3$) and, in this case, there is a more pronounced reduction in the OH stretching frequency. Fig 4.26 shows the IR spectra of the Creswell exinite maceral and the Creswell exinite maceral after acetylation and hydrolysis have taken place. The spectra shows that the exinite maceral has effectively reverted back to its original structure with only residual amounts of the acetylating reagent remaining.

Fig 4.27 shows the acetylated vitrinite maceral. Again, there is the a reduction of the OH vibration band at 3350 cm^{-1} and the appearance of the characteristic acetyl absorption bands.

Fig 4.28 shows the IR spectrum of the acetylated inertinite maceral. As before, there is a reduction in the OH stretching frequency and the appearance of bands showing acetylation has taken place. Fig 4.29 shows a comparison between the Creswell inertinite maceral and the Creswell inertinite maceral after acetylation and hydrolysis have taken place. Again, the structures are essentially similar with only residual amounts of the acetylating reagent still incorporated.

Fig 4.30 shows a multi-spectral display showing all the acetylated Creswell coal macerals and the acetylated Creswell raw coal on one IR plot. The spectra shows that, in each instance, a similar reaction is occurring i.e the reduction in the OH vibration band and the appearance of absorptions corresponding to acetyl bands. Fig 4.31 shows an IR comparison of the 3 Creswell macerals after acetylation and hydrolysis have taken place and the raw Creswell coal.

From the titration results for the acetylated Creswell macerals and acetylated raw Creswell coal, the percentage O_{OH} / O_{total} was calculated. The calculations are shown in Table 4.20.

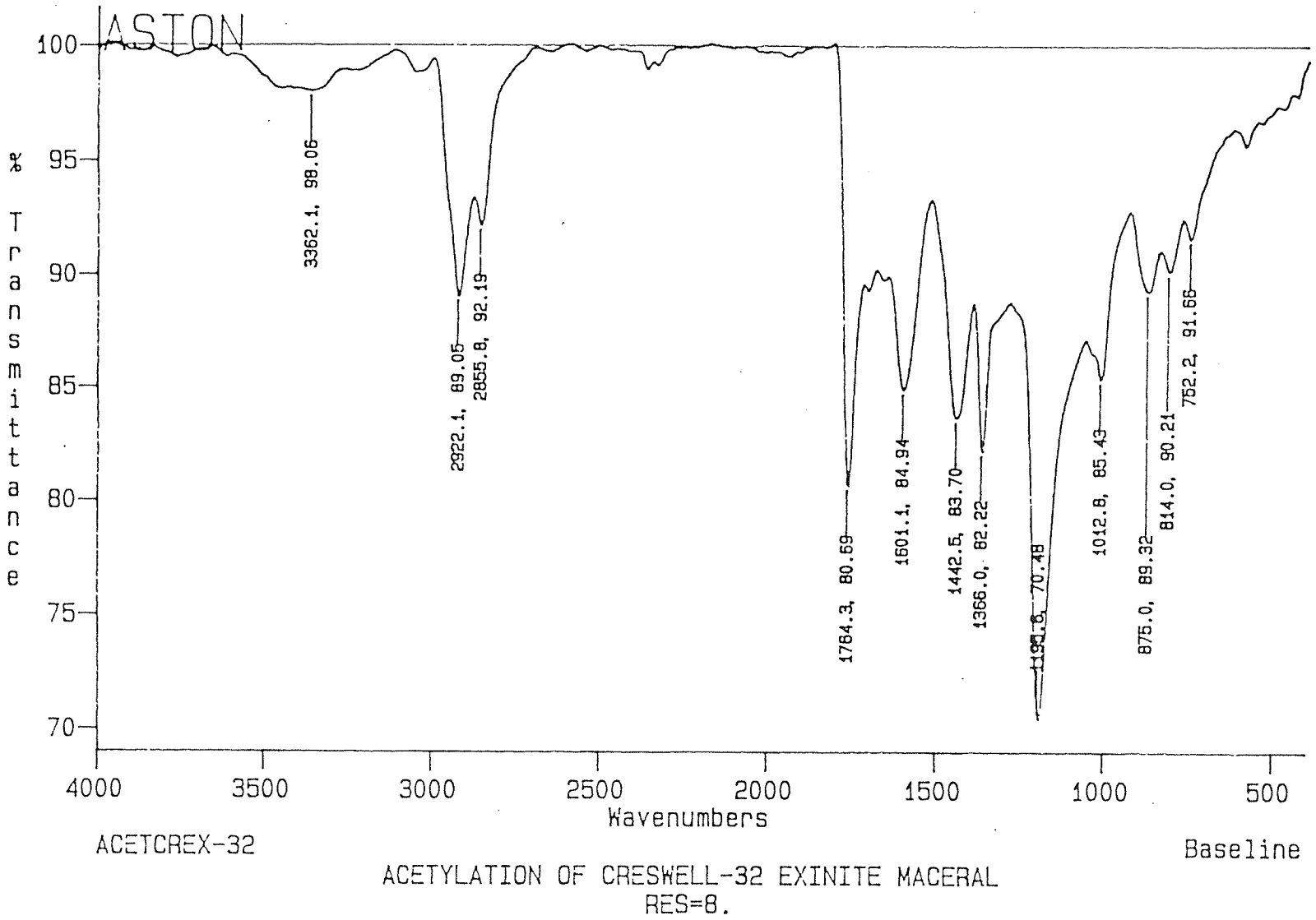

Fig4.25
IR of the acetylated Creswell exinite maceral

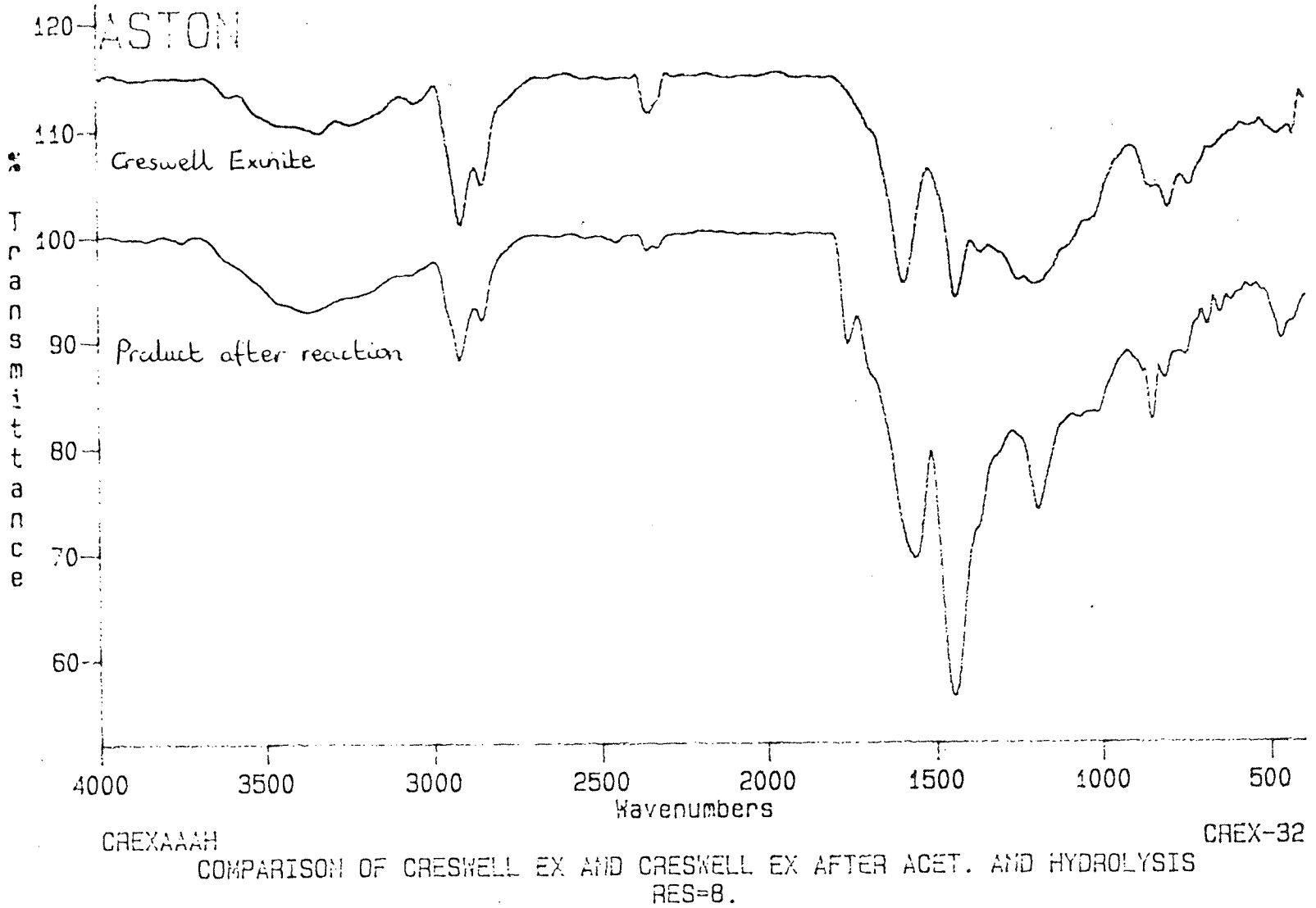

Fig4.26
IR comparison of Creswell exinite and the Creswell exinite after acetylation and hydrolysis

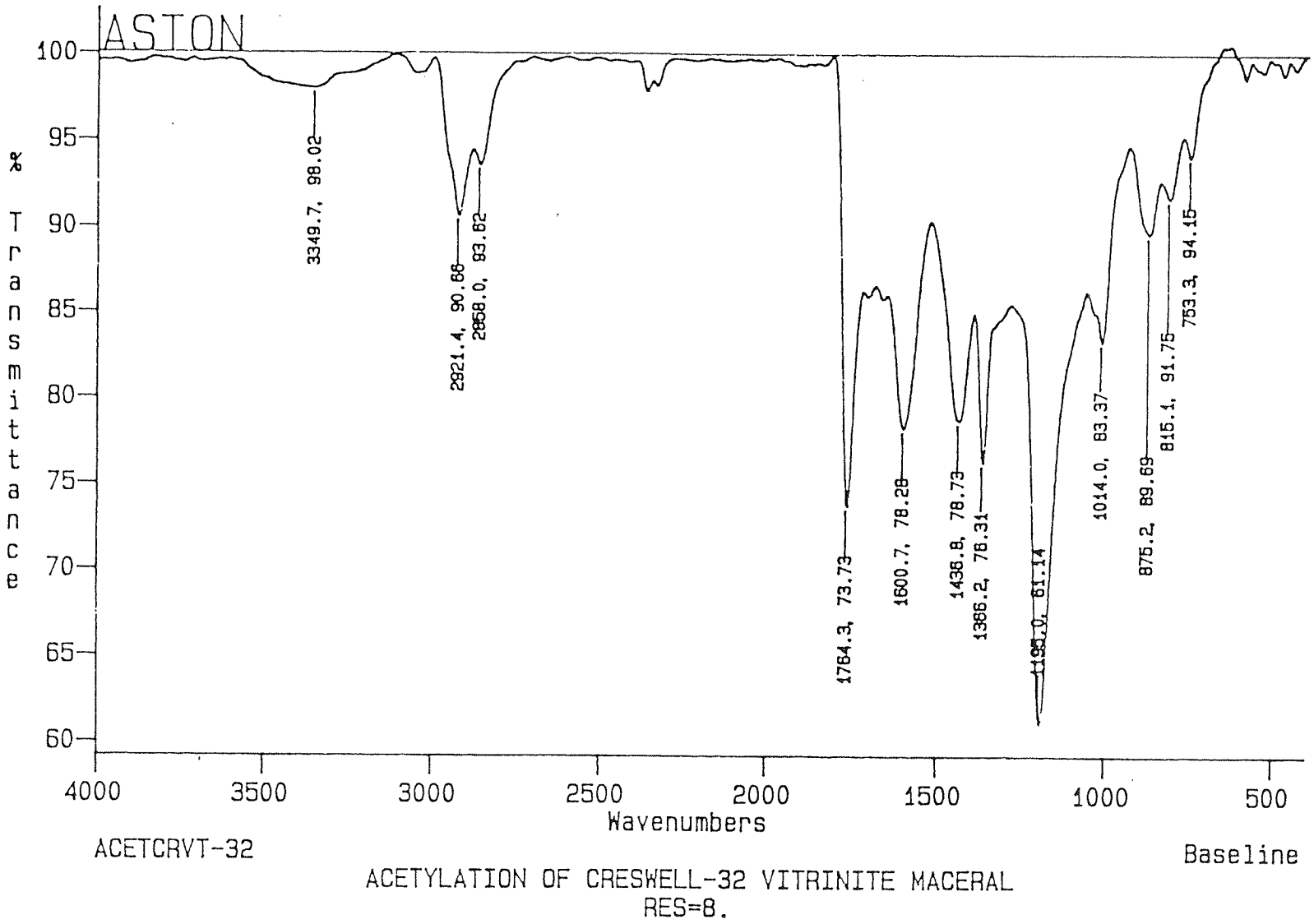

Fig4.27
IR of the acetylated Creswell vitrinite maceral

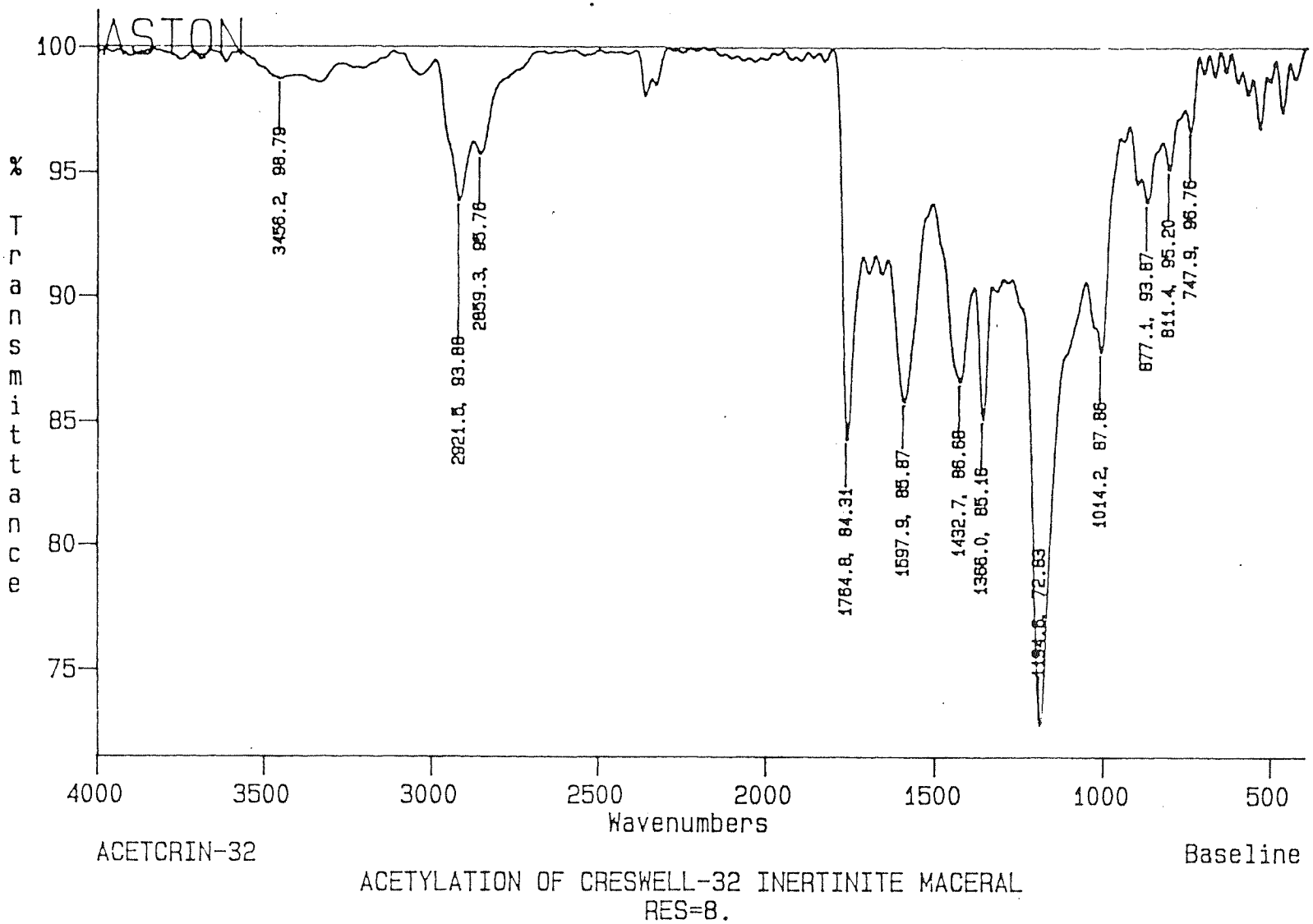

Fig4.28
IR of the acetylated Creswell inertinite maceral

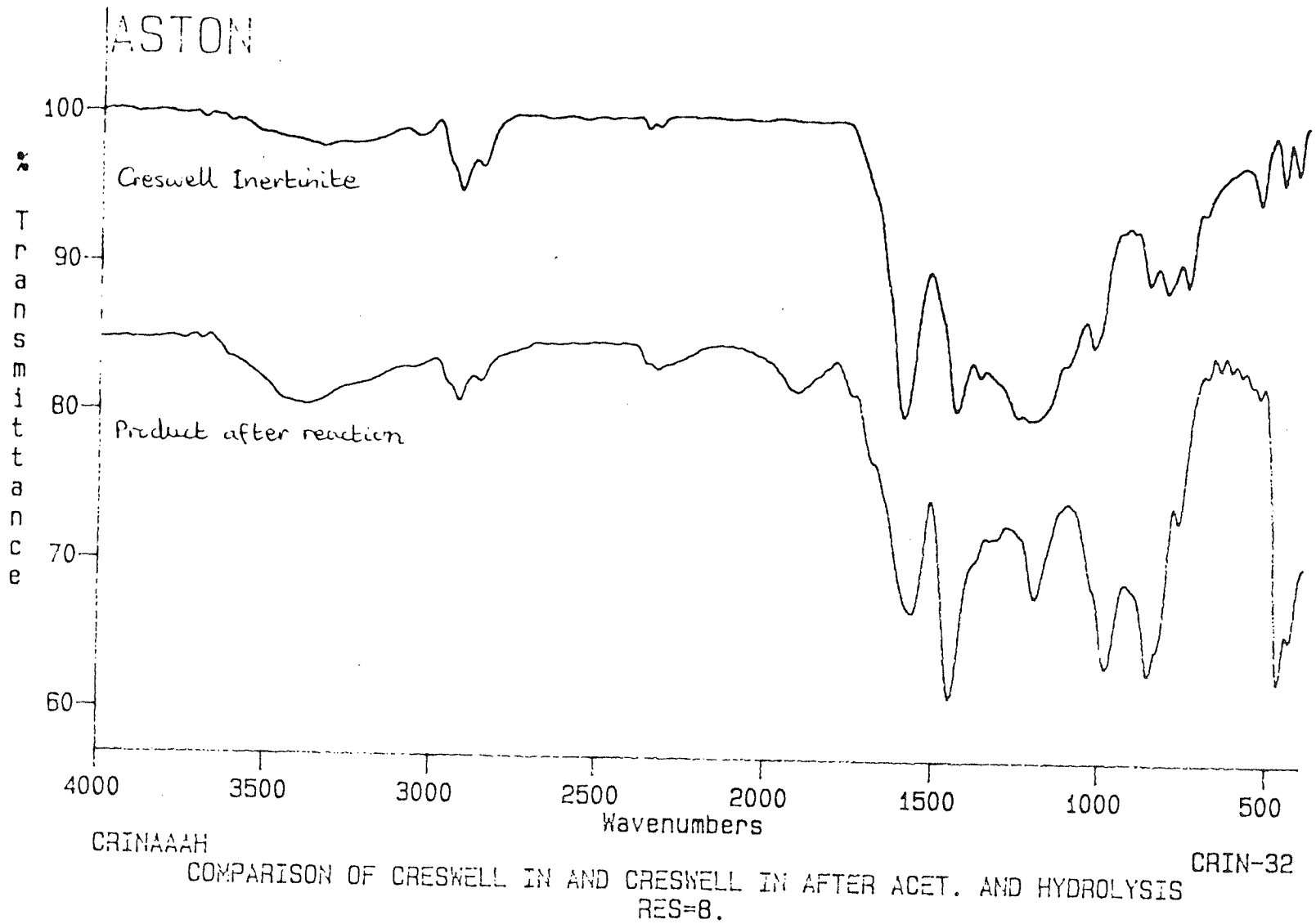

Fig4.29
IR comparison of the Creswell inertinite and the Creswell inertinite after acetylation and hydrolysis

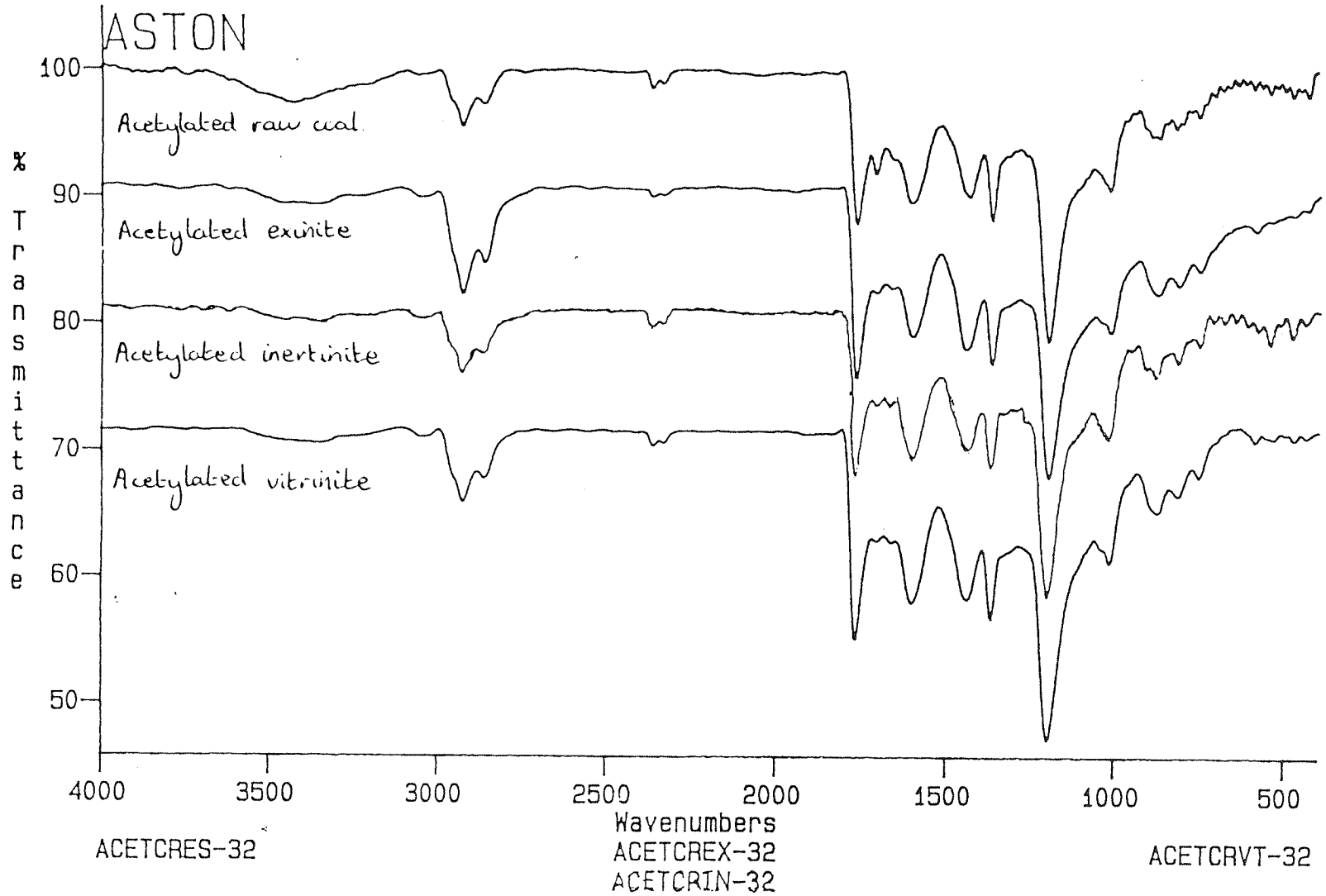

Fig4.30
IR of the acetylated Creswell macerals and the acetylated raw Creswell coal

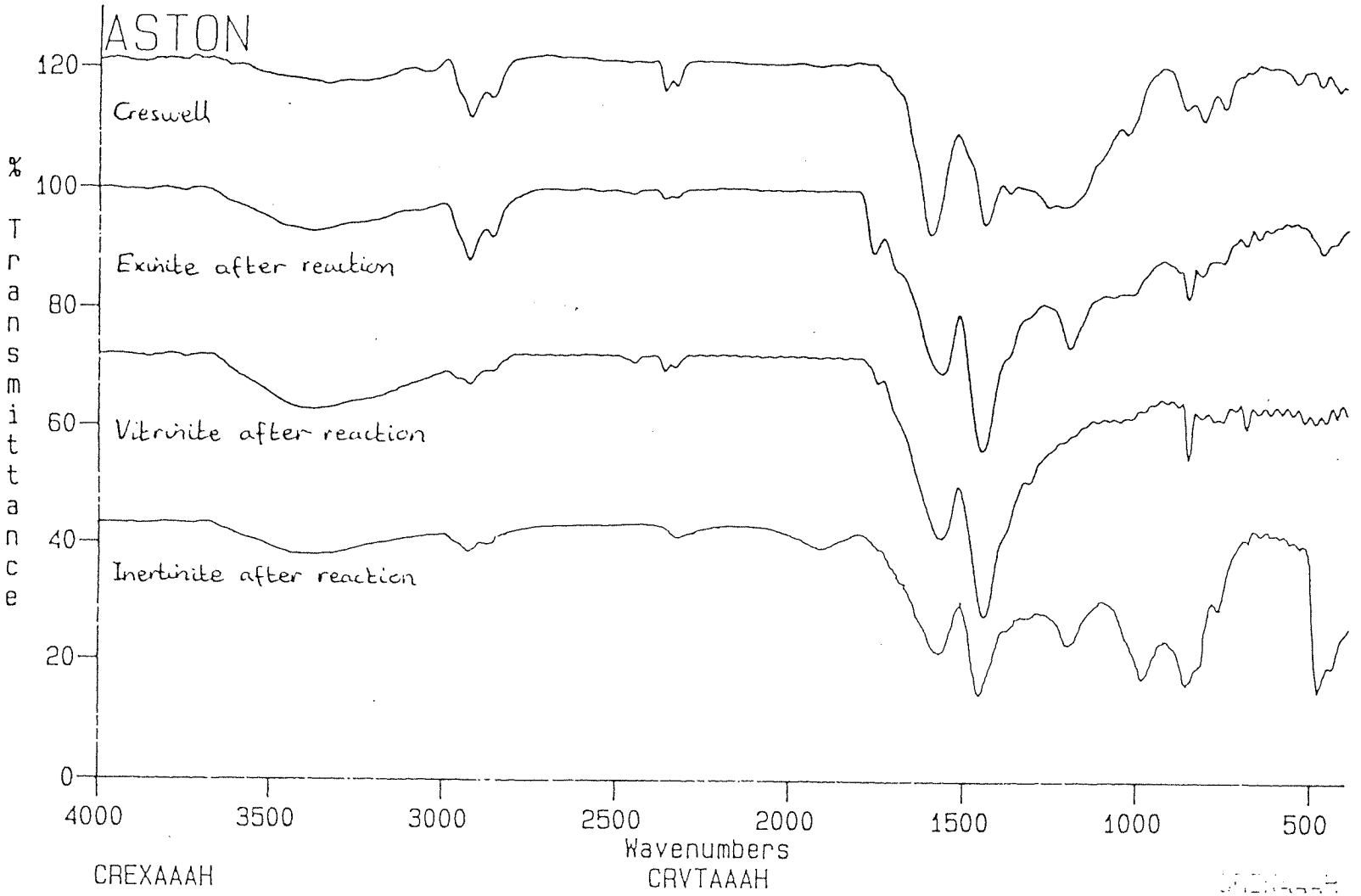

Fig4.31
IR of the Creswell macerals after acetylation and hydrolysis and the raw dried Creswell coal

Table 4.20

Calculation of the percentage O_{OH} / O_{total} for the Creswell coal macerals and the raw Creswell coal

Coal (Maceral)	Total titre (cm^3)	Acetyl content (A) m.equiv.g^{-1}	Hydroxyl content (H) m.equiv.g^{-1}	Calculated O_{dmmf} (%)	O_{dmmf} converted to m.equiv.g^{-1}	O_{OH} / O_{total} (%)
Creswell coal	1.51	1.4920	1.5918	5.6	3.5000	45
Creswell exinite	1.23	1.2079	1.2724	4.9	3.0625	42
Creswell vitrinite	3.88	3.8976	4.6605	8.2	5.1250	91
Creswell inertinite	2.28	2.2736	2.5136	7.6	4.7500	53

4.3.3 Acetylation of Cortonwood and Cortonwood macerals

It was attempted to acetylate the raw Cortonwood coal and the Cortonwood exinite, vitrinite and inertinite macerals. Table 4.21 gives some analytical data on the raw Cortonwood coal

Table 4.21 Analytical data for the raw Cortonwood coal (≤32 μm)

ANALYSIS	DATA	
Ultimate analysis (%)	Carbon (dmmf)[a]	87.2
	Hydrogen (dmmf)	5.6
	Oxygen (dmmf)	4.8
	Nitrogen (dmmf)	1.7
	Organic sulfur (db)[b]	0.60
	Sulfate sulfur (db)	0.02
	Pyritic sulfur (db)	0.36
Proximate analysis (%)	Moisture (ad)[c]	1.0
	Ash (ad)	2.2
	Volatile matter (ad)	34.7
	Fixed carbon (ad)	62.1

[a]dmmf = dry, mineral matter free
[b]db = dry basis
[c]ad = as analysed

The coal macerals were initially acetylated for 30 mins in the Sharp Carousel II microwave oven. Hydrolysis was carried out by refluxing with barium hydroxide solution for 24 hrs. Unfortunately the amount of acetic acid released on hydrolysis was very small in each case. Consequently it was decided to increase the microwave reaction time for acetylation to 2 hrs, after which the extent of acetylation was assessed by FT-IR analysis. It was found that, after this extended acetylation reaction time, a significant reaction had taken place - there was a reduction in the OH stretching band and the appearance of strong absorptions corresponding to the acetylation of the coal. Further testing involved reacting the Cortonwood macerals for 3 hrs in the microwave oven during the acetylation stage. Examination by FT-IR, however, showed that no further significant reaction had occurred. From these results it was decided that 2 hrs was an optimum reaction time for the acetylation of the Cortonwood macerals in the microwave oven. The hydrolysis step involved refluxing the acetylated Cortonwood macerals with barium hydroxide solution for 24 hrs (It was found that refluxing for more than 24 hrs did not result in the release of significantly greater amounts of acetic acid being liberated). Table 4.22 shows the titration values obtained for the acetylation of the Cortonwood macerals (2 hr reaction time in the microwave oven and 24 hrs refluxing with barium hydroxide solution). The results in Table 4.22 are displayed graphically in figs 4.32 - 4.34.

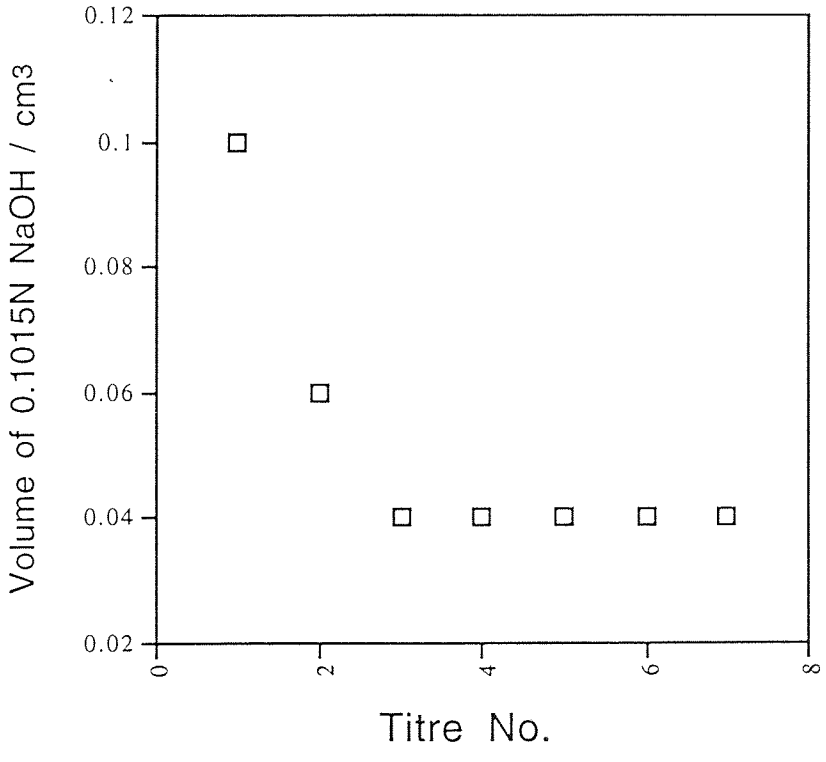

Fig4.32 Plot of the titration of liberated acetic acid with 0.1015N NaOH for the Cortonwood exinite maceral

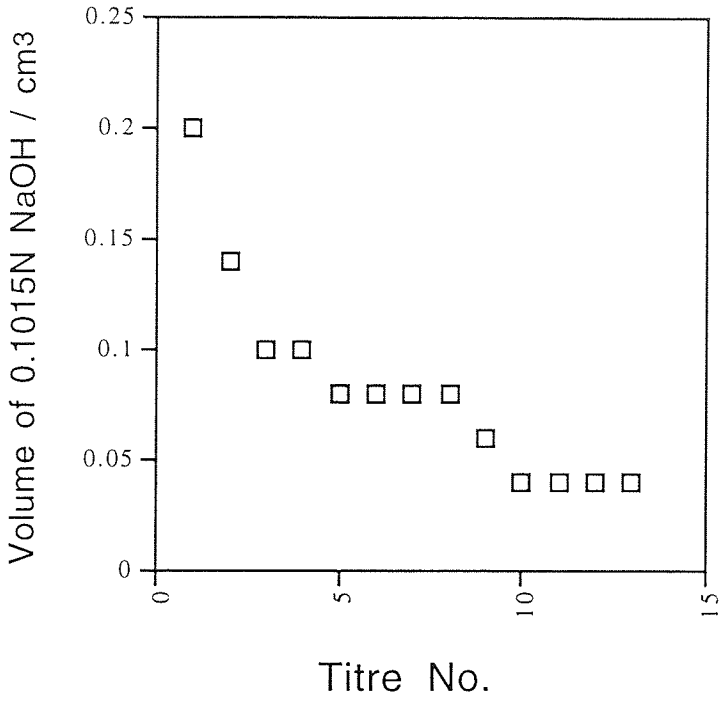

Fig4.33

Plot of the titration of liberated acetic acid with 0.1015N NaOH for the Cortonwood vitrinite maceral

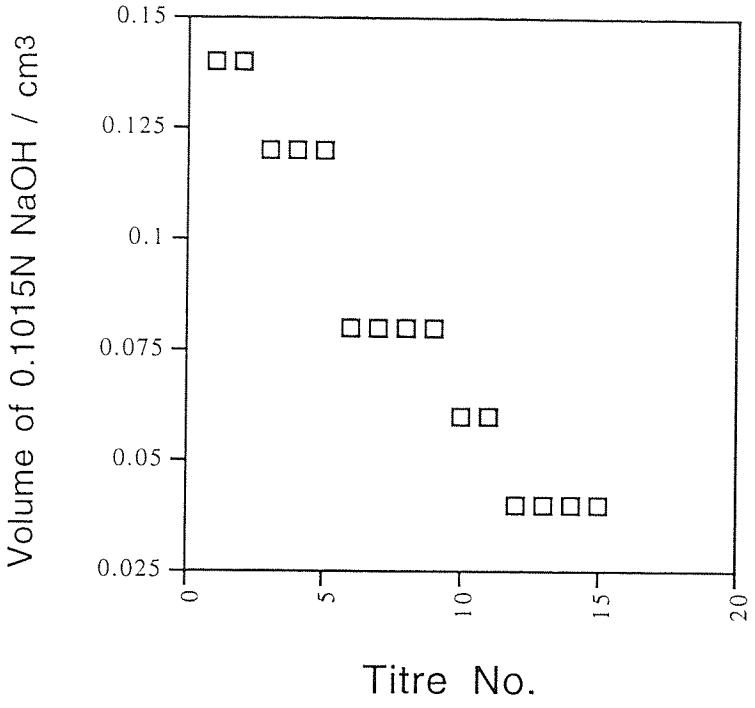

Fig4.34

Plot of the titration of liberated acetic acid with 0.1015N NaOH for the Cortonwood inertinite maceral

Total titration values of 0.16, 0.92 and 1.08 cm^3 were obtained for the Cortonwood exinite, vitrinite and inertinite macerals respectively.

Table 4.22 Titration results for the Cortonwood coal macerals

Titre No.	1	2	3	4	5	6	7	8	9	10	11	12	13	14
Exinite	0.10	0.06	0.04	0.04	0.04	-	-	-	-	-	-	-	-	-
Vitrinite	0.20	0.14	0.10	0.10	0.08	0.08	0.08	0.08	0.06	0.04	0.04	0.04	-	-
Inertinite	0.14	0.14	0.12	0.12	0.12	0.08	0.08	0.08	0.08	0.06	0.06	0.04	0.04	0.04

Next, it was attempted to acetylate the raw Cortonwood coal. The coal was acetylated for 2 hrs in the microwave oven and refluxed for 24 hrs with barium hydroxide solution, but only 0.06 cm^3 of acetic acid was found to be liberated. An attempt was made to try and improve on this figure by increasing the reflux time, first to 2 days and then to 3 days, but without success. The reaction time for acetylation was then increased to 3 hrs using a "high" setting on the microwave oven followed by refluxing for 3 days, but still there was very little reaction and only a very small amount of acetic acid was liberated (0.06 - 0.08 cm^3). Fig 4.35 shows the IR spectrum of the raw Cortonwood coal. The absorption due to hydroxyl functionality is clearly visible at 3406 cm^{-1}. Fig 4.36 shows the IR spectrum of the acetylated Cortonwood raw coal after a reaction time of 2 hrs in the microwave oven. The OH band is still clearly visible at 3440 cm^{-1}, but some acetylation appears to have taken place, as indicated by the bands at 1761 cm^{-1} (C=O), 1195 cm^{-1} (C-O) and 1365 cm^{-1} (C-CH_3 deformations). Fig 4.37 shows a comparison of the raw Cortonwood coal and the acetylated Cortonwood raw coal (2 hr reaction time). A further comparison of the acetylation of the raw Cortonwood coal after 2 hrs and 3 hrs in the microwave oven can be seen in Fig 4.38. The plot shows that the extent of reaction is essentially similar. Later in the study, a new microwave oven was acquired (the MES-1000). It was decided to attempt the acetylation of the raw Cortonwood coal using this new equipment, as greater control of temperature and pressure parameters was now possible. The raw Cortonwood coal was acetylated for 2 hrs in the MES-1000 microwave oven with maximum values of 200°C and 180 psi set for the containment vessel. Fig 4.39 shows the IR spectrum of the acetylated Cortonwood coal obtained by this method. In this instance, there is a much larger reduction in the intensity of the OH band at 3444 cm^{-1} indicating that a significant acetylation reaction has occurred. Because the containment vessel was constrained by an Ultem polyetherimide sleeve in the MES-1000 to help stop deformations at high pressures, it was decided to also attempt the hydrolysis step in the MES-1000. Unfortunately, the barium hydroxide solution chemically weakened the pyrex thermowell, containing the fibre-optic probe, after only 5 mins of reaction. This caused the thermowell to fracture and be ejected from the containment vessel. Because of the large expense which would have been incurred had the fibre-optic probe been damaged, it was decided not to attempt this method of hydrolysis again and revert back to the bench top hydrolysis method.

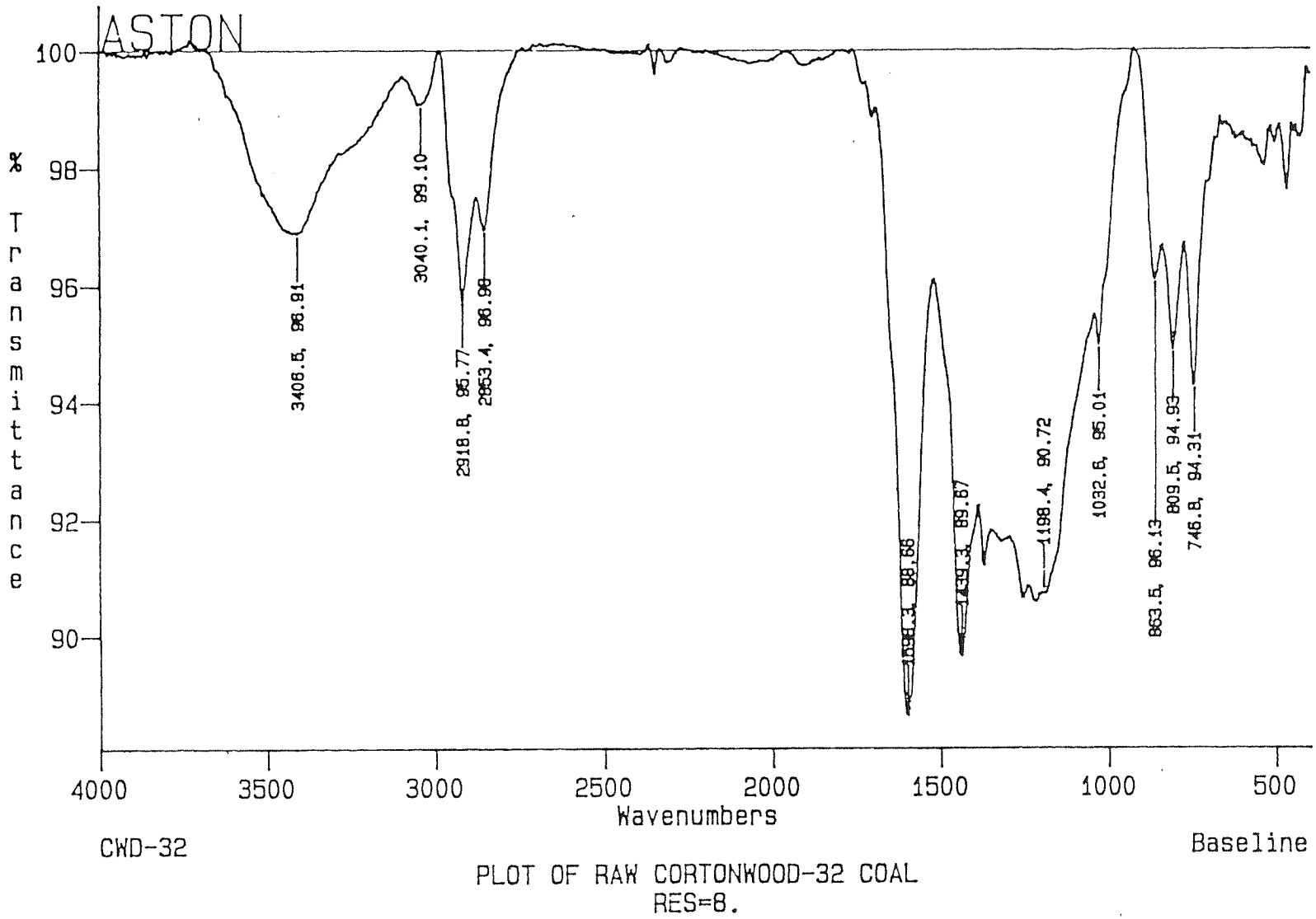

Fig4.35
IR of the raw Cortonwood coal

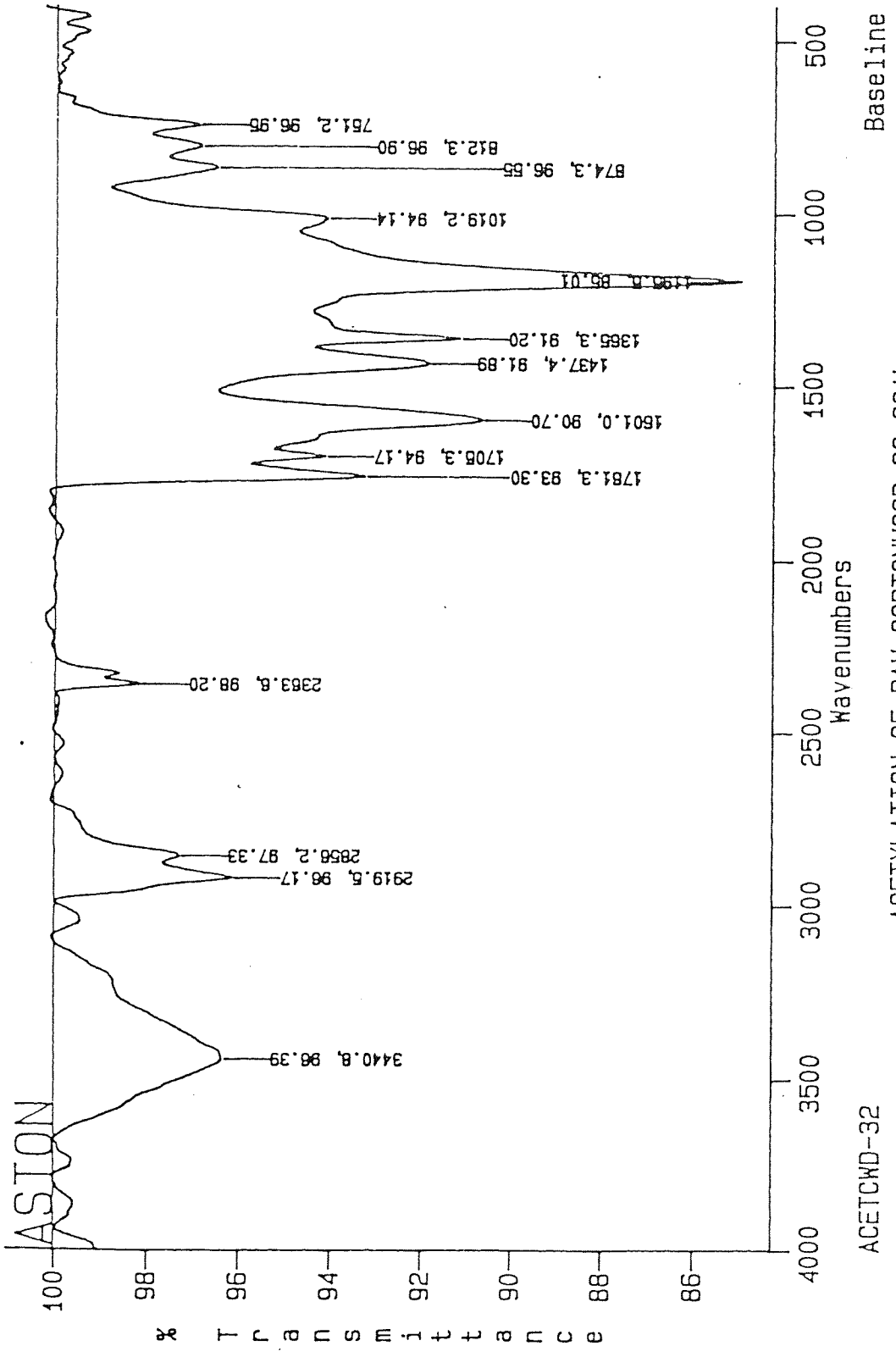

Fig4.36
IR of the acetylated raw Cortonwood coal

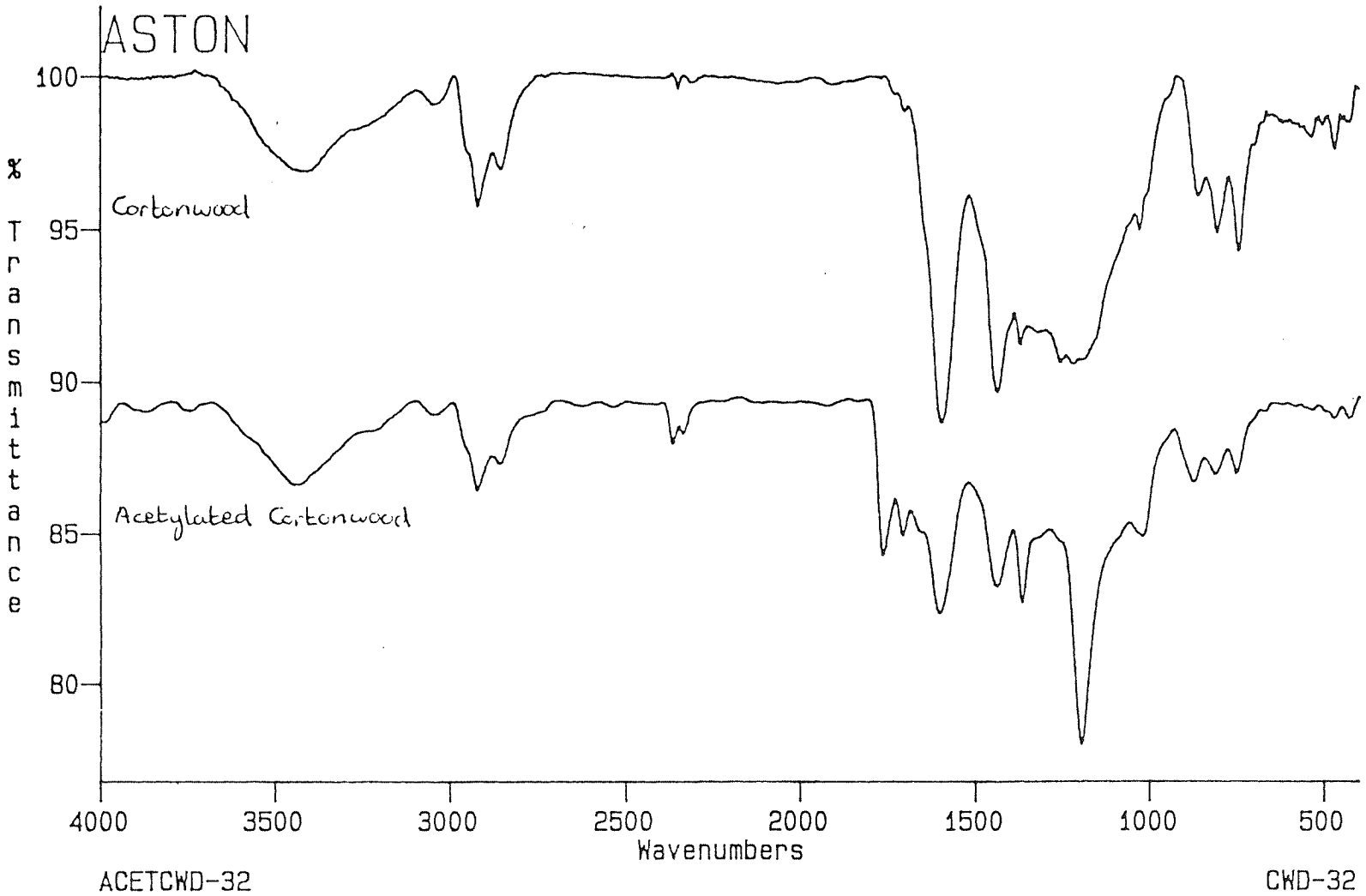

Fig4.37
IR comparison of the raw Cortonwood coal and the acetylated Cortonwood coal

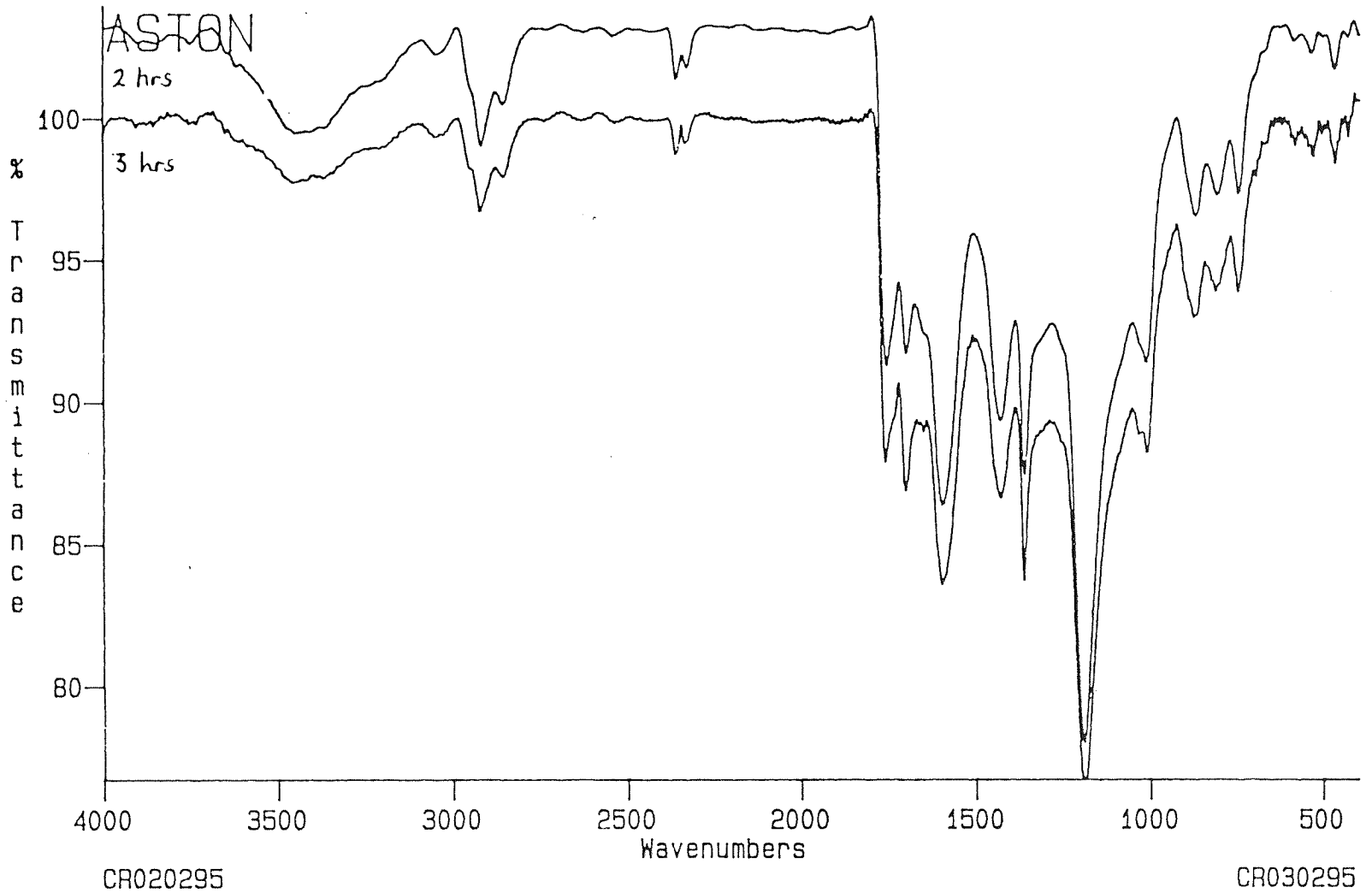

Fig4.38
IR of the acetylated raw Cortonwood coal after 2 hrs and 3 hrs mw heating

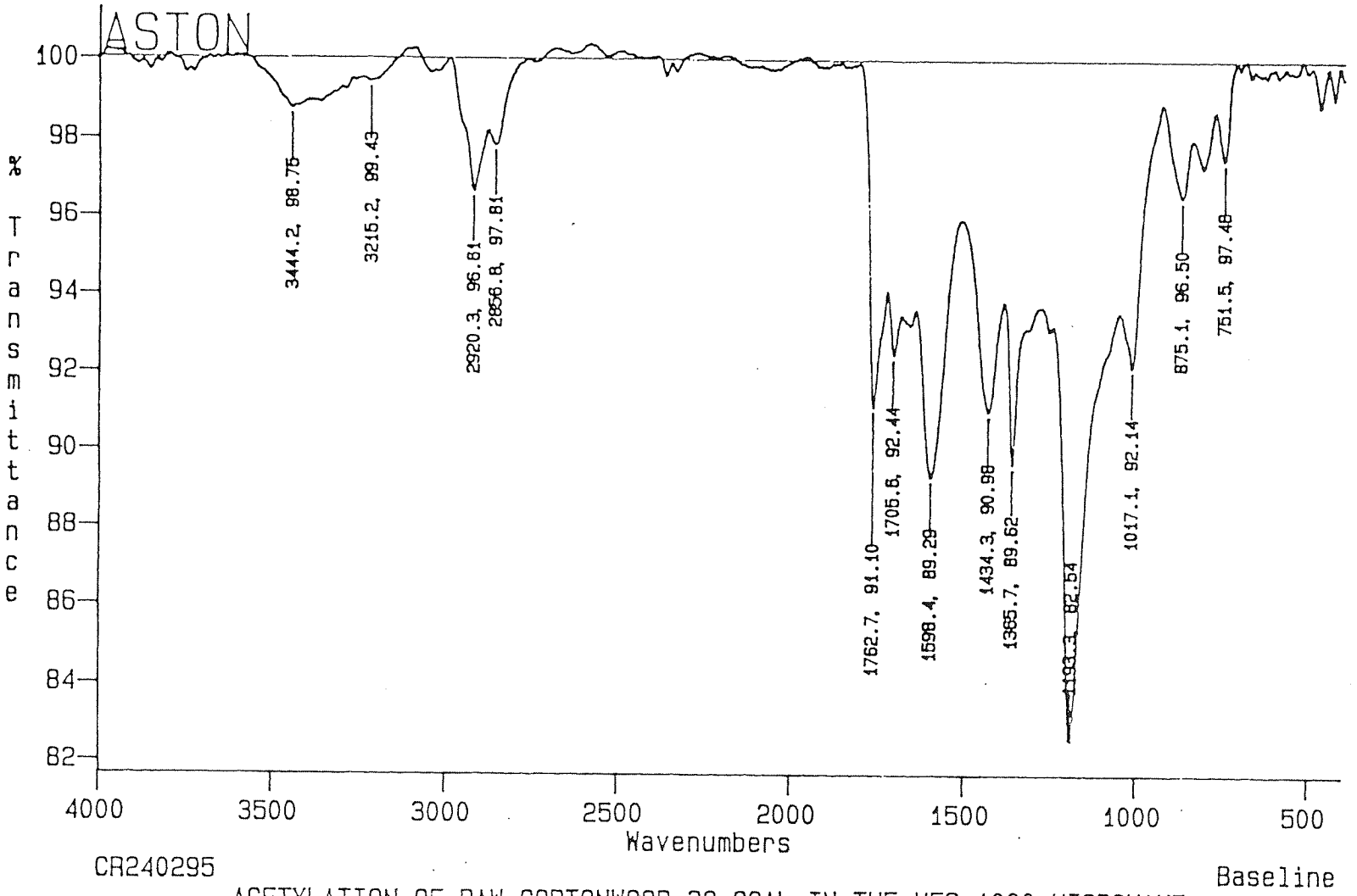

Fig4.39
IR of the acetylated raw Cortonwood coal using the MES-1000 mw oven

The acetylated Cortonwood coal (from the MES-1000 reaction - 2 hr reaction time) was refluxed for 48, 72 and 96 hrs with barium hydroxide solution in separate reactions, but all failed to liberate the acetic acid to any significant extent.

Fig 4.40 shows the IR spectrum of the acetylated Cortonwood exinite coal maceral. There is a significant reduction in the OH band at approximately 3400 cm^{-1} and the appearance of absorptions corresponding to the acetyl group at 1760 cm^{-1} (C=O), 1196 cm^{-1} (C-O) and 1366 cm^{-1} ($C-CH_3$). Fig 4.41 shows the IR spectrum of the acetylated Cortonwood vitrinite maceral. Again, there is a major reduction in intensity of the OH band and the presence of characteristic acetyl bands. Similarly for fig 4.42 - the acetylated Cortonwood inertinite maceral. Fig 4.43 shows an IR comparison of the acetylated Cortonwood raw coal and the acetylated Cortonwood macerals (all coals acetylated for 2 hrs in the Sharp Carousel II microwave oven).

From the titration values obtained for the Cortonwood macerals, the percentage O_{OH} / O_{total} was calculated. The calculations are shown in Table 4.23.

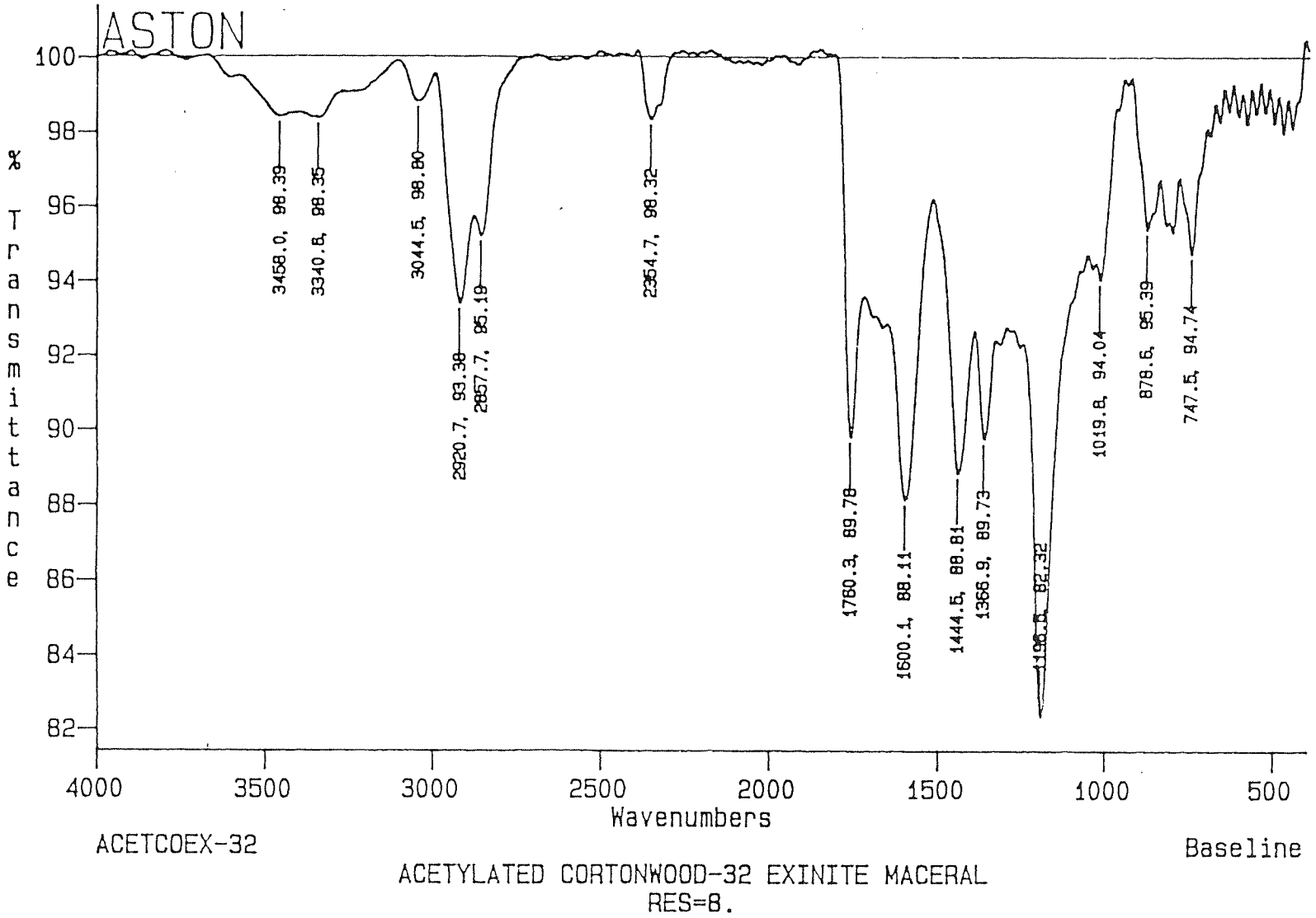

Fig4.40
IR of the acetylated Cortonwood exinite maceral

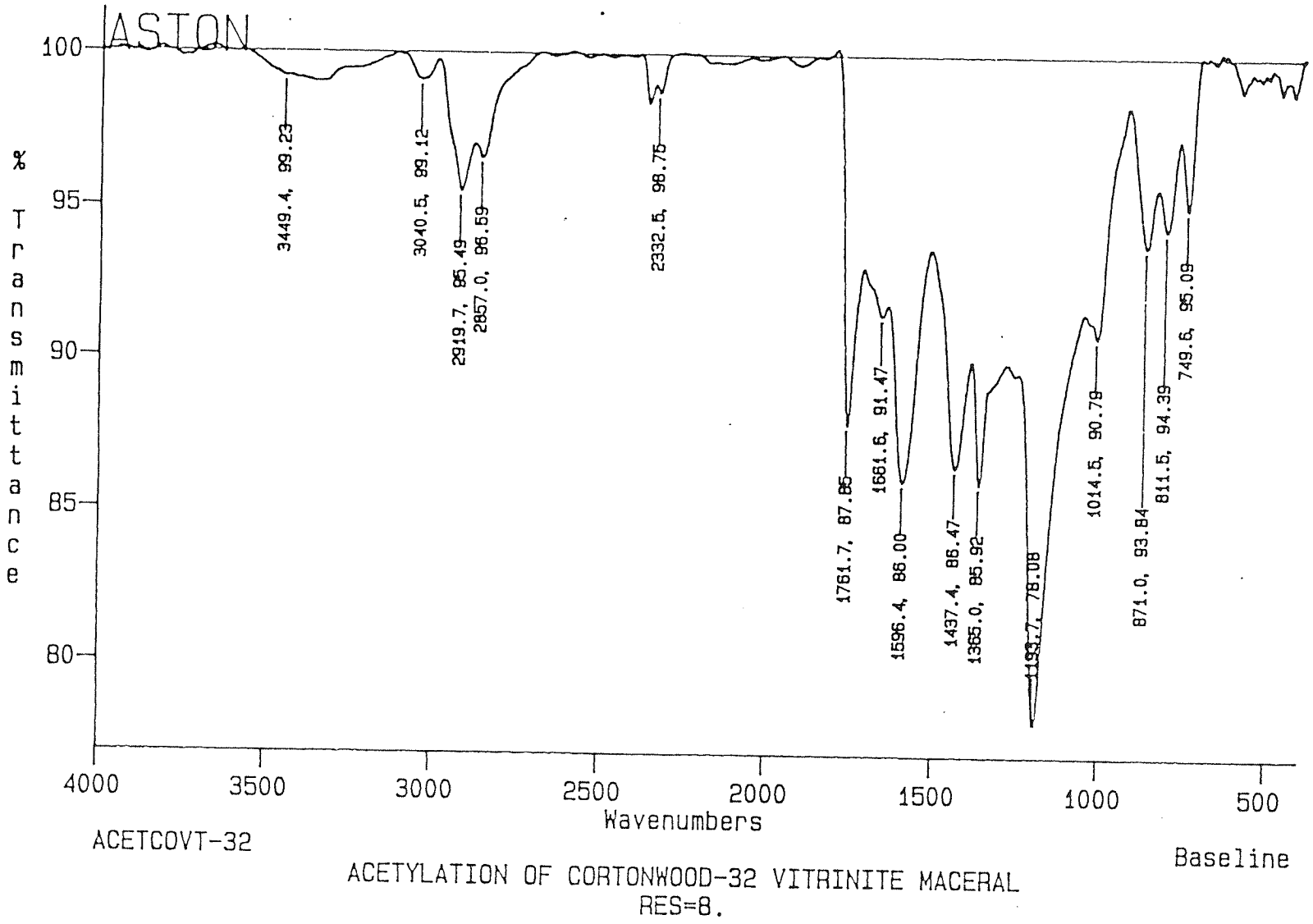

Fig4.41
IR of the acetylated Cortonwood vitrinite maceral

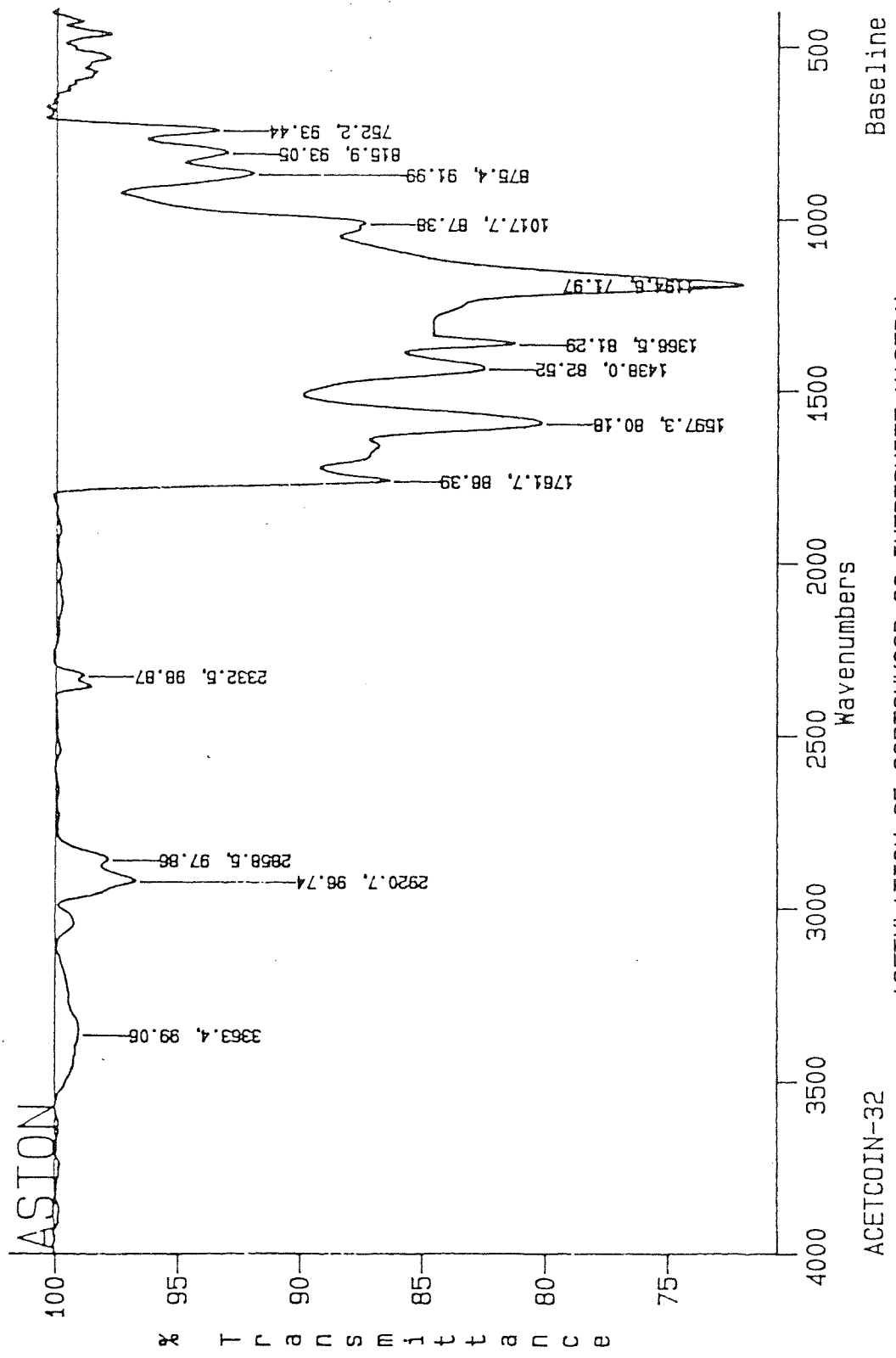

Fig4.42
IR of the acetylated Cortonwood inertinite maceral

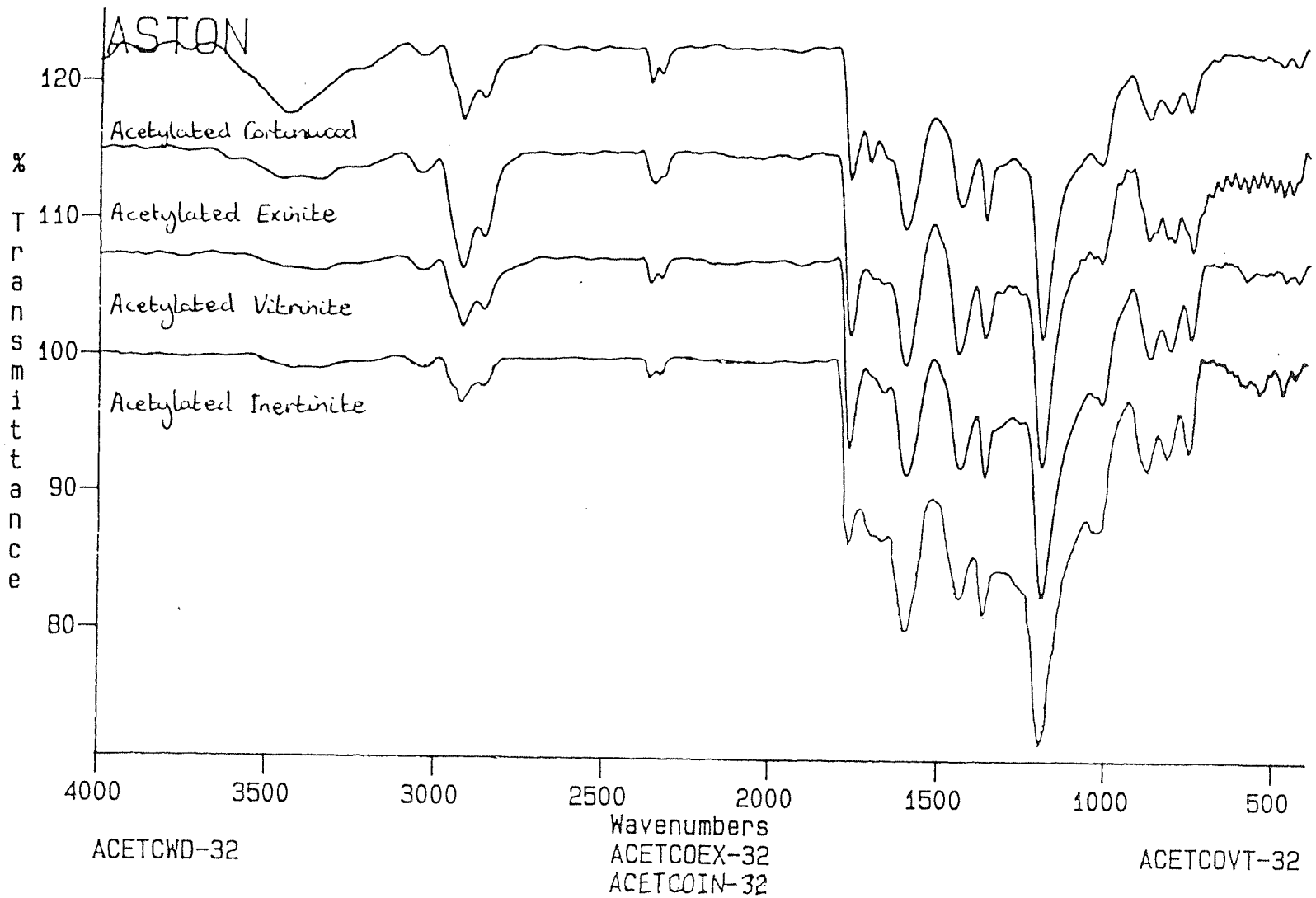

Fig4.43
IR comparison of the acetylated Cortonwood macerals
and the acetylated raw Cortonwood coal

Table 4.23 Calculation of the percentage O_{OH} / O_{total} for the Cortonwood coal macerals

Coal Maceral	Total titre (cm^3)	Acetyl content (A) m.equiv.g^{-1}	Hydroxyl content (H) m.equiv.g^{-1}	Calculated O_{dmmf} (%)	O_{dmmf} converted to m.equiv.g^{-1}	O_{OH} / O_{total} (%)
Cortonwood exinite	0.16	0.1218	0.1224	4.6	2.8750	04
Cortonwood vitrinite	0.92	0.8932	0.9280	4.2	2.6690	35
Cortonwood inertinite	1.08	1.0556	1.1046	6.2	3.8750	29

Acetylation of the phenol-formaldehyde resin was also attempted in the MES-1000 microwave oven. The resin (0.5g) was acetylated for a total reaction time of 4 hrs and 5 mins using an acetic anhydride / pyridine mixture. Table 4.24 shows the reaction parameters for the reaction.

Table 4.24
MES-1000 reaction parameters for the acetylation of the phenol-formaldehyde resin

STAGE	1	2	3	4	5
Power (%)	40	20	20	20	20
Pressure (psi)	180	180	180	180	180
Run time (mins)	05	60	60	60	60
Temperature (°C)	180	180	180	180	180

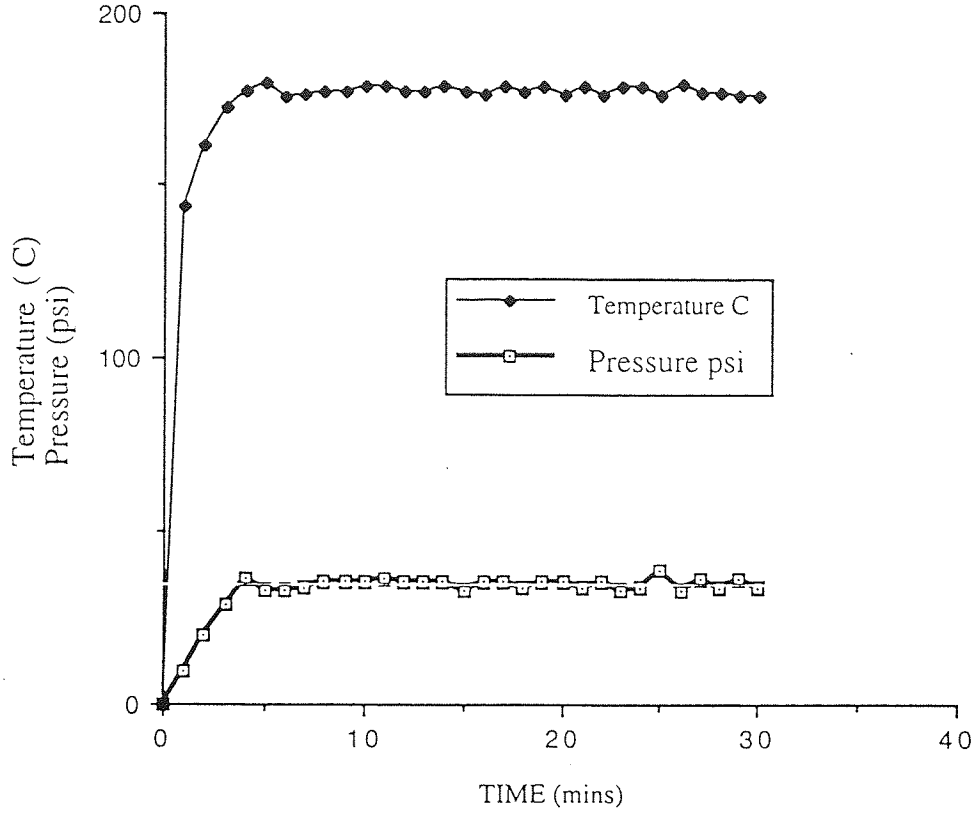

Fig4.44

Temperature and pressure profile (for the first 30 mins) for the acetylation of the phenol-formaldehyde resin

Fig 4.45 shows the IR spectrum of the phenol-formaldehyde resin and fig 4.46 shows the IR of the acetylated resin. There is a considerable reduction in the OH band and absorptions which can be assigned to acetyl bands are clearly present. Fig 4.47 shows an IR comparison between the resin and the acetylated resin - the plot shows that some reaction has indeed taken place. The acetylated resin was refluxed with barium hydroxide solution for 48 hrs, acidified with conc. H_3PO_4 and titrated with 0.1015N NaOH. The titration showed that no acetic acid had been liberated, yet the IR spectra (fig 4.48) shows that the acetylated resin has effectively reverted back to the original resin after hydrolysis. A possible explanation for this anomaly is that the acetic acid was released fairly rapidly into solution during hydrolysis and, because the mixture was left to hydrolyse for so long, the liberated acetic acid may have evaporated via the top of the condenser.

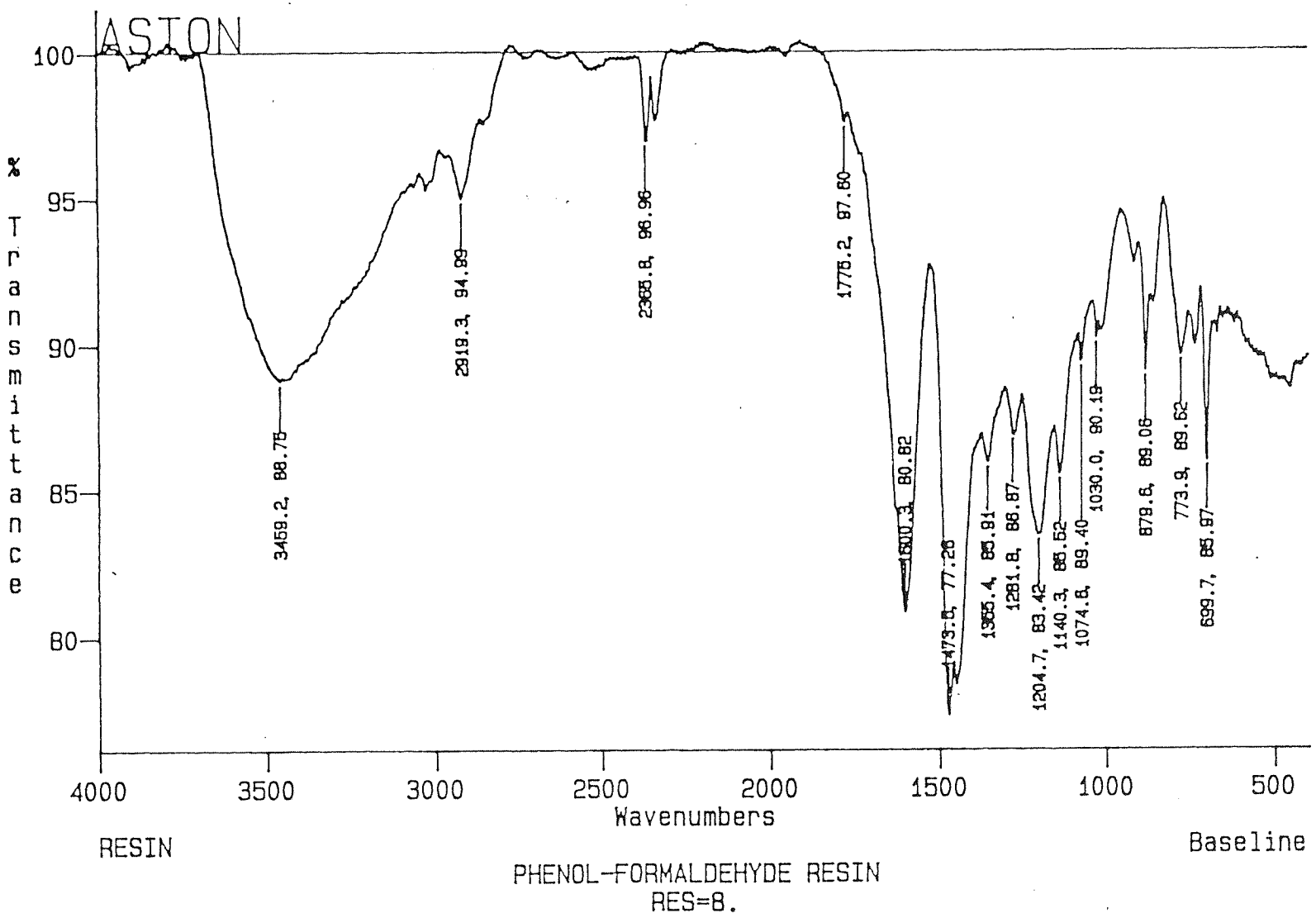

Fig4.45
IR of the phenol-formaldehyde resin

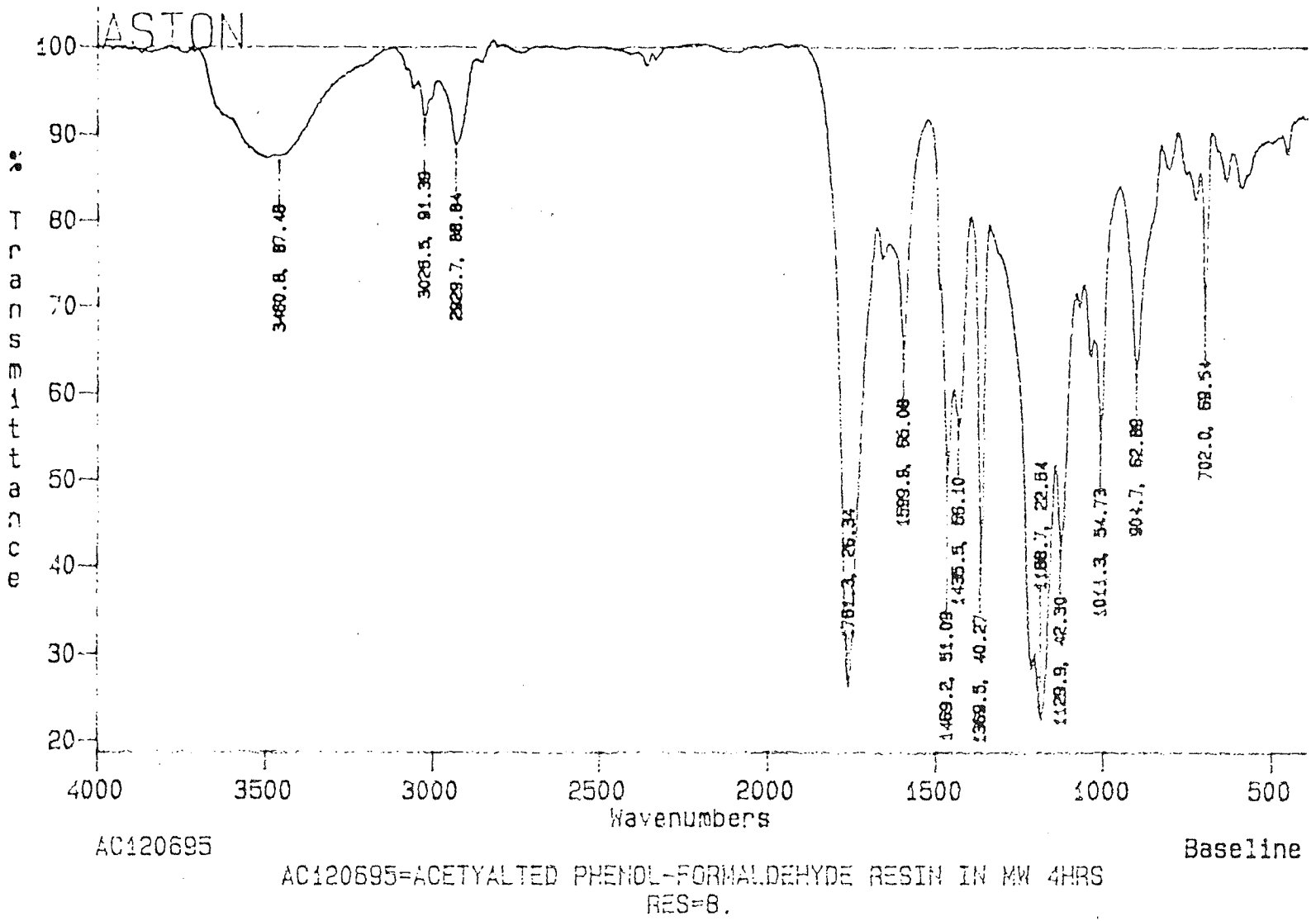

Fig4.46
IR of the acetylated phenol-formaldehyde resin after 4 hrs mw heating

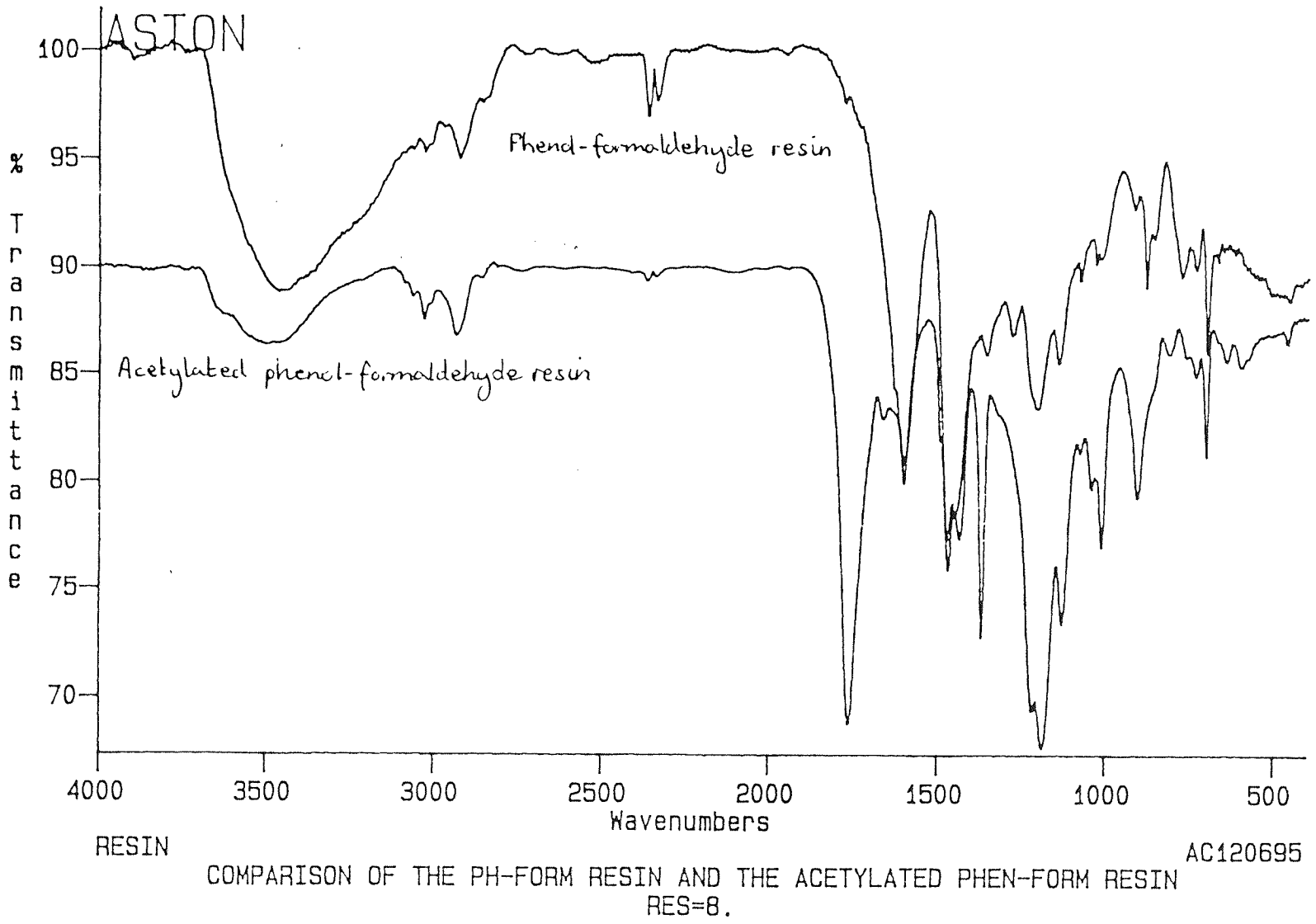

Fig4.47
IR comparison of the phenol-formaldehyde resin and the acetylated phenol-formaldehyde resin

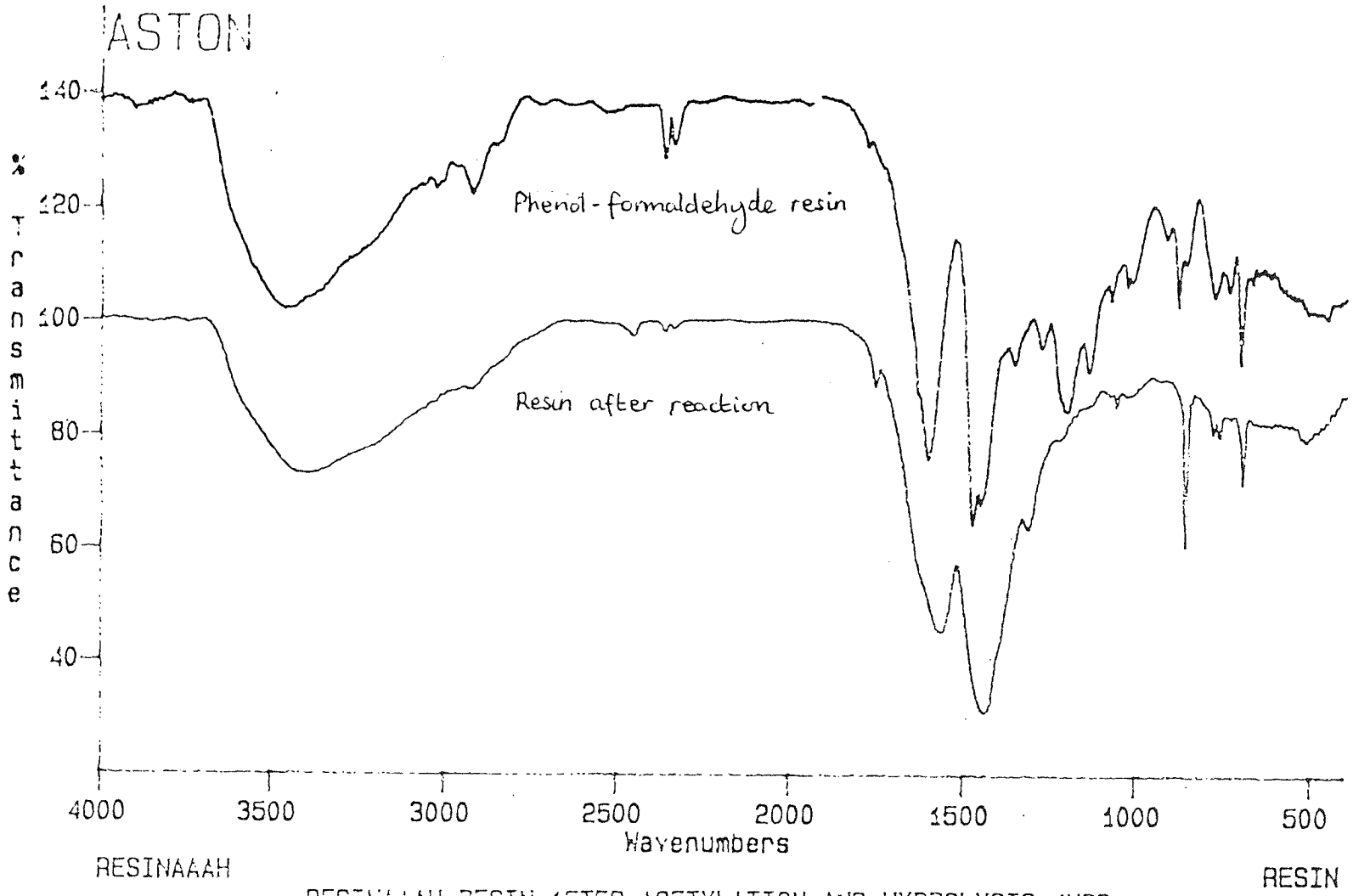

Fig4.48
IR of the phenol-formaldehyde resin after acetylation and hydrolysis

4.3.4 General conclusions

The Creswell coal showed very good separation of its macerals. In each case the maceral concentrate was found to predominate over the other 2 maceral groups. It is reasonable to assume that any reactions which take place using these maceral concentrates will be influenced primarily by the dominant maceral group. The calculated oxygen (dry, mineral matter free) values show that the Creswell exinite maceral contains the least oxygen, then the inertinite and finally, the vitrinite maceral group contains the most. The reason for the low value for exinite lies in its origins - the exinite maceral is derived mainly from lignin and waxy plant material. This waxy plant material is made up of mainly straight-chain aliphatic compounds linked by ester groups, with lesser amounts of aliphatic alcohol and carboxylic acid groupings (although these are rare in middle rank coals). It is also due to this type of structure that the exinite maceral group has the highest H / C ratio compared to the other two maceral groups. The exinite maceral gave an O_{OH} / O_{total} value of 42% indicating that almost two-fifths of the oxygen is present in the form of hydroxyl functionality. With the inertinite maceral group, this value is increased to just over half the total oxygen content and almost all the oxygen present in the vitrinite component is in the form of hydroxyl groups. The bulk coal gave an O_{OH} / O_{total} value of 45% after only 30 mins reaction time (acetylation) in the domestic microwave oven. These results compare favourably with work carried out by Bailey et al[41]. Bailey and his co-workers obtained values of 35% (after 10 hrs conventional heating) and 65% (after a reaction time of 2 hrs in the microwave oven) for the percentage O_{OH} / O_{total} for Creswell coal (using the same reagents). The highest value Bailey obtained for the percentage O_{OH} / O_{total} of Creswell coal was 90% using the ketene reagent for a reaction time of 23 hrs, whereas we have managed to obtain a value of 91% O_{OH} / O_{total} for the Creswell vitrinite (which makes up the bulk of the Creswell coal) after only 30 mins microwave heating in a conventional microwave oven at a medium-high setting.

The Cortonwood coal showed excellent separations for the exinite and inertinite macerals. If we consider the Cortonwood raw coal as the Cortonwood vitrinite maceral, we see that the exinite maceral again has the lowest oxygen content, only in this instance the inertinite maceral group has the highest oxygen content (on a dmmf basis). The exinite maceral gave an O_{OH} / O_{total} value of only 4% indicating that very little of the oxygen present is in the form of hydroxyl functionality. It is therefore reasonable to assume that the bulk of the oxygen in this maceral is in the form of ester and ether linkages. The O_{OH} / O_{total} value for the inertinite maceral indicates that almost one-third of the oxygen in the maceral is present as hydroxyl functionality.

The Cortonwood vitrinite maceral (which gave a poor maceral separation) gave an O_{OH} / O_{total} value of 35% - the concentration of vitrinite in this maceral is relatively small and it would be expected that the other two maceral groups (present in significant amounts) had some influence during reaction. It was partly due to this reason that it was attempted to acetylate the raw Cortonwood coal (containing a higher proportion of the vitrinite maceral group). As mentioned earlier, the acetylation of the raw Cortonwood coal was eventually possible, but the subsequent hydrolysis step proved very difficult to implement - even after 96 hrs refluxing there was no significant hydrolysis. Bailey carried out the hydrolysis in the microwave oven (reacting the acetylated coal for about 1 hr with barium hydroxide solution), but when we tried to repeat this procedure, superheating of the reagents resulted in venting of the reagent or damage to the apparatus. It may be concluded that the hydrolysis of Cortonwood coal is a very slow process, probably due to Cortonwood having a greater steric demand compared to the Creswell coal (see chapter 3). Consequently prolonged reaction times are required when carrying out the hydrolysis step via refluxing on the bench top. Bailey required 3 hrs for complete microwave hydrolysis of the Cortonwood coal and obtained a value of 50% O_{OH} / O_{total}. Unfortunately this approach is not viable in our case.

FT-IR spectroscopy has proved itself to be a potentially powerful technique for studying the chemical transformations undergone by coals and coal macerals during reaction. In this study it has been used to rapidly assess the extent of acetylation - derivatisation leads to a reduction in the vibrations due to OH and gives rise to bands due to acetate groups. The opposite is true after hydrolysis of the acetylated sample. Although there is a reduction in the OH band intensity after derivatisation, the OH absorption does not disappear completely. The residual absorption remaining can be attributed to traces of moisture and groups, such as NH, which absorb in the same region.

The use of microwave heating greatly enhances acetylation reactions over conventional bench top methods. Unfortunately this technique was not able to be successfully implemented for the hydrolysis stage of the reaction, which needed to be carried out via reflux and still required substantial experimental time. After acetylation of the coals and coal macerals, the efficiency of microwave heating in the domestic microwave cavity was again tested by heating a 100 cm^3 sample of distilled water, placed on the centre of the turntable, for 1 min (on a medium-high setting) and measuring the initial and final temperature of the distilled water. It was found that the temperature rise had fallen by approximately 15°C compared to the values obtained when tested 7 months earlier.

This has serious implications if reaction times are to be compared over a prolonged period of time. We may conclude that the magnetron in the domestic microwave oven tends to "run down" and lose power with continued use. This is one advantage of using the MES-1000 microwave system, in which the magnetron is built to higher specifications and has a higher wear tolerance. There is also the added advantage that temperature and pressure parameters can be accurately controlled with the MES-1000. Consequently all future microwave experiments were carried out in the MES-1000 microwave system.

SILYLATION

5.1 INTRODUCTION

5.1.1 General Introduction

Silylation involves the introduction of a ^{29}Si magnetic label into the coal via selective reaction with the hydroxyl functional groups. The ^{29}Si is commonly incorporated in the form of trialkylsilyl (usually trimethylsilyl) derivatives followed by quantitative analysis using ^{29}Si MASNMR. The trimethylsilyl ethers and trimethylsilyl esters (if carboxylic functional groups are present) obtained via derivatisation are thermally stable and resistant to oxidation. The starting product may also be recovered from the ether / ester by hydrolysis. FT-IR has been shown to be a useful technique to subjectively follow the extent of silylation.

5.1.2 Literature review

Much of the early work on the silylation of coals was carried out by S. Friedman et al[28], 1961. Friedman and his co-workers developed a new method for the determination of hydroxyl groups in coal based on the formation of trimethylsilyl ethers [$ROSi(CH_3)_3$]. Initially reactions were carried out on aliphatic alcohols using hexamethyldisilazane (HMDS) :

$$2\,ROH + (CH_3)_3SiNHSi(CH_3)_3 \rightarrow 2\,ROSi(CH_3)_3 + NH_3$$

The reaction was shown to proceed rapidly and quantitatively. The testing was then extended to model (phenol) compounds and found to proceed with equal facility. Next attempts were made to silylate hydroxy-carbonyl compounds, which were postulated to exist in coals. The first compound tested was 1,5-dihydroxyanthraquinone. Previous work had shown that this compound only underwent silylation under very harsh reaction conditions i.e heating its dipotassium salt with dimethyl sulfate at 140°C. Friedman, however, found that the bis(trimethylsilyl) ether was readily formed on refluxing with HMDS and one drop of trimethylchlorosilane (TMCS) for 24 hrs. Hydrogen-bonded 1,4-dihydroxyanthraquinone and 1,8-dihydroxyanthraquinone were also reacted with similar results. Friedman also managed to quantitatively silylate highly hindered 2,6-di-tert-butylphenol by reacting it with HMDS in the presence of TMCS and pyridine and refluxing for 24 hrs.

The success of these reactions lead Friedman and his fellow workers to develop a reaction for the derivatisation of hydroxyl groups in coal. This involved reacting the coal with HMDS in pyridine, either with or without TMCS, and refluxing the reaction mixture under nitrogen for 3 days. After reaction the product was dried and analysed for silicon - from this value the hydroxyl value was calculated. Friedman concluded that both extremely hindered and hydrogen-bonded hydroxyl groups could be quantitatively derivatised. He also found that the stability of the trimethylsilyl ethers of coal were excellent and moisture had little effect on the derivatised product (refluxing with water for 1 hr caused only slight hydrolysis and 72 hrs refluxing effected hydrolysis of only one-third of the silicon introduced into the coal). For the middle rank coals tested, Friedman obtained reproducible values for the hydroxyl content to within ±0.02 per cent. These values showed good agreement with previous acetylation work done on the coals.

Later work carried out by Seyferth et al[71] showed that silylation was a good method for increasing the solubility (in benzene) of pyridine-soluble coal-derived products. Seyferth and his co-workers showed that the conversion of hydroxyl groups in preasphaltenes to trimethylsilyl ethers decreased the polarity of the sample and imparted some ability for benzene solubilisation to the preasphaltene fraction. The silylation procedure Seyferth used was that developed by Friedman et al[28] using hexamethyldisilazane (HMDS) in the presence of small amounts of trimethylchlorosilazane (TMCS). Derivatisation by silylation resulted in 40 - 58% of the preasphaltene (pyridine-soluble, benzene-insoluble) fraction being completely converted to a benzene-soluble product.

Similar work has also been carried out by Snape and Bartle[72] and Patel et al[73]. Snape and Bartle managed to silylate the pyridine extract from Daw Mill coal - a low rank British coal (82% carbon daf). The procedure involved refluxing the benzene-insoluble extracts with pyridine, HMDS and TMCS for only 1 hr. The solvent and quantities of silylating reagents used gave rapid and total conversion of hydroxyl groups and were found to yield larger conversions than either refluxing in benzene or using smaller quantities of silylating reagent. The conversion of hydroxyl groups to their trimethylsilyl ether derivatives in the extracts was confirmed by infra-red spectra, which was recorded as smears in chloroform-d using sodium chloride plates. The silylated extracts were also analysed by ^{1}H and ^{13}C to determine the hydroxyl content and proportion of aliphatic and aromatic carbon respectively. The hydroxyl values obtained by Snape and Bartle were slightly higher than those quoted in previous literature and the ^{13}C nmr showed that all the benzene-insoluble fractions were highly aromatic.

Work done by Patel et al[73] showed that the solubility of solvent-refined coal and solvent-refined lignite increased dramatically in benzene and chloroform upon silylation of the samples with hexamethyldisilazane (HMDS). They postulated that the reason for this was the disruption of intramolecular association forces (such as Π-Π bonding) and intermolecular hydrogen-bonding (mainly due to hydroxyl groups).

More recent work has been carried out by Monsef-Mirzai et al[42], 1995. Monsef-Mirzai and her co-workers have tested a range of silylating reagents :

1. N-(trimethylsilyl) imidazole (TMSI)
2. 1-(trimethylsilyl) pyrrolidine (TMSPY)
3. N,O-bis(trimethylsilyl) acetamide (BSA)
4. Hexamethyldisilazane (HMDS)
5. Trimethlychlorosilane (TMCS)

These reagents have been tested both by themselves and in mixtures on model compounds and coals. Ten phenol compounds (including 1,2-dihydroxybenzene, pyrogallol, 1-napthol, 2-napthol and 2,6-di-tert-butylphenol) were tested with various reagents using microwave, reflux and ultrasonic techniques. Model compounds were used for 2 reasons - to evaluate the effectiveness of the various silylation agents and to use those silylated derivatives, which are solids, to evaluate methods of determining spin-lattice relaxation times for ^{29}Si. It was found that a mixture of BSA : TMSI : TMCS (1 : 1 : 1) was the best reagent to ensure complete silylation of even the most sterically-hindered -OH groups. Microwave heating was also shown to be the most effective method of driving reactions rapidly to equilibrium, proving superior to conventional reflux and ultrasound techniques. Eleven coals (9 British coals and 2 American coals) were also investigated in this extensive study. Again, microwave heating was the preferred method for silylation. The N,O-bis(trimethylsilyl) acetamide (BSA) was found to be the most powerful reagent for the silylation of the coals. A problem, however, with this reagent was that the by-product and leaving group (acetamide) stayed tenaciously on the coal. Consequently N-(trimethylsilyl) imidazole (TMSI) was selected for the silylation of the coals - again this is a powerful silylating reagent and the leaving group (imidazole) comes off with the solvent on separation of the products.

The time for complete silylation varied depending upon which coal was used. The samples were analysed by FT-IR, elemental analysis and quantitative ^{29}Si MASNMR.

The testing carried out in this chapter utilised N-(trimethylsilyl) imidazole (TMSI) as the silylating reagent for the Creswell and Cortonwood coals and coal macerals. The samples were analysed by FT-IR and quantitative ^{29}Si MASNMR.

5.2 EXPERIMENTAL

The coals and coal macerals were silylated as outlined in section 2.8. In order to obtain quantitative ^{29}Si (^{29}Si has a natural abundance of 4.70%, a receptivity of 2.09 compared to ^{13}C and a spin 1/2) data from the coal compounds, it is important to ensure that the magnetisation produced by one radio-frequency pulse has decayed to equilibrium before a second pulse is applied. The ratio of resonant nuclei occupying chemically and magnetically distinct sites, and the concentration of these resonating nuclei, will only be truly reflected if the delay between pulses is $\geq 5\ T_1$, where T_1 is the spin-lattice relaxation time. Clearly, if nuclei are present in different chemical environments, it must be the maximum T_1 value which determines the pulse delay. Spin-lattice relaxation times were determined by Dr M.C Perry at Aston University (Chemical Engineering and Applied Chemistry Dept.) using new pulse sequence software supplied by Brüker.

Spin-lattice relaxation times determined for the silylated coals and silylated model compounds were in the order of approximately 8 seconds and approximately 25 seconds respectively. For the standard, three possibilities were considered - silylated model compounds, triphenylsilane and laponite (a synthetic smectite clay). With the silylated model compounds, it was found that the ^{29}Si resonances overlapped with the ^{29}Si signals from the silylated coal. The triphenylsilane gave a long spin-lattice relaxation time and strong Si-H decoupling was required. The laponite, however, was a good compromise - it is inert, has a reasonable spin-lattice relaxation time (T_1 = 25 seconds) and its resonance is well removed from the -$OSiMe_3$ signal. Consequently it was decided to use the laponite as a standard.

For quantitative ^{29}Si measurements known weights of the silylated coal and laponite were placed in the zirconium dioxide rotor and separated using a 'kel-f' spacer. A pulse delay of $6T_1$ (laponite) was used and data accumulated until a satisfactory signal / noise ratio was achieved. The peak areas were integrated to give the ratio of the silicon present in the standard (known) and the sample under investigation. The concentration of hydroxyl groups in the original coal was then calculated assuming a 1 : 1 molar relationship with the complexed silicon.

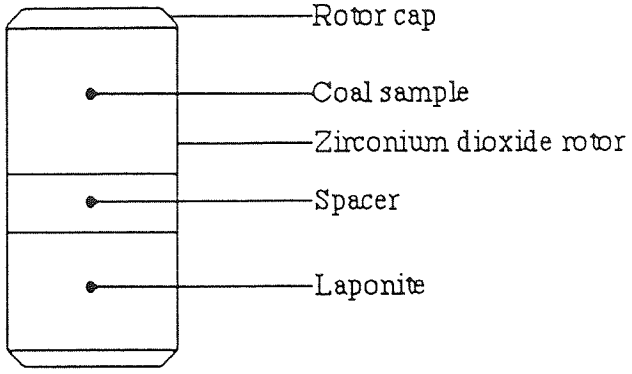

Fig5.01

Zirconium dioxide rotor used for quantitative ^{29}Si measurements

5.3 RESULTS AND DISCUSSION

5.3.1 Silylation of resins

All the resins were dried overnight prior to reaction and reacted for 1 hr and 2 hrs in the MES-1000 microwave oven on a 20% power setting. The three resins tested were :

1. Phenol-formaldehyde resin
2. 1 : 1 Phenol : 2,6-di-tert-butylphenol-formaldehyde co-resite
3. 3 : 1 Phenol : 2,6-di-tert-butylphenol-formaldehyde co-resite

Fig 5.02 shows the IR spectrum of the phenol-formaldehyde resin. A broad absorption centred at 3459 cm^{-1} can be seen which is indicative of polymeric hydroxyl groups. A smaller absorption due to $-CH_2-$ linkages also appears at 2919 cm^{-1}. A band due to alcoholic C-O stretching vibrations is also visible at 1140 cm^{-1} and absorptions due to characteristic aromatic vibrations can also be seen at 1600 cm^{-1} (C=C stretch), 700 cm^{-1} and 1474 cm^{-1} (C-H bending). Fig 5.03 shows the IR spectra for the attempted silylation of the phenol-formaldehyde resin after 1 hr and 2 hrs reaction time in the microwave oven. As can be seen there appears to be little change after 2 hrs of heating compared to the 1 hr reaction. Fig 5.04 shows the IR spectrum, with the prominent peaks highlighted, of the silylated phenol-formaldehyde resin after 2 hrs microwave reaction time. There is still a notable peak at 3418 cm^{-1} indicating that not all of the hydroxyl groups have been silylated, but there are significant peaks at 841 cm^{-1} and 1253 cm^{-1} due to $-OSiCH_3$ and $-SiCH_3$ respectively, showing that some silylation has taken place. Fig 5.05 shows an IR comparison between the silylated and unreacted phenol-formaldehyde resin, where the changes in structure are clearly distinguishable. Fig 5.06 shows the IR spectra of the unreacted 1 : 1 co-resite. Again, the absorptions due to the hydroxyl functionality, the methylene bridges and the aromatic moieties are all discernible, with additional bands due to the $-CH_3$ groups in the tert-butyl substituents - these can be seen on either side of the band at 2922 cm^{-1} and are due to symmetric and asymmetric $-CH_3$ stretching. Other prominent $-CH_3$ bands are masked by bands already present in the resin structure. Fig 5.07 shows the IR comparison of the 1 : 1 co-resite after 1 hr and 2 hrs reaction time in the microwave oven. In both cases there appears to be little reaction.

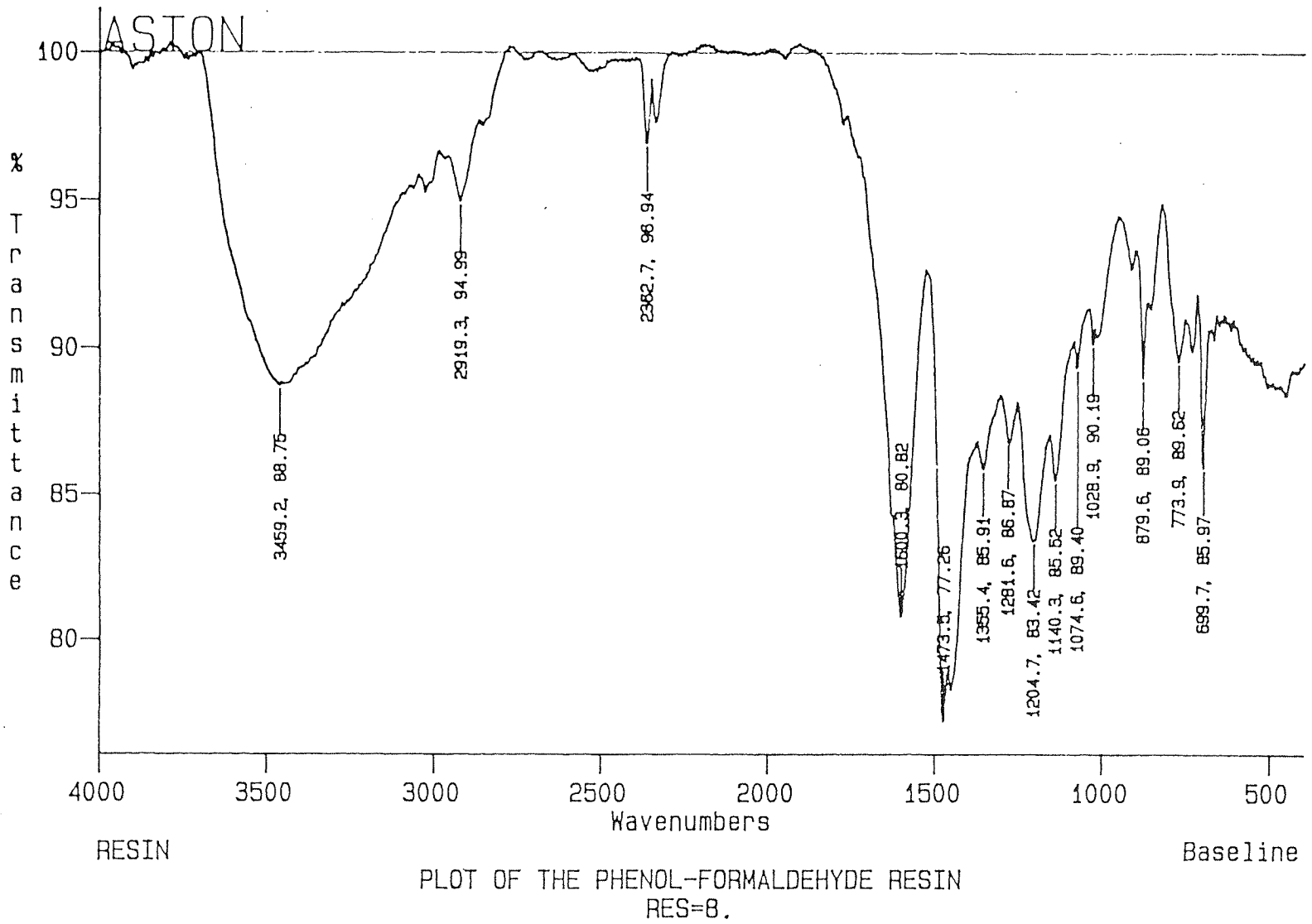

Fig5.02
IR of phenol-formaldehyde resin

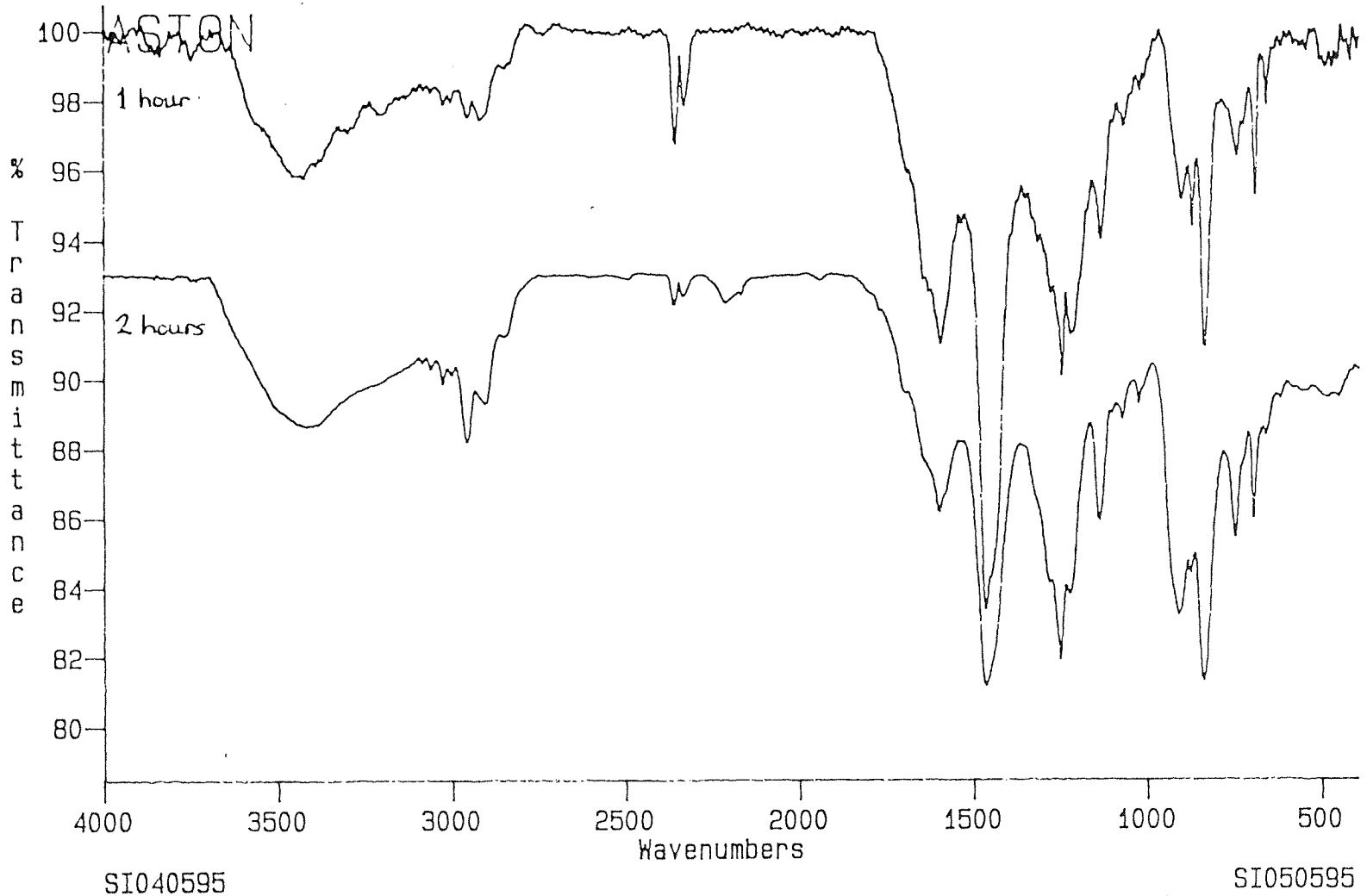

Fig5.03
IR of silylated phenol-formaldehyde resin after 1 hr and 2 hrs mw heating

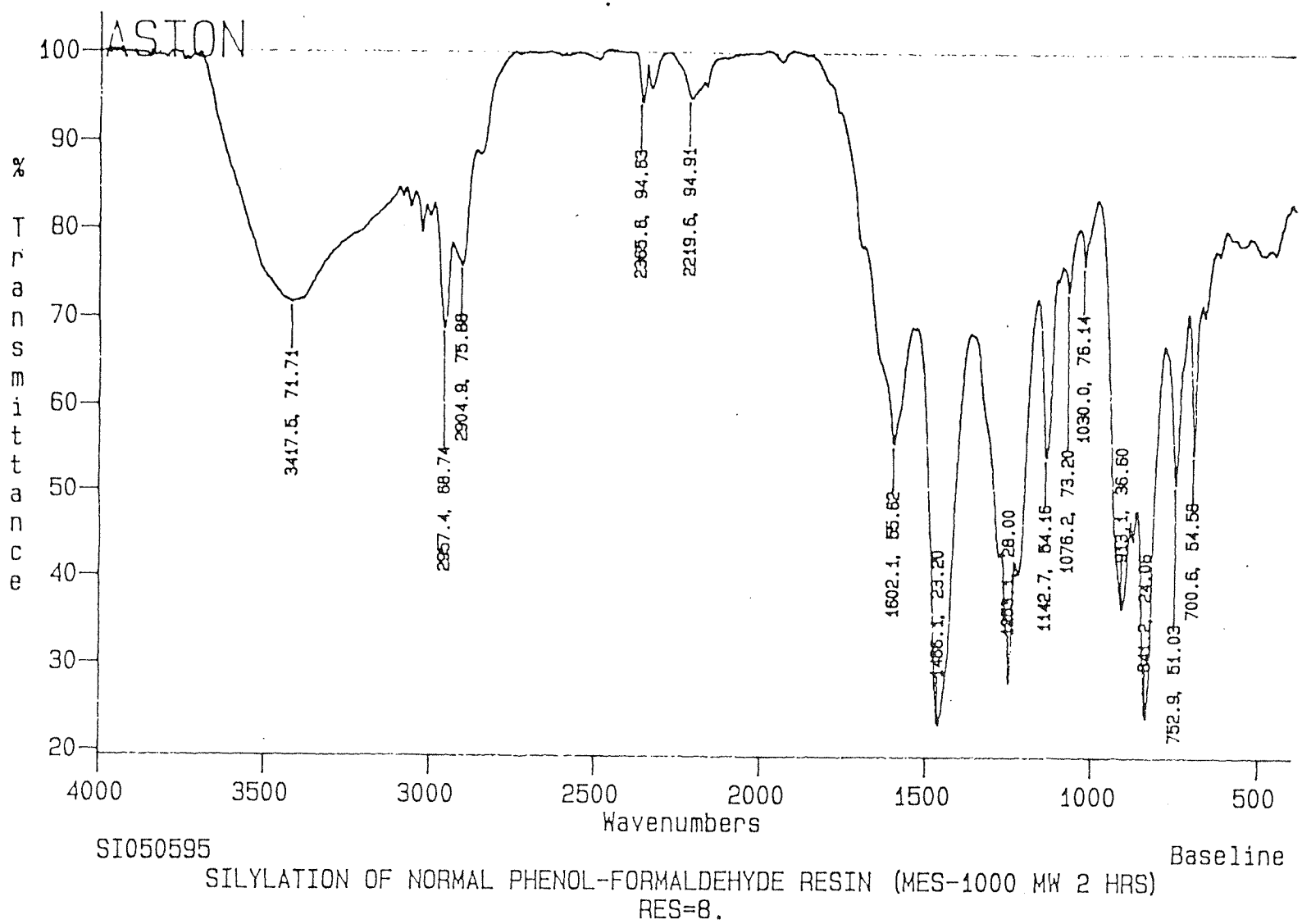

Fig5.04
IR of silylated phenol-formaldehyde resin after 2 hrs mw heating

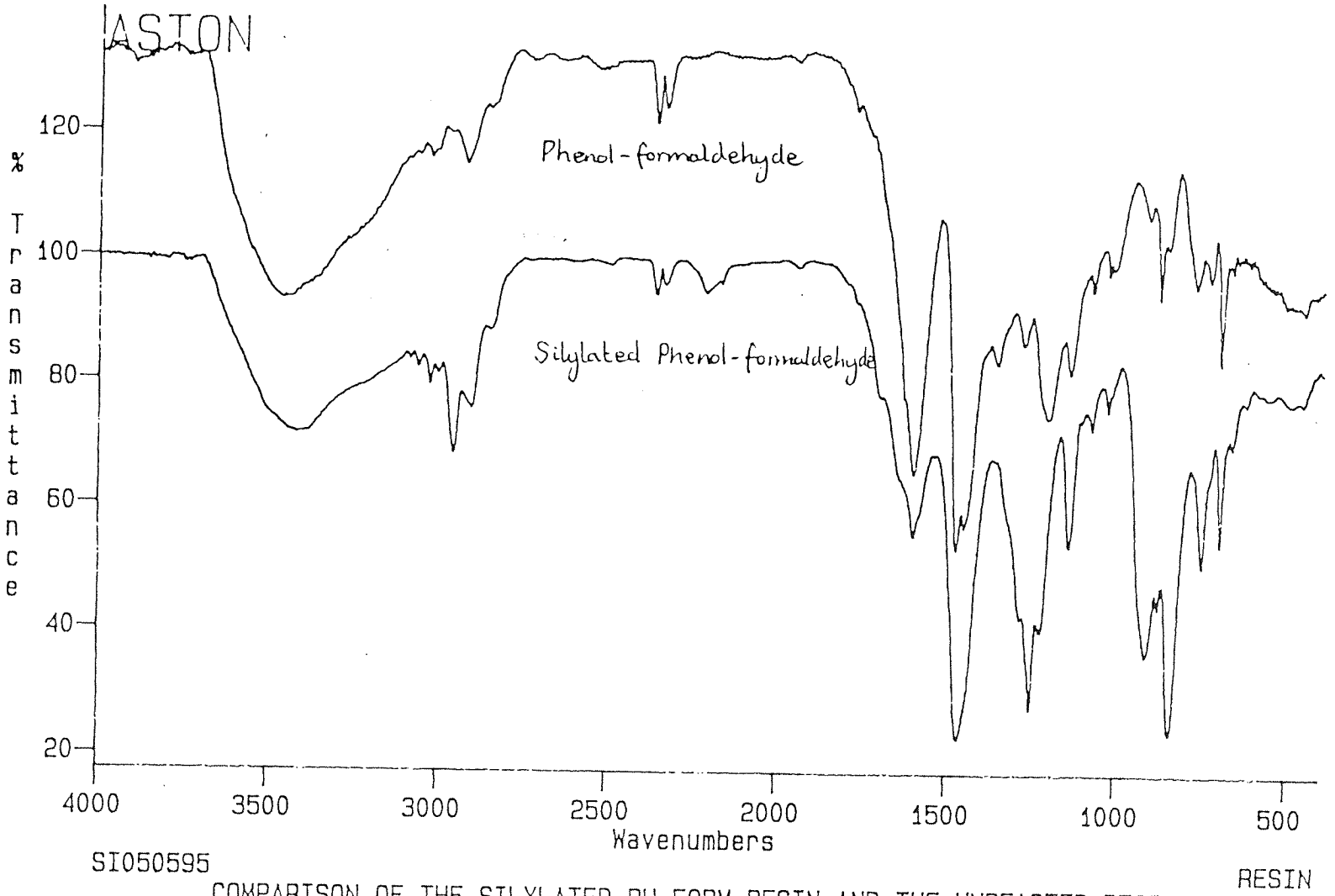

Fig5.05
IR comparison of the silylated phenol-formaldehyde resin
and the unreacted phenol-formaldehyde resin

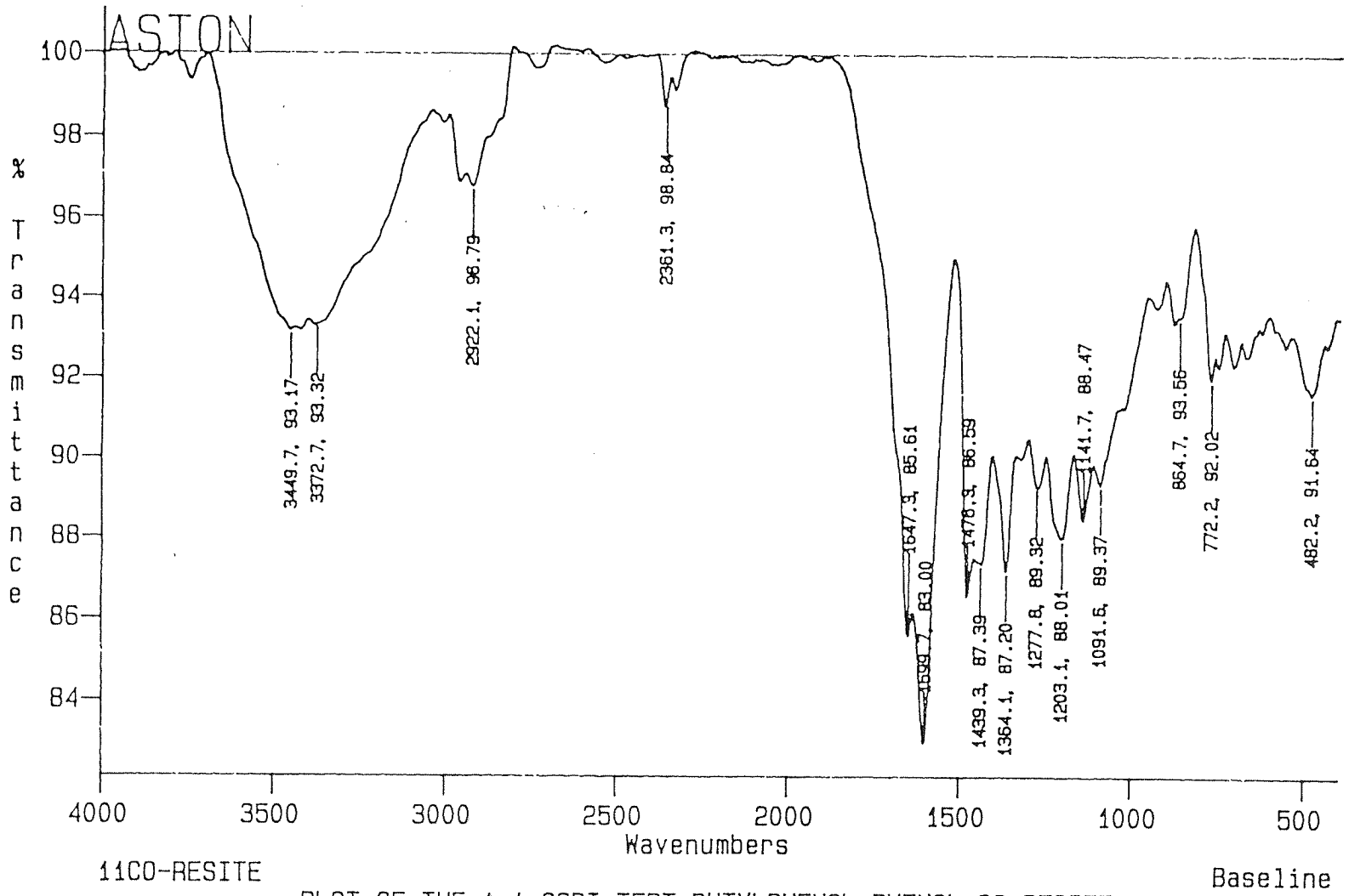

Fig5.06
IR of the 1:1 co-resite

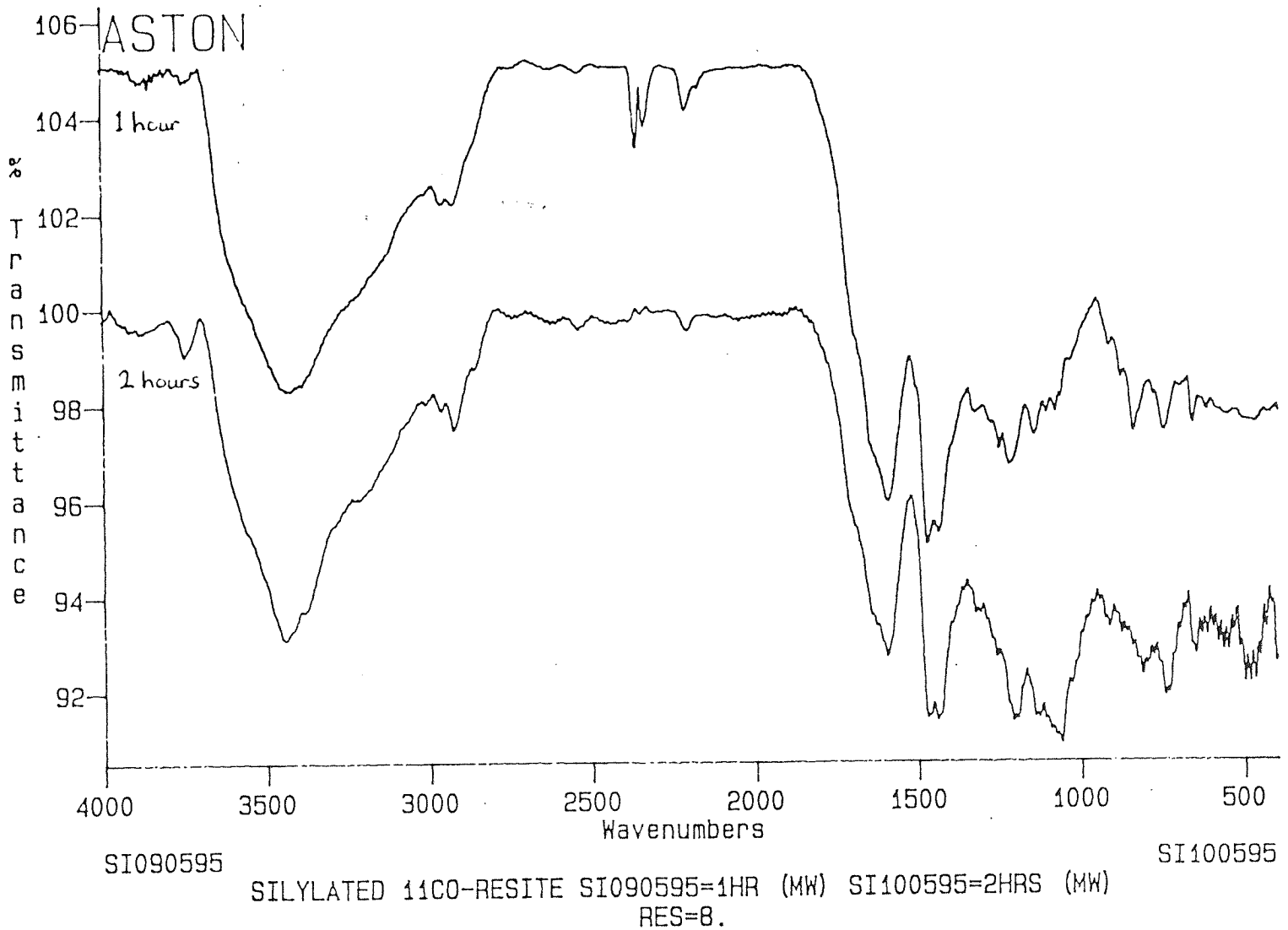

Fig5.07
IR of the silylated 1:1 co-resite after 1 hr and 2 hrs mw heating

Fig 5.08 shows the IR peaks for the attempted silylation of the 1 : 1 co-resite (2 hrs microwave reaction time). The structure of the 1 : 1 co-resite is essentially unchanged and the peaks denoting silylation are markedly absent. It was found that there was still no change in the structure even after 3 hrs reaction in the microwave oven. Fig 5.09 shows the IR plot of the 3 : 1 co-resite - this has an IR structure, which is similar to both the phenol-formaldehyde resin and the 1 : 1 co-resite, which is as expected. Fig 5.10 shows a multispectral IR plot of all three unreacted resins for comparison. The 3 : 1 co-resite was reacted for 1 hr and 2 hrs in the MES-1000 microwave oven and the resulting IR spectra can be seen in fig 5.11. In this case there is a noticeable difference between the 1 hr and 2 hr reactions. As the IR plot shows there appears to be an increased reaction after 2 hrs of microwave heating, denoted by the increase of the bands at 816 cm^{-1} υ-($OSiCH_3$) and at 1258 cm^{-1} υ-($SiCH_3$). Fig 5.12 shows the peaks prominent in the silylated 3 : 1 co-resite (2 hr microwave reaction time) and fig 5.13 shows an IR comparison between the unreacted 3 : 1 co-resite and the silylated 3 : 1 co-resite - the IR bands due to silylation are more distinguishable in this plot.

The silylated resins were also analysed by ^{29}Si CP MASNMR. A qualitative analysis was carried out on the silylated phenol-formaldehyde resin (fig 5.14). This produced a good quality nmr spectrum with a major resonance at 17.5 ppm. This resonance is due to -$OSi(CH_3)_3$ and is consistent with silylated phenols. There is also a much weaker higher-field signal centred at -3.8 ppm - one possible explanation for this resonance may be the formation of small amounts of bis-trimethylsilyl oxide at higher temperatures during the reaction. The silylated 1 : 1 co-resite was also analysed qualitatively using ^{29}Si CP MASNMR. The results can be seen in fig 5.15. There is a resonance at 19.2 ppm denoting some silylation has occurred and a signal of similar intensity at 7.1 ppm. This higher field signal is due to the formation of trimethyl silanol $(CH_3)_3SiOH$, a hydrolysis by-product. The origin of this is likely to be the hydrolysis of the TMSI silylating reagent by water tenaciously held (probably hydrogen-bonded) within the resin polymer matrix. There is also a less intense signal at -7.8 ppm - again this could be due to bis-trimethylsilyl oxide formation. Fig 5.16 shows the quantitative ^{29}Si CP MASNMR spectrum for the silylated 3 : 1 co-resite. The product resonance appears at 18.1 ppm and the laponite (the synthetic smectite standard) resonance appears at -93.6 ppm. There is also a substantial peak representing the formation of trimethyl silanol at 8.2 ppm. The calculation for the amount of hydroxyl oxygen silylated in the 3 :1 co-resite was carried out thus :

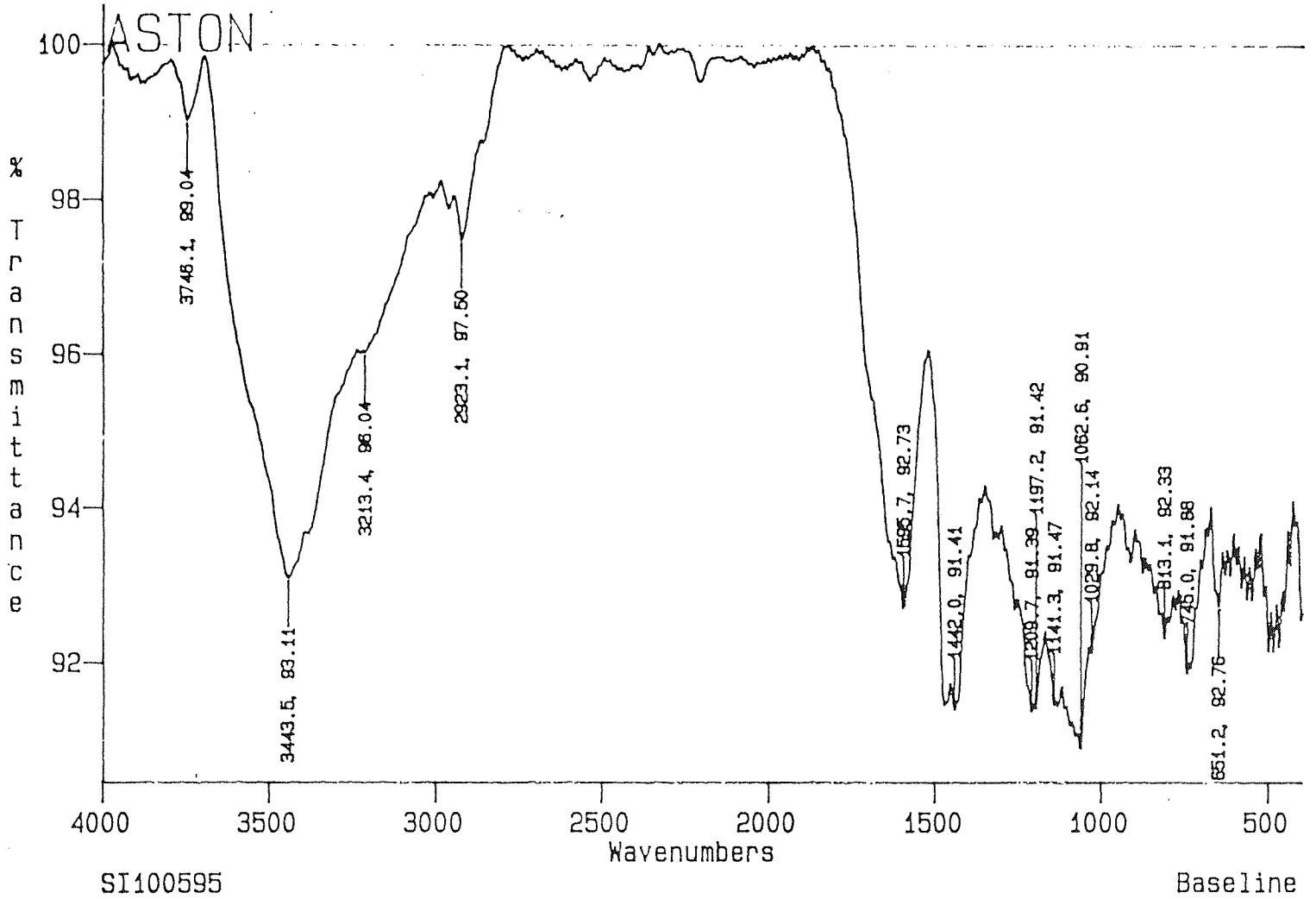

Fig5.08
IR of the silylated 1:1 co-resite after 2 hrs mw heating

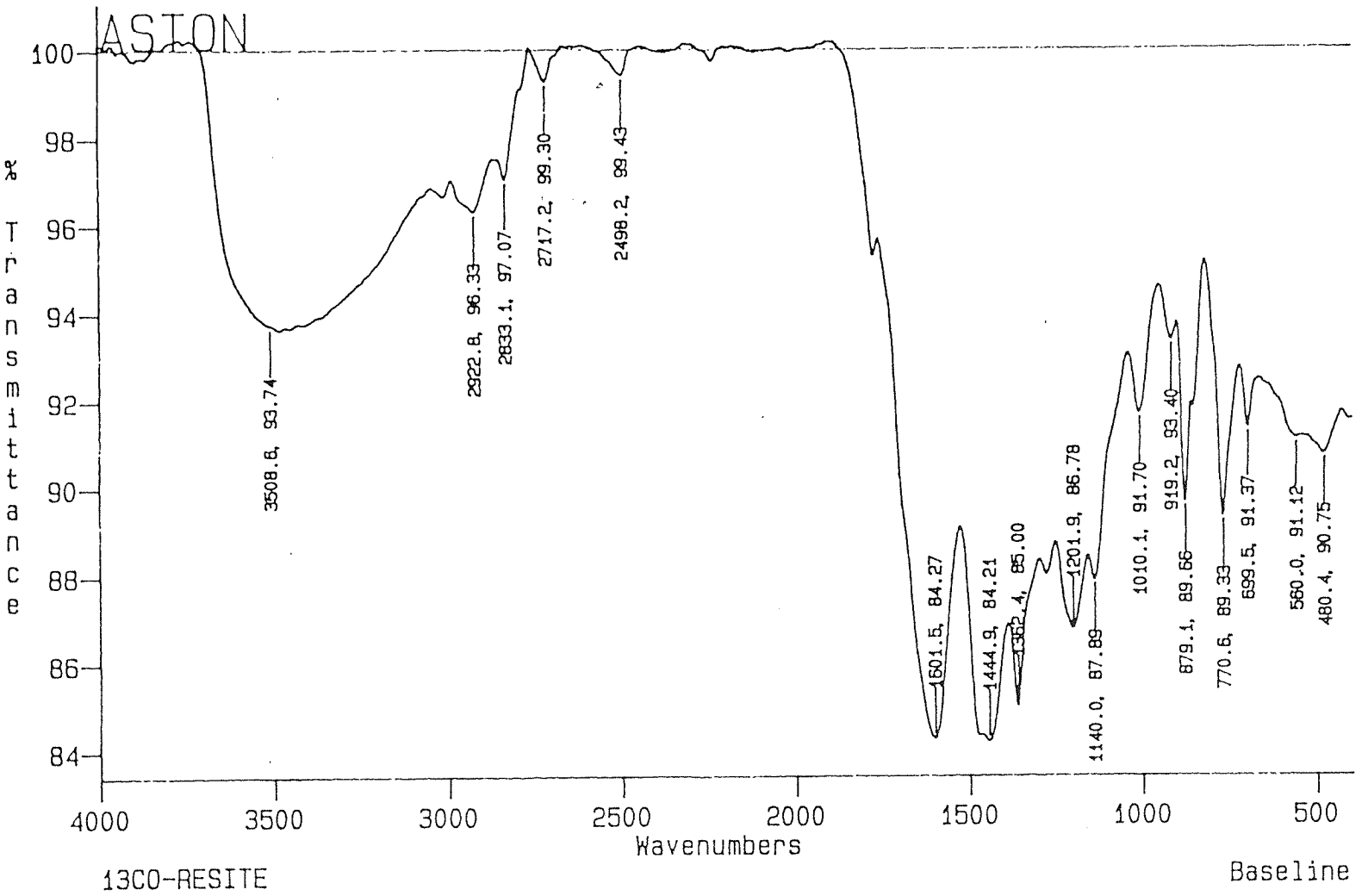

RES=8.

Fig5.09
IR of the 3:1 co-resite

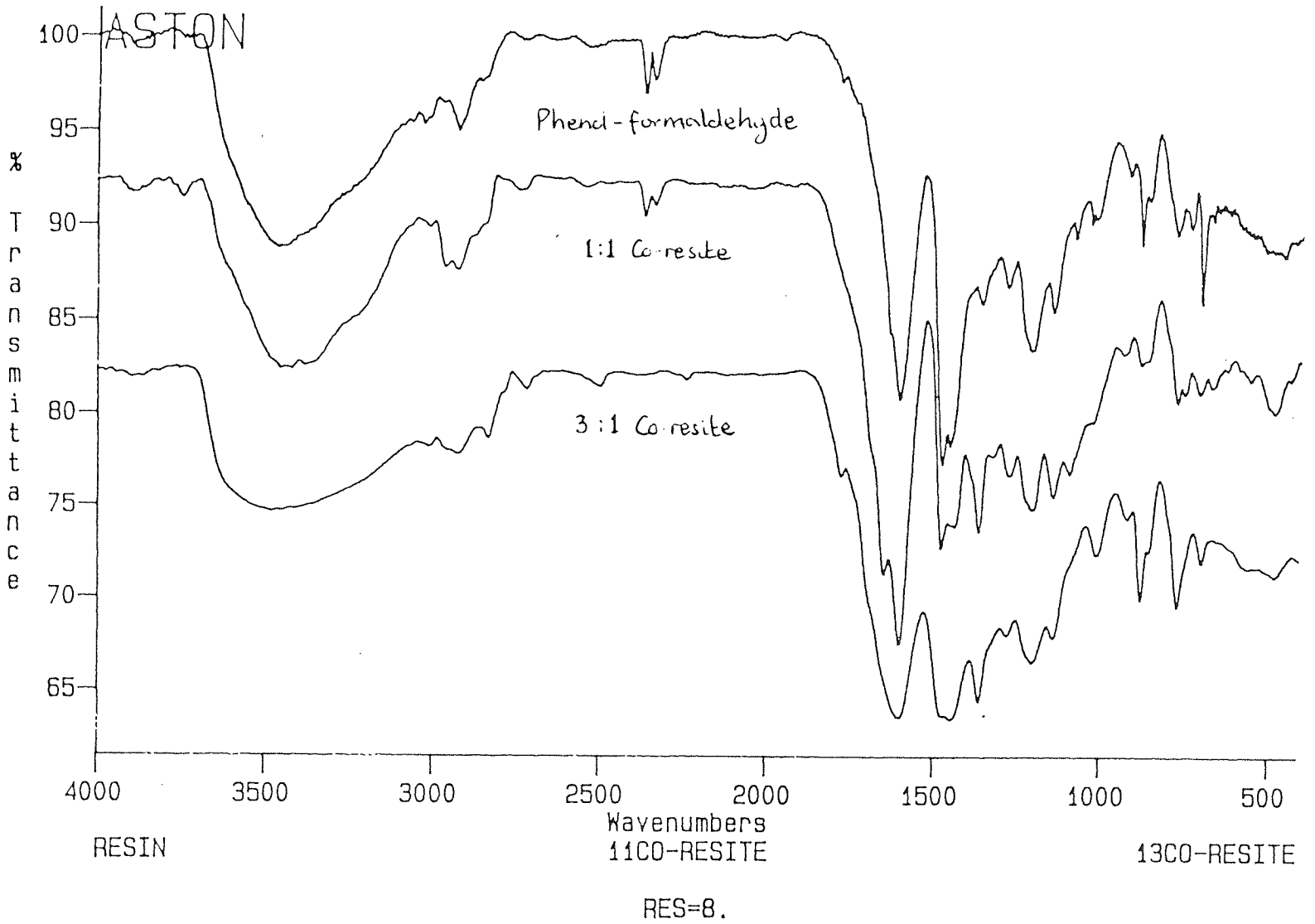

Fig5.10
Multispectral IR display of the phenol-formaldehyde resin and the 1:1 and 3:1 co-resites

Fig5.11
IR of the silylated 3:1 co-resite after 1 hr and 2 hrs mw heating

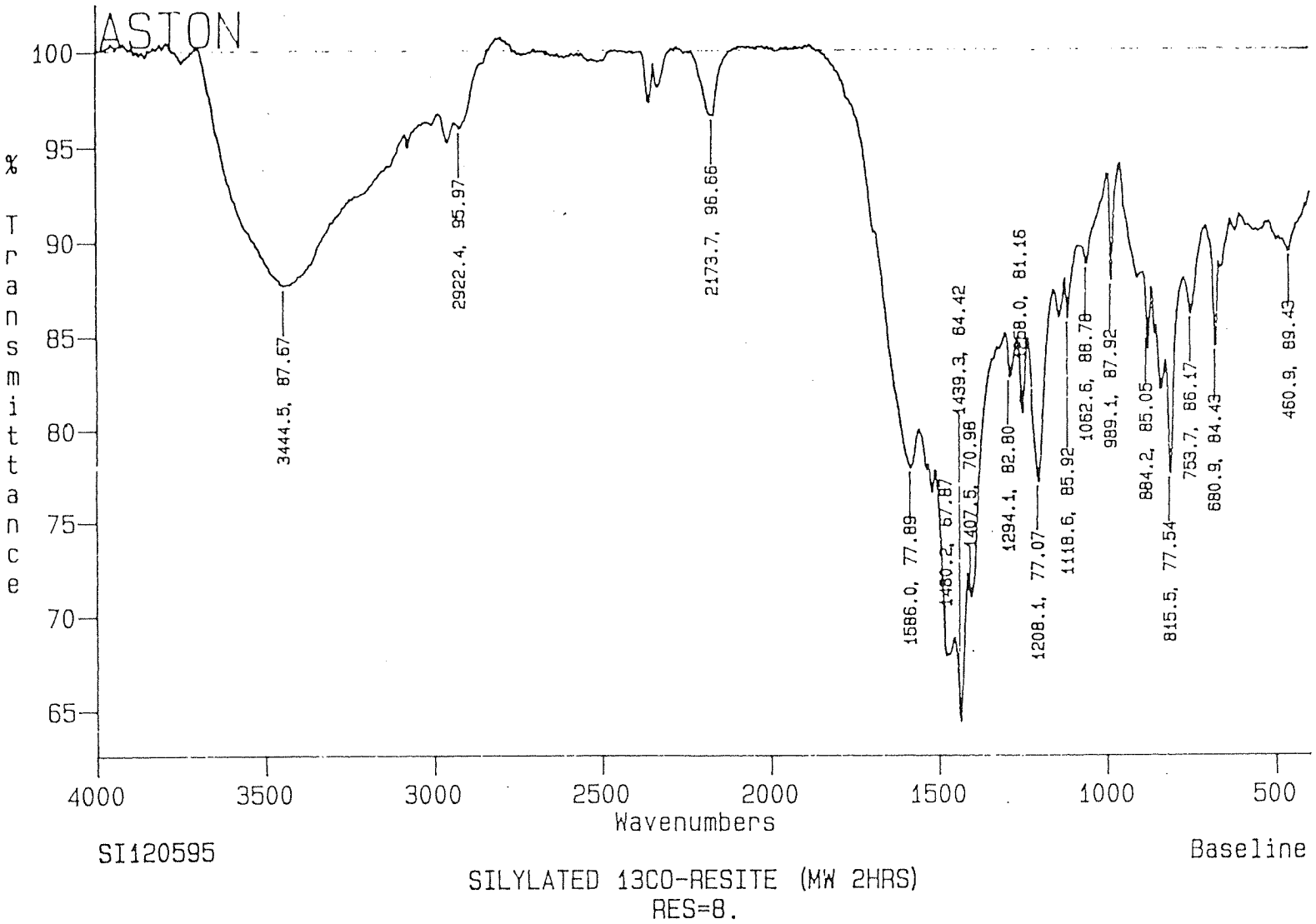

Fig5.12
IR of the silylated 3:1 co-resite after 2 hrs mw heating

Fig5.13
IR comparison of the silylated 3:1 co-resite and the unreacted 3:1 co-resite

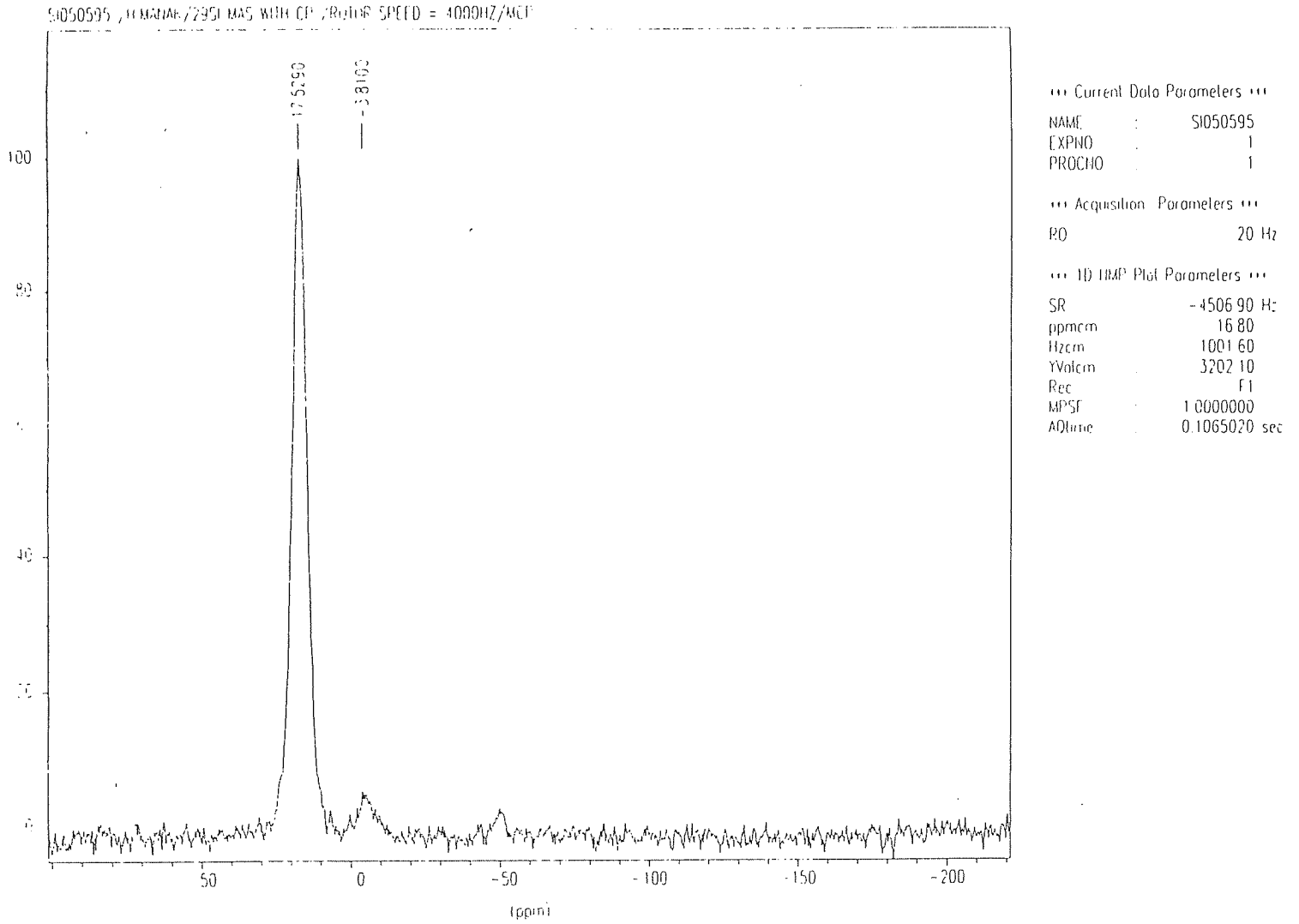

Fig5.14
Qualitative ^{29}Si CP MASNMR of the silylated phenol-formaldehyde resin
(2 hrs mw heating)

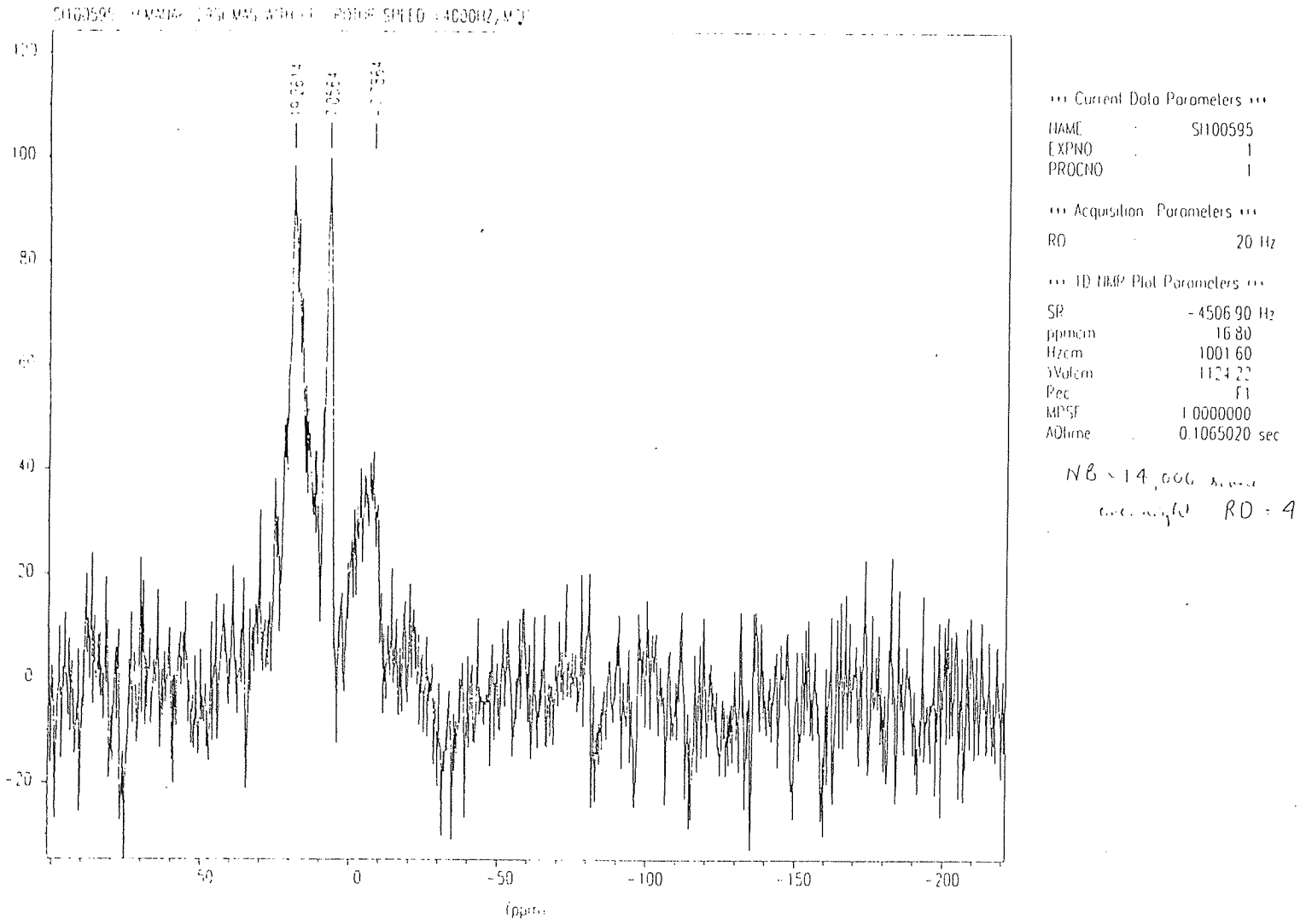

Fig5.15
Qualitative ^{29}Si CP MASNMR of the silylated 1 : 1 co-resite
(2 hrs mw heating)

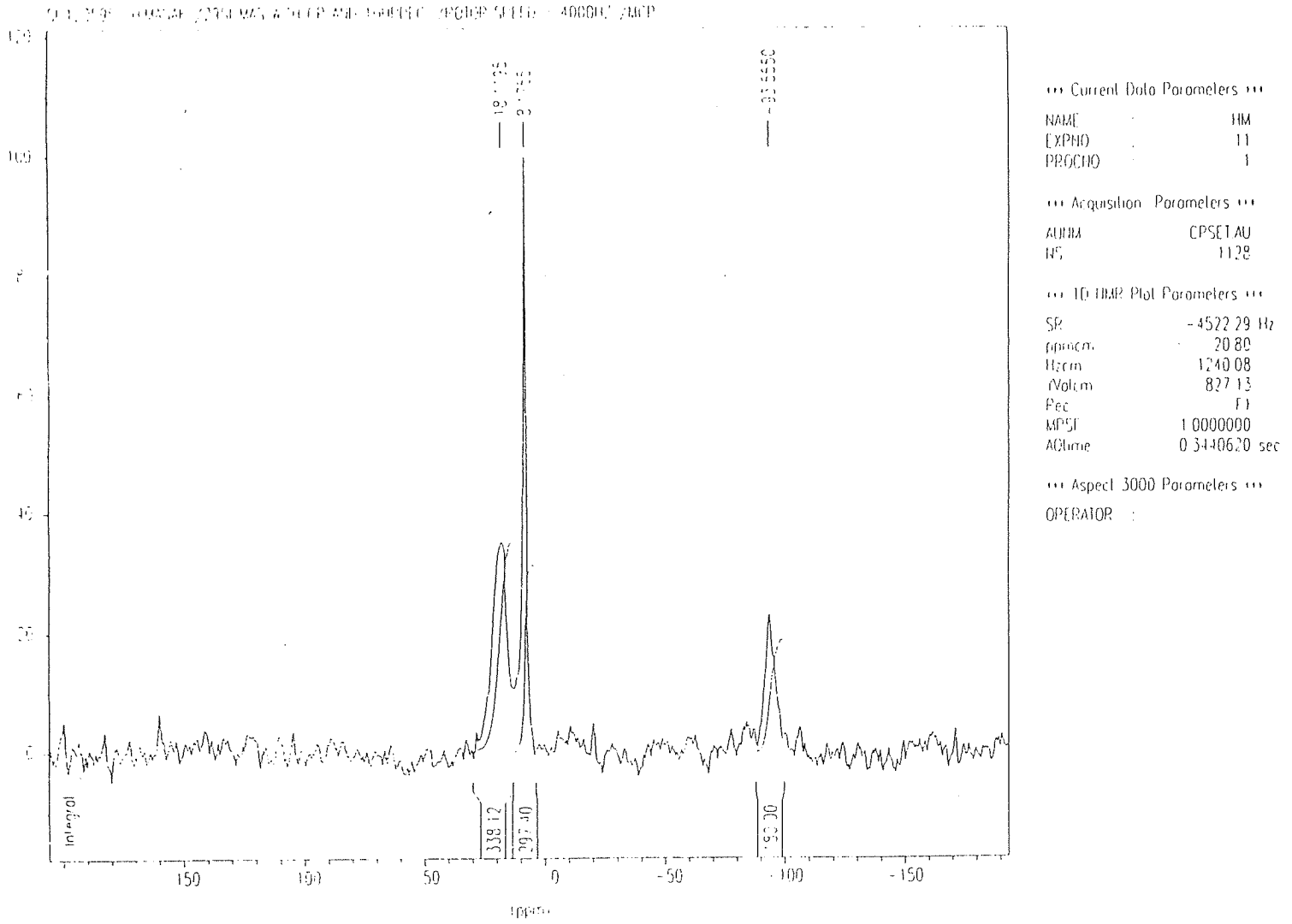

Fig5.16
Quantitative ^{29}Si CP MASNMR of the silylated 3 : 1 co-resite
(2 hrs mw heating)

mass of rotor + spacer + lid	= 1.9237g
mass of rotor + spacer + lid + laponite	= 1.9621g
mass of rotor + spacer + lid + laponite + silylated 3 : 1 co-resite	= 2.1406g

Hence

mass of laponite	= 0.0384g
mass of silylated 3 : 1 co-resite	= 0.1785g

The structure of laponite is $Si_{8.0}Mg_{5.34}Li_{0.66}O_{20}[OH]_4Na_{0.66}$

So the atomic weight of laponite is :
(8.0 x 28.0855) + (5.34 x 24.305) + (0.66 x 6.941) + (20 x 15.9994) + (4 x 17.0073) + (0.66 x 22.98977) = 762.244g

But there are 8 silicon atoms in laponite, so in order to determine the contribution from one silicon atom, we must divide this value by 8 :

762.244 / 8 = 95.28g

The % O (as -OH) silylated is then calculated using the following equation :

$$\% \ O = (M_O / m_r).(m_S / M_S).(I_r / I_S) \times 100\%$$

where M_O = atomic weight of oxygen
m_r = weight of resin
m_S = weight of standard
M_S = molecular weight of standard
I_r = signal area of resin
I_S = signal area of standard

For the silylated 3 : 1 co-resite :

$$\% \text{ O} = (15.9994 / 0.1785).(0.0384 / 95.28).(338.12 / 180.00).100\% = 6.8 \%$$

The 3 : 1 co-resite was sent to MEDAC Ltd at Brunel University for elemental analysis (C, H, O), but unfortunately, the amount of oxygen present could not be determined routinely. The elemental percentage of C and H were, however, determined in duplicate. The values for the two runs were 60.39% C, 4.80% H and 60.58% C, 4.84% giving average values of 60.49% C, 4.82% H for the 3 : 1 co-resite. If we assume that the sample is completely pure and there are no impurities present, then the rest of the sample must consist solely of oxygen. Hence :

$$\% \text{ O (in 3 : 1 co-resite)} = 100.00 - (60.49 + 4.82) \%$$

$$\% \text{ O (in 3 : 1 co-resite)} = 34.69 \%$$

The quantitative ^{29}Si data for the silylated 3 : 1 co-resite informs us that 6.8% of this oxygen has been silylated. Thus :

$$\% \text{ O (silylated in the 3 : 1 co-resite)} = (6.8 / 34.7).100 \%$$

$$\% \text{ O (silylated in the 3 : 1 co-resite)} = 19.6 \%$$

The silylated pure phenol-formaldehyde resin (1hr and 2hr microwave reaction times) and silylated 1 : 1 mixture of 2,6-di-tert-butylphenol and phenol co-resite (1hr and 2hr microwave reaction times) were analysed quantitatively using solid-state ^{13}C nmr by John Andrésen at the University of Strathclyde. Two techniques were used to obtain each nmr spectra - cross polarisation (CP) and single pulse excitation (SPE). Table 5.01 compares the results obtained via the two methods for the silylated pure phenol-formaldehyde resin and the silylated 1 : 1 co-resite (both 1 hr reaction times in the microwave oven). The areas of the various peaks are also listed.

Table 5.01

Results from the SPE / CP ^{13}C MASNMR analysis of the silylated pure phenol-formaldehyde resin and the silylated 1 : 1 co-resite

Carbon (ppm)	Ar-O (≈150) %	Aromatic (≈125) %	Aliphatic (40-20) %	Methyl (20-10) %
Silylated phenol-formaldehyde resin - 1hr microwave reaction time	10 (SPE)[a] 8 (CP)[b]	77 (SPE) 75 (CP)	13 (SPE) 17 (CP)	0 (SPE) 0 (CP)
Silylated 1 : 1 co-resite - 1hr microwave reaction time	12 (SPE) 12 (CP)	70 (SPE) 67 (CP)	15 (SPE) 17 (CP)	3 (SPE) 4 (CP)

[a]Single pulse excitation method
[b]Cross-polarisation method

Figs 5.17a and 5.17b show the solid-state ^{13}C nmr spectra for the silylated pure phenol-formaldehyde resin (1hr microwave reaction time) obtained using SPE and CP techniques respectively. Similarly, figs 5.18a and 5.18b show the solid-state ^{13}C nmr spectra for the silylated 1 : 1 co-resite (1hr microwave reaction time) obtained using SPE and CP techniques respectively. In both cases the main peaks can be attributed to aromatic carbon atoms followed by aliphatic carbon atoms and then aromatic-oxygen carbon atoms. Methyl carbon atoms appear to be present in only small concentrations in the silylated 1 : 1 co-resite indicating that the original sample of this co-resite was not a 1 : 1 mixture of 2,6-di-tert-butylphenol and phenol. Indeed, analysis of the original co-resite showed that the ratio was closer to an 18 : 1 mixture of phenol and 2,6-di-tert-butylphenol respectively.

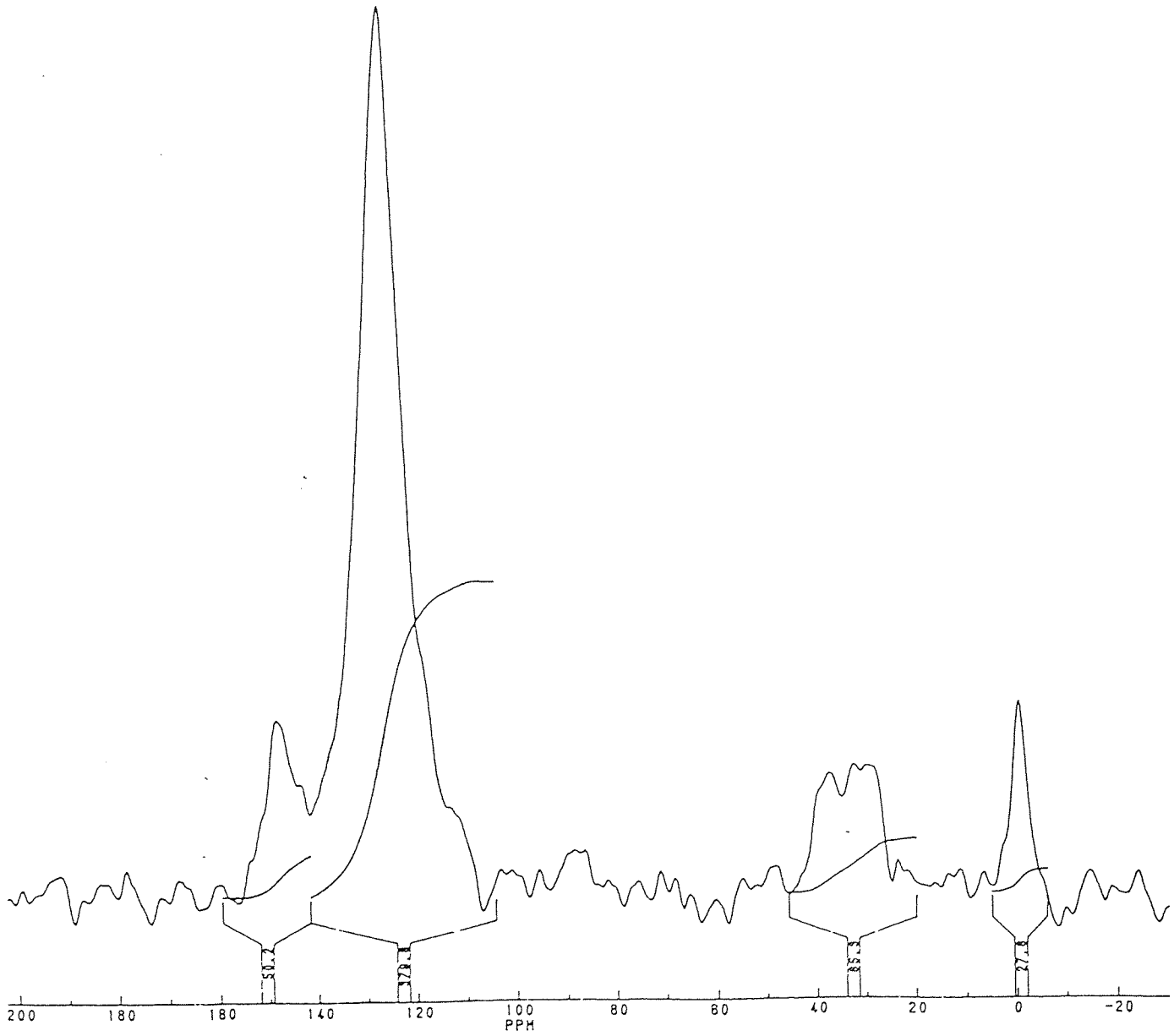

Fig5.17a
^{13}C SPE MASNMR of the silylated phenol-formaldehyde resin
(1 hr mw heating)

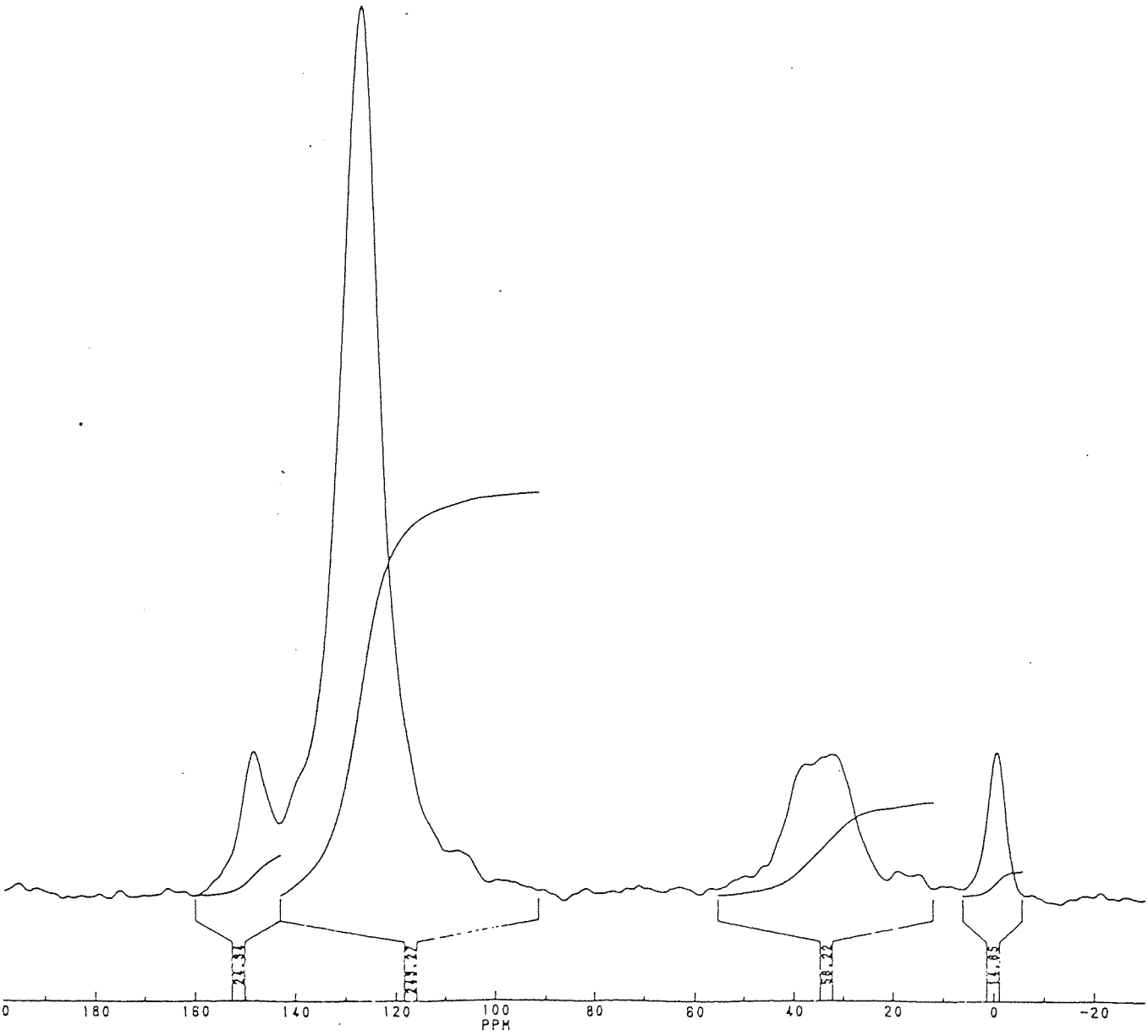

Fig5.17b
^{13}C CP MASNMR of the silylated phenol-formaldehyde resin
(1 hr mw heating)

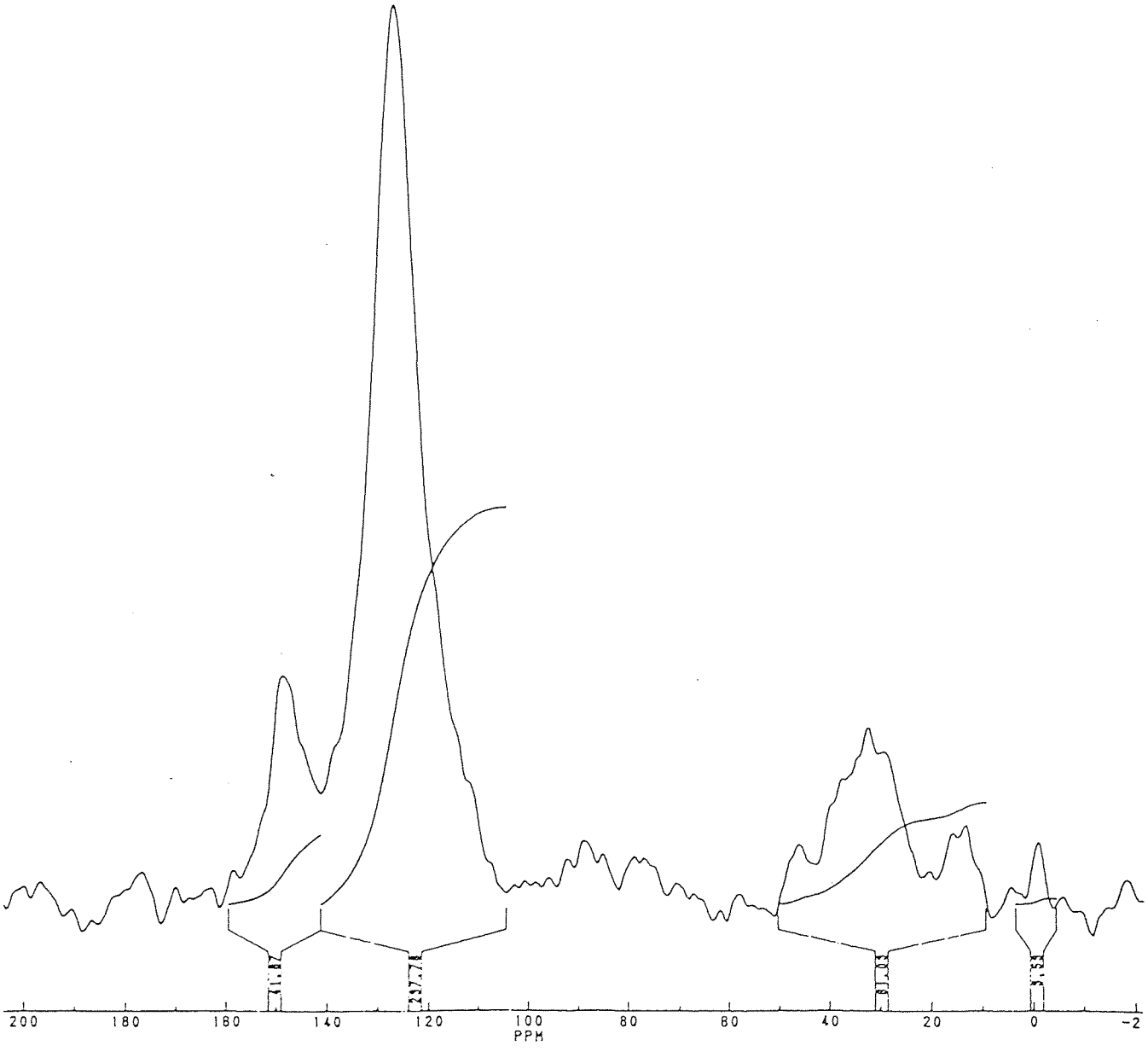

Fig5.18a
^{13}C SPE MASNMR of the silylated 1 : 1 co-resite
(1 hr mw heating)

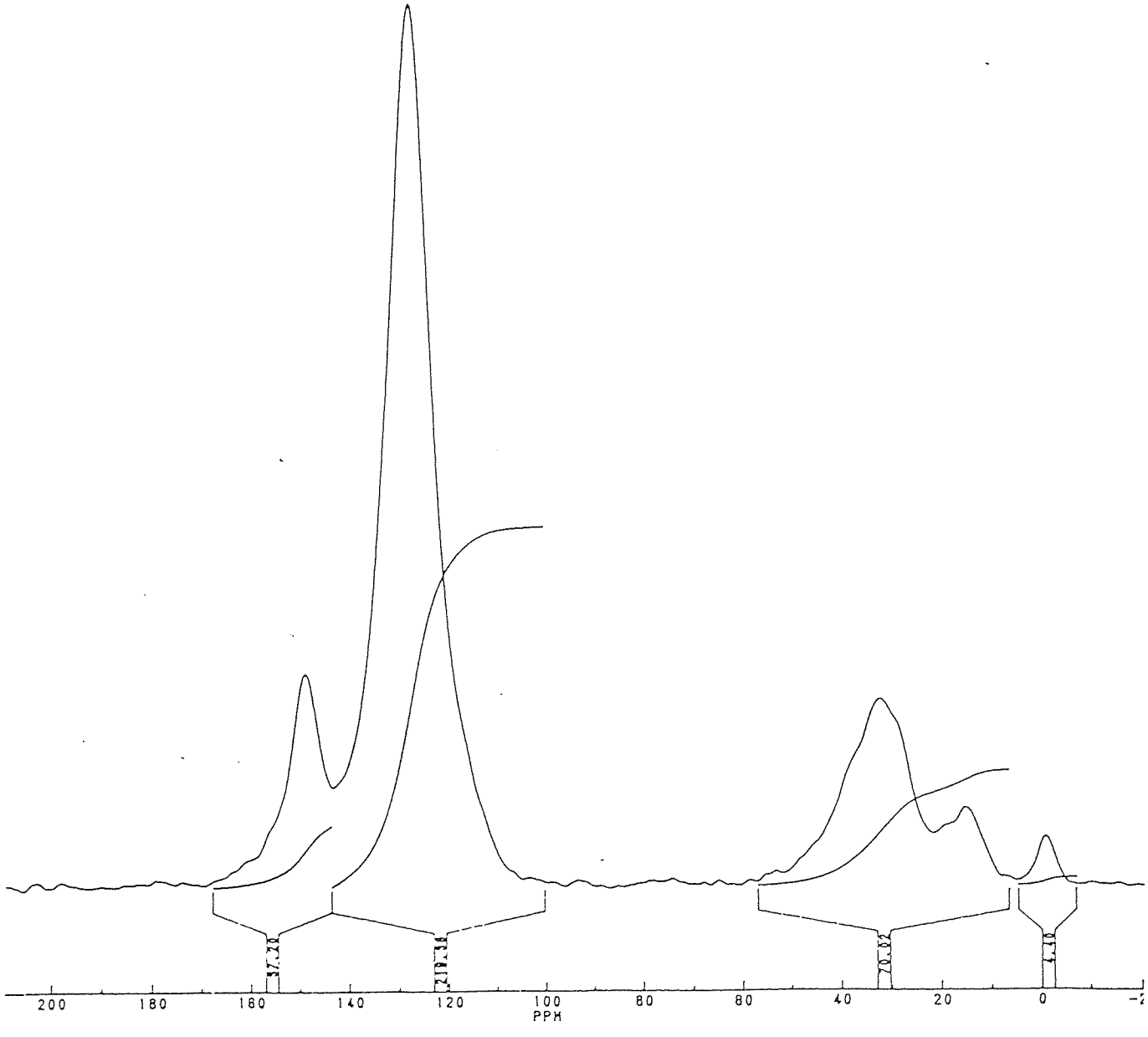

Fig5.18b
^{13}C CP MASNMR of the silylated 1 : 1 co-resite
(1 hr mw heating)

The high content of aromatic protons in the polymeric samples provides a suitable environment for cross polarisation of the samples. Consequently the results from CP and SPE are very similar and the cross polarisation technique may be used to analyse similar resites. Table 5.02 shows the percentage of methyl carbon atoms attached to the silicon atoms (trimethyl silyl carbons) and the percentage of aromatic carbon atoms attached to oxygen (Ar-O) in the silylated phenol-formaldehyde and (formerly) 1 : 1 co-resite samples. From these values the extent of silylation was calculated.

Table 5.02

Calculation of the degree of silylation for the phenol-formaldehyde resin and the (formerly) 1 : 1 co-resite

Carbon-13 nmr	Ar-O %	$(CH_3)_3Si$ %	$(CH_3)_3Si$ / 3[a] %	O_{OH} / O_{total} %
Silylated phenol-formaldehyde resin - 1hr microwave reaction time	10.0 (SPE)[b] 8.0 (CP)[c]	5.7 (SPE) 4.5 (CP)	1.9 (SPE) 1.5 (CP)	19 (SPE) 19 (CP)
Silylated 1 : 1 co-resite - 1hr microwave reaction time	12.0 (SPE) 12.0 (CP)	0.9 (SPE) 1.5 (CP)	0.3 (SPE) 0.5 (CP)	03 (SPE) 04 (CP)

[a]This value is divided by 3 because there are 3 methyl groups per silylated phenol group
[b]Single pulse excitation method
[c]Cross-polarisation method

The quantitative solid-state ^{13}C CP / SPE MASNMR results show that the extent of silylation is low in both cases. Silylation of 19% of the total phenol in the phenol-formaldehyde resin was effected and only 3 - 4% in the former 1 : 1 co-resite. The small extent of silylation observed for the former 1 : 1 co-resite, as shown by quantitative ^{13}C CP / SPE MASNMR, correlates very well with the results obtained from FT-IR and ^{29}Si CP MASNMR analysis.

In summary, silylation did occur with the phenol-formaldehyde resin and the 3 : 1 co-resite, but there was hardly any silylation with the (former) 1 : 1 co-resite - as indicated by the FT-IR, ^{29}Si CP MASNMR and the ^{13}C CP / SPE MASNMR results. Perhaps, this is not surprising, considering that the former 1 : 1 co-resite has the largest proportion of 2,6-di-tert-butylphenol incorporated into the resin matrix. These groups make it difficult for the silylating reagent (TMSI) to silylate the proximal hydroxyl groups due to the increased steric demand. Consequently, less reaction would be expected to occur. These observations are consolidated by our findings. We would also expect the pure phenol-formaldehyde to show the greatest degree of silylation, followed by the 3 : 1 co-resite and then the 1 : 1 co-resite. The pure phenol-formaldehyde and 3 : 1 co-resite gave % O silylated values of approximately 19% and the 1 : 1 co-resite gave a value of approximately 3 - 4%. The figure for the 1 : 1 co-resite is the lowest, as expected, but the 3 : 1 co-resite appears to show the same extent of silylation as the pure phenol-formaldehyde resin. This implies that very little of the 2,6-di-tert-butylphenol moieties were actually incorporated into the 3 : 1 co-resite and the 3 : 1 co-resite is, in fact, only a very slightly modified version of the pure phenol-formaldehyde resin. It should also be noted that increased reaction time can sometimes result in a greater extent of reaction, as was found in the case of the 3 : 1 co-resite - unfortunately a similar trend with the 1 : 1 co-resite was not observed. The results from the ^{29}Si CP MASNMR analysis seem to conclude that a substantial amount of water was still present in the resins (especially the co-resites). This indicates that either a vigorous drying procedure or a prolonged drying period is required prior to reaction. The results from the quantitative ^{13}C CP / SPE MASNMR analyses show that the co-resite mixtures may not always have the phenol and substituted-phenol components present in the ratios originally reacted, as shown by analysis of what was believed to be a 1 : 1 mixture of 2,6-di-tert-butylphenol and phenol co-resite. It is, therefore, highly probable that the 3 : 1 (phenol : 2,6-di-tert-butylphenol) co-resite may also have a different ratio to that previously thought. However, it is also probably safe to assume that this 3 : 1 co-resite will have a greater proportion of phenol to 2,6-di-tert-butylphenol present in its co-resite compared to the former 1 : 1 co-resite. Consequently, the impact of this finding on this set of experiments is not as drastic as first thought, as we are more concerned with trends that are observed as the degree of steric hindrance increases, rather than absolute values.

The results show that the presence of even small amounts of 2,6-di-tert-butylphenol, as with the 18 : 1 (formerly 1 : 1) co-resite, are sufficient to drastically reduce the extent of silylation. The reason for this is probably due to the 2,6-di-tert-butylphenol groups occupying boundary positions in the co-resites - this effectively leaves only the para-position open to form a methylene linkage. In this way the bulky 2,6-di-tert-butylphenol groups become concentrated at the edges of the structure and the silylating reagent must diffuse past these bulky groups in order to react with other phenol groups in the core of the polymer matrix - this results in poor mass transport and, subsequently, a lower reaction is observed.

5.3.2 Silylation of Creswell and Creswell macerals

The Creswell coal and coal macerals (≤ 32μm) were dried under N_2 at 110°C for between 2-3 days before silylation was attempted. The silylation reaction involves the reaction of phenol substituents in the coal with the TMSI reagent to produce the trimethyl silylphenol and imidazole :

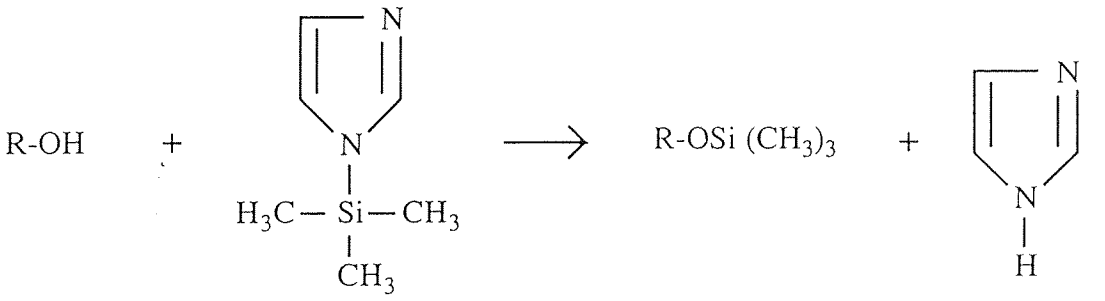

Substituted Phenol — Trimethylsilylimidazole — Silylated Substituted Phenol — Imidazole

The Creswell coal and its macerals were all reacted for 4 hrs in the MES-1000 microwave oven, after which the product was isolated and analysed by FT-IR and quantitative ^{29}Si MASNMR (as outlined in section 5.2) to determine the extent of silylation. The parameters programmed into the MES-1000 microwave oven were the same for each reaction to ensure that standard conditions were maintained throughout. Table 5.03 shows the MES-1000 reaction parameters used.

Table 5.03

MES-1000 reaction parameters used for the silylation of the Creswell coal and coal macerals

STAGE	1	2	3	4	5
Power (%)	40	20	20	20	20
Pressure (psi)	180	180	180	180	180
Run time (mins)	05	60	60	60	60
Temperature (°C)	200	200	200	200	200

Fig 5.19 shows the temperature / pressure profile with respect to time (for the first 30 mins of reaction) for the silylation reaction of the raw Creswell coal. As can be seen there is a sharp increase in temperature and an almost linear associated increase with pressure during the first 5 mins of reaction. During this time period the microwave output power was set at 40% to ensure a fairly rapid attainment of the programmed parameters. After this initial 5 min period of reaction at 40% power, the MES-1000 initiated stage.2 of the reaction which involved decreasing the microwave power to 20%. In the process of this changeover, the magnetron is temporarily deactivated for 5 seconds, which results in the slight decrease in temperature and pressure observed on the plot after the 5 min reaction period. During stages 2 - 5 of the reaction, the microwave power output was maintained at 20%. This resulted in a gradual increase in temperature and pressure until either the pre-set temperature or pressure value was reached. As soon as these pre-set values were attained, the magnetron was deactivated until the fibre-optic probe or pressure sensing line detected the monitored value had again fallen below the pre-set programmed value - when the magnetron was again switched on and so on. In this way, the pre-set temperature or pressure value (whichever was attained first) was maintained for the duration of the remaining part of the reaction. Fig 5.20 shows the temperature / pressure profile for the silylation of the Creswell exinite maceral. In this instance both the temperature and pressure increased very rapidly and there is a marked increase in pressure, over the first 5 min period of reaction, compared to the silylation reaction utilising the raw Creswell coal. This, perhaps, is not surprising considering that the exinite maceral has a high volatile matter content.

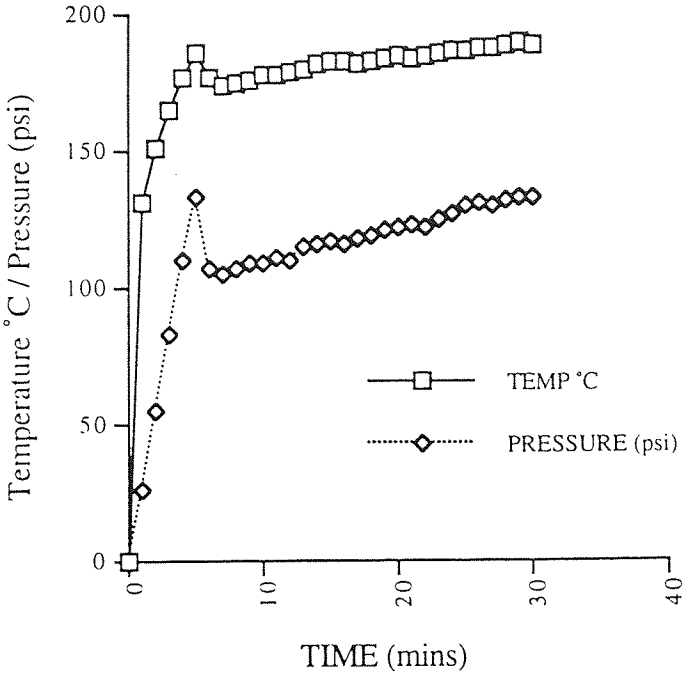

Fig5.19

Temperature / pressure profile for the silylated raw Creswell coal

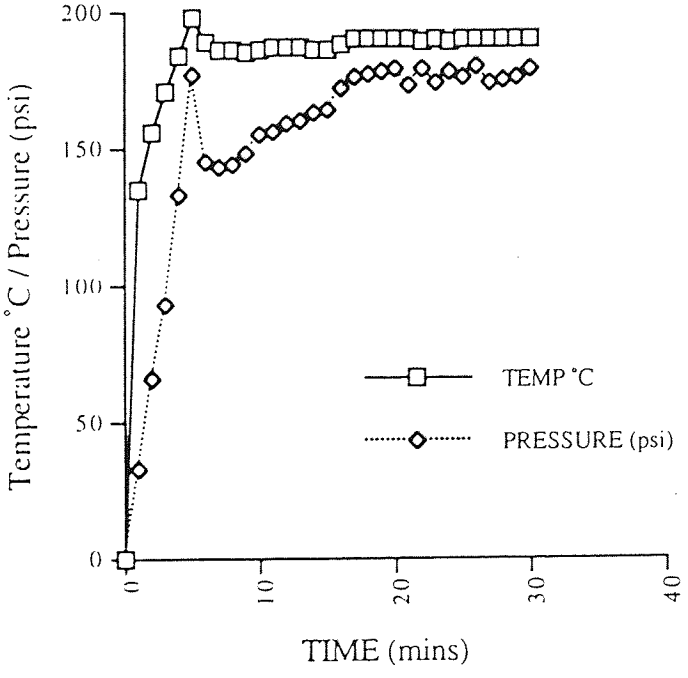

Fig5.20

Temperature / pressure profile for the silylated Creswell exinite maceral

Fig 5.21 shows the temperature / pressure profile for the silylation of the Creswell vitrinite maceral. In this case a high pressure is reached fairly rapidly. This pressure falls significantly as stage 2 of the reaction is initiated and then continues to increase gradually as the temperature is maintained at the pre-set level. Fig 5.22 shows the temperature / pressure profile for the silylation of the Creswell inertinite maceral - both temperature and pressure peak at lower values, compared to the other 2 maceral groups, after the first 5 mins of reaction. This is probably due to inertinite being generally less reactive than the other 2 macerals groups.

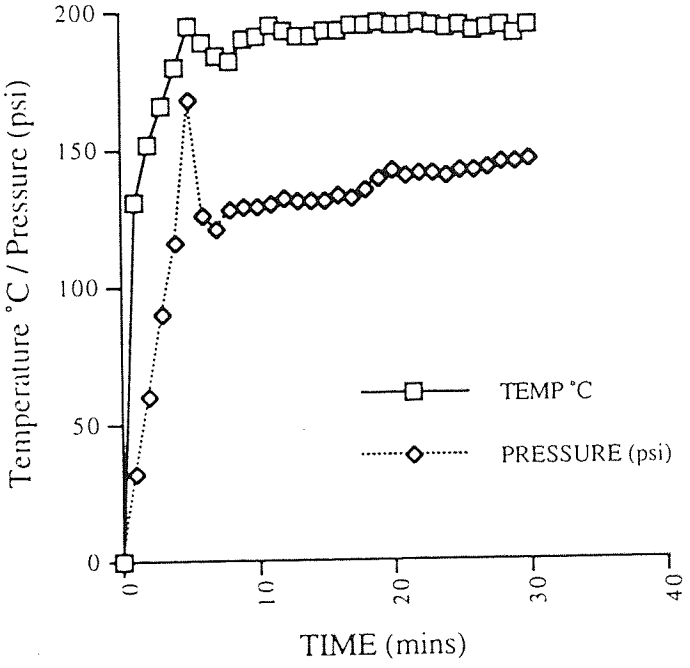

Fig5.21
Temperature / pressure profile for the silylated Creswell vitrinite maceral

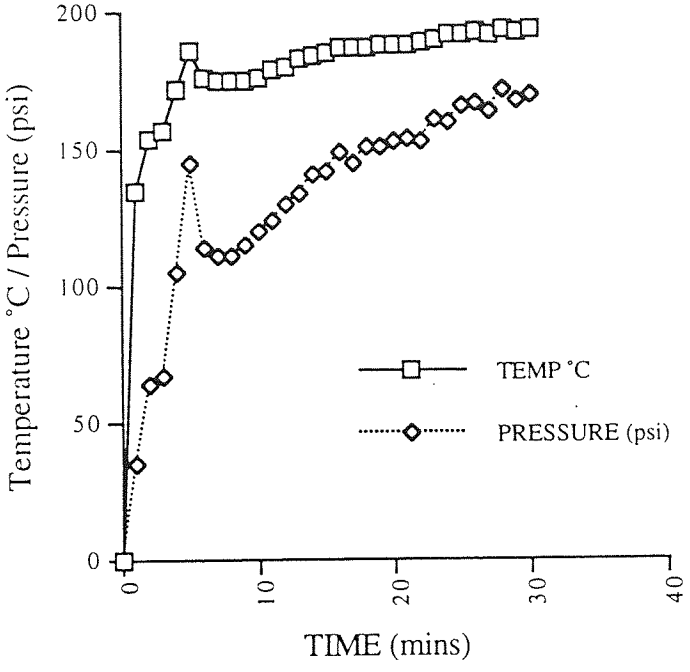

Fig5.22

Temperature / pressure profile for the silylated Creswell inertinite maceral

Fig 5.23 shows the IR plot for the silylated raw Creswell coal. There is a significant reduction in the -OH stretching frequency at 3437 cm^{-1} and the appearance of well-defined bands at 843 cm^{-1} and 1251 cm^{-1} corresponding to $-OSiCH_3$ and $-SiCH_3$ stretching respectively. Fig 5.24 shows an IR comparison of the silylated raw Creswell coal and the unreacted raw Creswell coal - the differences between the 2 structures are much more apparent in this plot. Fig 5.25 shows the IR plot of the silylated Creswell exinite maceral. Again, there are bands corresponding to $-OSiCH_3$ (841 cm^{-1}) and $-SiCH_3$ (1250 cm^{-1}) and there is also a decrease in the -OH stretching frequency centred at 3449 cm^{-1}. Fig 5.26 shows the IR plot of the silylated Creswell vitrinite maceral - again the peaks denoting silylation has occurred are apparent at 842 cm^{-1} and 1251 cm^{-1} and there is also a decrease in the -OH stretching frequency centred at 3442 cm^{-1}. Fig 5.27 shows the IR plot of the silylated Creswell inertinite maceral - the peaks expected due silylation are absent and there appears to be no appreciable change in the band due to -OH stretching at 3408 cm^{-1}. Fig 5.28 shows an IR comparison of the attempted silylation of Creswell inertinite and the unreacted Creswell inertinite maceral. The plot shows that there is no significant difference between the two spectra indicating that silylation of the Creswell inertinite maceral was unsuccessful. Fig 5.29 shows a multispectral IR plot of the 3 silylated Creswell maceral groups - the Creswell exinite and vitrinite maceral groups clearly show signs of silylation, whereas the Creswell inertinite maceral group appears to show no change. Table 5.04 summarises the IR results.

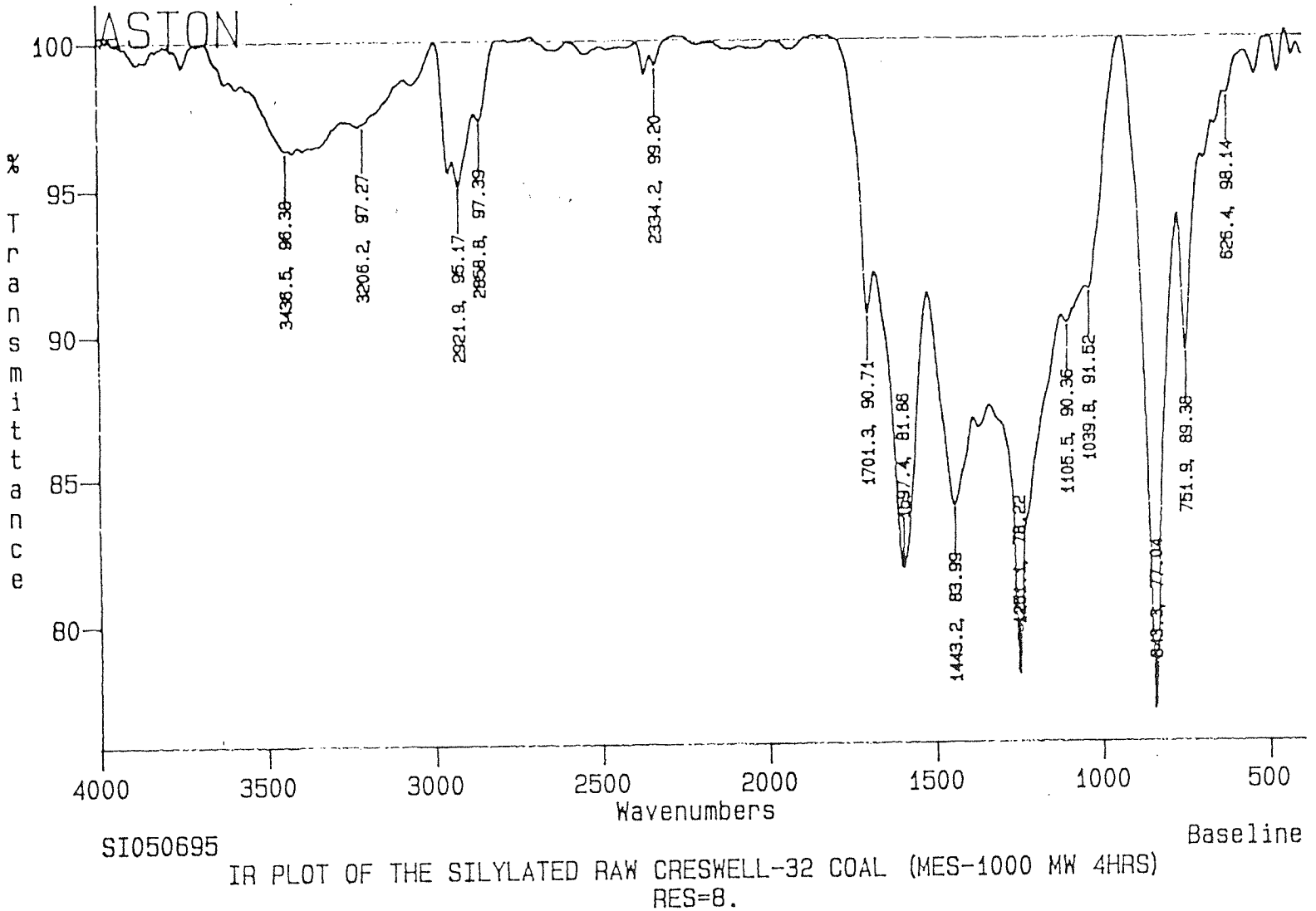

Fig5.23
IR of the silylated raw Creswell coal (4 hrs mw heating)

Fig5.24
IR comparison of the silylated raw Creswell coal
and the unreacted raw Creswell coal

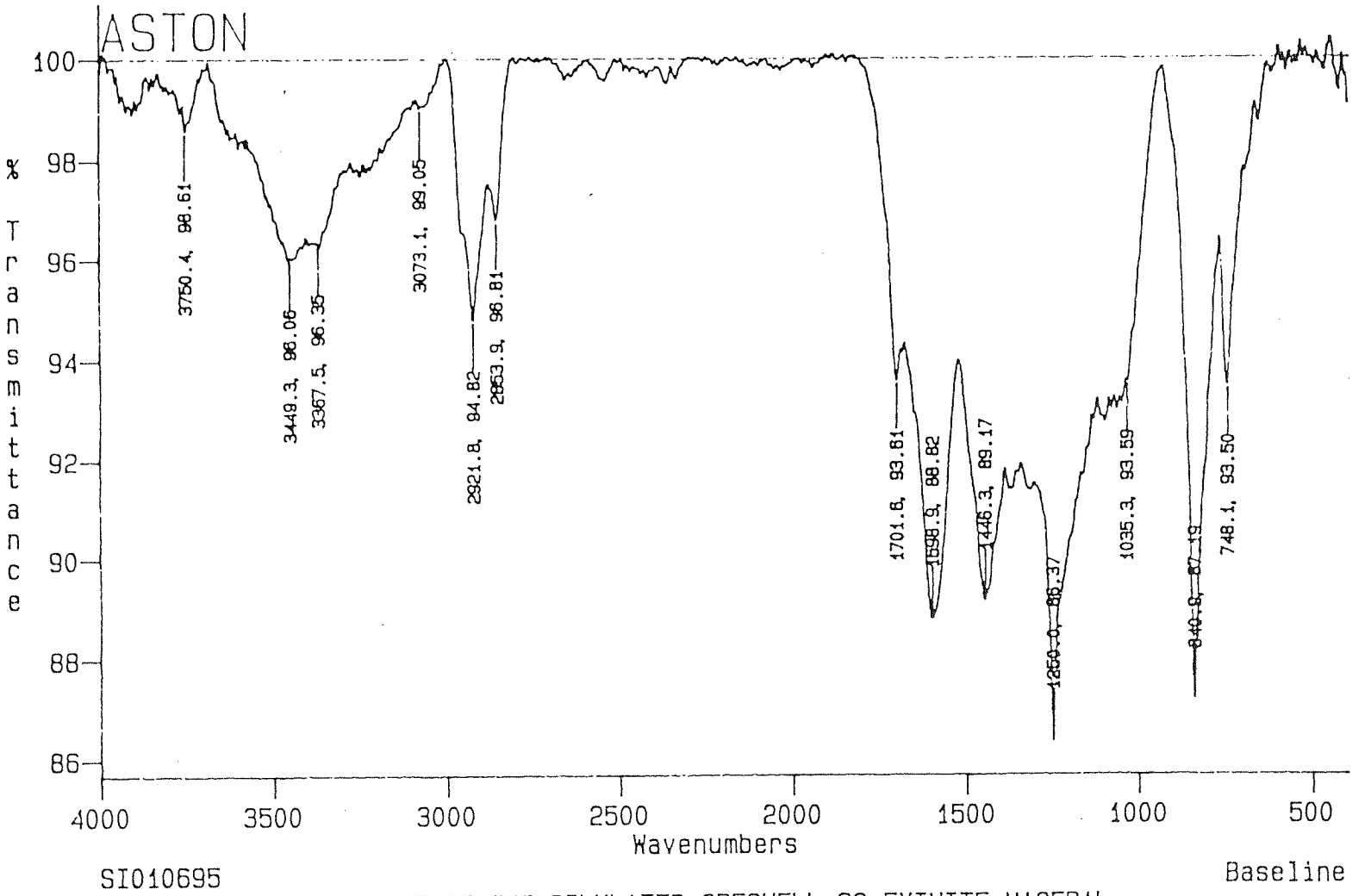

IR PLOT OF THE SILYLATED CRESWELL-32 EXINITE MACERAL
RES=8.

Fig5.25
IR of the silylated Creswell exinite maceral

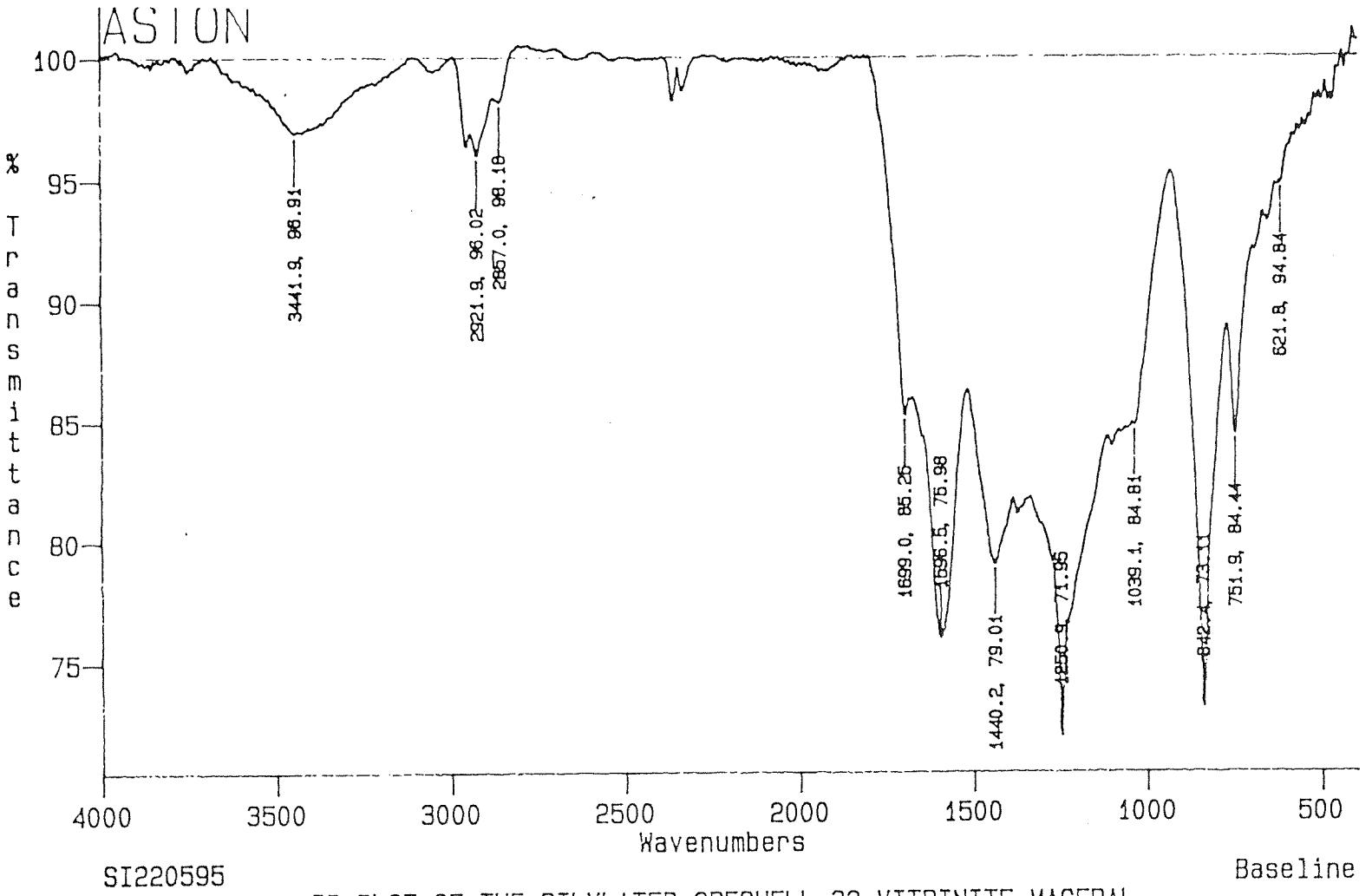

Fig5.26
IR of the silylated Creswell vitrinite maceral

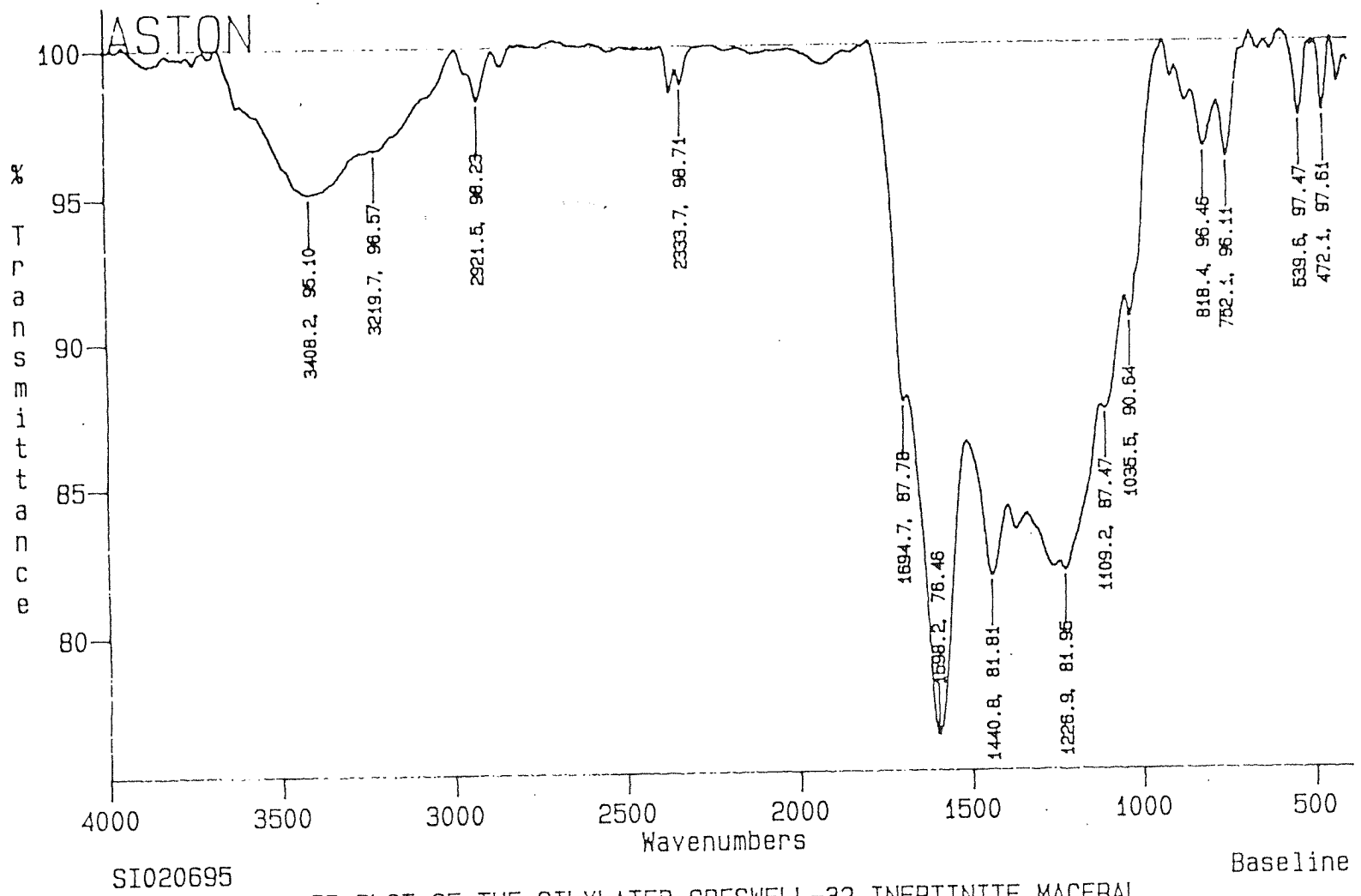

Fig5.27
IR of the silylated Creswell inertinite maceral

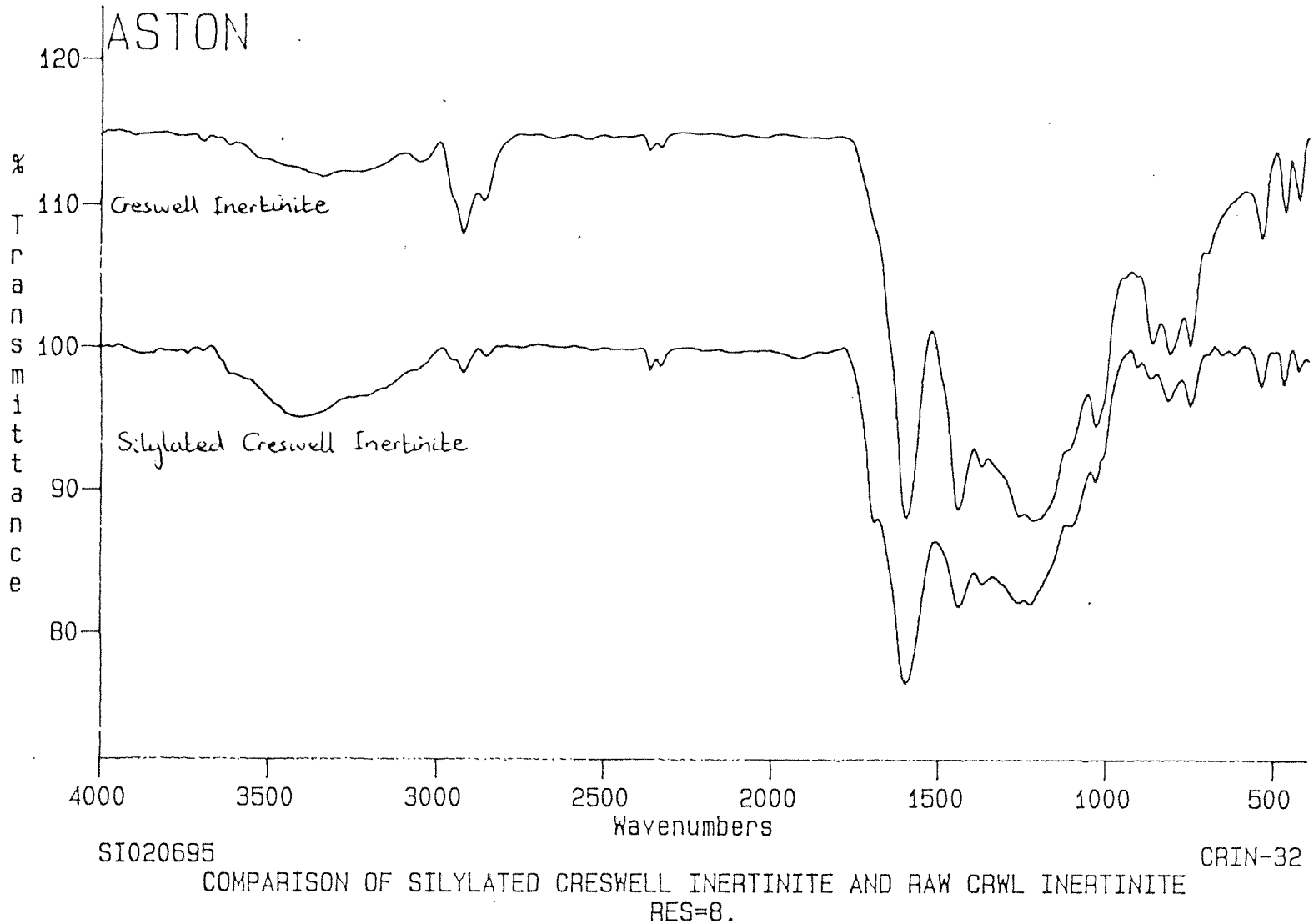

Fig5.28
IR comparison of the silylated Creswell inertinite
and the unreacted Creswell inertinite

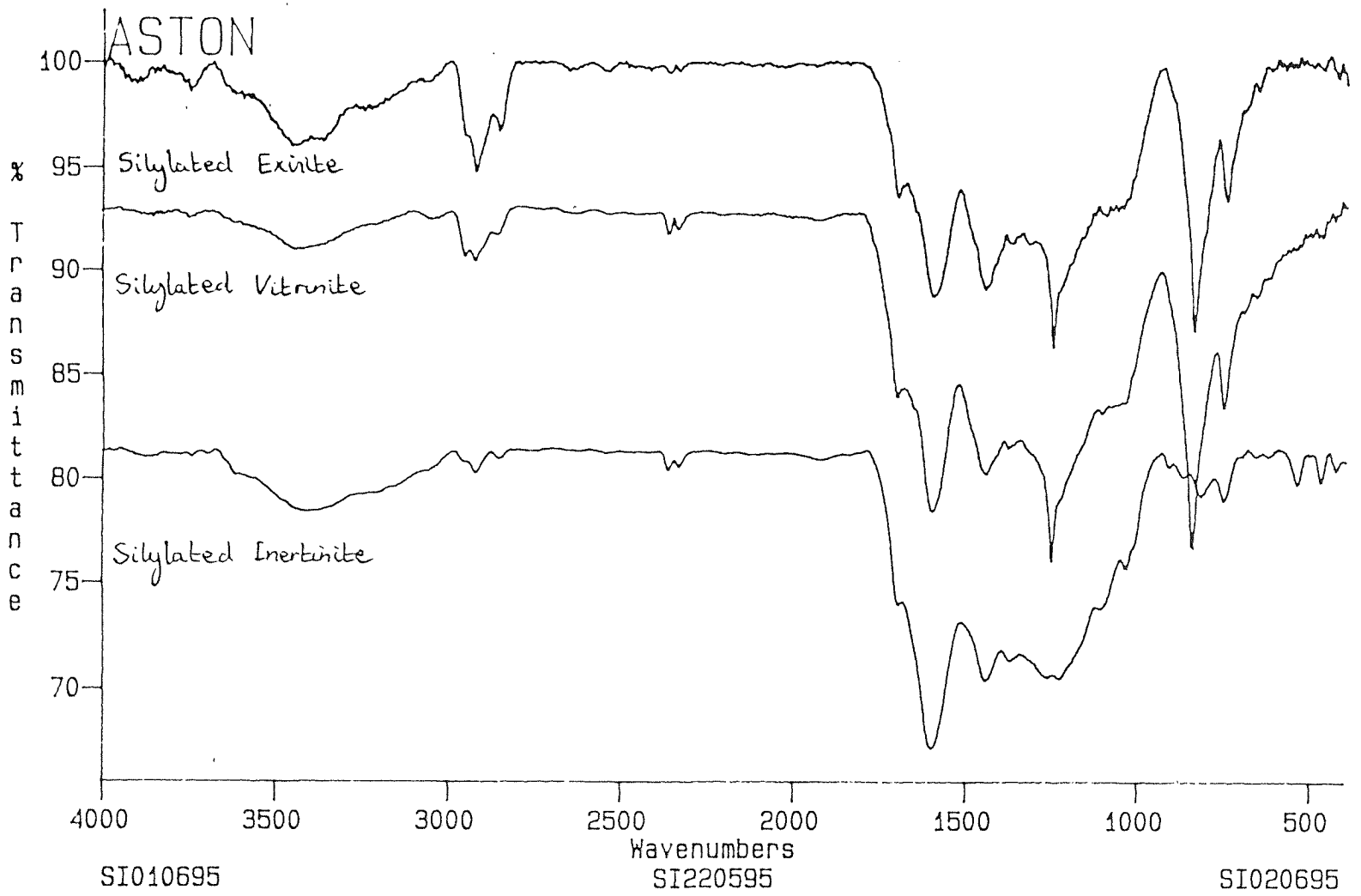

Fig5.29
IR comparison of the silylated Creswell macerals

Table 5.04

Summary of the IR results for the silylation of the Creswell coal and Creswell macerals

Silylated coal / coal macerals	$\upsilon(-OSiCH_3)$	$\upsilon(-SiCH_3)$	$\upsilon(-OH)$
Creswell coal	843 cm^{-1}	1251 cm^{-1}	3436 cm^{-1}
Creswell exinite	840 cm^{-1}	1250 cm^{-1}	3449 cm^{-1}
Creswell vitrinite	842 cm^{-1}	1250 cm^{-1}	3441 cm^{-1}
Creswell inertinite	———	———	3408 cm^{-1}

The silylated raw Creswell coal and Creswell macerals were analysed by quantitative ^{29}Si MASNMR to determine the extent of silylation. All ^{29}Si resonances are reported relative to tetramethylsilane (TMS). Fig 5.30 shows the nmr spectrum for the silylated raw Creswell coal. The major resonance occurs at 20.2 ppm corresponding to the formation of silylated phenols of moderate steric hindrance. There is also a higher field signal at 8.2 ppm - this is due to the formation of $(CH_3)_3SiOH$ (trimethyl silanol), which is believed to be a hydrolysis by-product. The peak at -93.1 ppm is due to the laponite standard. Fig 5.31 shows the ^{29}Si nmr spectrum for the silylated Creswell exinite maceral. The peak due to the silylated phenol groups is apparent at 17.4 ppm, as is the peak due to trimethyl silanol formation at 6.6 ppm. The laponite resonant peak is evident at -94.3 ppm. Fig 5.32 shows the ^{29}Si nmr spectrum for the silylated Creswell vitrinite maceral. The three major resonances are at 20.6 ppm, 7.9 ppm and -93.2 ppm corresponding to silylated phenols, trimethyl silanol and the laponite standard respectively. Fig 5.33 shows the ^{29}Si nmr spectrum for the silylated Creswell inertinite maceral. In this case silylation does not appear to have taken place - there is only one main resonance peak at -93.5 ppm due to the laponite standard. It is interesting to note that the resonance due to the formation of trimethyl silanol is also absent. This may be due to the fact that inertinite is largely made up of condensed aromatic units and has a low H / C ratio compared to the other 2 maceral groups - these units probably have less affinity for moisture and are probably easier to dry compared to structures found in the other 2 maceral groups - we would also expect inertinite to contain less -OH than the exinite and vitrinite maceral groups.

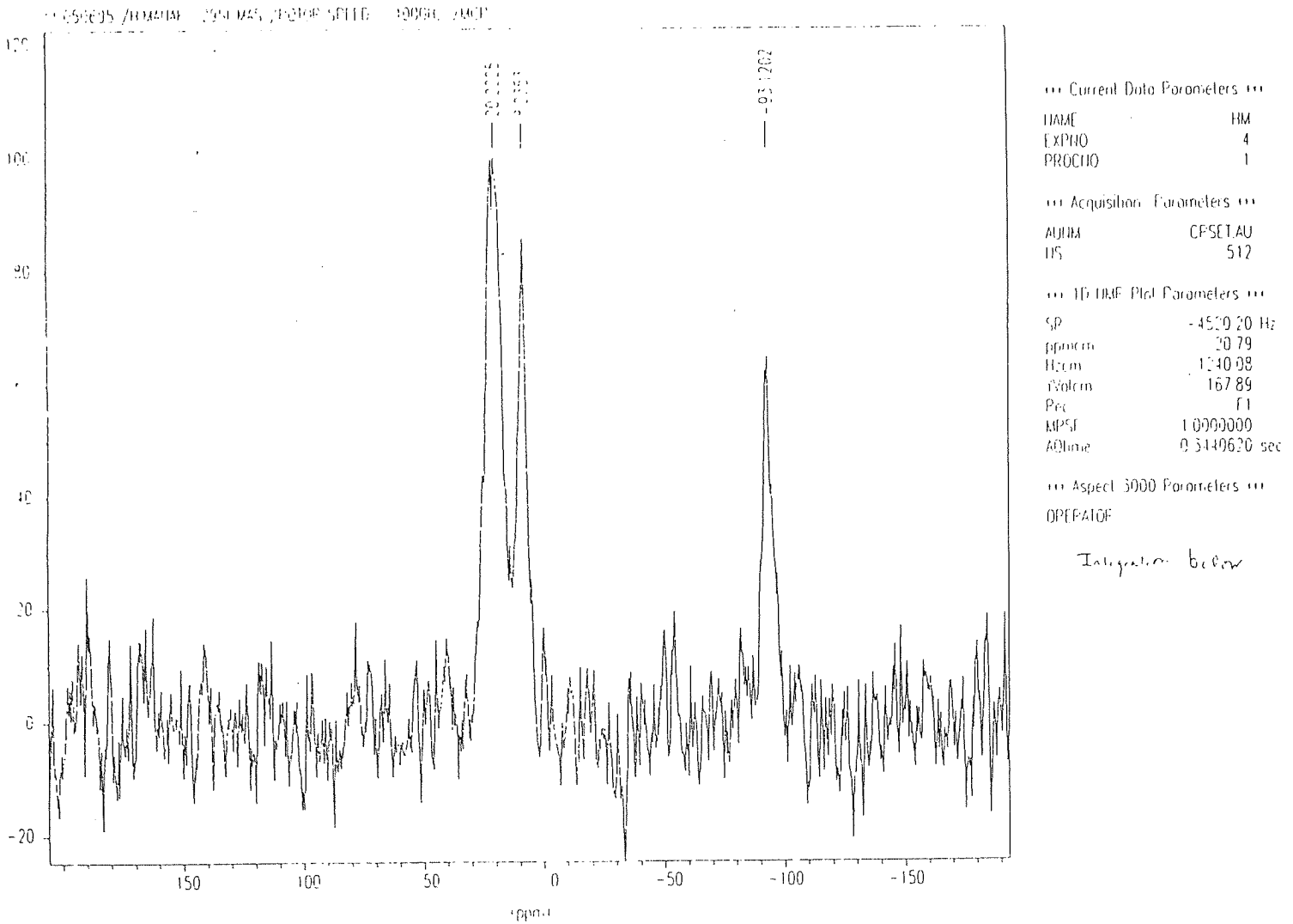

Fig5.30
Quantitative ^{29}Si MASNMR of the silylated raw Creswell coal

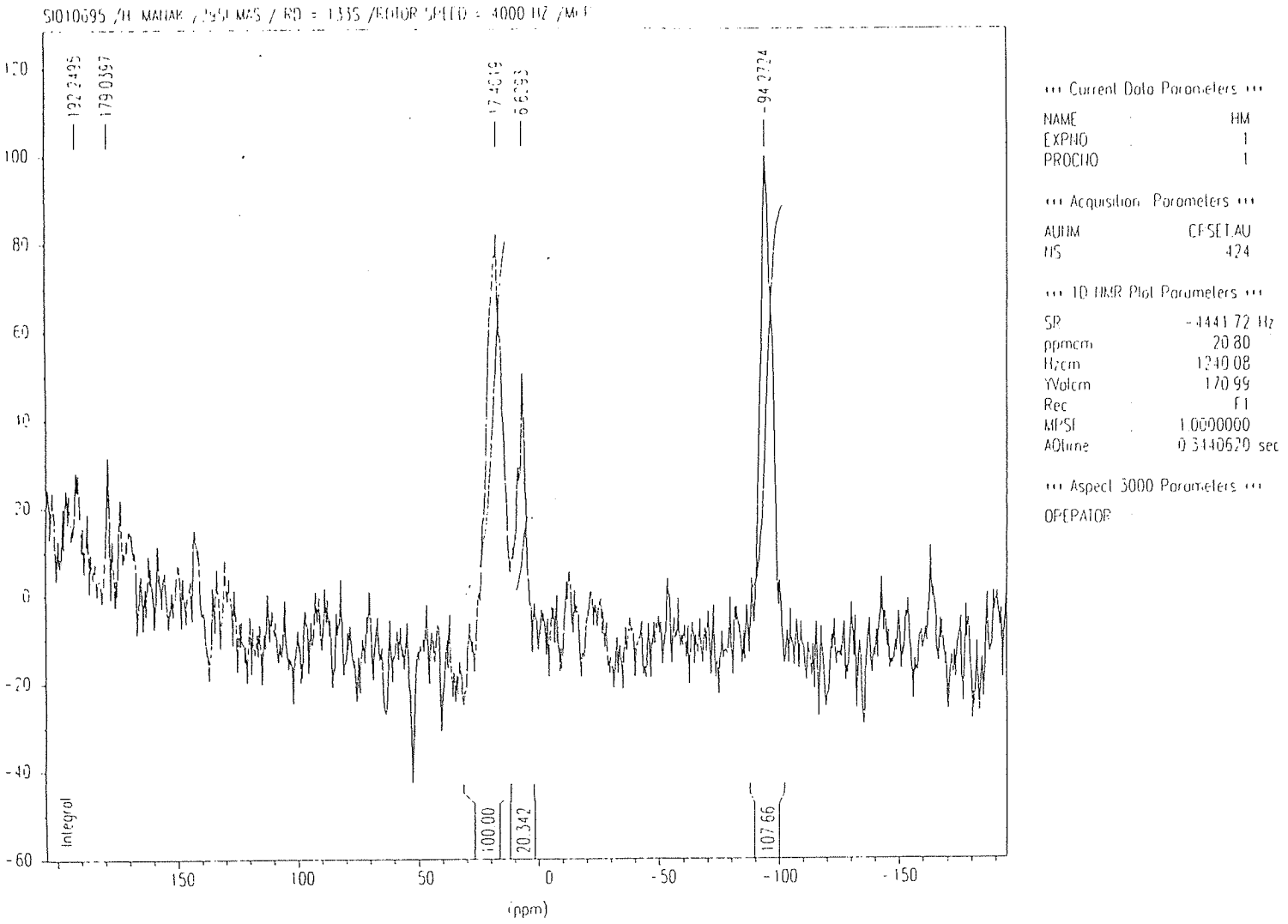

Fig5.31
Quantitative ^{29}Si MASNMR of the silylated Creswell exinite maceral

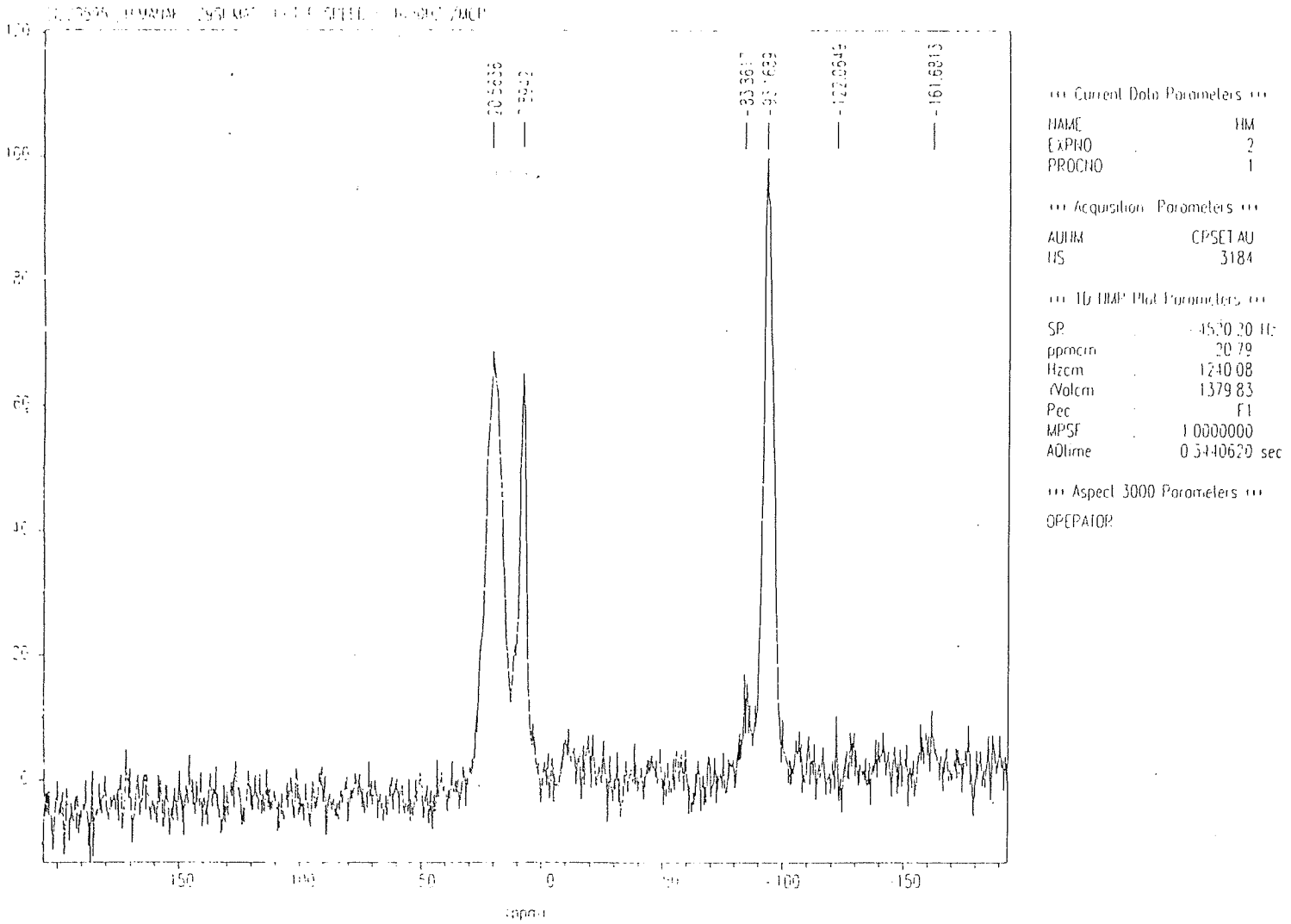

Fig5.32
Quantitative ^{29}Si MASNMR of the silylated Creswell vitrinite maceral

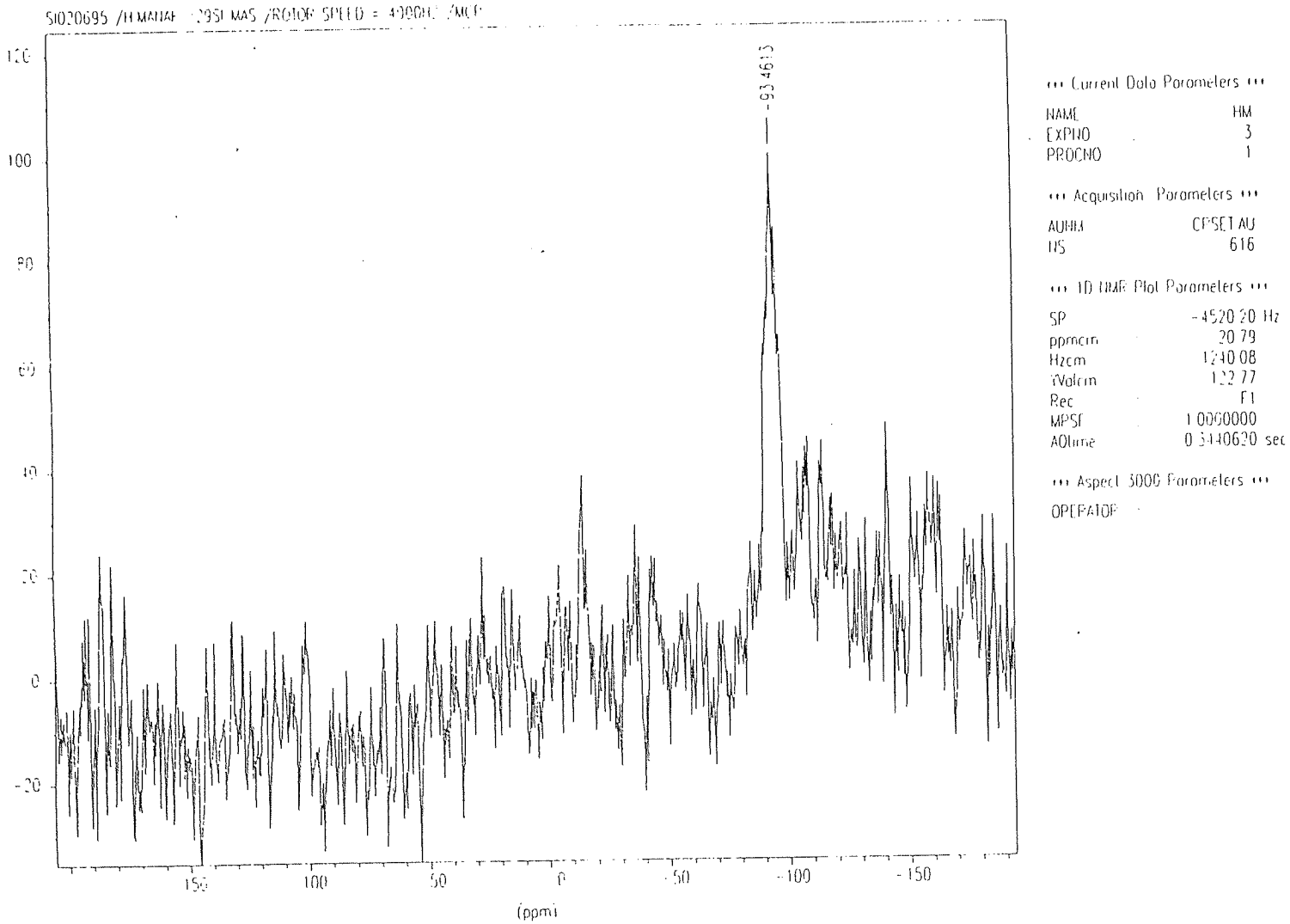

Fig5.33
Quantitative ^{29}Si MASNMR of the silylated Creswell inertinite maceral

Table 5.05 summarises the results obtained from the quantitative ^{29}Si MASNMR analysis of the silylated raw Creswell and silylated Creswell macerals.

Table 5.05
Resonant peaks from the ^{29}Si MASNMR analysis of the silylated Creswell raw coal and silylated Creswell coal macerals

Silylated coal / coal macerals	Resonance due to silylated phenols (ppm)	Resonance due to $(CH_3)_3SiOH$ (ppm)	Resonance due to laponite standard (ppm)
Creswell coal	20.2	8.2	-93.1
Creswell exinite	17.4	6.6	-94.3
Creswell vitrinite	20.6	7.9	-93.2
Creswell inertinite	___	___	-93.5

Table 5.06 shows the integration values obtained for the silylated raw Creswell and Creswell macerals and the laponite standards.

Table 5.06
Integration values from ^{29}Si MASNMR for the silylated Creswell coal and Creswell macerals and the laponite standards

Silylated coal / coal macerals	Signal area of silylated coal / coal maceral	Signal area of laponite standard
Creswell coal	458.31	180.00
Creswell exinite	100.00	107.66
Creswell vitrinite	194.62	180.00
Creswell inertinite	_____	_____

Because of the poor spectral quality i.e the poor baseline plots in the ^{29}Si MASNMR spectra, it was decided to calculate the % O (as phenolic -OH) silylated in the Creswell coal and coal macerals using four different techniques :

1. Using the computer integration values from the normal ^{29}Si MASNMR spectra
2. Using a "cut-out-and-weigh" method on the normal ^{29}Si MASNMR spectra
3. Using the computer integration values from the deconvoluted ^{29}Si MASNMR spectra
4. Using a "cut-out-and-weigh" method on the deconvoluted ^{29}Si MASNMR spectra

The results were calculated using the following equation :

$$\% \ O = (M_O / m_C).(m_S / M_S).(I_C / I_S) \times 100\%$$

where M_O = atomic weight of oxygen
m_C = weight of silylated coal
m_S = weight of standard
M_S = molecular weight of standard
I_C = signal area of silylated coal
I_S = signal area of standard

The calculations (using technique No.1) for the silylated Creswell coal and coal macerals can be found in Appendix III.

The % O (as phenolic -OH) in the silylated creswell coal and macerals was also calculated using an alternative method, whereby the relevant silylated coal and laponite standard peaks were expanded, cut out using scissors and weighed (to 3 decimal places) to give the relative signal area of each peak (technique No.2). This method assumes that the density of the plot-paper is uniform. Table 5.07 shows the results obtained using this method.

Table 5.07

Results from the weighings of the silylated coal and laponite standard peaks for the Creswell coal and Creswell macerals

Coal / Coal Maceral	Weight of silylated coal peak / g	Weight of laponite standard peak / g
Creswell raw coal	0.128	0.051
Creswell exinite maceral	0.120	0.092
Creswell vitrinite maceral	0.091	0.077
Creswell inertinite maceral	——	——

The values from Table 5.07 were used to calculate alternative % O values for the silylated Creswell coal and coal macerals. The calculations (using technique No.2) for the silylated Creswell raw coal and silylated Creswell macerals can be found in Appendix III.

The silylated Creswell coal and Creswell maceral ^{29}Si MASNMR spectra were also deconvoluted and the values for the extent of silylation (using both computer integration (technique No.3) and weighing methods (technique No.4)) utilising this technique were compared to those obtained from the normal ^{29}Si MASNMR spectra. Figs 5.34 - 5.36 show the deconvoluted ^{29}Si plots for the silylated raw Creswell, the silylated Creswell exinite and the silylated Creswell vitrinite respectively. Table 5.08 shows the integration values obtained from the deconvoluted plots.

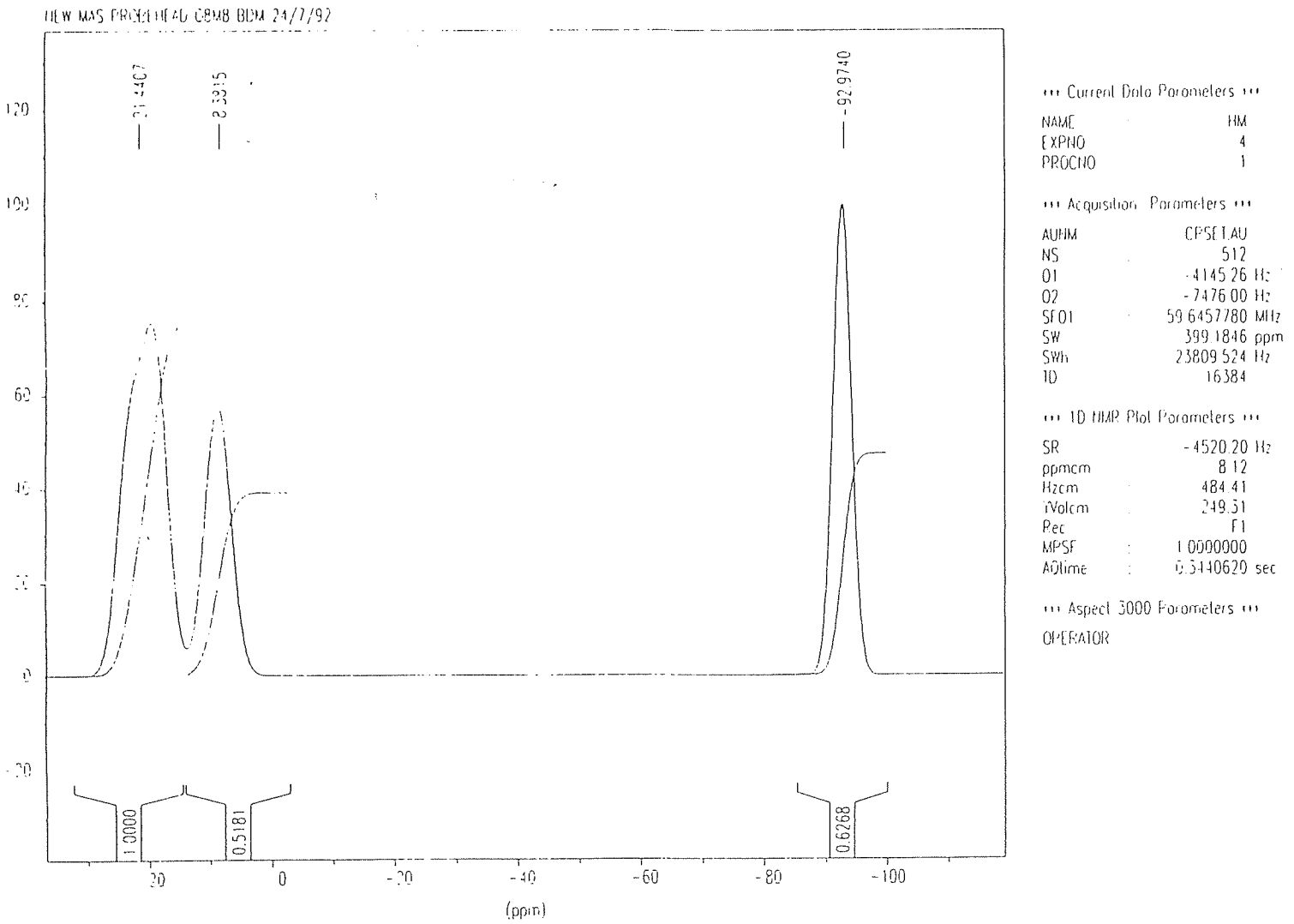

Fig5.34
Deconvoluted ^{29}Si MASNMR spectrum for the silylated raw Creswell coal

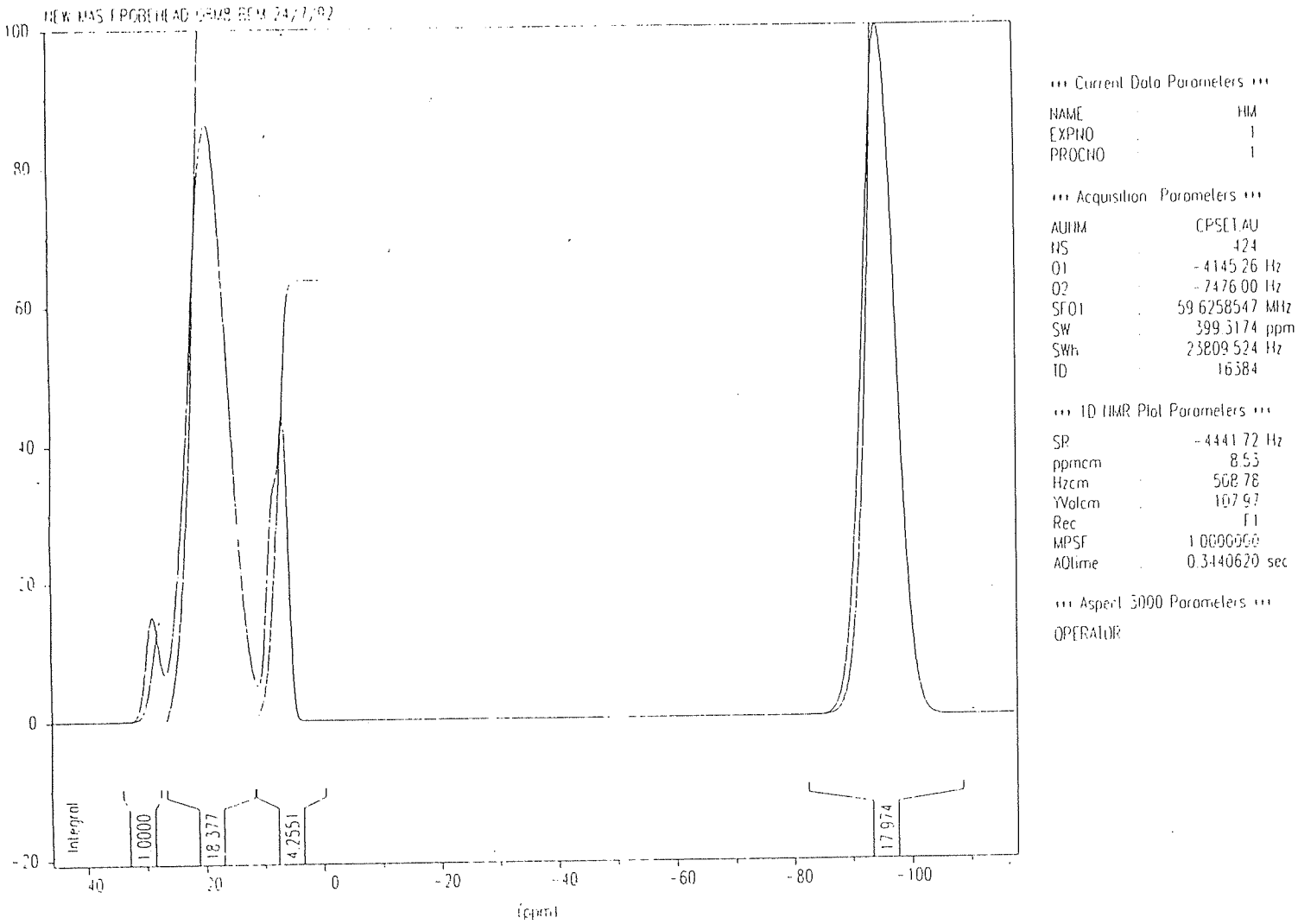

Fig5.35
Deconvoluted ^{29}Si MASNMR spectrum for the silylated Creswell exinite maceral

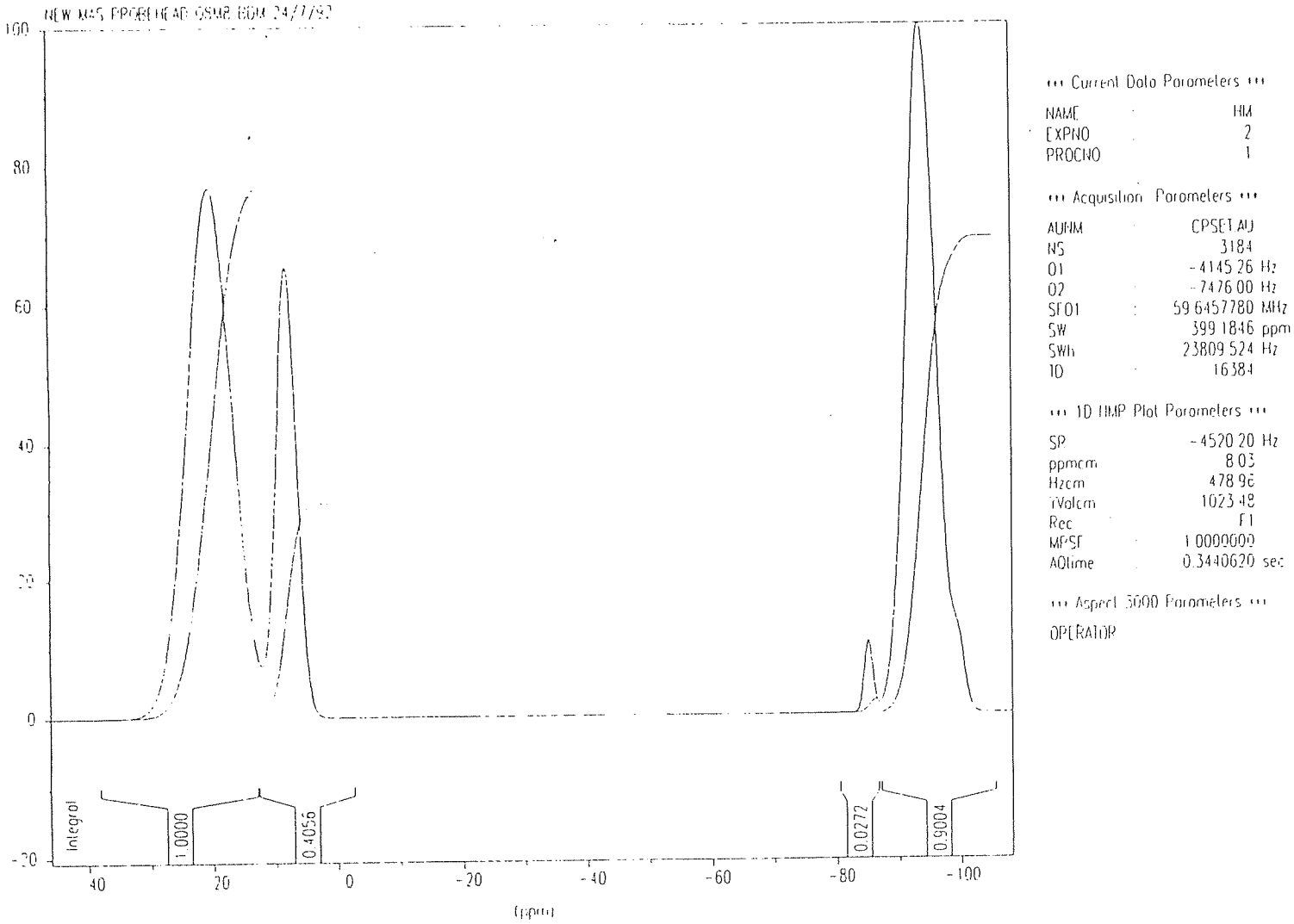

Fig5.36
Deconvoluted ^{29}Si MASNMR spectrum for the silylated Creswell vitrinite maceral

Table 5.08

Integration values from the deconvoluted ^{29}Si MASNMR spectra for the silylated Creswell coal and Creswell macerals and the laponite standards

Silylated coal / coal macerals	Signal area of silylated coal / coal maceral	Signal area of laponite standard
Creswell coal	1.0000	0.6268
Creswell exinite	1.0000	0.9276
Creswell vitrinite	1.0000	0.9004
Creswell inertinite	———	———

The deconvoluted spectra were expanded and the relevant silylated coal and laponite standard peaks were cut out and weighed (to 3 dp) to give the relevant signal area of each peak. Table 5.09 shows the results from the weighings.

Table 5.09

Results from the weighings (deconvolution method) of the silylated coal and laponite standard peaks for the Creswell coal and Creswell macerals

Coal / Coal Maceral	Weight of silylated coal peak / g	Weight of laponite standard peak / g
Creswell raw coal	0.049	0.041
Creswell exinite maceral	0.080	0.093
Creswell vitrinite maceral	0.088	0.090
Creswell inertinite maceral	———	———

From the figures in Tables 5.08 and 5.09 the % O (as phenolic -OH) was calculated for the silylated Creswell coal and Creswell macerals (using the deconvolution method). Tables 5.10 and 5.11 summarise the results from the silylation of the Creswell coal and Creswell macerals. It is obvious that techniques No.1 and No.2 (using the normal ^{29}Si MASNMR spectra) are giving nonsense results because of the uncertainty attached to where the baseline is taken. Deconvolution of the ^{29}Si MASNMR spectra, however, produced better results. This is probably due to averaging of the ^{29}Si MASNMR spectra to give a better approximation for the baseline.

Table 5.10

Results for the % O (as phenolic -OH) from the silylation of the Creswell coal and Creswell macerals

Coal / Coal Maceral	Total % O_{dmmf}	Results from Silylation (normal spectra)		Results from Silylation (deconvoluted spectra)	
		Technique No.1 % O (as -OH) Integration method	Technique No.2 % O (as -OH) Weighing method	Technique No.3 % O (as -OH) Integration method	Technique No.4 % O (as -OH) Weighing method
Creswell raw coal	5.6	9.9	9.8	6.2	4.7
Creswell exinite	4.9	9.0	12.7	10.5	8.3
Creswell vitrinite	8.2	4.9	5.4	5.0	4.4
Creswell inertinite	7.6	—	—	—	—

Table 5.11

The results for the % O_{OH} / O_{total} from the silylation of the Creswell coal and Creswell macerals

Coal / Coal Maceral	Results from Silylation (normal spectra)		Results from Silylation (deconvoluted spectra)	
	Technique No.1 % O_{OH} / O_{total} Integration method	Technique No.2 % O_{OH} / O_{total} Weighing method	Technique No.3 % O_{OH} / O_{total} Integration method	Technique No.4 % O_{OH} / O_{total} Weighing method
Creswell raw coal	177	175	111	84
Creswell exinite	184	259	214	169
Creswell vitrinite	60	66	61	54
Creswell inertinite	—	—	—	—

5.3.3 Silylation of Cortonwood and Cortonwood macerals

The Cortonwood coal and coal macerals (≤ 32μm) were dried under N_2 at 110°C for between 2-3 days before silylation was attempted. The Cortonwood coal and its macerals were all reacted for 4 hrs in the MES-1000 microwave oven, after which the product was isolated and analysed by FT-IR and quantitative ^{29}Si MASNMR (as outlined in section 5.2) to determine the extent of silylation. The parameters programmed into the MES-1000 microwave oven were the same for each reaction to ensure that standard conditions were maintained throughout. Table 5.12 shows the MES-1000 reaction parameters used.

Table 5.12

MES-1000 reaction parameters used for the silylation of the Cortonwood coal and coal macerals

STAGE	1	2	3	4	5
Power (%)	40	20	20	20	20
Pressure (psi)	180	180	180	180	180
Run time (mins)	05	60	60	60	60
Temperature (°C)	200	200	200	200	200

Fig 5.37 shows the temperature / pressure profile with respect to time (for the first 30 mins of reaction) for the silylation reaction of the raw Cortonwood coal. As with the silylation of the raw Creswell coal, there is a sharp increase in temperature and an associated linear increase with pressure during the first stage of reaction. After 5 mins there is a slight decrease in temperature and a corresponding decrease in pressure due to deactivation of the magnetron for a short time before initiation of the second stage of the reaction. During this second stage of reaction the temperature and pressure both increased gradually until the pre-set values were attained. Figs 5.38, 5.39 and 5.40 show the temperature / pressure profiles for the silylation of the Cortonwood exinite, vitrinite and inertinite macerals respectively.

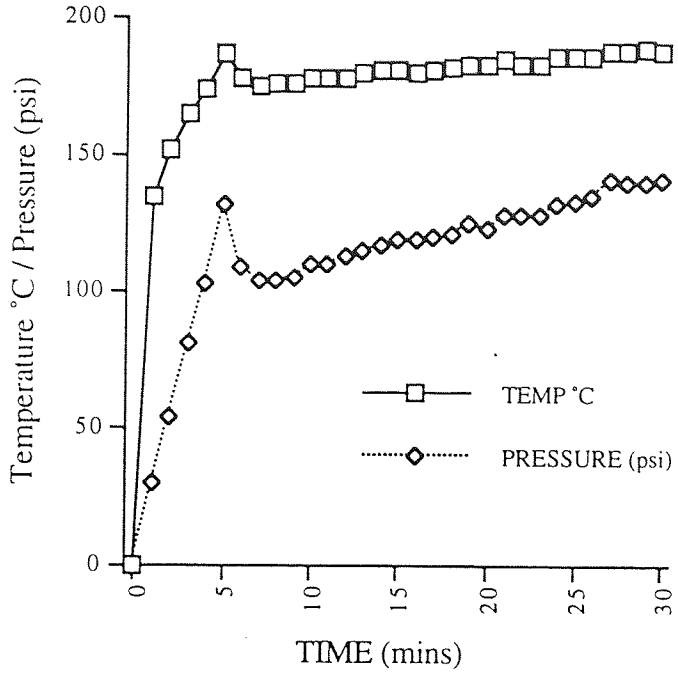

Fig5.37

Temperature / pressure profile for the silylated raw Cortonwood coal

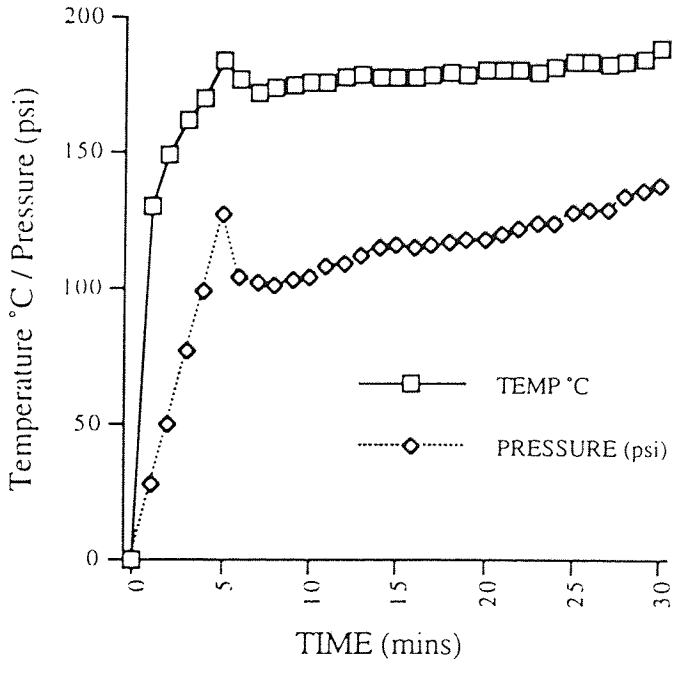

Fig5.38

Temperature / pressure profile for the silylated Cortonwood exinite maceral

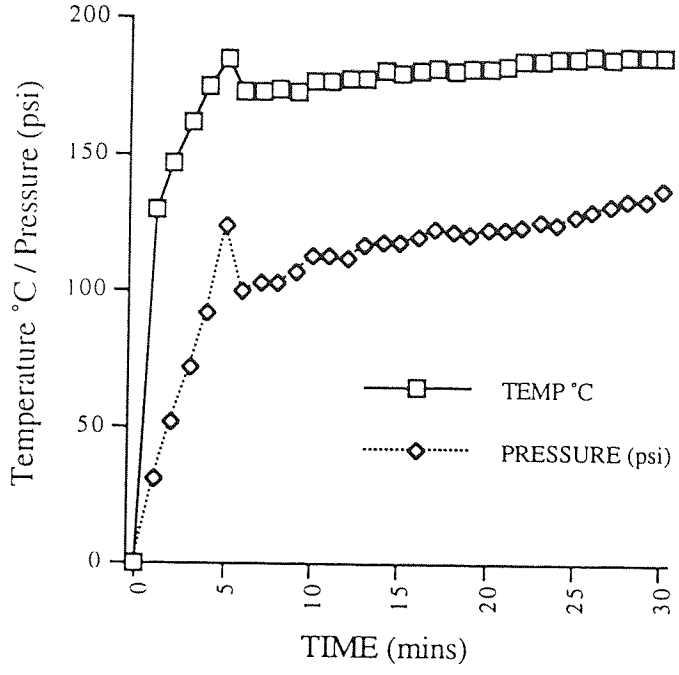

Fig5.39

Temperature / pressure profile for the silylated Cortonwood vitrinite maceral

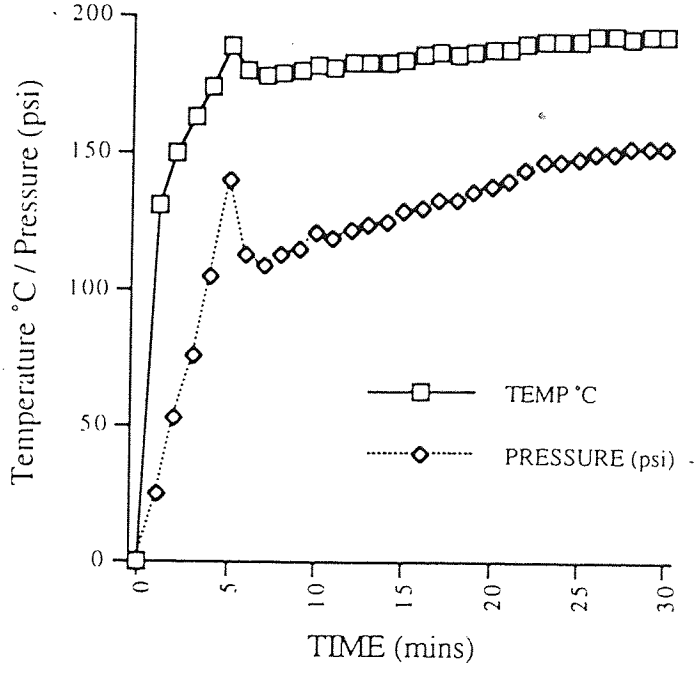

Fig5.40

Temperature / pressure profile for the silylated Cortonwood inertinite maceral

All these plots have similar curves and there are no significant differences between these plots and silylation of the bulk coal. There were, however, noticeable differences in the temperature / pressure profiles for the Creswell coal and Creswell macerals. This could be a possible indication of the relative unreactivity of the Cortonwood coal and coal macerals compared to the Creswell and Creswell coal macerals.

Fig 5.41 shows the IR plot for the silylated raw Cortonwood coal. There is a significant reduction in the -OH stretching band at 3429 cm^{-1} and distinct bands due to $-OSiCH_3$ and $-SiCH_3$ appear at 842 cm^{-1} and 1250 cm^{-1} respectively. Fig 5.42 shows an IR comparison of the silylated raw Cortonwood coal and the unreacted raw Cortonwood coal - the differences between the 2 structures are much more apparent in this plot. Fig 5.43 shows the IR plot of the silylated Cortonwood exinite maceral. In this instance there is still a significant band due to -OH stretching centred at 3444 cm^{-1}, but peaks due to $-OSiCH_3$ (841 cm^{-1}) and $-SiCH_3$ (1250 cm^{-1}) are also present. These peaks due to silylation are not as sharp as observed in previous IR spectra of silylated coals and coal macerals. Fig 5.44 shows the IR spectrum of the silylated Cortonwood vitrinite maceral - there is a large reduction in the -OH stretching band centred at 3447 cm^{-1} and very well-defined peaks at 842 cm^{-1} and 1250 cm^{-1} denoting silylation has been successful. Fig 5.45 shows the IR spectrum of the silylated Cortonwood inertinite maceral - again there is a noticeable reduction in the -OH stretching band at 3448 cm^{-1} and the appearance of distinct bands at 844 cm^{-1} and 1252 cm^{-1} indicating that silylation has occurred. Fig 5.46 shows a multispectral IR plot of the 3 silylated Cortonwood maceral groups - all show absorptions (at approximately 840 cm^{-1} and 1250 cm^{-1}) denoting that silylation has taken place. The silylated Cortonwood exinite maceral, however, does not appear to have achieved the same extent of silylation as the other two maceral groups. Table 5.13 summarises the IR results.

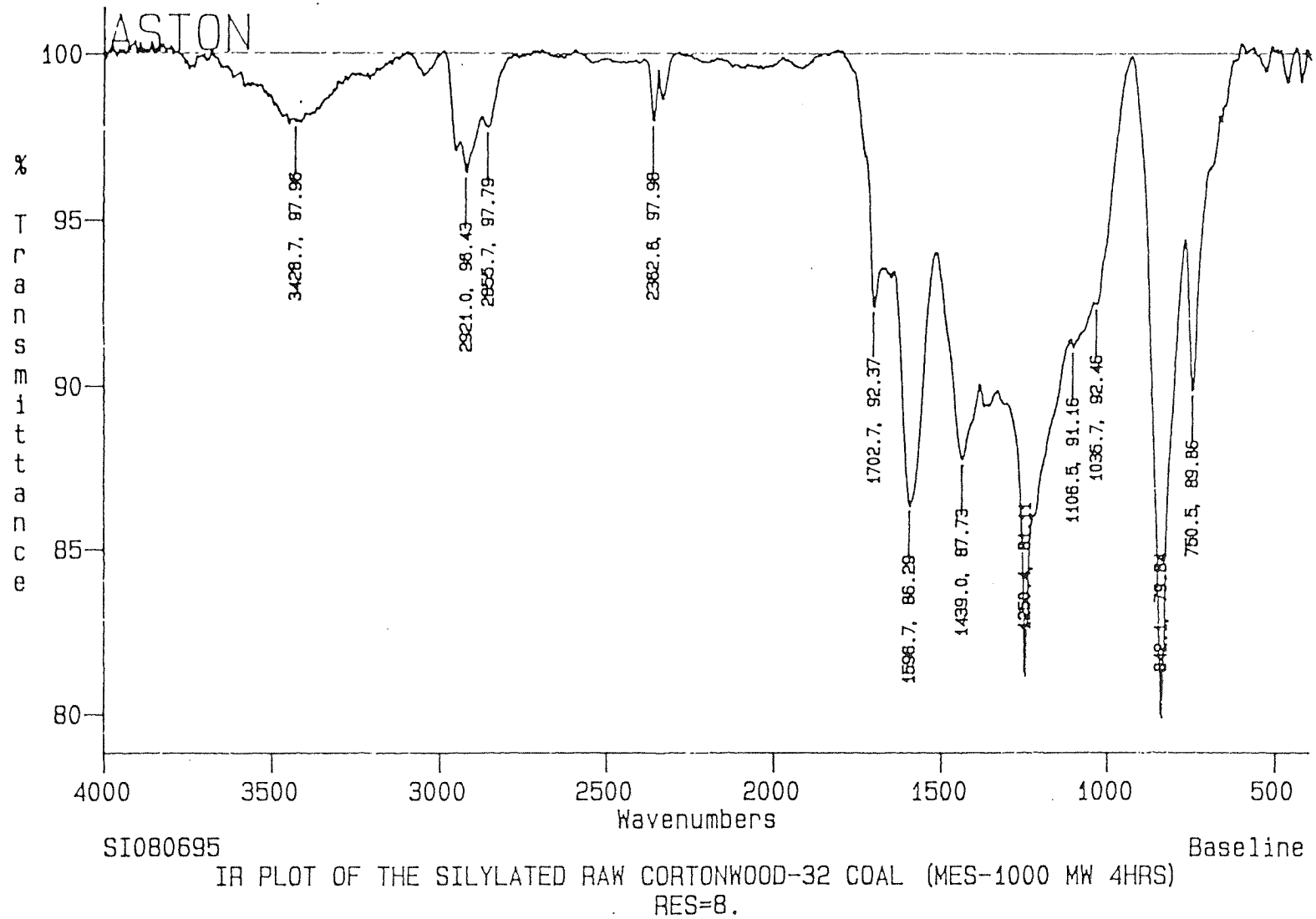

Fig5.41
IR of the silylated raw Cortonwood coal (4 hrs mw heating)

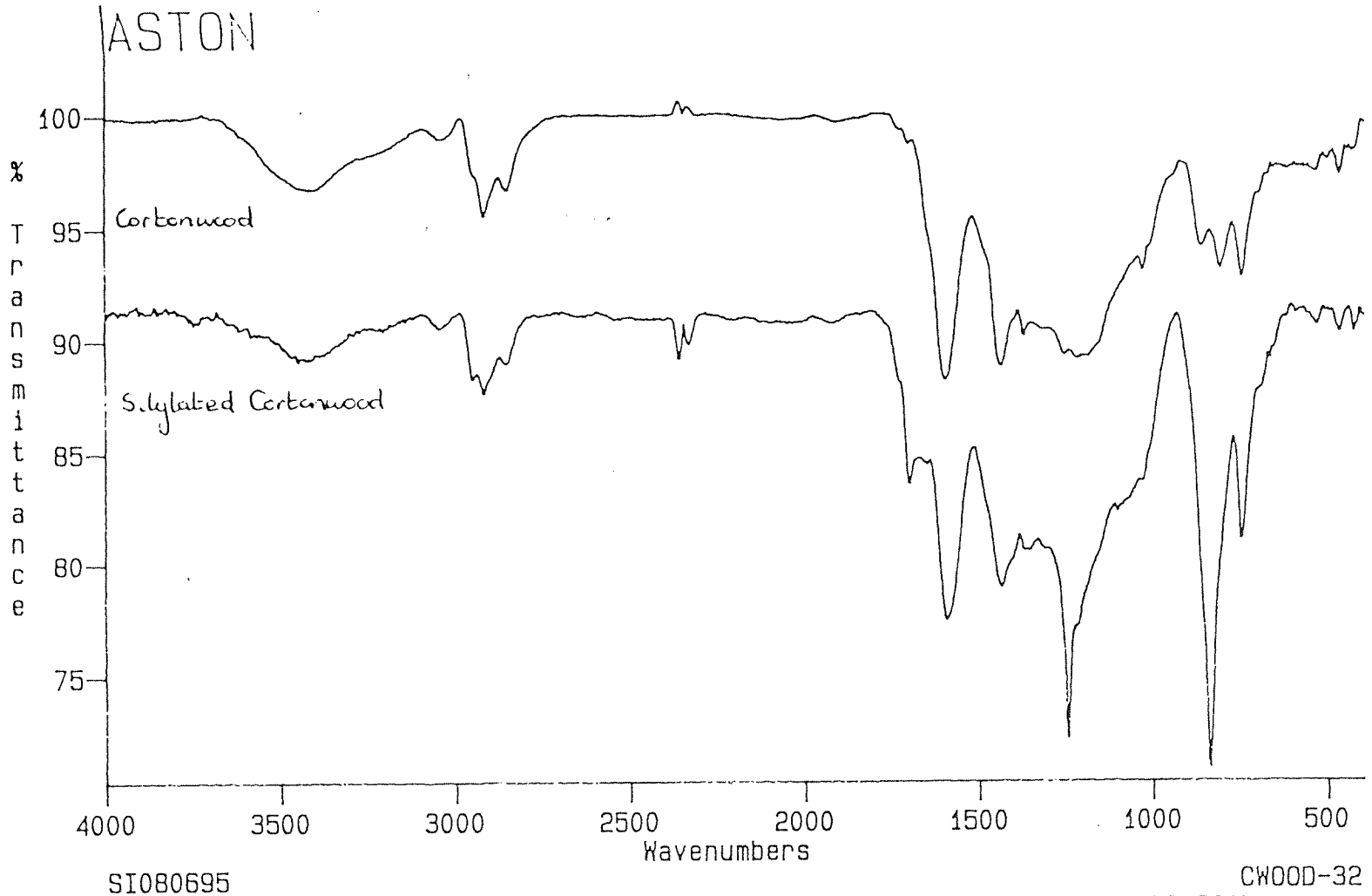

Fig5.42
IR comparison of the silylated raw Cortonwood coal
and the unreacted raw Cortonwood coal

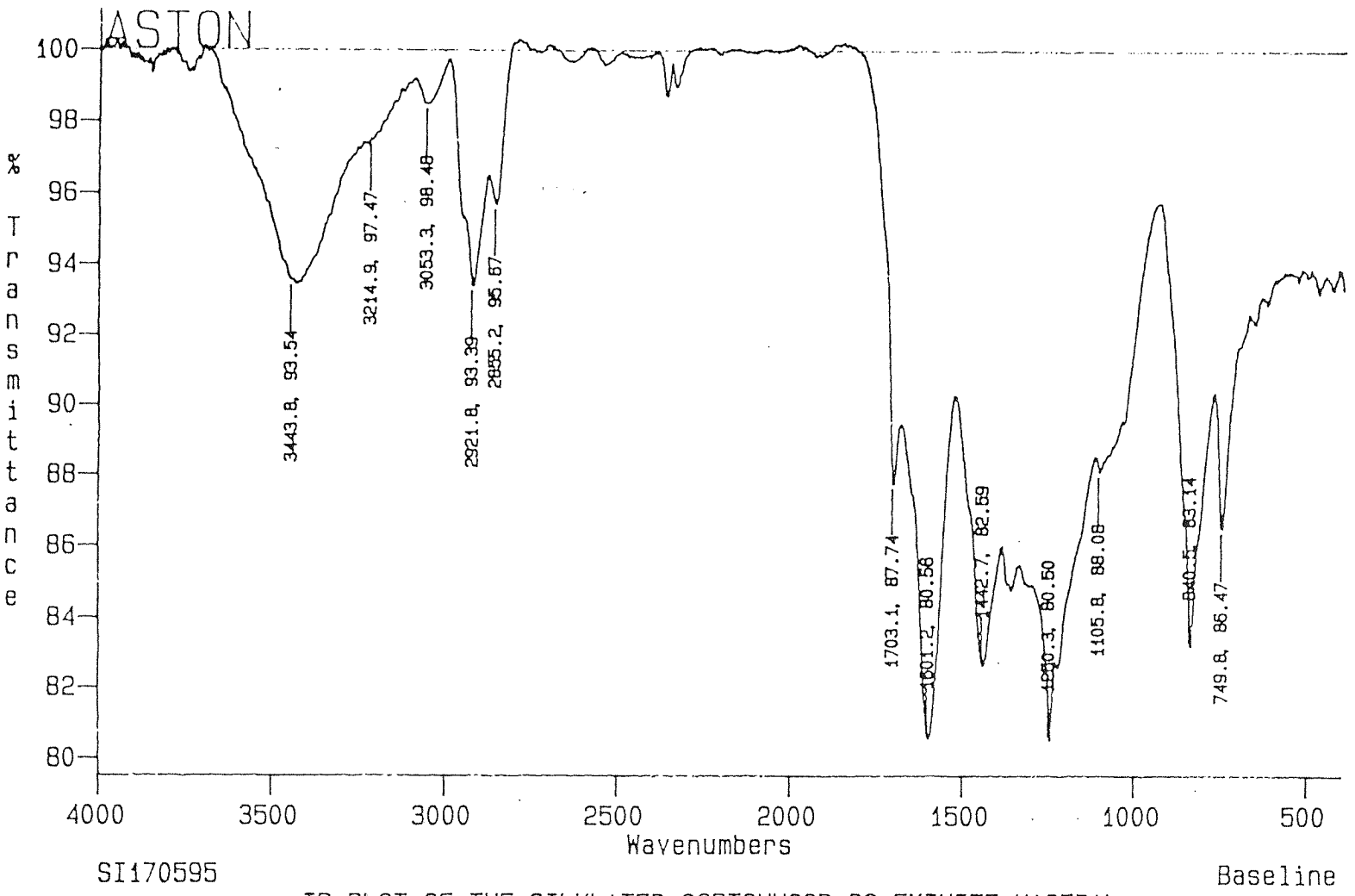

IR PLOT OF THE SILYLATED CORTONWOOD-32 EXINITE MACERAL
RES=8.

Fig5.43
IR of the silylated Cortonwood exinite maceral

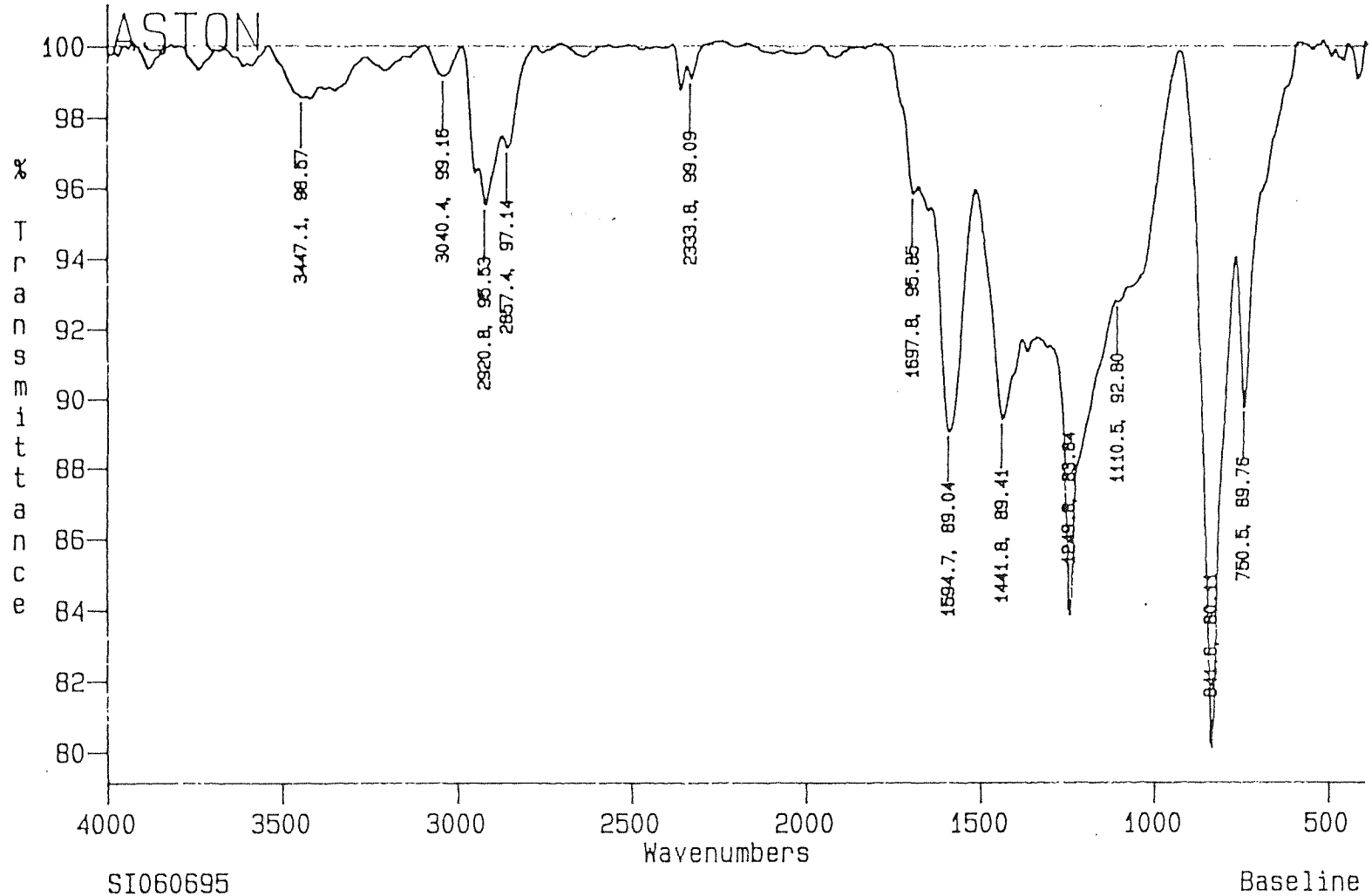

IR PLOT OF THE SILYLATED CORTONWOOD-32 VITRINITE MACERAL
RES=8.

Fig5.44
IR of the silylated Cortonwood vitrinite maceral

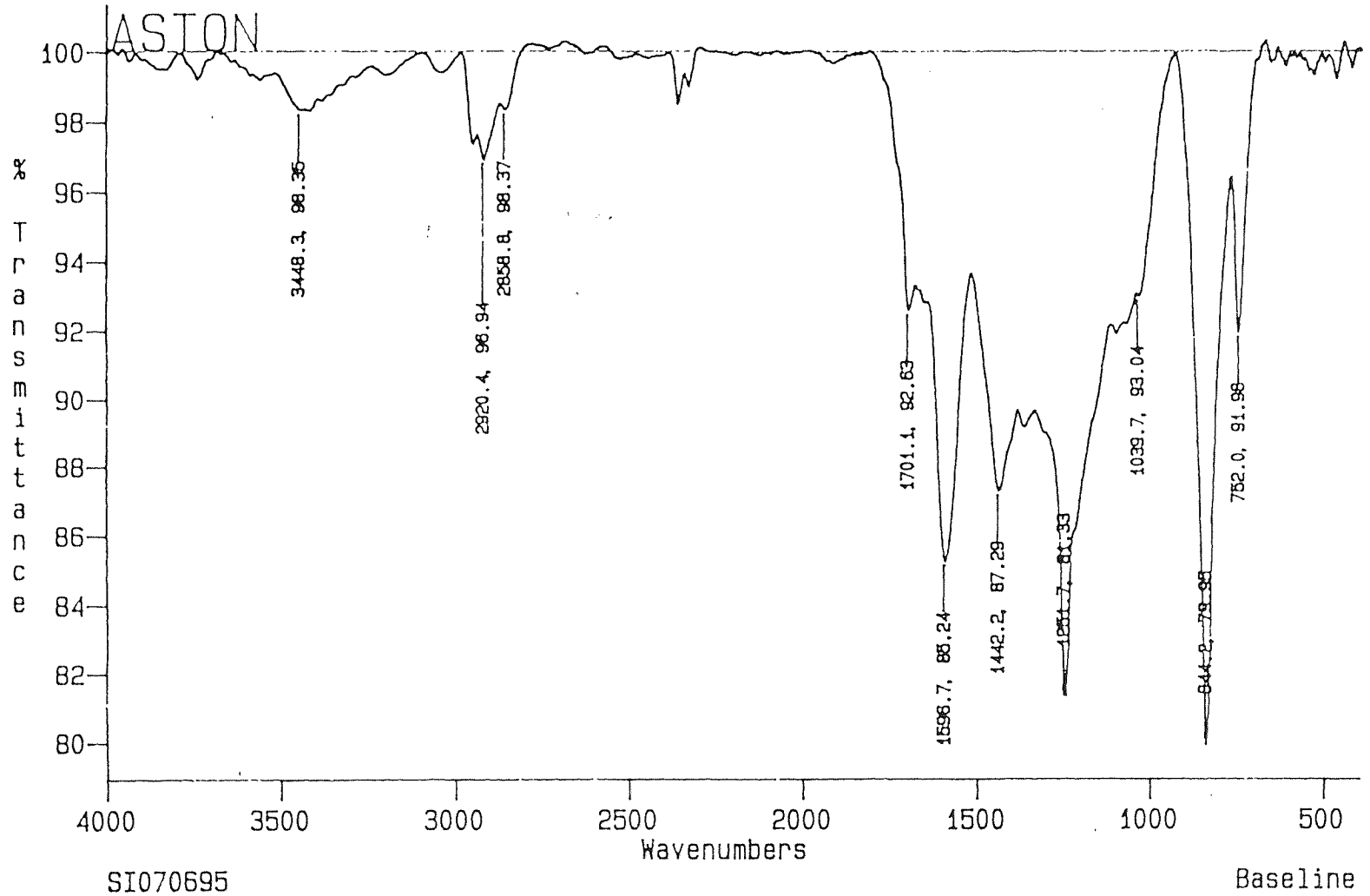

Fig5.45
IR of the silylated Cortonwood inertinite maceral

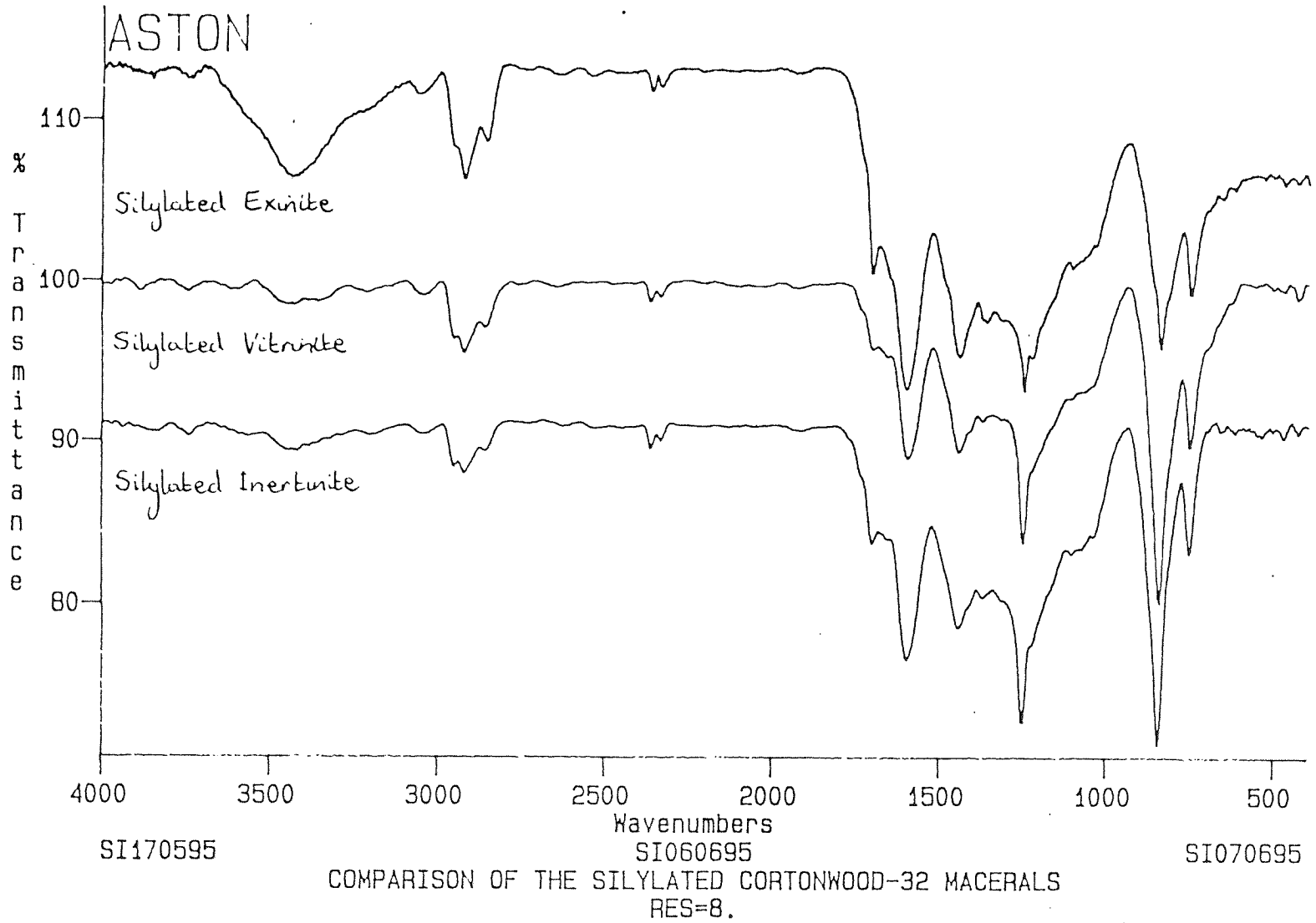

Fig5.46
IR comparison of the silylated Cortonwood macerals

Table 5.13

Summary of the IR results for the silylation of the Cortonwood coal and Cortonwood macerals

Silylated coal / coal macerals	$\upsilon(-OSiCH_3)$	$\upsilon(-SiCH_3)$	$\upsilon(-OH)$
Cortonwood coal	842 cm^{-1}	1250 cm^{-1}	3429 cm^{-1}
Cortonwood exinite	841 cm^{-1}	1250 cm^{-1}	3444 cm^{-1}
Cortonwood vitrinite	842 cm^{-1}	1250 cm^{-1}	3447 cm^{-1}
Cortonwood inertinite	844 cm^{-1}	1252 cm^{-1}	3448 cm^{-1}

The silylated raw Cortonwood coal and Cortonwood macerals were analysed by quantitative ^{29}Si MASNMR to determine the extent of silylation. All ^{29}Si resonances are reported relative to tetramethylsilane (TMS). Fig 5.47 shows the nmr spectrum for the silylated raw Cortonwood coal. Unfortunately the peaks due to the silylated coal were very low in intensity and not detected during the analysis. Integration of the peaks, however, did produce a value for the region where we would expect to find the silylated coal peak. Calculations for the extent of silylation of the raw Cortonwood coal were made based on this integration value (coupled with the integration value obtained for the laponite standard). Fig 5.48 shows the ^{29}Si nmr spectrum for the silylated Cortonwood exinite maceral. The resonance due to the silylated phenol groups in the coal maceral is evident at 19.4 ppm. The laponite standard peak appears upfield at -93.2 ppm. Fig 5.49 shows the ^{29}Si nmr spectrum for the silylated vitrinite Cortonwood maceral. There are three major resonance peaks at 20.2 ppm, 7.6 ppm and -94.4 ppm corresponding to silylated phenols, trimethyl silanol and the laponite standard respectively. Fig 5.50 shows the ^{29}Si nmr spectrum for the silylated Cortonwood inertinite maceral. The two main peaks detected occur at 18.4 ppm and -93.7 ppm corresponding to the silylated coal maceral and the laponite standard respectively. Table 5.14 summarises the results obtained from the quantitative ^{29}Si MASNMR analysis of the silylated Cortonwood raw coal and coal macerals.

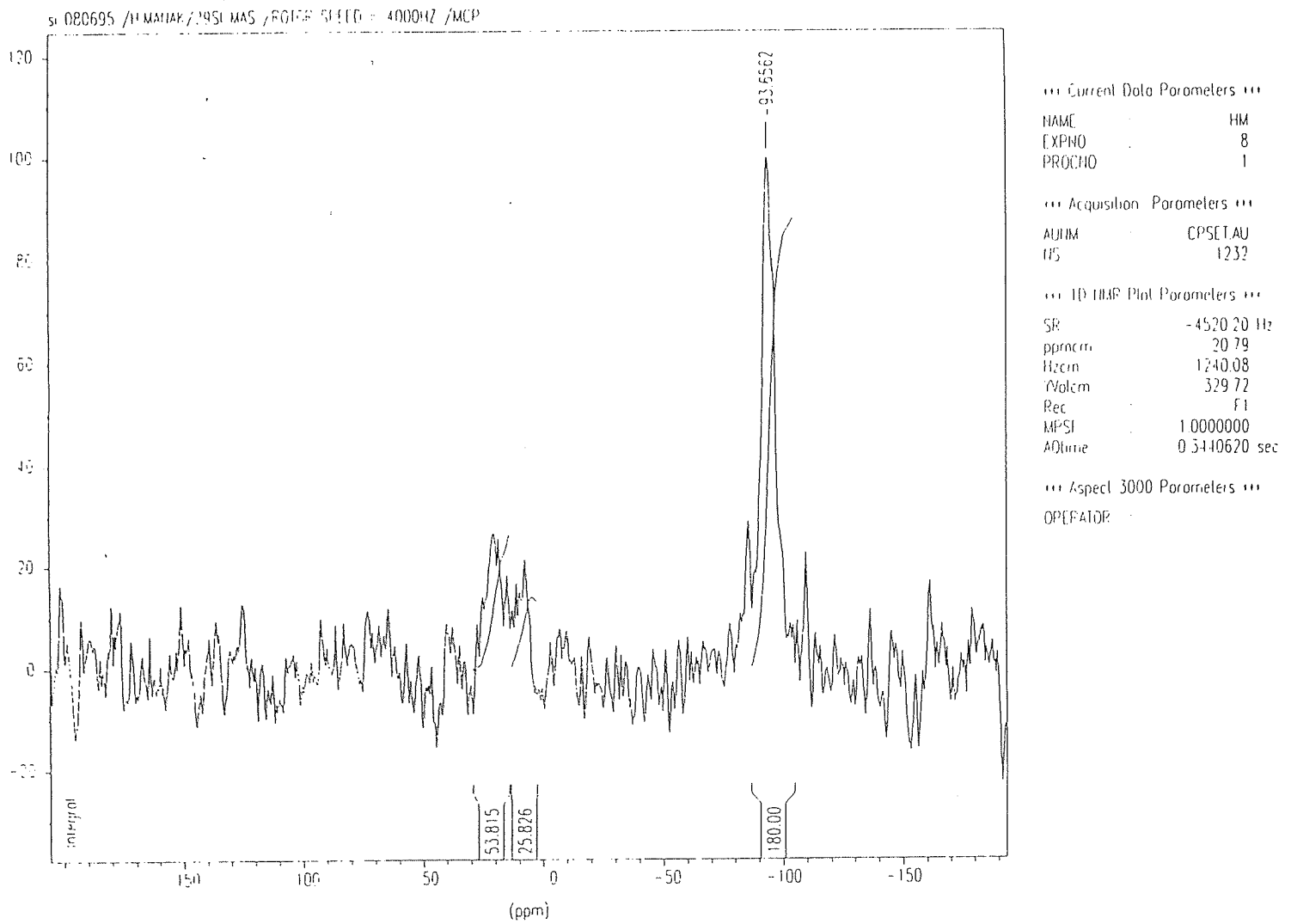

Fig5.47
Quantitative ^{29}Si MASNMR of the silylated raw Cortonwood coal

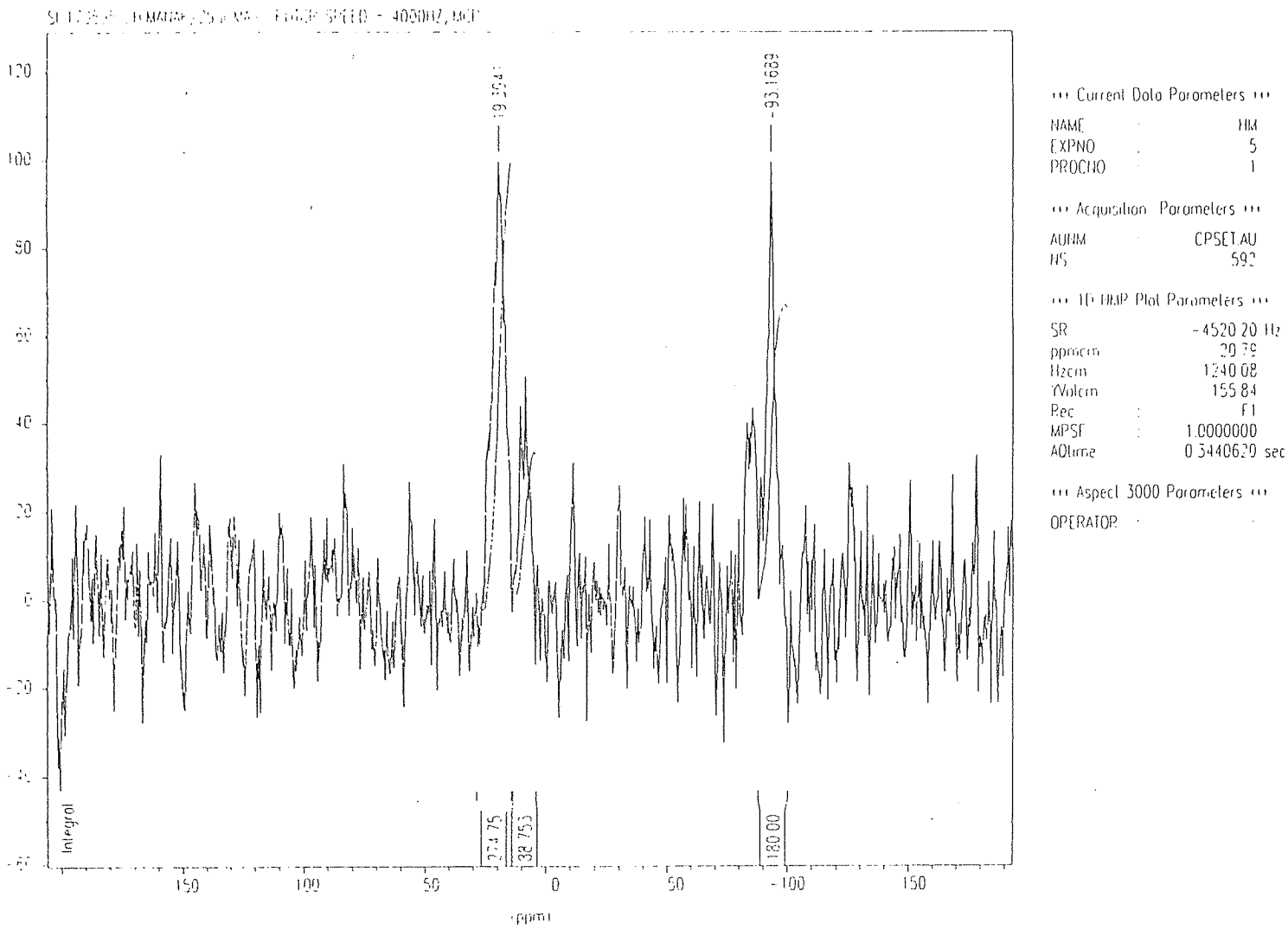

Fig5.48
Quantitative ^{29}Si MASNMR of the silylated Cortonwood exinite maceral

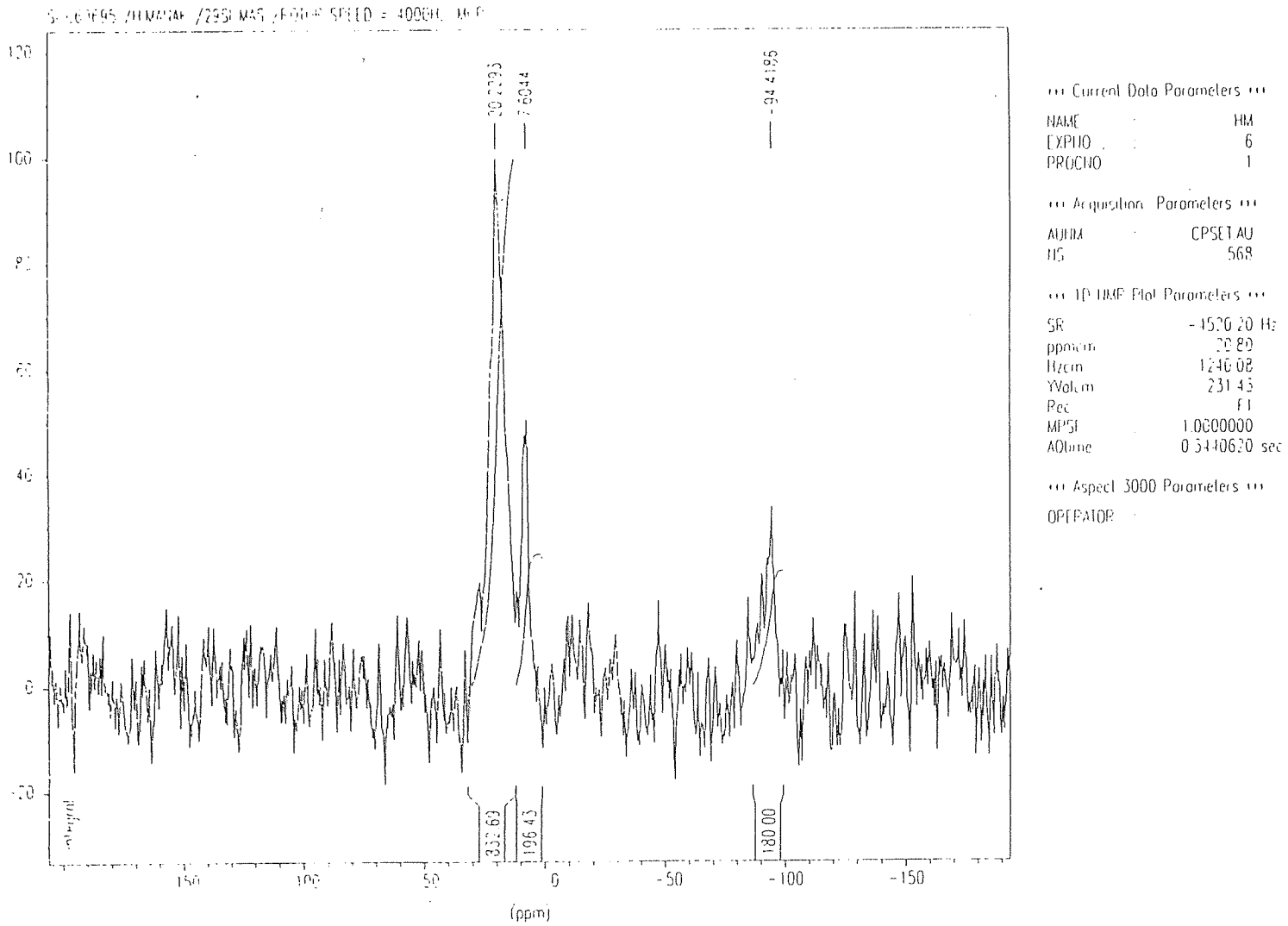

Fig5.49
Quantitative ^{29}Si MASNMR of the silylated Cortonwood vitrinite maceral

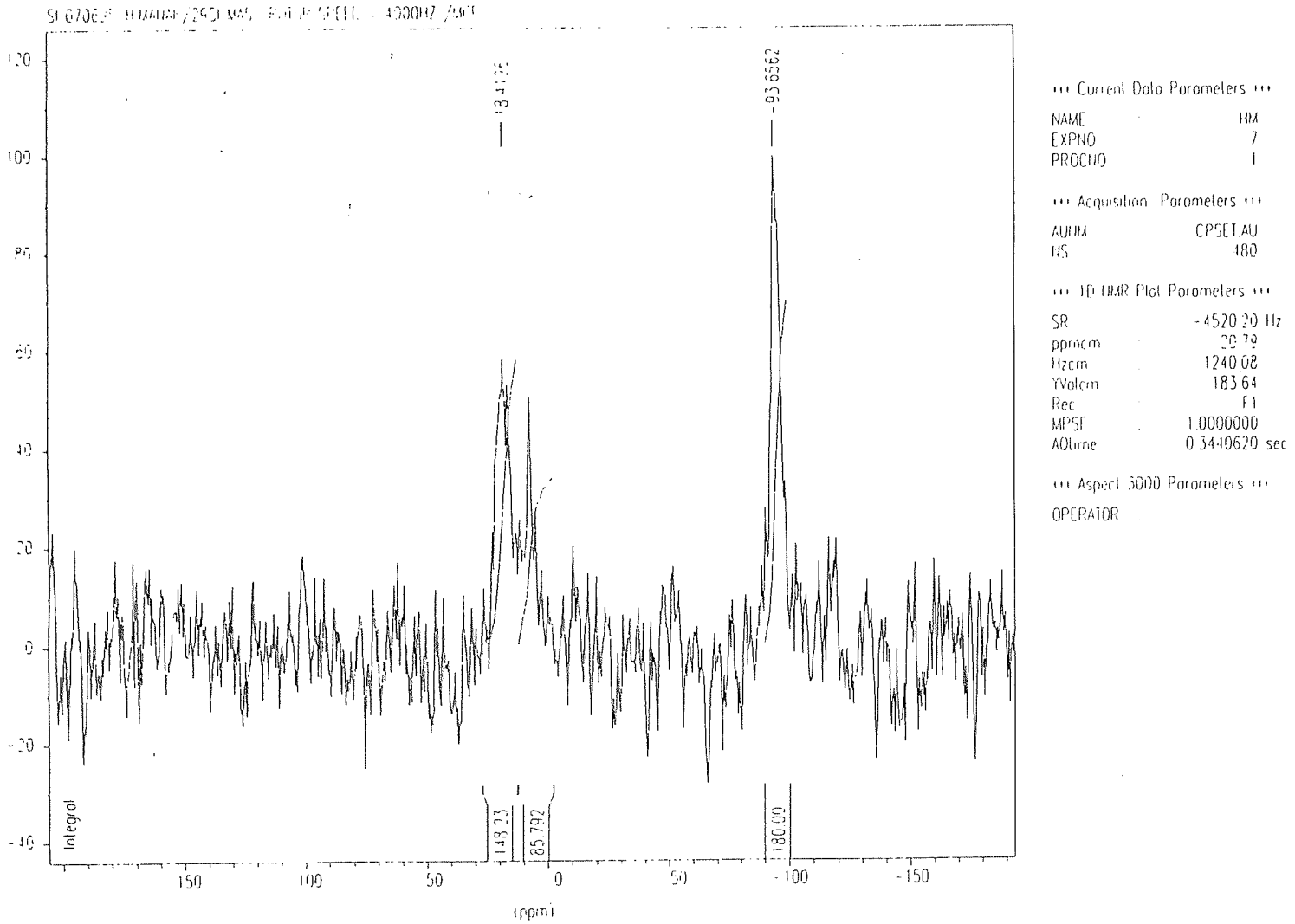

Fig5.50
Quantitative ^{29}Si MASNMR of the silylated Cortonwood inertinite maceral

Table 5.14

Resonant peaks from the ^{29}Si MASNMR analysis of the silylated Cortonwood raw coal and silylated Cortonwood coal macerals

Silylated coal / coal macerals	Resonance due to silylated phenols (ppm)	Resonance due to $(CH_3)_3SiOH$ (ppm)	Resonance due to laponite standard (ppm)
Cortonwood coal	—	—	-93.7
Cortonwood exinite	19.4	—	-93.2
Cortonwood vitrinite	20.2	7.6	-94.4
Cortonwood inertinite	18.4	—	-93.7

Table 5.15 shows the integration values obtained for the silylated raw Cortonwood coal and coal macerals, and the laponite standards.

Table 5.15

Integration values from ^{29}Si MASNMR for the silylated Cortonwood coal and Cortonwood macerals and the laponite standards

Silylated coal / coal macerals	Signal area of silylated coal / coal maceral	Signal area of laponite standard
Cortonwood coal	53.82*	180.00
Cortonwood exinite	274.75	180.00
Cortonwood vitrinite	832.69	180.00
Cortonwood inertinite	148.23	180.00

*For the silylated raw Cortonwood coal, the silylated coal peak was very small and consequently not detected during quantitative ^{29}Si MASNMR analysis.

From these results the % O (as phenolic -OH) silylated in the Creswell coal and coal macerals was calculated using the following equation :

$$\% \ O = (M_O / m_C).(m_S / M_S).(I_C / I_S) \times 100\%$$

where M_O = atomic weight of oxygen
m_C = weight of silylated coal
m_S = weight of standard
M_S = molecular weight of standard
I_C = signal area of silylated coal
I_S = signal area of standard

The calculations (using technique No.1) for the silylated Cortonwood coal and silylated Cortonwood macerals can be found in Appendix III.

The % O (as phenolic -OH) in the silylated Cortonwood coal and coal macerals was also calculated using the alternative "cut-out-and-weigh" method (technique No.2) to give the relative signal areas of the silylated coal to the silylated laponite standard.

Table 5.16

Results from the weighings of the silylated coal and laponite standard peaks for the Cortonwood coal and Cortonwood macerals

Coal / Coal Maceral	Weight of silylated coal peak / g	Weight of laponite standard peak / g
Cortonwood raw coal	0.054	0.092
Cortonwood exinite maceral	0.103	0.077
Cortonwood vitrinite maceral	0.116	0.034
Cortonwood inertinite maceral	0.095	0.091

The values in Table 5.16 were used to calculate alternative % O values for the silylated Cortonwood coal and coal macerals. The calculations (using technique No.2) for the silylated Cortonwood coal and silylated Cortonwood macerals can be found in Appendix III.

As with the silylated Creswell coal and Creswell macerals, the silylated Cortonwood coal and Cortonwood maceral ^{29}Si MASNMR spectra were deconvoluted and the % O (as phenolic -OH) calculated using the integration and weighing methods. Figs 5.51 - 5.54 show the deconvoluted ^{29}Si MASNMR plots for the silylated raw Cortonwood coal and the silylated Cortonwood exinite, vitrinite and inertinite macerals respectively. Table 5.17 shows the integration values associated with the aforementioned plots.

Table 5.17

Integration values from the deconvoluted ^{29}Si MASNMR spectra for the silylated Cortonwood coal and coal macerals and the laponite standards

Silylated coal / coal macerals	Signal area of silylated coal / coal maceral	Signal area of laponite standard
Cortonwood coal	1.0000	4.0144
Cortonwood exinite	1.0000	0.7592
Cortonwood vitrinite	1.0000	0.1551
Cortonwood inertinite	1.0000	1.2158

The deconvoluted spectra were expanded and the relevant silylated coal and laponite standard peaks were cut out and weighed (to 3 dp) to give the relevant signal area of each peak. Table 5.18 shows the results from the weighings.

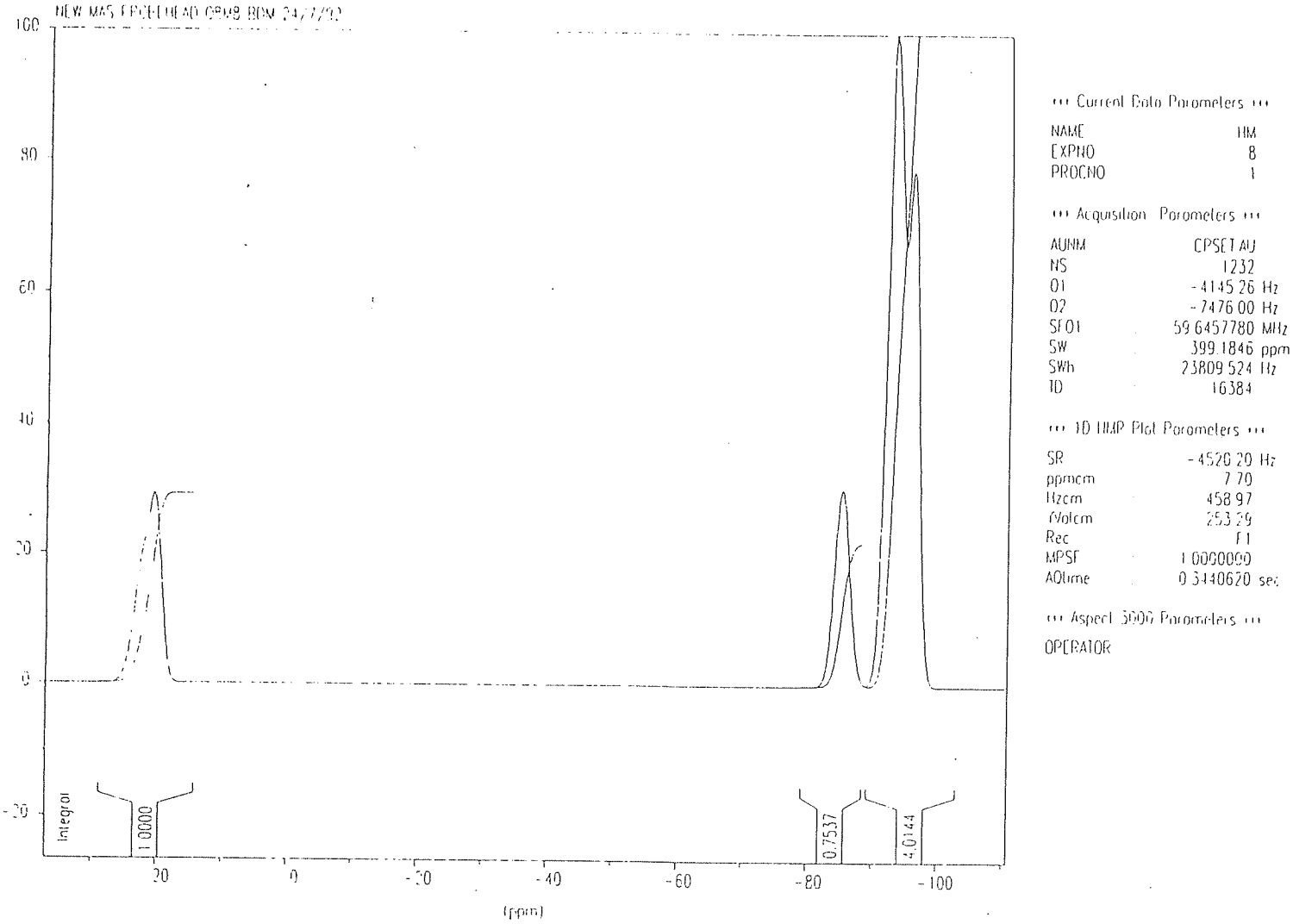

Fig5.51
Deconvoluted ^{29}Si MASNMR spectrum for the silylated raw Cortonwood coal

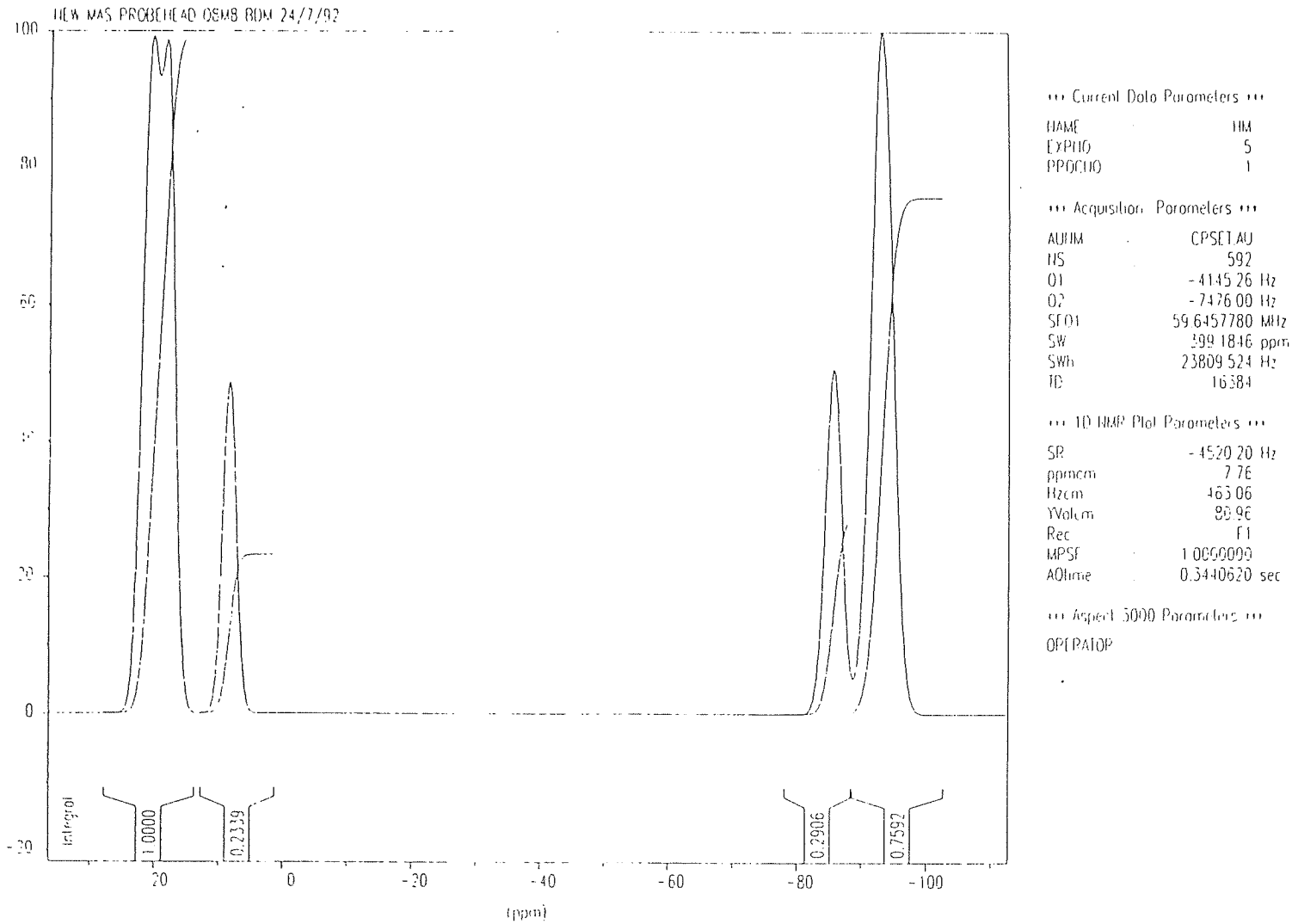

Fig5.52
Deconvoluted ^{29}Si MASNMR spectrum for the silylated Cortonwood exinite maceral

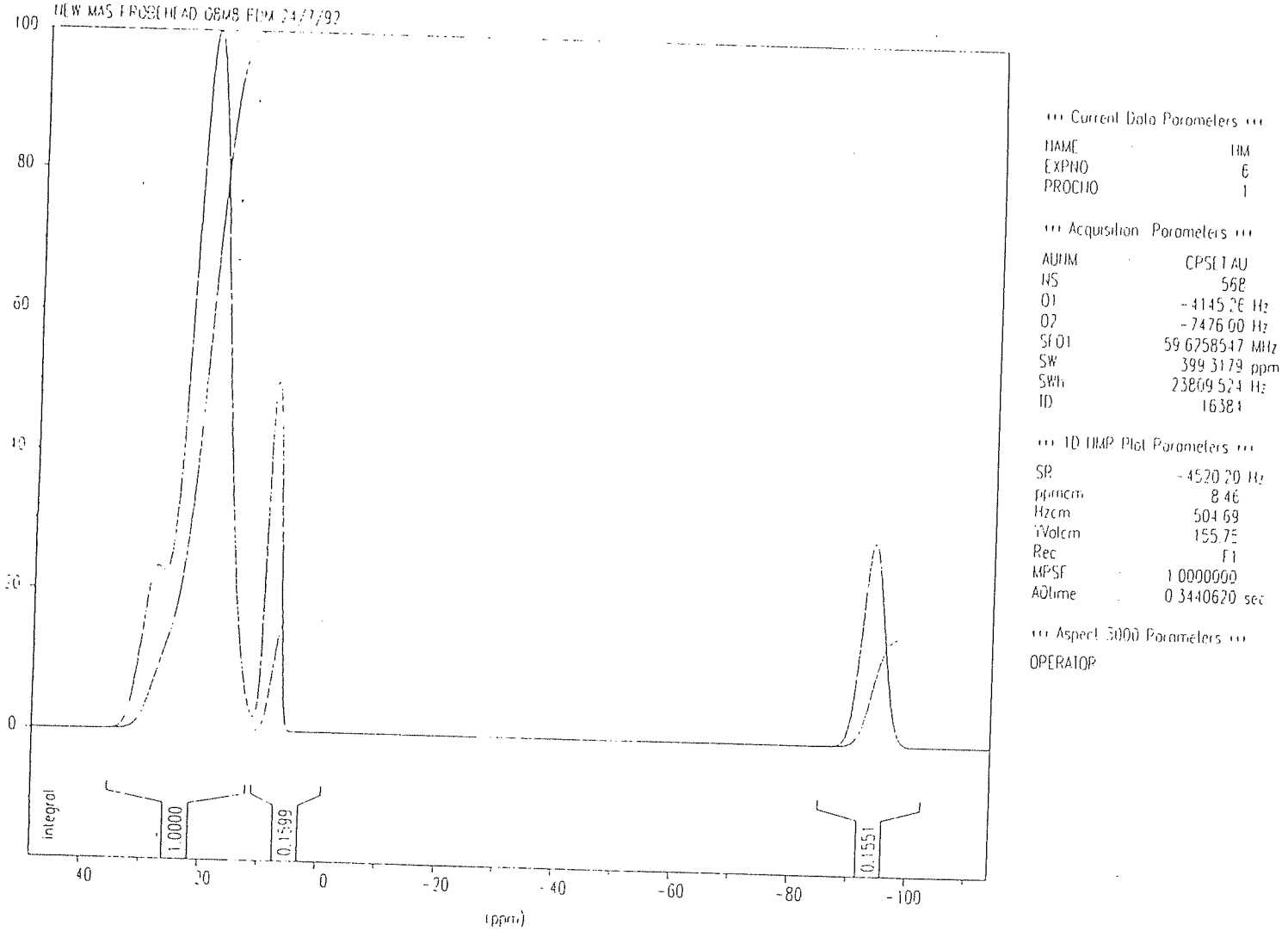

Fig5.53
Deconvoluted ^{29}Si MASNMR spectrum for the silylated Cortonwood vitrinite maceral

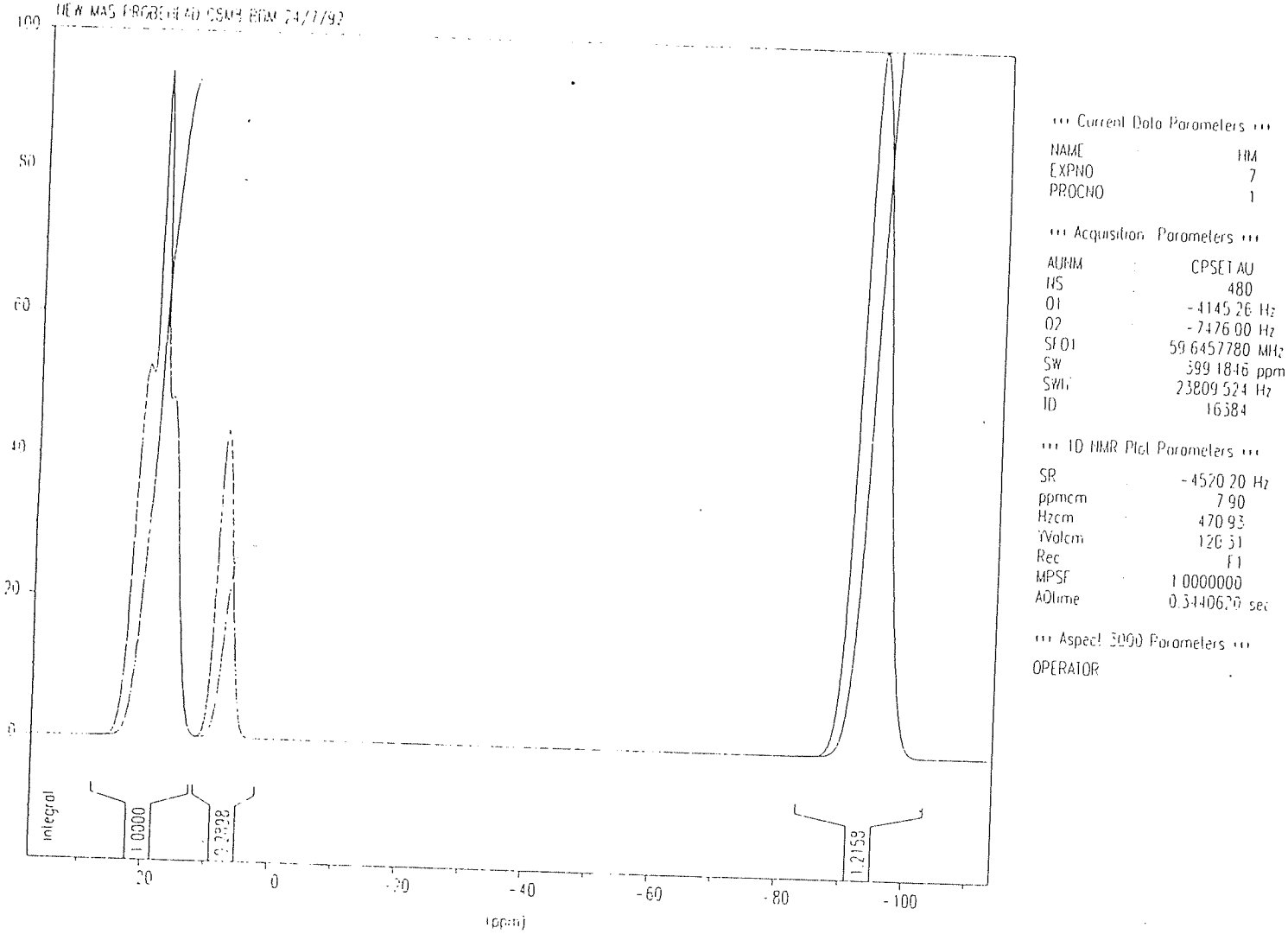

Fig5.54
Deconvoluted ^{29}Si MASNMR spectrum for the silylated Cortonwood inertinite maceral

Table 5.18

Results from the weighings (deconvolution method) of the silylated coal and laponite standard peaks for the Cortonwood coal and coal macerals

Coal / Coal Maceral	Weight of silylated coal peak / g	Weight of laponite standard peak / g
Cortonwood raw coal	0.014	0.064
Cortonwood exinite	0.063	0.064
Cortonwood vitrinite	0.097	0.022
Cortonwood inertinite	0.056	0.091

From the figures in Tables 5.17 and 5.18 the % O (as phenolic -OH) was calculated for the silylated Cortonwood coal and Cortonwood macerals (using the deconvolution method). Tables 5.19 and 5.20 summarise the results from the silylation of the Cortonwood coal and Cortonwood macerals. Once again, techniques No.1 and No.2 produced nonsense results, owing to the ambiguity attached to where the baseline is taken. Techniques No.3 and No.4 produced relatively better results.

Table 5.19

Results for the % O (as phenolic -OH) from the silylation of the Cortonwood coal and Cortonwood macerals

Coal / Coal Maceral	Total % O_{dmmf}	Results from Silylation (normal spectra)		Results from Silylation (deconvoluted spectra)	
		Technique No.1 % O (as -OH) Integration method	Technique No.2 % O (as -OH) Weighing method	Technique No.3 % O (as -OH) Integration method	Technique No.4 % O (as -OH) Weighing method
Cortonwood raw coal	4.8	5.6	11.1	4.7	4.1
Cortonwood exinite	4.6	6.4	5.6	5.5	4.1
Cortonwood vitrinite	4.2	15.7	11.6	21.9	15.0
Cortonwood inertinite	6.2	5.5	6.9	5.4	4.1

Table 5.20

The results for the % O_{OH} / O_{total} from the silylation of the Cortonwood coal and Cortonwood macerals

Coal / Coal Maceral	Results from Silylation (normal spectra)		Results from Silylation (deconvoluted spectra)	
	Technique No.1 % O_{OH} / O_{total} Integration method	Technique No.2 % O_{OH} / O_{total} Weighing method	Technique No.3 % O_{OH} / O_{total} Integration method	Technique No.4 % O_{OH} / O_{total} Weighing method
Cortonwood raw coal	117	231	98	85
Cortonwood exinite	139	122	120	89
Cortonwood vitrinite	374	276	521	357
Cortonwood inertinite	89	111	87	66

5.3.4 General conclusions

The phenol-formaldehyde resin and the two co-resites all showed some degree of silylation. The pure phenol-formaldehyde showed evidence of silylation from the FT-IR results and gave a very good quality ^{29}Si CP MASNMR spectrum with the main resonance due to the silylated phenolic groups centred at 17.5 ppm. The 1 : 1 co-resite showed little evidence of silylation (even after 2 hrs of microwave heating) from the FT-IR results, but a ^{29}Si MASNMR resonance at 19.2 ppm denoted that some silylation had taken place. Results from the 3 : 1 co-resite were more conclusive - FT-IR showed an increased reaction had occurred after 2 hrs of microwave heating and the ^{29}Si MASNMR spectrum produced a peak centred at 18.1 ppm. The silylated pure phenol-formaldehyde resin and silylated 1 : 1 co-resite were analysed by quantitative solid-state ^{13}C MASNMR at the University of Strathclyde using both cross polarisation (CP) and single pulse excitation (SPE) techniques for comparison. It was shown that the high content of aromatic protons in the polymeric samples provided a suitable environment for cross polarisation of the samples and consequently, the results from CP and SPE were very similar. Thus, cross polarisation was shown to be a reliable technique for the quantitative analysis of these silylated resin samples.

The quantitative ^{13}C CP / SPE MASNMR results showed that the extent of silylation was low in both cases - 19% O_{OH} / O_{total} for the pure phenol-formaldehyde resin and 3 - 4% O_{OH} / O_{total} for the 1 : 1 co-resite. A very interesting fact to emerge during the analysis of the 1 : 1 co-resite was that the ratio of 2,6-di-tert-butylphenol to phenol in the co-resite was much less than previously thought (18 : 1 as opposed to 1 : 1). This also has implications for the other (nominal) 3 : 1 (2,6-di-tert-butylphenol : phenol) co-resite - we would expect the actual ratio of phenol : 2,6-di-tert-butylphenol to be much higher than 3 : 1 (in fact, much higher than 18 : 1). The extent of silylation for the 3 : 1 co-resite was calculated using quantitative solid-state ^{29}Si MASNMR (using a synthetic smectite clay as the standard). The value for % O_{OH} / O_{total} calculated for the silylated 3 : 1 co-resite, via integration of the ^{29}Si MASNMR spectrum, was 19.6%. An alternative method, whereby the ^{29}Si MASNMR spectrum was deconvoluted and the relevant peaks cut out and weighed, produced a % O_{OH} / O_{total} value of 14.7% for the silylated 3 : 1 co-resite. This value appears to be more accurate than the former value, as it tends to fit in with the trend we would expect for silylation of the resins. In relative terms we would expect the pure phenol-formaldehyde resin to show the greatest degree of silylation and the 1 : 1 co-resite (which contained the largest number of 2,6-di-tert-butylphenol groups) to show the least - this is consolidated by our findings.

The results also show that even very small concentrations of 2,6-di-tert-butylphenol moieties in the structure are sufficient to drastically reduce the extent of silylation - it is postulated that the reason for this is that the bulky 2,6-di-tert-butylphenol groups tend to occupy boundary positions in the structure, which make it difficult for the silylating reagent to diffuse into the polymer matrix to effect further silylation. As such, the resins do not appear to be suitable for our purposes as models for coals, for the obvious reason that the substituted-phenol groups in coal are much more widely dispersed throughout the structure.

The Creswell coal and Creswell macerals were silylated for 4 hrs in the MES-1000 microwave oven and analysed quantitatively using solid-state ^{29}Si MASNMR. Two different procedures were used to evaluate the extent of silylation - these involved using the normal ^{29}Si MASNMR spectra and the deconvoluted ^{29}Si MASNMR spectra. The silylated Creswell raw coal gave an average % O_{OH} / O_{total} value of 176% using the normal ^{29}Si MASNMR spectrum and an average of 97.5% O_{OH} / O_{total} using the deconvoluted ^{29}Si MASNMR spectrum. The latter figure is in good agreement with work carried out by Monsef-Mirzai et al[42] on the silylation of raw Creswell coal. They calculated a value of 92% O_{OH} / O_{total} for the Creswell raw coal after a 2 hr microwave reaction time (at 100% microwave power using a 650 Watt microwave oven). Our value of 97.5% O_{OH} / O_{total} was obtained after a 4 hr microwave reaction time, but using only 20% microwave power (in a 950 ± 50 Watt microwave oven). The results also show that using the deconvoluted ^{29}Si MASNMR spectrum appears to afford us more accurate results. The very high values obtained using the normal ^{29}Si MASNMR spectrum are probably due to difficulties in determining where the actual baseline is under the peak, as it is from the baseline that calculations need to be made in order to ascertain the signal area. The Creswell exinite produced % O_{OH} / O_{total} average values of 221.5% and 191.5% for the normal and deconvoluted ^{29}Si MASNMR spectra respectively. These values are unusually high and the cause of this may have a number of contributory factors - firstly, the baseline on the silylated Creswell exinite ^{29}Si MASNMR plot has a fairly high degree of uncertainty and there is still a noticeable amount of noise on the plot. The Creswell exinite maceral also has a significantly higher proportion of sulfur (as shown by ultimate analysis) in its constitution compared to the Creswell raw coal and the other two maceral groups. Silylation of this additional sulfur during reaction could contribute to the ^{29}Si MASNMR silylated coal resonance on the plot resulting in an over-estimation of the amount of -OH present.

Another factor, which could be involved, is error in determining the ultimate analysis - the analysis was not carried out in duplicate and, as such, there is some ambiguity attached to the values obtained - if this is true, however, then there is also uncertainty attached to the other maceral ultimate analysis values. The silylated Creswell vitrinite produced average values of 63% and 57.5% O_{OH} / O_{total} for the normal and deconvoluted ^{29}Si MASNMR spectra respectively showing that the greater proportion of oxygen in the Creswell vitrinite maceral is in the form of the hydroxyl functionality. The ^{29}Si MASNMR spectrum gave a very good resolution and there was less noise compared to the raw Creswell and exinite spectra, which is probably why the figures from the two different methods are in fairly good agreement. The Creswell inertinite maceral group showed no signs of silylation, even after 4 hrs of microwave heating. Perhaps, this is not surprising, considering that the inertinite maceral group is the least reactive of the three maceral groups and tends to have a lower % O content compared to the Creswell raw coal and the other two maceral groups.

The silylated Cortonwood raw coal produced % O_{OH} / O_{total} average values of 174% and 91.5% for the normal and deconvoluted spectra respectively. Because the relative height of the silylated coal peak is very small compared to the laponite standard peak, it is very difficult to ascertain where the coal peak boundaries and baseline are in the normal spectra - this could be a major contributory factor in the over-estimation of % O_{OH} / O_{total} when considering the normal ^{29}Si MASNMR spectrum. Again, the value obtained from the deconvoluted ^{29}Si MASNMR spectrum is in fairly good agreement with silylation work carried out by Monsef-Mirzai et al[42], who obtained a value of 84% O_{OH} / O_{total} for raw Cortonwood coal after 3 hrs microwave reaction time (the deconvoluted-weighing method gave a value of 85% O_{OH} / O_{total} for the raw Cortonwood coal after 4 hrs microwave heating at a lower microwave power output than that used by Monsef-Mirzai's microwave oven). This shows that the method is indeed reproducible. The silylated Cortonwood exinite gave average values of 130.5% and 104.5% O_{OH} / O_{total} for the normal and deconvoluted spectra respectively - again, the higher value may be put down to ambiguity in determining the baseline on the ^{29}Si MASNMR plot. A more reliable figure for the silylated Cortonwood exinite is obtained using the deconvoluted-weighing method - 89% O_{OH} / O_{total}. The results obtained for the silylated Cortonwood vitrinite, using both methods, are far too high. The high values may be explained by looking back at the maceral separations - the Cortonwood vitrinite fraction was found to contain significant concentrations of both the exinite and inertinite macerals. We would therefore expect more N and S (both capable of being silylated) to be present in the Cortonwood "vitrinite" fraction as a result of this.

This would result in a greater amount of silicon reagent being incorporated and subsequently, higher values would be observed. There is also the added ambiguity of determining where the baseline is and there are also two shoulders on either side of the main silylated coal peak indicating a more varied -OH environment - probably due to exinite and vitrinite infiltration - which makes it difficult to define the silylated coal peak boundary. The Cortonwood vitrinite results are, therefore, effectively meaningless in the context of these maceral comparisons. The silylated Cortonwood inertinite maceral did show some silylation, in contrast to the Creswell inertinite. Values of 100% and 76.5% O_{OH} / O_{total} were obtained using the normal and deconvoluted spectra respectively (with a value of 66% O_{OH} / O_{total} for the deconvoluted-weighing method).

Because the ^{29}Si MASNMR resonance peaks (for the silylated resins and silylated Creswell and Cortonwood raw coals and coal macerals) were too broad, it was not possible to distinguish individual resonances due to specific chemical environments for the silylated resins and coals. Consequently, it was decided to look at the width-at-half-height of the relevant silylated product peaks to ascertain whether any individual maceral contained a significantly greater (or less) proportion of variable environments. Table 5.21 shows the width-at-half-height of the various silylated resin / coal products.

Table 5.21
Width-at-half-height from the ^{29}Si MASNMR spectra for the silylated resins / coal products

Silylated resin / coal / maceral	Width-at-half-height (Hz)
Pure phenol-formaldehyde resin (mw reaction time 2 hrs)	359
18 : 1 phenol : 2,6-di-tert-butylphenol - formaldehyde co-resite (mw reaction time 2 hrs)	594
3 : 1 (nominally) phenol : 2,6-di-tert-butylphenol - formaldehyde co-resite (mw reaction time 2 hrs)	430
Raw Creswell coal	500
Creswell exinite maceral	590
Creswell vitrinite maceral	514
Creswell inertinite maceral	—
Raw Cortonwood coal	421
Cortonwood exinite maceral	387
Cortonwood vitrinite maceral	448
Cortonwood inertinite maceral	436

The silylated resins appear to follow the pattern expected - that is, the silylated pure phenol-formaldehyde resin was found to have the narrowest width, because of the limited environments available to the -OH groups and the (formerly 1 : 1) 18 : 1 co-resite had the greatest width due to more 2,6-di-tert-butylphenol groups being available per phenol group, allowing for the likelihood of a more varied -OH environment compared to the 3 : 1 co-resite (which has a greater number of phenol groups compared to 2,6-di-tert-butylphenol groups). In the case of the silylated Creswell coal and coal macerals, the Creswell exinite maceral group appears to have a more varied -OH environment than the Creswell raw coal or the Creswell vitrinite (which both have similar frequency widths - this does not seem unusual considering that the bulk of the raw Creswell coal is made up of the vitrinite maceral group). The Creswell inertinite did not show silylation. The Cortonwood coal and coal macerals tended to show less varied -OH environments compared to the Creswell coal and coal macerals. In this case, the Cortonwood exinite shows the smallest frequency-width indicating a less varied -OH environment. Interestingly, exinite can have different compositions for a given rank with variances being caused by differences in chemical composition of the original plant matter or development during coalification. The differences between the Creswell and Cortonwood exinite macerals may be due to this factor. The largest width-at-half-height occurs with the Cortonwood vitrinite - this is probably due to the poor separation of the Cortonwood vitrinite concentrate resulting in substantial exinite and inertinite infiltration. The Cortonwood raw coal and the Cortonwood inertinite show similar -OH environments. This is probably due to the inertinite maceral group constituting a fairly large proportion of the raw Cortonwood coal (18% inertinite, compared to only 5% exinite). A possible improvement in the quality of the baseline in the ^{29}Si MASNMR spectra may result if the samples were allowed longer instrument time.

Overall silylation produced good results with higher values derived from the normal ^{29}Si MASNMR spectra compared to the deconvoluted spectra. The results appear to indicate that the preferential method for calculating the extent of silylation - when poor quality baseline ^{29}Si MASNMR spectra are obtained (as in the case of the silylated Creswell and Cortonwood raw coals and coal macerals) - is to deconvolute the original ^{29}Si MASNMR spectrum and then cut-out and weigh the relevant silylated coal / maceral peaks and the laponite standard peaks to determine the relative signal areas.

However, when good quality ^{29}Si MASNMR spectra are obtained, as with the silylated 3 : 1 co-resite, computer integration of the normal ^{29}Si MASNMR spectra is a reliable and feasible method for % O (as phenolic -OH) determination - the ^{29}Si results for the 3 : 1 co-resite gave excellent agreement with the ^{13}C resin results (within experimental error).

In the case of the Creswell coal, the raw coal produced very good results in good approximation to work carried out previously in the literature. The Creswell exinite gave higher values than expected, but indications are that a significant proportion of the exinite was silylated. The Creswell vitrinite produced average values which were in very good agreement using both the calculation methods. The results indicated that, although the Creswell vitrinite contains the largest amount of oxygen compared to the other two macerals groups, less of this oxygen is in the form of easily accessible -OH groups. The Creswell inertinite showed no inclination to silylate. The relative order of OH content, as determined by this silylation work, for the Creswell macerals is exinite > vitrinite > inertinite.

The Cortonwood raw coal also gave very good silylation results, in good agreement with the published literature silylation work. The silylated Cortonwood exinite showed that the majority (in fact, nearly all) the oxygen present was in the form of -OH and the silylated Cortonwood inertinite, in contrast to the Creswell inertinite (which showed no silylation), showed that a large proportion of its oxygen (approximately 66%) was in the form of -OH accessible to the silylating reagent. These differences show the variances which can occur, not only from maceral to maceral within a certain coal, but also between the same macerals of different coals of similar rank. The origin of these differences probably arises during the coalification stage of the individual coal. It was not possible to determine the relative order of OH content for the Cortonwood macerals, because the Cortonwood vitrinite maceral gave a poor maceral separation.

METHYLATION

6.1 INTRODUCTION

6.1.1 General Introduction

It was attempted, initially, to methylate model compounds followed by methylation of the Creswell and Cortonwood coals and coal macerals. This was to be followed by subsequent *in situ* analysis by FT-IR and nmr techniques. Three methods of methylation were attempted :

1. Methylation using methyl iodide
2. Methylation using methyl formate
3. Methylation using a phase-transfer method

Different methods were used in order to ascertain which would be the most suitable for the coals and coal macerals utilised. The second stage of the experiment was to introduce an isotopically-labelled version of the reagent (chosen from the first part of the experiment) into the coals and coal macerals to determine quantitatively (using ^{13}C CP MASNMR) the nature of the hydroxyl groups in the coals.

6.1.2 Literature review

Much of the early work on the alkylation of coals was carried out by Heinz Sternberg et al[74], 1971 and Sternberg and Delle Donne[75], 1974. They managed to increase the solubility in benzene of bituminous and subbituminous coals by first alkylating the coals. This reaction involved the formation of a "coal anion" by reacting the coal with alkali metal (potassium) in tetrahydrofuran solvent in the presence of naphthalene.

$$\text{Coal} + n\,C_{10}H_8^{-} \rightarrow \text{Coal}^{n-} + n\,C_{10}H_8$$

Sternberg postulated that an electron transfer reaction was taking place, whereby the naphthalene acted as an electron-carrier from the insoluble alkali metal to the insoluble coal. It was found that the use of ether-type solvents tended to increase the rate of electron transfer from the alkali metal to the coal. Sternberg also discovered that a larger amount of naphthalene was required for high volatile bituminous and subbituminous coals than for anthracite and low volatile bituminous coals to achieve anion formation.

This is probably due to the fact that the former coals contain considerable amounts of hydroxyl groups, which are powerful proton donors and reduce the naphthalene anion to dihydronaphthalene. Dihydronaphthalene does not accept electrons and consequently cannot act as an electron transfer reagent. Hence it was necessary to use an excess of naphthalene. When coal is treated with naphthalene anions, electrons are transferred to both aromatic hydrocarbons and aryl ethers :

$$2\,C_{10}H_8^- + ArH \rightarrow ArH^{2-} + 2\,C_{10}H_8$$

$$C_{10}H_8^- + Ar\text{-}O\text{-}R \rightarrow (Ar\text{-}O\text{-}R)^- + C_{10}H_8$$

However, the intermediate aryl ether anion $(Ar\text{-}O\text{-}R)^-$ is unstable and decomposes in the presence of excess naphthalene anions :

$$(Ar\text{-}O\text{-}R)^- \rightarrow Ar\text{-}O^- + R^-$$

$$C_{10}H_8^- + R^- \rightarrow C_{10}H_8 + R^{2-}$$

The naphthalene anion also abstracts protons from phenolic hydroxyl groups to produce the corresponding phenate ions.

$$2\,C_{10}H_8 + 2\,ArOH \rightarrow 2\,ArO^- + C_{10}H_{10} + C_{10}H_8$$

Subsequent treatment of the anions formed via these reactions with alkyl halide results in the alkylation of the coal. Sternberg et al[74] proposed that the reason for the increased solubility in benzene was due in part to the presence of alkyl groups which prevented the stacking of the aromatic clusters.

Further work using the technique developed by Sternberg was carried out by Wachowska[76-77]. Wachowska found that the solubility of alkylated coals in benzene was dependant upon the type (rank) of coal, the degree of its substitution with alkyl groups and the length of the substituent alkyl chain. She tested five different coals varying in rank from 78 - 93 wt% carbon and found that reaction times varying between 96 and 144 hrs were required for complete coal anion formation. The H / C ratio for all the coals was considerably raised after alkylation and there was a marked increase in yield of the benzene extracts from the alkylated coals with increasing chain length of the alkyl substituent (methyl, ethyl, butyl and octyl alkyl substituents were compared). The number of alkyl groups incorporated per 100 C atoms, however, increased in going from octyl to methyl substituents. Reduction was also found to be accompanied by a degradation of the coal substance due to cleavage of the ether linkages. Ignasiak et al[78] later suggested using an alkali metal / liquid NH_3 mixture for the reductive alkylation of coal instead of naphthalene (which is liable to attack low rank coals). This procedure was more rapid than Sternberg's method and did not require an organic solvent (which may interact with the coal). Also, when concentrated metal solutions were used, many of the free-radical reactions that tend to accompany alkylation were eliminated.

Work studying the proton and carbon nmr spectra of butylated coal (alkylated using Sternberg's method) was carried out by Stock et al[79]. Stock's results showed that both C-butylation and O-butylation were taking place and electron transfer, proton abstraction, ether cleavage and elimination reactions all played an important part in Sternberg's process. Stock also concluded that both nucleophilic and free radical substitution reactions were occurring.

In 1979 Liotta[35] devised a novel method for the selective alkylation of acidic hydroxyl groups in coal. Previously, it was thought that chemical changes in coal could only be carried out without solvents like pyridine (which swells the coal matrix) if elevated temperatures and pressures were used. It was also believed that a loss in selectivity occurred which increased with the severity of the reaction conditions. A consequence of this is that other changes occur in the structure and thus only limited information is obtained about the original structure. Liotta, however, devised a selective O-alkylation procedure which proceeded rapidly under very mild reaction conditions
- the conditions were so mild and so specific to hydroxyl groups (phenol, aliphatic and carboxylic) that essentially no other chemical transformations took place.

The reaction was carried out at ambient conditions under a dry N_2 blanket. The coal was suspended in tetrahydrofuran and stirred mechanically while a 40% aqueous solution of tetrabutylammonium hydroxide base was added via a burette. The extent of reaction was monitored by the pH of the solution, so that just enough base was added to remove all the acidic protons from the coal. The reaction may be summed up by the following equation :

$$\underset{\text{hydroxyl group}}{\text{Coal-OH}} + \underset{\text{base}}{(C_4H_9)_4NOH} \rightarrow \underset{\text{quaternary ammonium salt}}{\text{Coal-ON}(C_4H_9)_4} + \underset{\text{water}}{H_2O}$$

The mixture was stirred for 2 hrs and the alkylating agent (iodomethane) was then added in a two-fold excess.

$$\text{Coal-ON}(C_4H_9)_4 + CH_3I \rightarrow \text{Coal-OCH}_3 + (C_4H_9)_4NI$$

The reaction mixture was then stirred overnight and the product separated and dried under a vacuum at 100°C overnight. Illinois No.6 (a high volatile bituminous coal) and Rawhide (a subbituminous coal) were methylated with great success. The results were analysed by IR and ^1H nmr. Further work on alkylating these coals and the importance of secondary structure in coals was carried out by Liotta et al[80] in 1980.

Later Wachowska et al[81] used Sternberg's reductive alkylation procedure to cleave the ether linkages and octylate the vitrinite and semifusinite-rich fractions of Balmer 10 coal - a Canadian coking coal with a carbon content of approximately 88% (daf). Wachowska and her co-workers analysed the oxygen functional groups before and after ether cleavage and found that the number of ether linkages present in the original samples were approximately 1.5 per 100 C atoms. They also concluded that there was a greater amount of heterocyclic oxygen present in the semifusinite which could not be cleaved by the K / THF / Naphthalene system. Later Wachowska et al[82] continued their reductive alkylation work looking at the structures of coal extracts.

Ignasiak et al[83] succeeded in ethylating a low rank vitrinite coal via a non-reductive technique using ammonia. The product obtained from this non-destructive technique showed significant solubilisation in both chloroform and pyridine. The reaction involved the removal of acidic protons from the coal using liquid NH_3 in the presence of sodium or potassium amide.

$$\text{Vitrinite-(H)} + NH_3 \rightarrow \text{Vitrinite}^- + NH_4^+$$

This was followed by addition of ethyl bromide to effect alkylation.

$$\text{Vitrinite-Na(K)} + C_2H_5Br \rightarrow \text{Vitrinite-}C_2H_5 + \text{Na(K)Br}$$

The results showed that, overall, about 50% of the ethyl groups introduced into the vitrinite were not linked to hydroxyl oxygen. Ignasiak postulated that a significant proportion of the ethyl groups were linked to acidic carbon atoms.

Snape et al[84] have also shown that methylation of benzene-insoluble coal extracts is an excellent method for increasing the solubility of these fractions prior to spectroscopic analysis. The method utilised by Snape and his fellow workers involved the reaction of the extracts with iodomethane and tetra-n-butylammonium hydroxide base in THF solvent. The reactions were carried out at ambient temperatures and nuclear magnetic resonance spectroscopy showed that over 70% of the phenolic hydroxyl functional groups were methylated.

In 1986 Stock and Mallaya[85] succeeded in increasing the extractability in pyridine of six high rank coals (87 - 89% C - daf basis) via alkylation using Liotta's mild alkylating procedure[35]. There was a remarkable increase in pyridine extractability after O-butylation but only modest changes after O-methylation. Studies of the effects of O-methylation on the pyrolysis behaviour of coals have been carried out by Chu et al[86], who methylated the coals using the procedure devised by Liotta[35]. Significant increases in tar yields and a low-temperature fraction (150 - 300°C) were found for the low rank O-methylated coals. Chu and her co-workers proposed that methylation prevented the formation of new ether cross linkages through water elimination reactions of hydroxyl functional groups, thus allowing for the release of a low-temperature fraction as well as a higher temperature tar. Methanol and formaldehyde were the principal products from the pyrolysis of methylated carboxylic and aliphatic hydroxyls, whilst decomposition of methylated phenolic groups occurred at a slightly higher temperature and produced principally methane and carbon monoxide.

A new technique for the synthesis of methoxybenzenes from phenols and methyl formate via catalytic O-alkylation has recently been devised by Taleb and Jenner[87]. This technique involves a nucleophilic methylation by methyl formate using acetonitrile as solvent and cetyltrimethylammonium bromide (CTAB) as catalyst. The yields from the reaction are high and the procedure is simple and inexpensive - the CTAB may be recovered after distillation and re-used without appreciable loss in activity.

The work in this chapter involves the attempted methylation of the model compounds followed by subsequent methylation of the Creswell and Cortonwood coals and coal macerals, with a view to analysing the resulting products via spectroscopic techniques, to ascertain the nature of the hydroxyl functionalities in the coals and coal macerals.

6.2 EXPERIMENTAL

6.2.1 Method 1 - methyl iodide

The sample (3.26 mmol phenolic compound) and 6.52 mmol of silver tetrafluoroborate ($AgBF_4$) were dissolved, with stirring, in 11.0 cm^3 of dichloroethane under an inert atmosphere of argon. The methyl iodide (6.52 mmol) was then introduced via a syringe and the mixture was left to stir overnight. On completion of the reaction the mixture was filtered and washed with an excess of acetonitrile. The filtrate was then rotary evaporated to remove the solvent and the residue (if a solid) was dried overnight at 110°C under dry N_2.

6.2.2 Method 2 - methyl formate

The dried sample (10 mmol phenolic compound) was added to 50 mmol methyl formate ($HCOOCH_3$), 0.30 mmol cetyltrimethylammonium bromide catalyst and 7 cm^3 acetonitrile solvent. For the microwave method the reagents were put into a sealed teflon digestion vessel, placed in a microwave and irradiated with microwaves (usually for 30 mins). The bench top method involved refluxing the reagents (usually for 24 hrs). On completion of reaction the sample was rotary evaporated or filtered and washed with acetonitrile, depending on whether a solution or solid in solution were obtained.

6.2.3 Method 3 - phase-transfer

10 mmol of the phenolic compound, 20 mmol of 0.2M sodium hydroxide solution and 20 mmol of methyl iodide were placed in a separating funnel to give two immiscible layers. 1.0 cm^3 of 15-crown-5 ether was then added and the mixture was agitated and left to stand for two days. After two days the mixture was separated and silver nitrate ($AgNO_3$) was added to the aqueous solution to see how much silver iodide (AgI) precipitated. The layer containing the methylated phenol compound was rotary evaporated to isolate the product.

6.3 RESULTS AND DISCUSSION

6.3.1 Methylation using methyl iodide

This novel method for the attempted methylation of phenolic compounds involved dissolving the model compound and silver tetrafluoroborate (1 : 2 molar ratio respectively) in dichloromethane under inert argon whilst stirring. The next stage of the reaction was to add the methyl iodide (iodomethane) methylating reagent via syringe. The mixture was then left to stir under argon overnight. The reaction, if successful, should involve an S_N2 displacement by the phenolic oxygen on the silver-complexed halide. Because the alkylation is reversible due to the presence of the halide ion (which is also a good nucleophile), the reaction is carried out in the presence of silver tetrafluoroborate, which precipitates out as silver halide, leaving the poor nucleophile tetrafluoroborate as the solute anion.

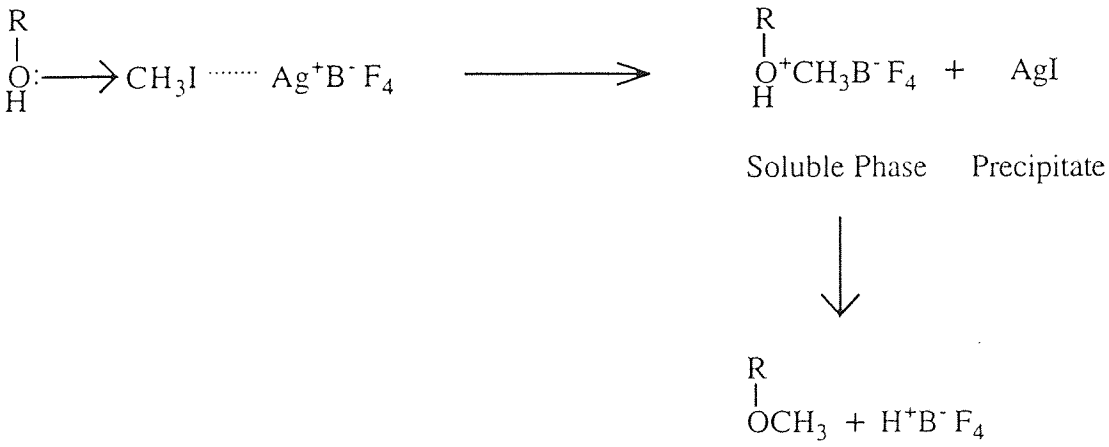

The reaction was initially carried out on the 2,6-dimethylphenol (model compound). On addition of the methyl iodide, the solution turned a cloudy-yellow colour, which, upon further mixing, changed to a yellow-green colour. After completion of the reaction a green-grey precipitate was observed. Fig 6.01 shows the IR plot of the solution obtained after rotary-evaporation of the solvent. The product is obviously not methylated 2,6-dimethylphenol in solution. There are a distinct lack of IR bands due to aryl-H vibrations at 750 - 850 cm^{-1} and aromatic ring frequencies at approximately 1500, 1580 and 1600 cm^{-1} are notable by their absence. Also there is the appearance of a major band at 1058 cm^{-1} - this is probably due to BF_4^- or iodate (originally occurring as an impurity in the methyl iodide).

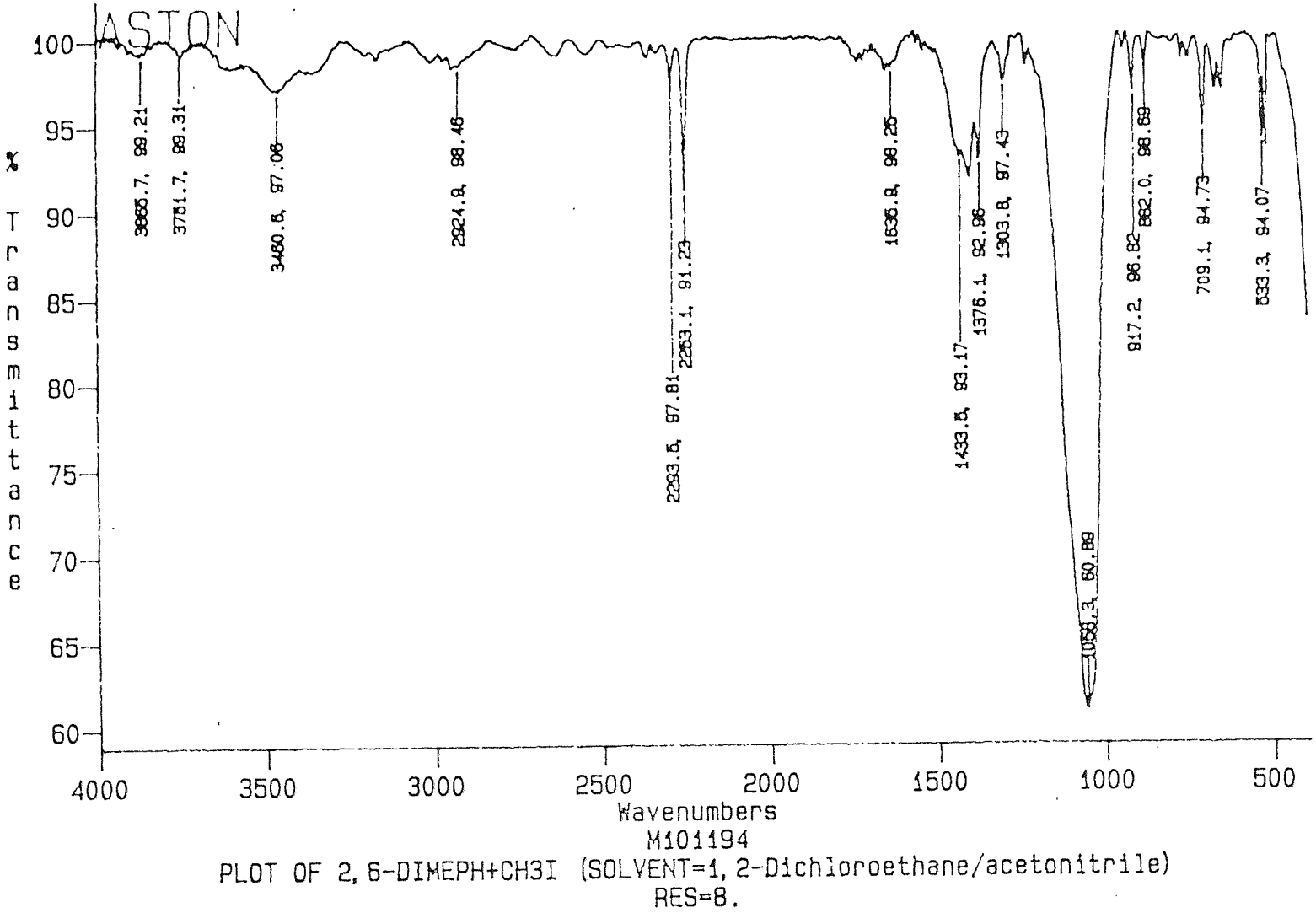

Fig6.01
IR of the methylated 2,6-dimethylphenol product (methyl iodide method)

Fig 6.02 shows an IR comparison between the product obtained and the unreacted 2,6-dimethylphenol compound. In this plot the differences are much more apparent.

Due to the unusual nature of the product, it was decided to look more closely at the reagents being used. It was discovered that the methyl iodide being utilised had been stored away for some time and contained substantial impurities. Fig 6.03 shows the IR plot of the methyl iodide used for the methylation of 2,6-dimethylphenol. The plot shows that the main peaks expected at approximately 2950 cm^{-1} (C-H stretching) and approximately 510 cm^{-1} (C-I stretching) are missing. Fig 6.04 shows an IR comparison of the contaminated methyl iodide reagent and the product. The plot shows that the main contributions appear to be due to the impure CH_3I reagent. An attempt was made to purify the methyl iodide by drying it for several days using molecular sieve 4A. This dried methyl iodide was then used to methylate the 2,6-dimethylphenol. Fig 6.05 shows the IR plot of the resulting product and fig 6.06 shows an IR comparison of the products obtained using the impure and dried CH_3I reagents - drying the impure methyl iodide did not appear to make any significant difference to the nature of the product.

Consequently, a new batch of methyl iodide was ordered from the Aldrich Chemical Company and this was analysed as soon as it was received. Fig 6.07 shows the IR spectrum of the new methyl iodide reagent. In this instance, the peaks we would expect to find are apparent - there is a sharp peak due to aliphatic C-H stretching at 2948 cm^{-1}, a substantial peak due to C-H deformations at 1423 cm^{-1} and a sharp peak due to C-I at 523 cm^{-1}. Fig 6.08 shows an IR comparison between the impure and new batch of methyl iodide, where the differences in structure are much more evident. The new batch of methyl iodide was now used in the attempted methylation of 2,6-dimethylphenol. On addition of the methyl iodide, the solution changed to a creamy-yellow colour and after the reaction was complete a green-grey precipitate was observed. Fig 6.09 shows the IR plot of the product. It appears that methylation has been unsuccessful - the sharp IR band expected at around 2950 cm^{-1} due to aliphatic C-H stretching has not materialised. There are also bands at 2293 cm^{-1}, 2253 cm^{-1} and 1423 cm^{-1}, 1375 cm^{-1} which are characteristic of acetonitrile, showing that not all the wash-solvent has been removed. Another dominant band (which also appeared in the impure CH_3I) appears at 1041 cm^{-1}. It is highly probable that this band is due to iodate. The results point to the conclusion that an alternative reaction is occurring preferentially to the one desired. IR analysis of the precipitate obtained from the reaction yielded no peaks in the 4000 - 400 cm^{-1} region (fig 6.10).

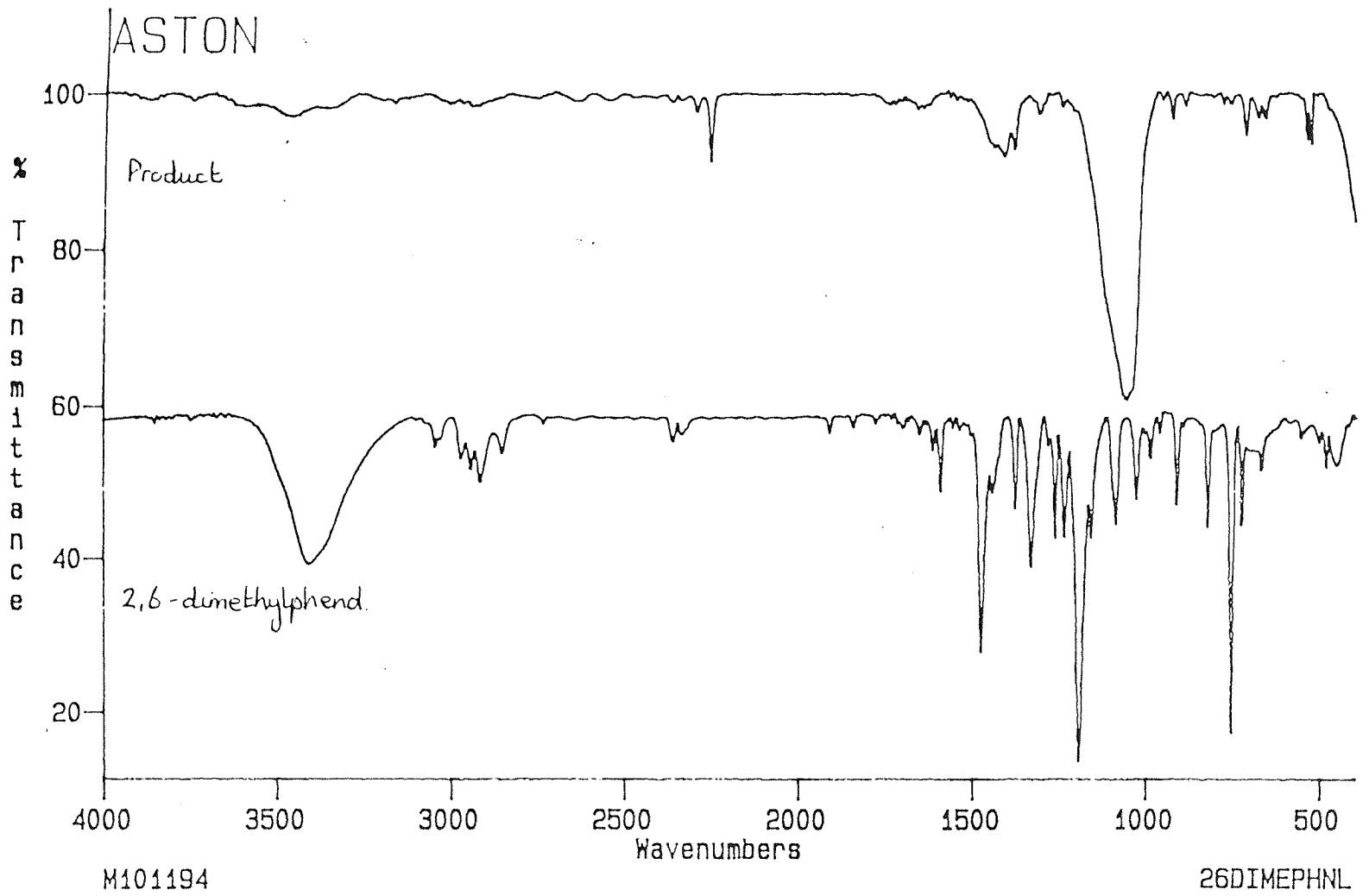

Fig6.02
IR of the methylated 2,6-dimethylphenol product and the unreacted 2,6-dimethylphenol (methyl iodide method)

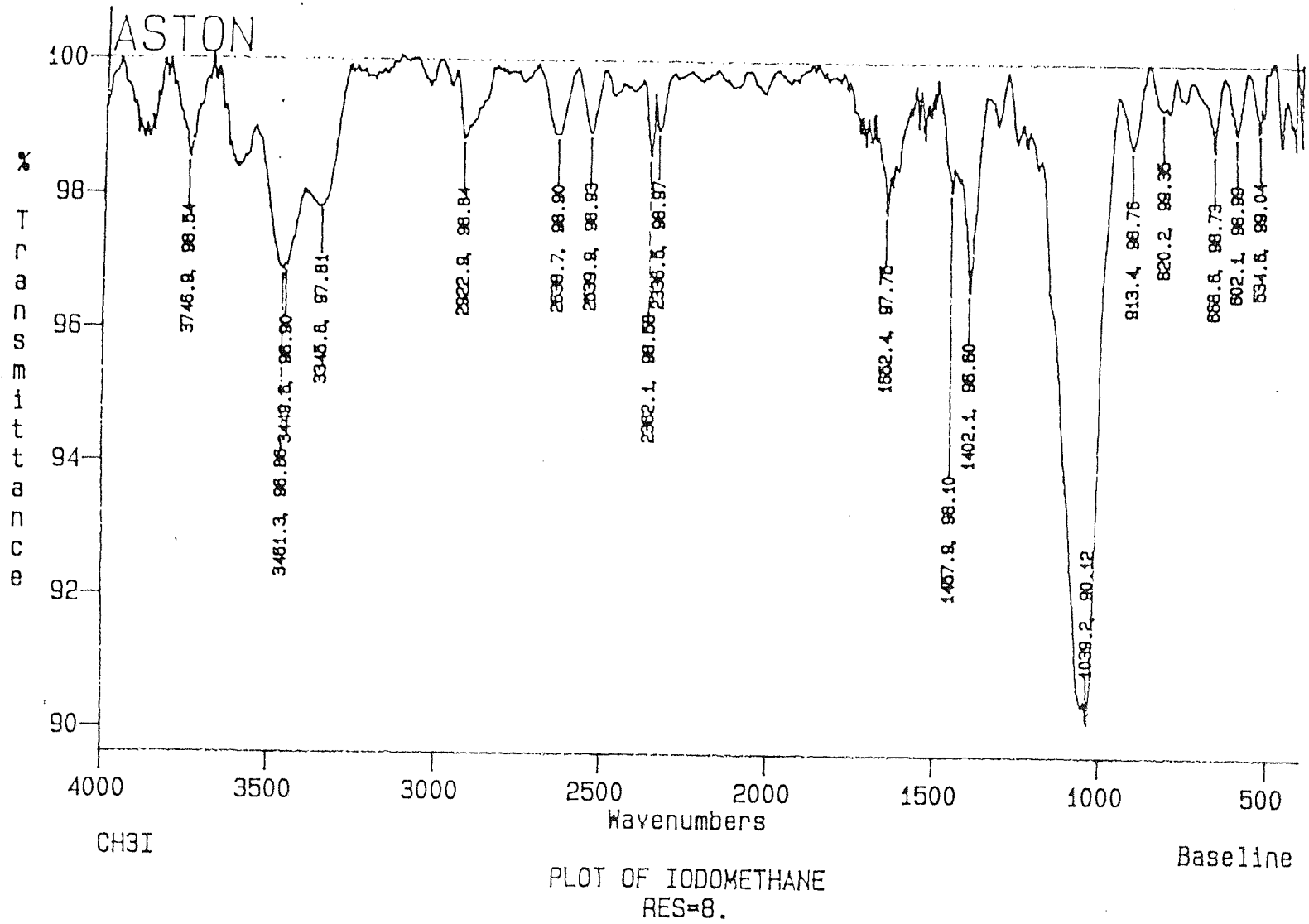

Fig6.03
IR of Iodomethane

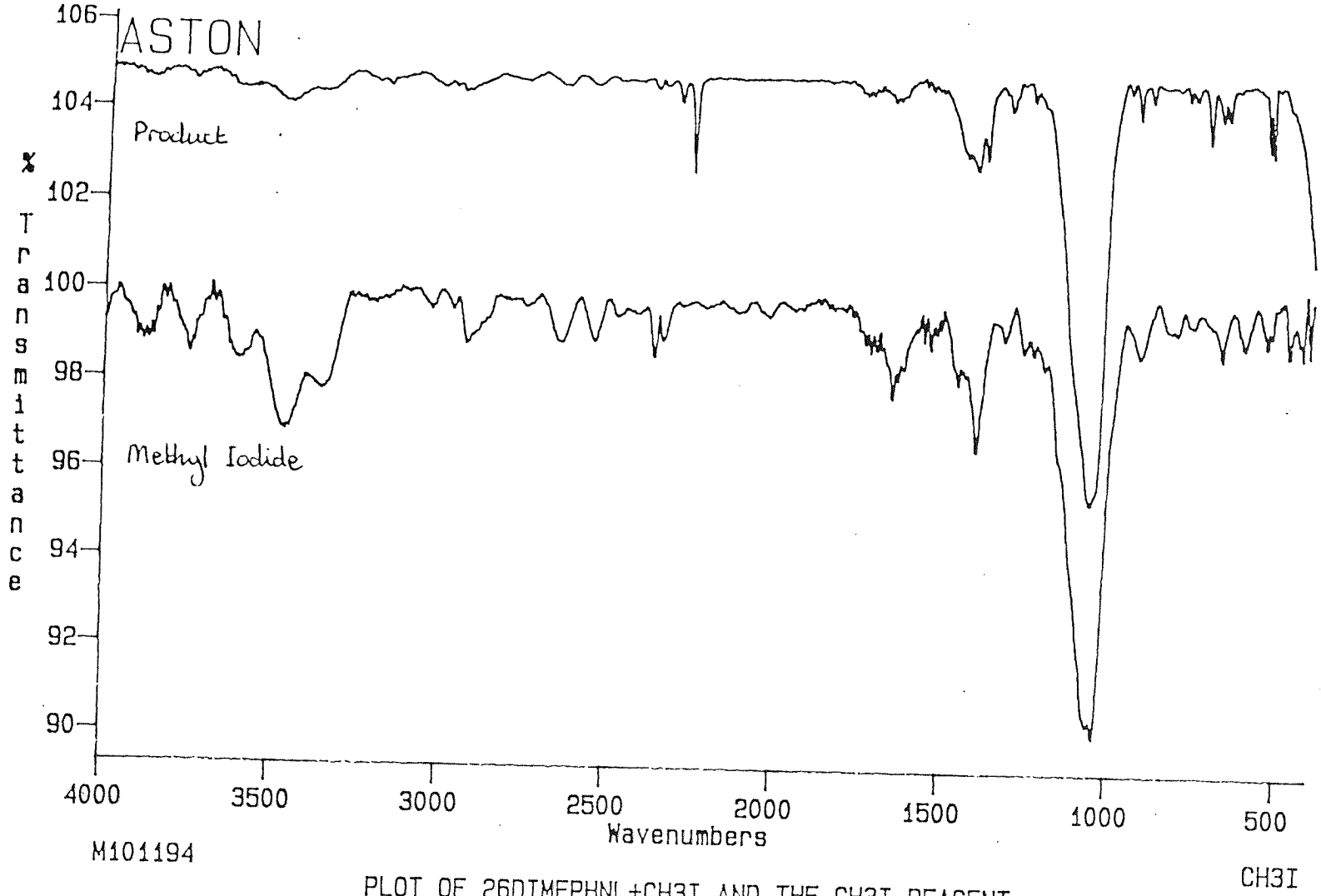

Fig6.04
IR of Iodomethane and the methylated 2,6-dimethylphenol product
(methyl iodide method)

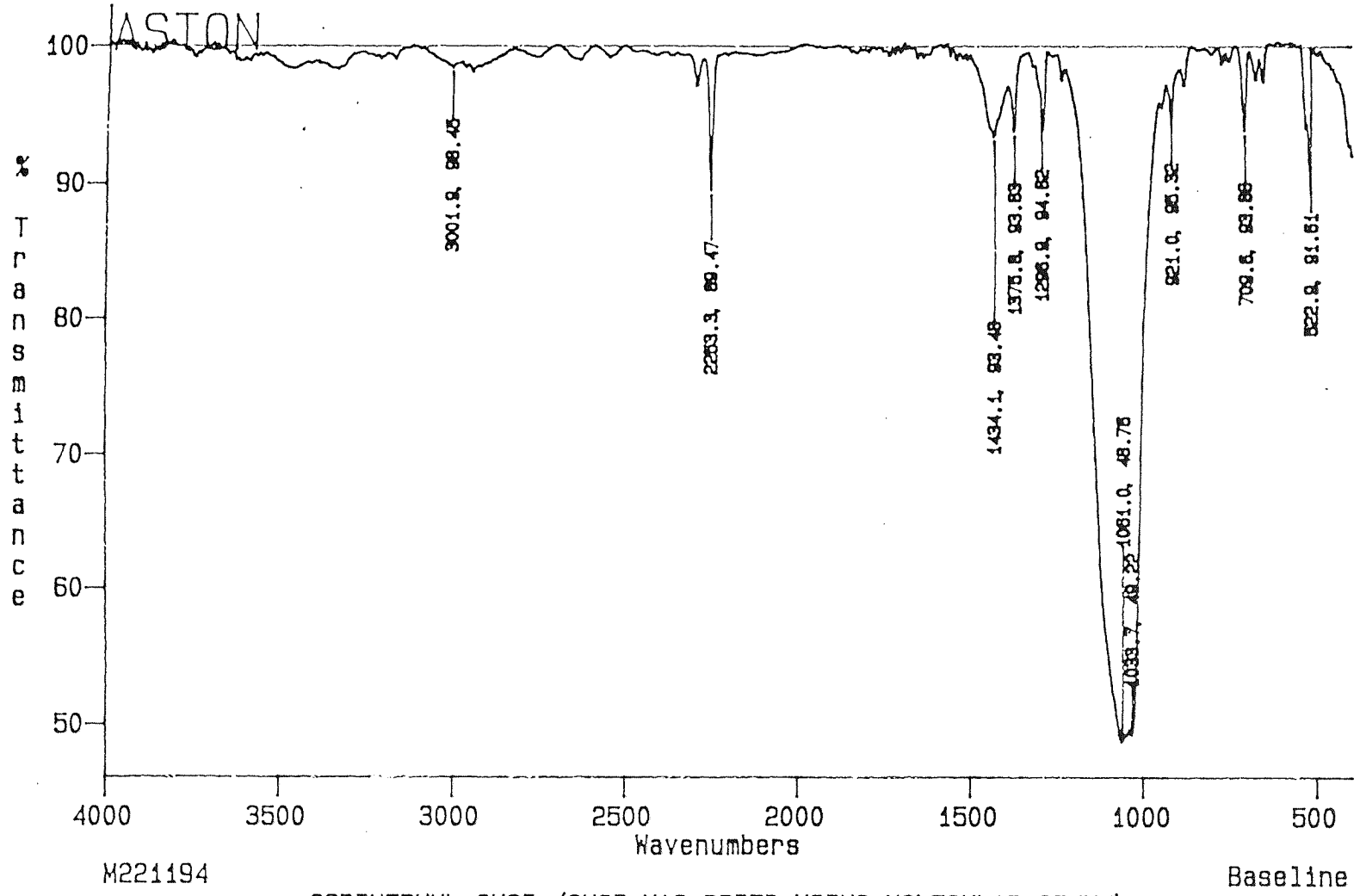

Fig6.05
IR of the methylated 2,6-dimethylphenol product using dried CH_3I (methyl iodide method)

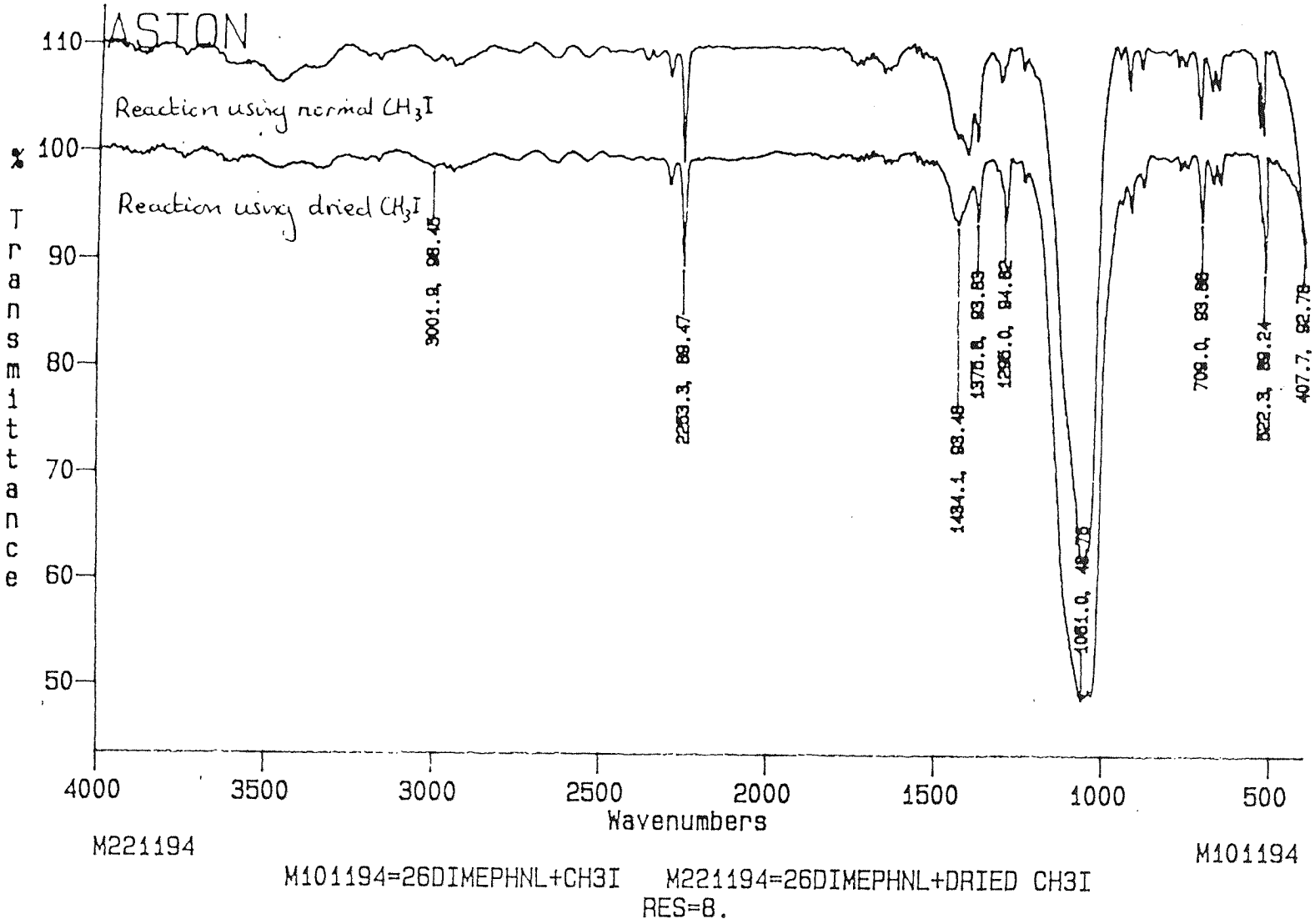

Fig6.06
IR of the methylated 2,6-dimethylphenol product using dried CH_3I and normal CH_3I (methyl iodide method)

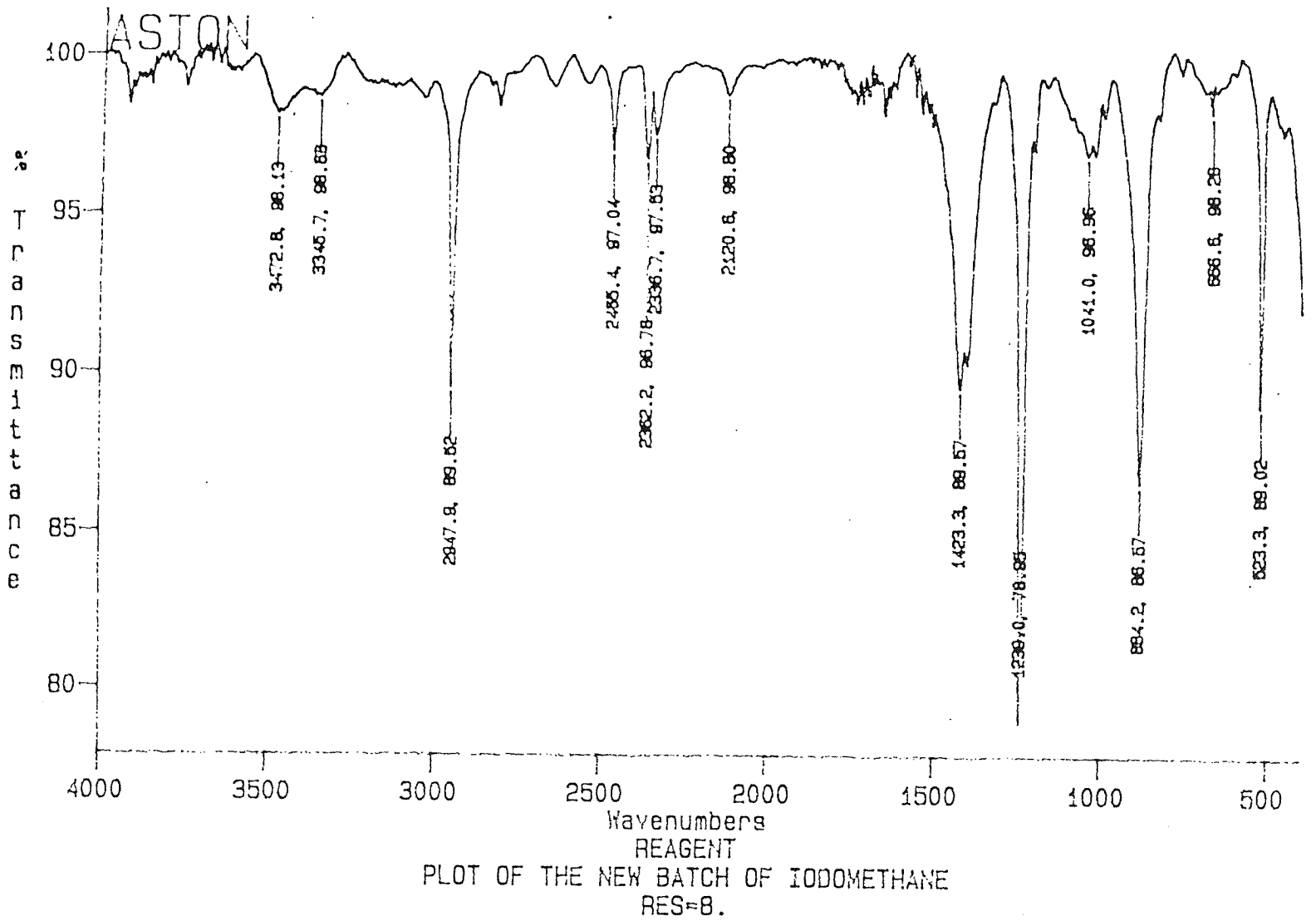

Fig6.07
IR of the new batch of Iodomethane

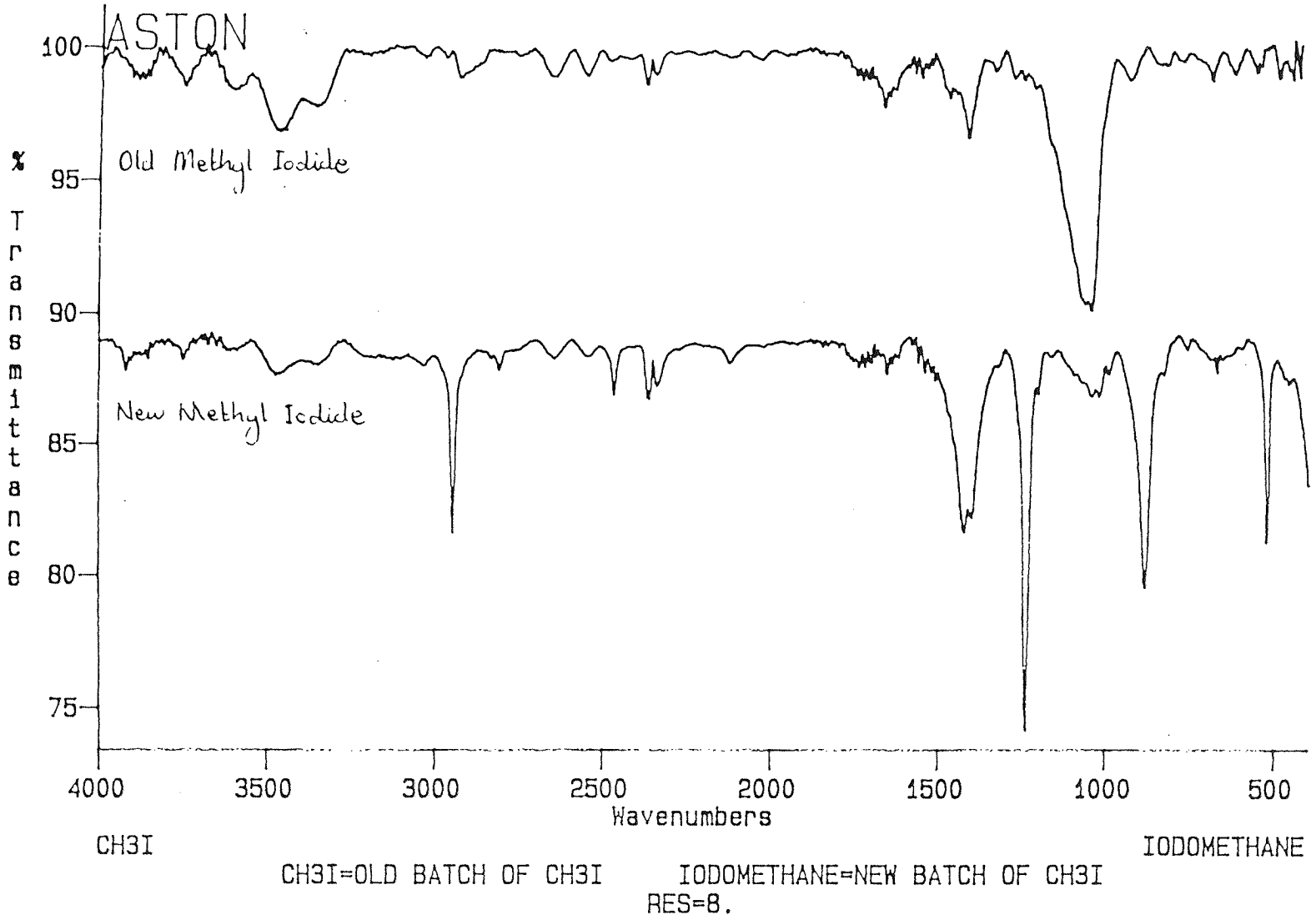

Fig6.08
IR comparison between the impure and new batch of Iodomethane

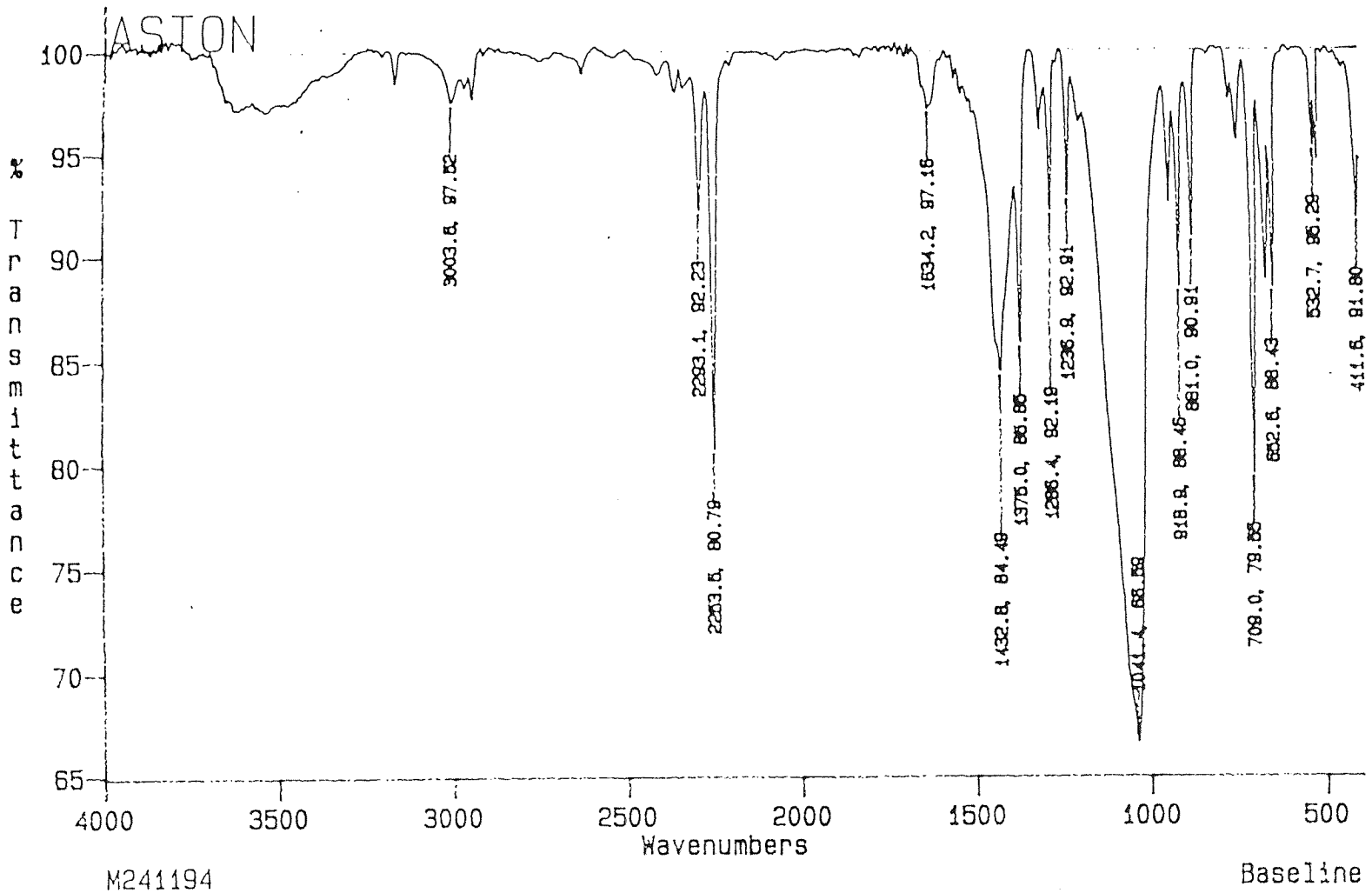

Fig6.09
IR of methylated 2,6-dimethylphenol product using the new batch of CH_3I (methyl iodide method)

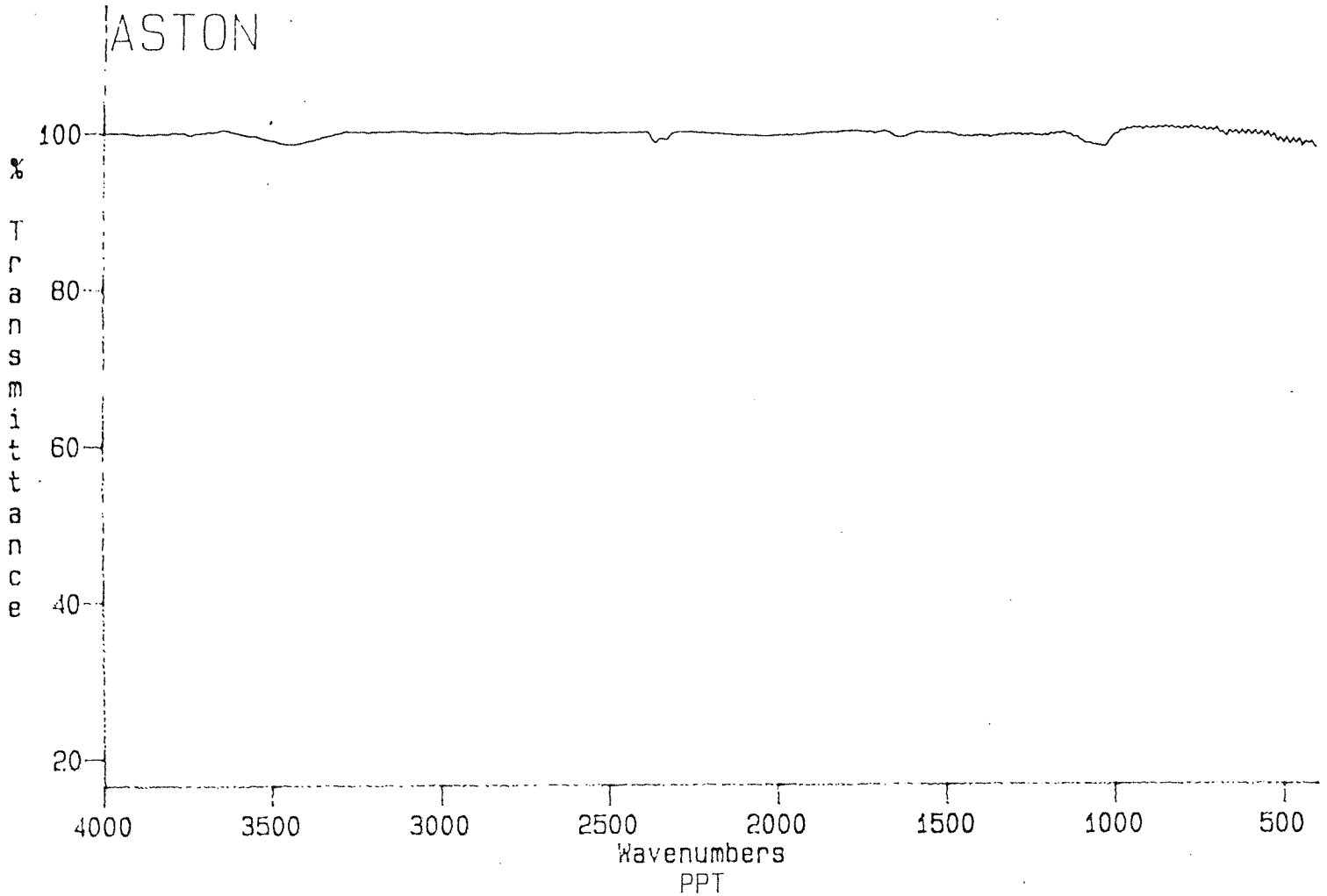

Fig6.10
IR of the ppt obtained from the methylation of 2,6-dimethylphenol using the new batch of CH_3I (methyl iodide method)

One possible explanation could be that the methyl iodide is reacting preferentially with small amounts of moisture present to form methanol and hydrogen iodide (which is subsequently converted to AgI precipitate) and the volatile model compound and methyl iodide may, in part, be lost in the inert argon gas stream. Mild heating of the reagents during reaction proved to have little effect. Due to these reasons and the sensitivity of the method, methylation via this route was considered unsuitable.

6.3.2 Methylation using methyl formate

This method was based on a procedure devised by Taleb and Jenner[15] which involves the synthesis of methoxybenzenes from phenols using methyl formate. Methyl formate was used as the methylating agent and a quaternary ammonium salt Q^+X^- (cetyltrimethylammonium bromide $C_{16}H_{33}N^+(CH_3)_3Br^-$) was used as a catalyst. The reaction may be summarised as :

$$R\text{-}OH \xrightarrow[Q^+X^-]{HCOOCH_3} R\text{-}OCH_3$$

The cetyltrimethylammonium bromide (CTAB) quaternary ammonium salt was used because the long alkyl chain ensures good solubility in organic solvents and leads to the formation of a highly reactive ion-pair :

$$HCOOCH_3 + Q^+X^- \longrightarrow HCOO^-Q^+ + CH_3X$$

$$CH_3X + PhO^- \longrightarrow PhOCH_3 + X^-$$

$$X^- + HCOO^-Q^+ \longrightarrow Q^+X^- + HCOO^-$$

$$HCOO^- \longrightarrow CO_2 + 1/2\,H_2$$

A direct attack by the phenoxide ion on the methyl formate may also occur :

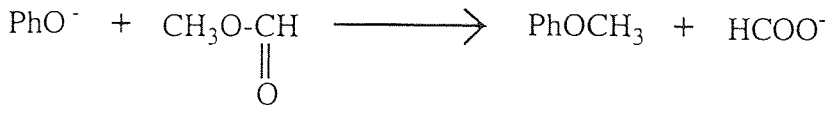

Acetonitrile was chosen as the solvent because it acts as a basic medium and also possesses polar properties. It also has the added advantage that it has been shown to extract only negligible amounts of the more labile components in coal. Excess methyl formate reagent was used to counteract the effects of decarboxylation under CTAB / acetonitrile conditions. All reactions were carried out in the MES-1000 microwave oven using an initial 5 min heating period at 40% microwave power followed by further microwave heating for the appropriate time at 20% microwave power. The MES-1000 microwave oven was programmed such that the upper temperature limit was set at 200°C and the upper limit on pressure was 180 psi.

Initially, the model compounds were reacted for 30 mins in the MES-1000 microwave oven. Fig 6.11 shows the IR spectra of the product obtained from the attempted methylation of 2,6-dimethylphenol. The unreacted 2,6-dimethylphenol is also shown for comparison. The spectrum remains effectively unchanged and very little reaction, if any, appears to have occurred. Fig 6.12 shows an IR comparison of the methylated 2,6-diisopropylphenol - again no methylation has taken place. Similarly for the attempted methylation of 2,6-di-tert-butylphenol (fig 6.13), 2,6-diphenylphenol (fig 6.14) and 2-phenylphenol (fig 6.15). The 2,4,6-tri-tert-butylphenol does, however, show an interesting difference after 30 mins of microwave heating. Fig 6.16 shows the IR spectra of the product obtained after methylation of 2,4,6-tri-tert-butylphenol and the unreacted 2,4,6-tri-tert-butylphenol. A broad absorption band appears in the product IR at approximately 2900 cm^{-1}. This band has been assigned to C-H deformations in the alkyl chain of the CTAB catalyst. Fig 6.17 shows the IR spectra of the methylated 2,4,6-tri-tert-butylphenol product and the CTAB catalyst. One possibility is that the phenolic compound has managed to form a stable ion-pair with the CTAB catalyst :

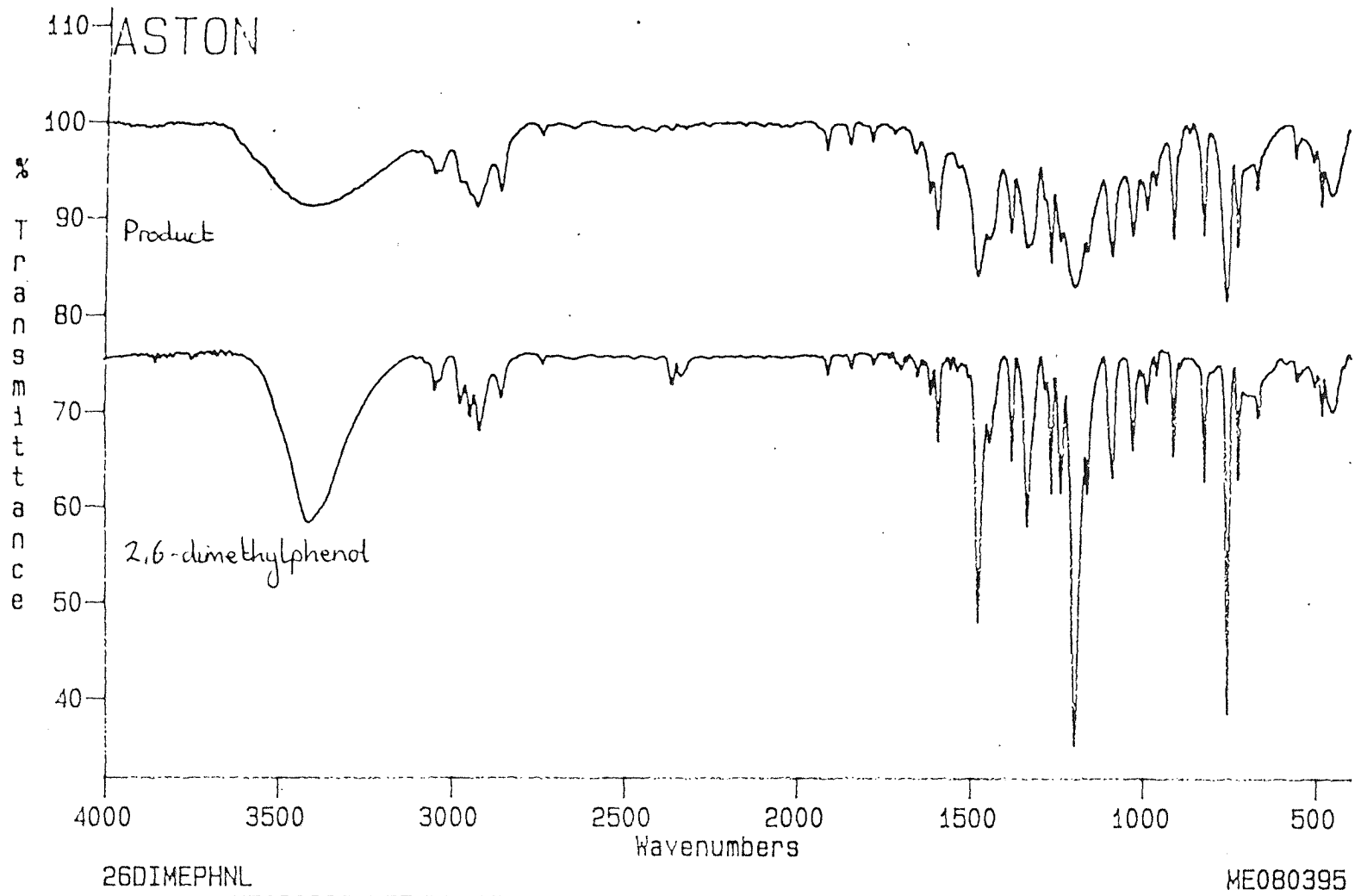

Fig6.11
IR of the methylated 2,6-dimethylphenol product (methyl formate method)

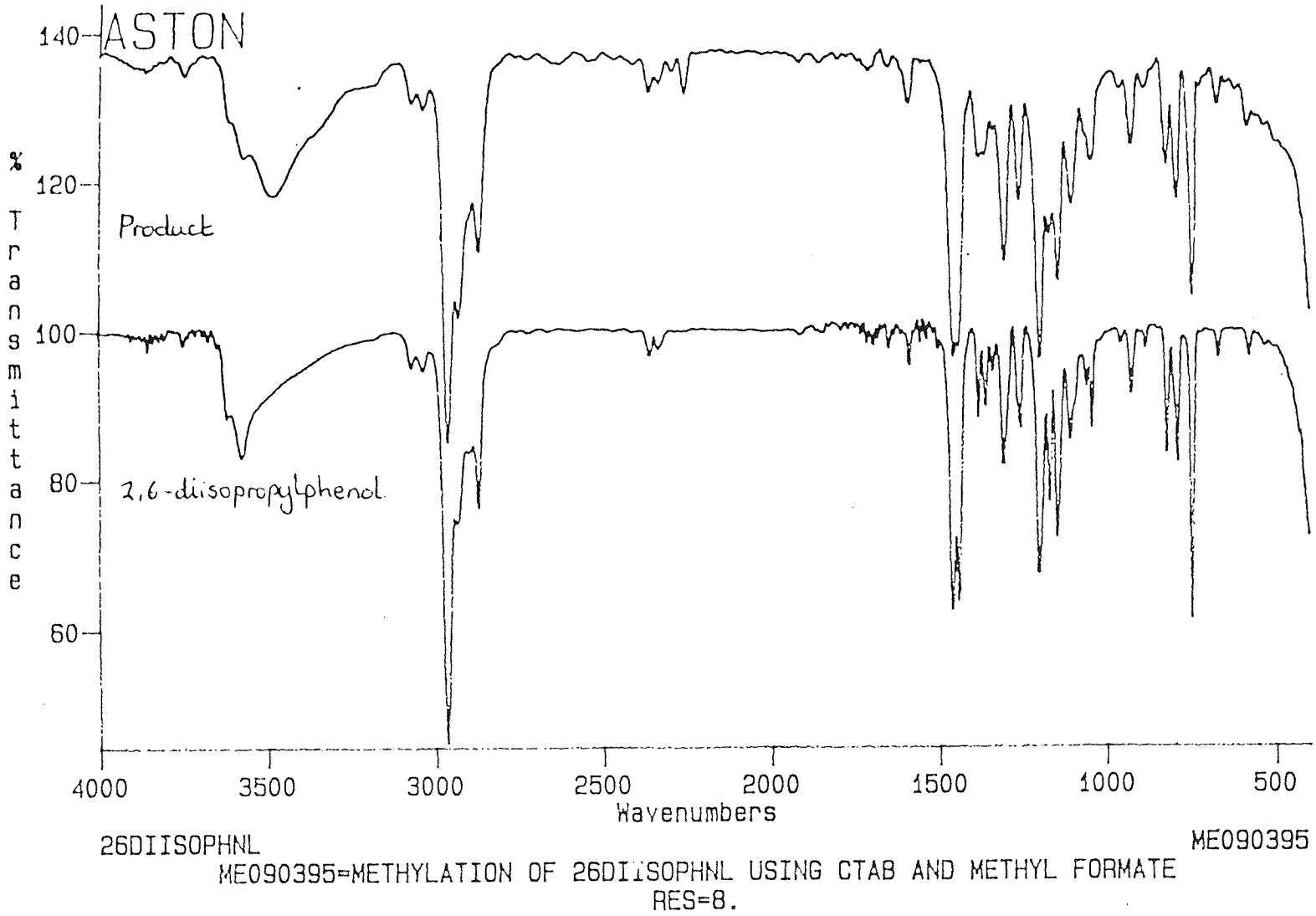

Fig6.12
IR of the methylated 2,6-diisopropylphenol product (methyl formate method)

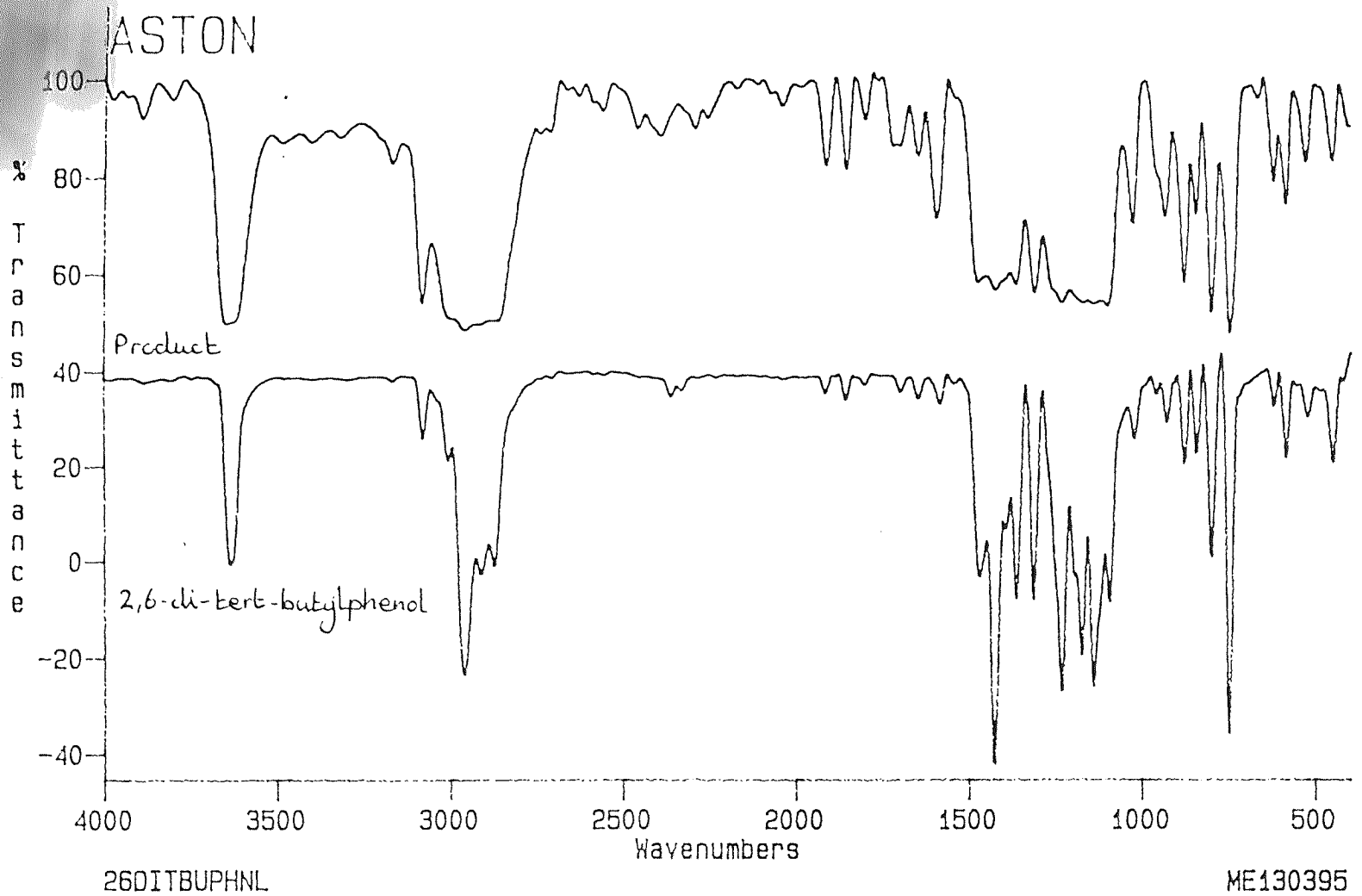

Fig6.13
IR of the methylated 2,6-di-tert-butylphenol product (methyl formate method)

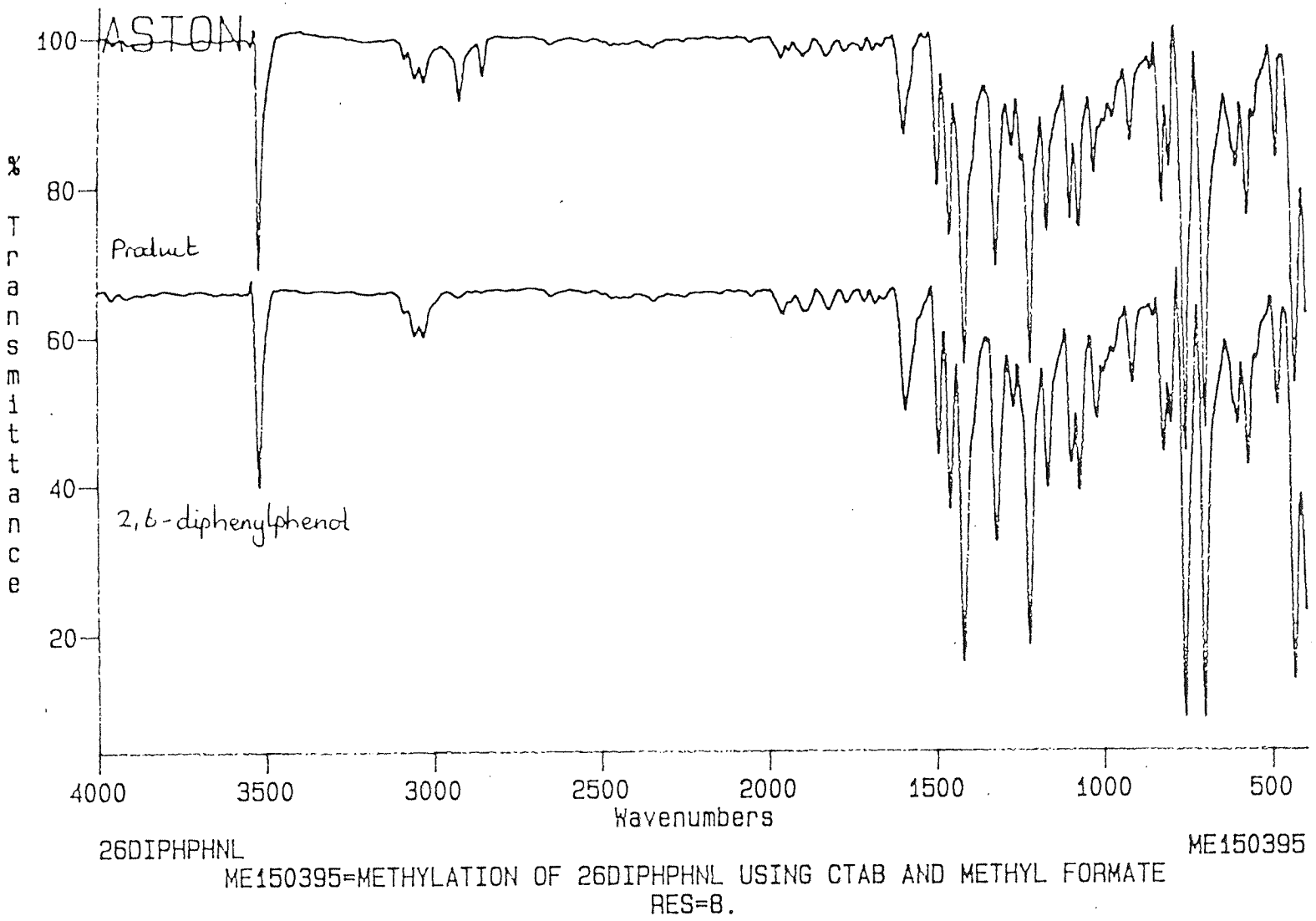

Fig6.14
IR of the methylated 2,6-diphenylphenol product (methyl formate method)

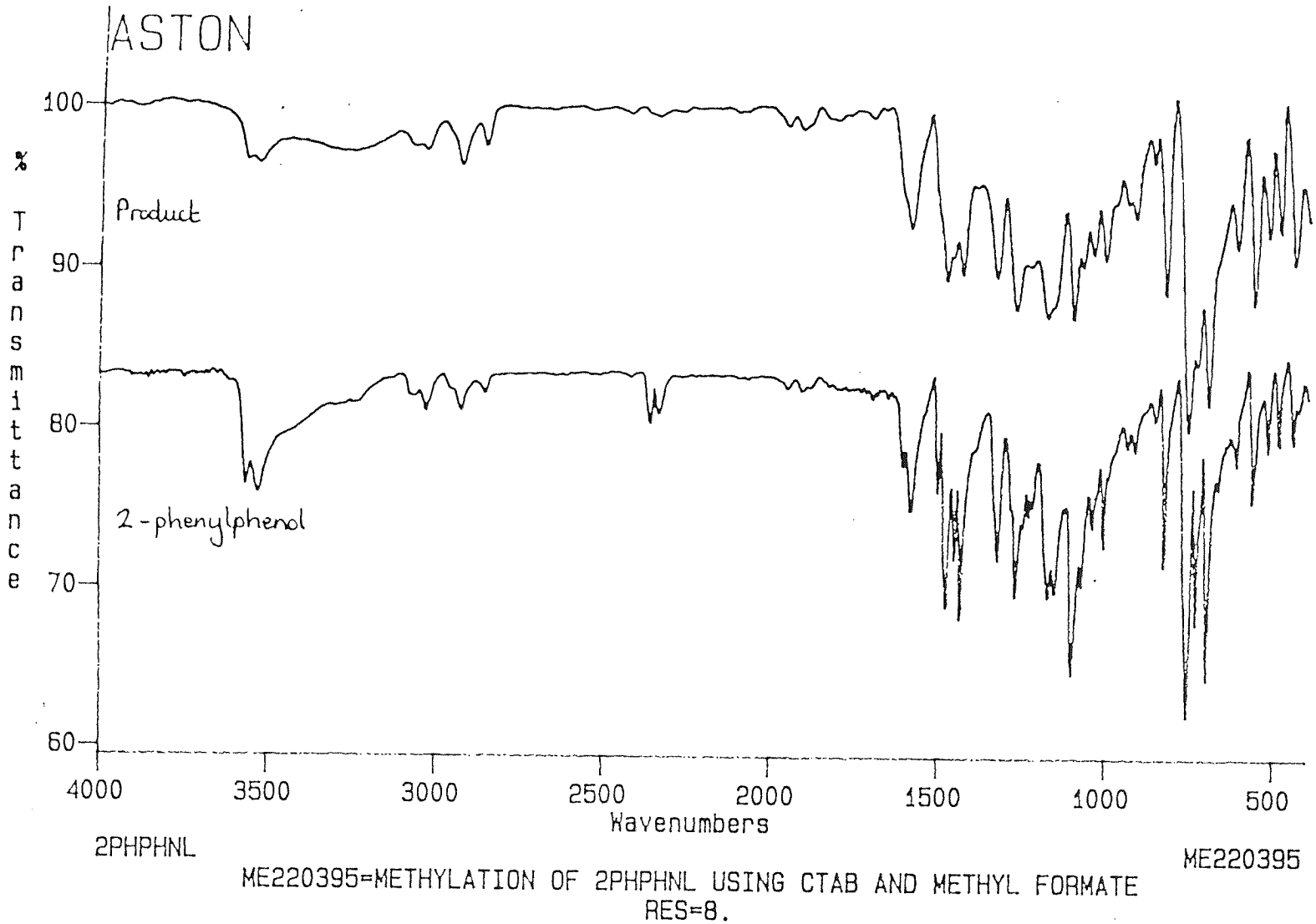

Fig6.15
IR of the methylated 2-phenylphenol product (methyl formate method)

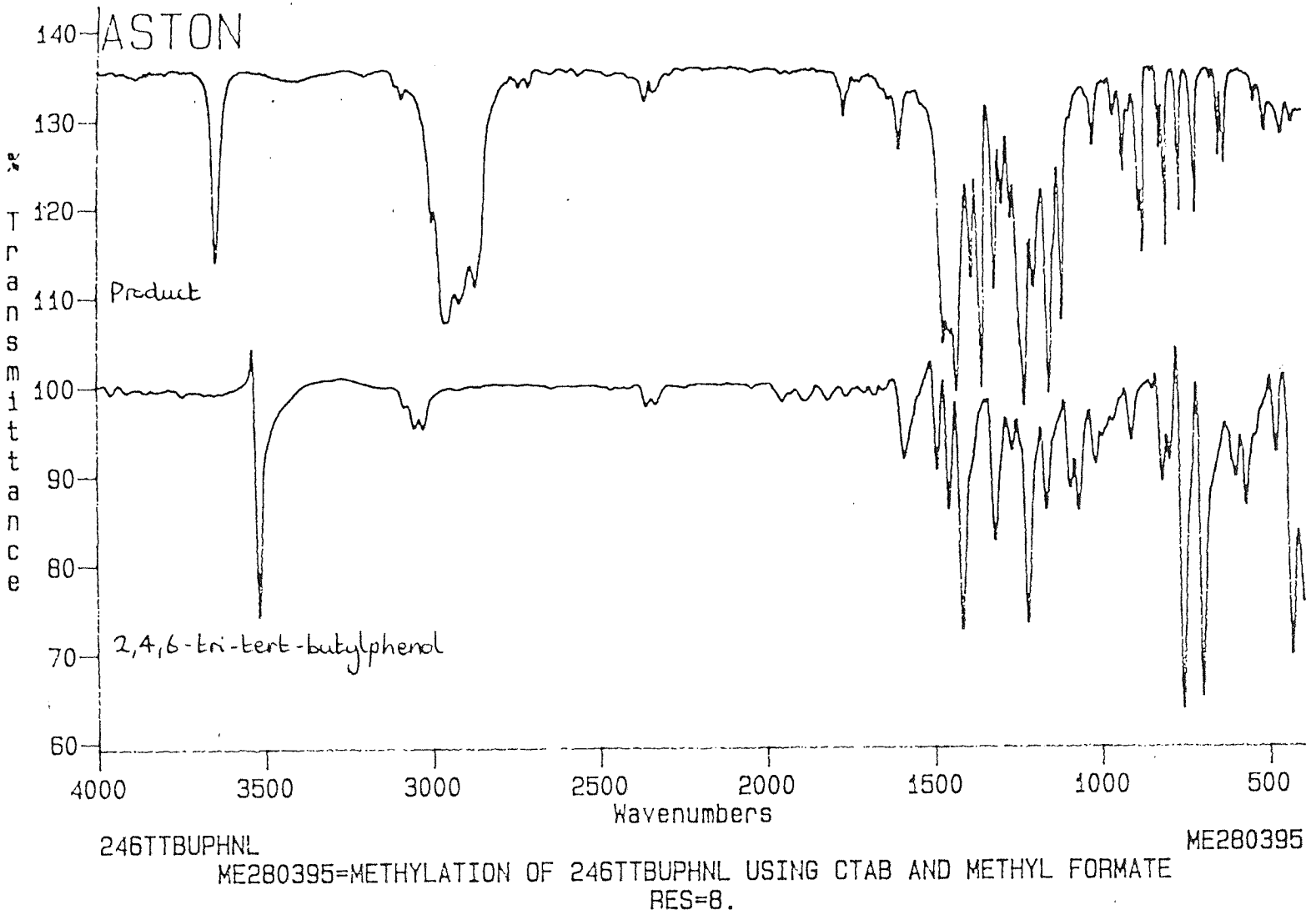

Fig6.16
IR of the methylated 2,4,6-tri-tert-butylphenol product (methyl formate method)

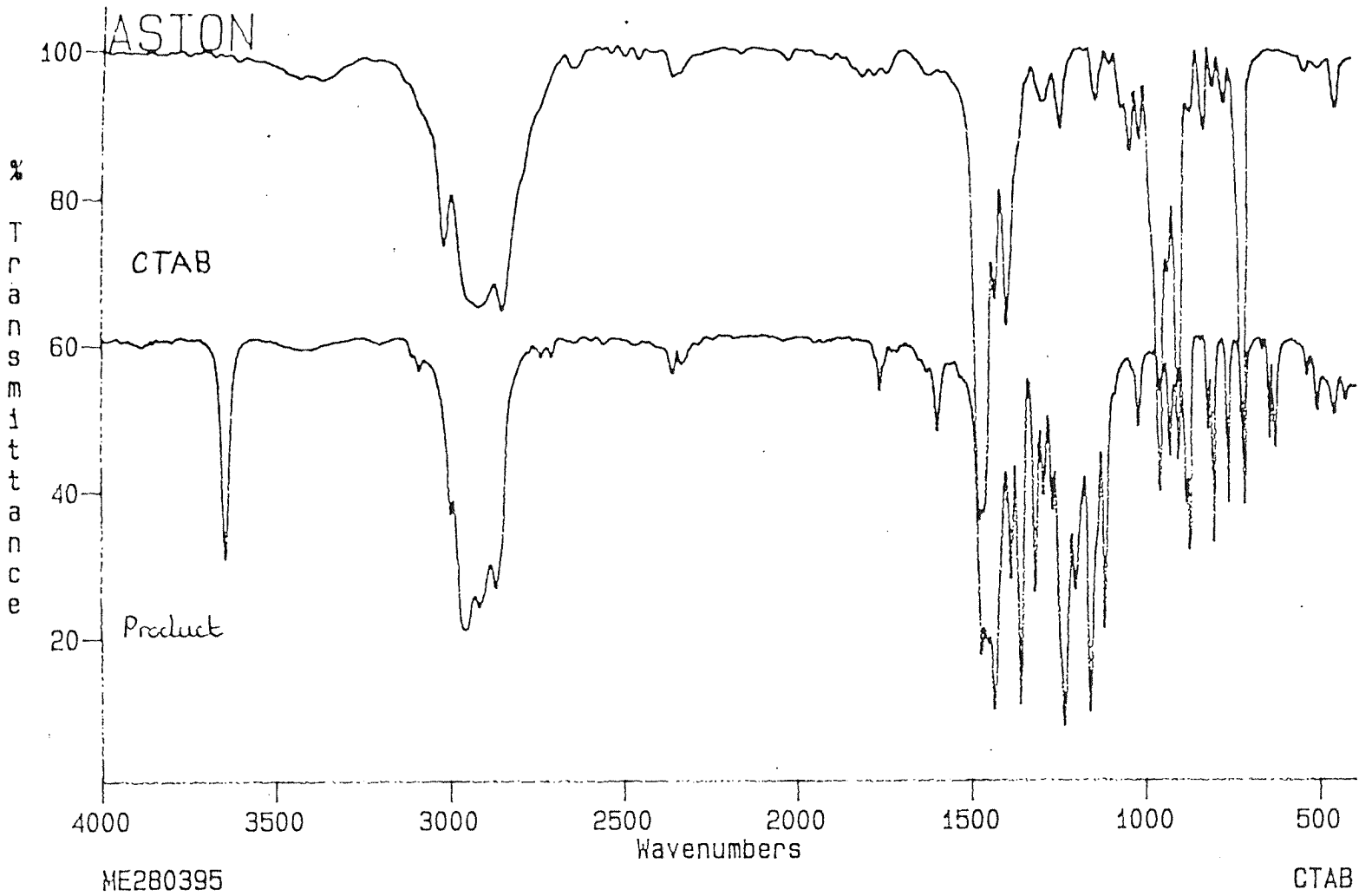

Fig6.17
IR of the methylated 2,4,6-tri-tert-butylphenol product
and CTAB (methyl formate method)

The reason why this phenomenon only occurs with this particular model compound is probably due to the stabilising electronic effects of an additional butyl group at the para-position of the benzene ring. This methyl group appears to be imparting extra stability to the aromatic ring structure allowing the stable cetyltrimethylammonium phenoxide ion-pair to exist. There also appears to be a solvation effect - a large anion and large cation produce lower solvation energies, which will favour the formation of ion-pairs in solution.

Table 6.01 Methylation of model compounds using methyl formate

Model Compounds	Evidence of methylation from FT-IR (after 30 mins microwave heating)
2,6-diphenylphenol	No
2,6-diisopropylphenol	No
2,6-di-tert-butylphenol	No
2,6-diphenylphenol	No
2-phenylphenol	No
2,4,6-tri-tert-butylphenol	No

It was decided to concentrate on attempting to methylate the 2,6-dimethylphenol compound. This model compound was reacted for 2 hrs in the MES-1000 microwave oven. Fig 6.18 shows the IR spectra of the 30 min microwave reaction (which did not react) and the 2 hr microwave reaction. The two spectra are effectively similar and still no significant reaction appears to have taken place. The 2,6-dimethylphenol was then reacted for 6 hrs. Fig 6.19 shows the IR for the subsequent product and a comparison with the 2 hr microwave reaction - again, no methylation has occurred.

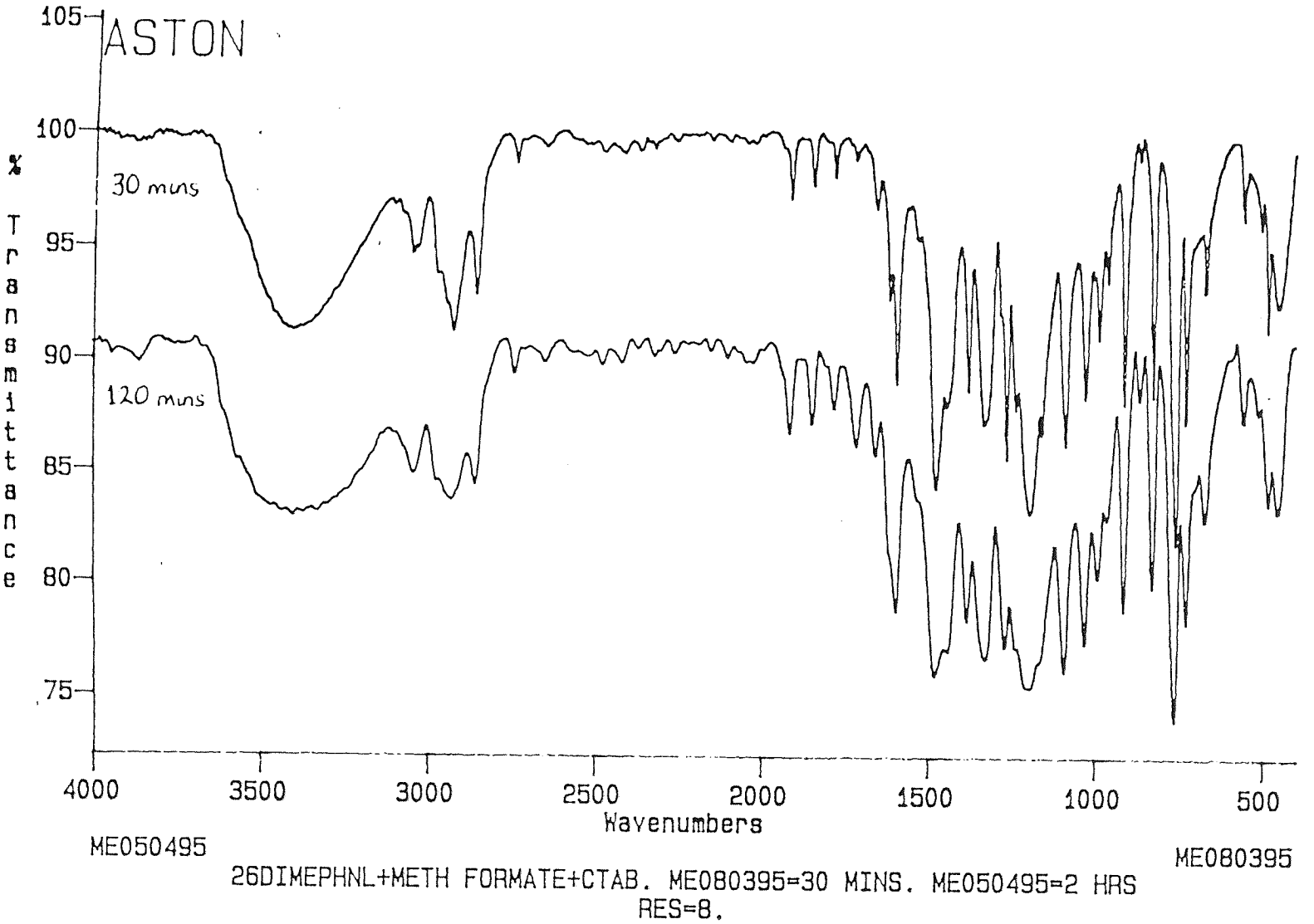

Fig6.18
IR of the methylated 2,6-dimethylphenol product after 30 mins and 120 mins mw heating (methyl formate method)

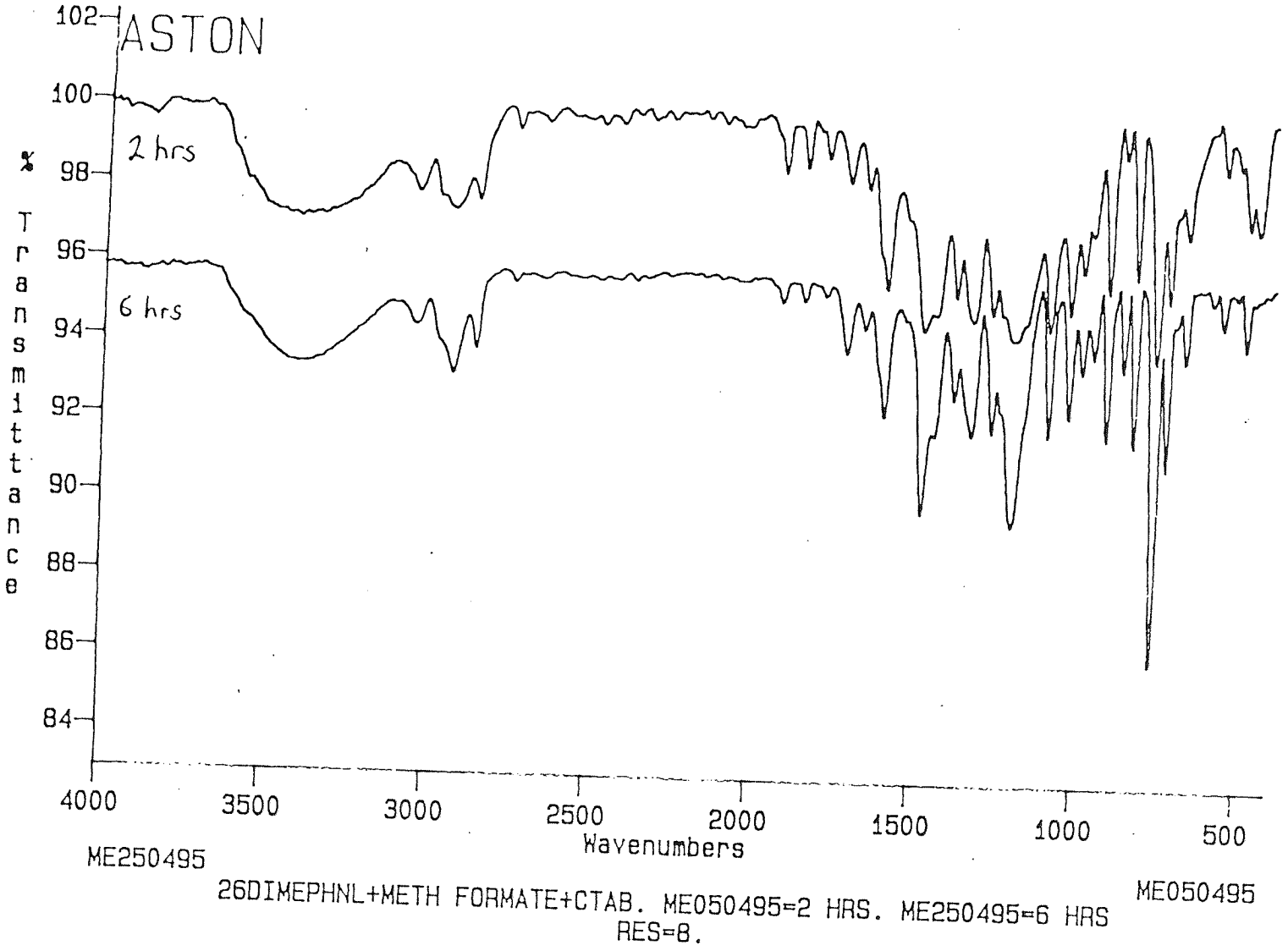

Fig6.19
IR of the methylated 2,6-dimethylphenol product after 6 hrs mw heating
(methyl formate method)

An alternative method of methylation, using the same reagents, was then attempted, whereby the reagents were refluxed for 24 hrs and 48 hrs on the bench top (figs 6.20 and 6.21 show the resulting IR spectra respectively). Still no methylation was observed.

6.3.3 Methylation via phase-transfer

This novel method involved the attempted methylation of 2,6-dimethylphenol, using methyl iodide methylating reagent, via a phase-transfer method. The model compound was dissolved in aqueous sodium hydroxide to give a light-orange solution. This was then poured into a separating funnel and the methyl iodide was added. Two immiscible layers were observed with the colourless methyl iodide at the bottom. The crown ether (15-crown-5) was then added to the separating funnel. The role of the crown ether was to promote the solubility of the alkali metal from one phase to another i.e to act as a transport medium between the two phases. The separating funnel was then agitated and left to stand for 2 days, after which the top layer was a cloudy light-pink colour and the bottom layer (containing the methylated product) was a light yellow colour.

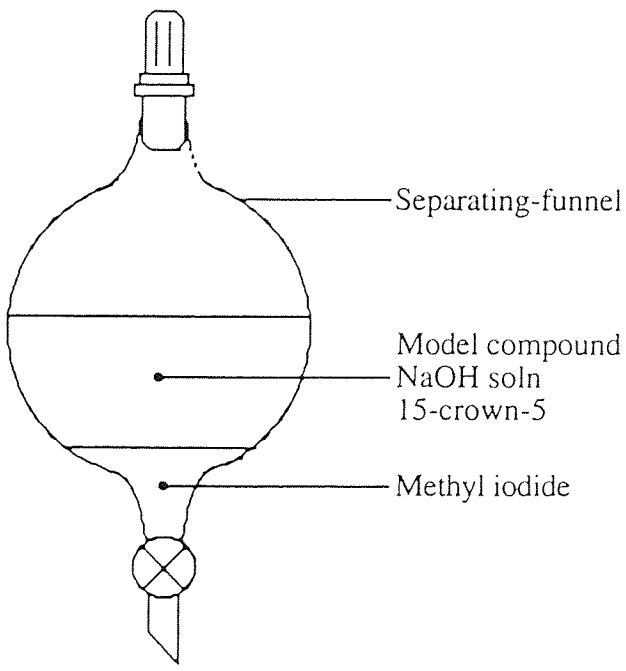

Fig 6.22 Methylation via phase-transfer

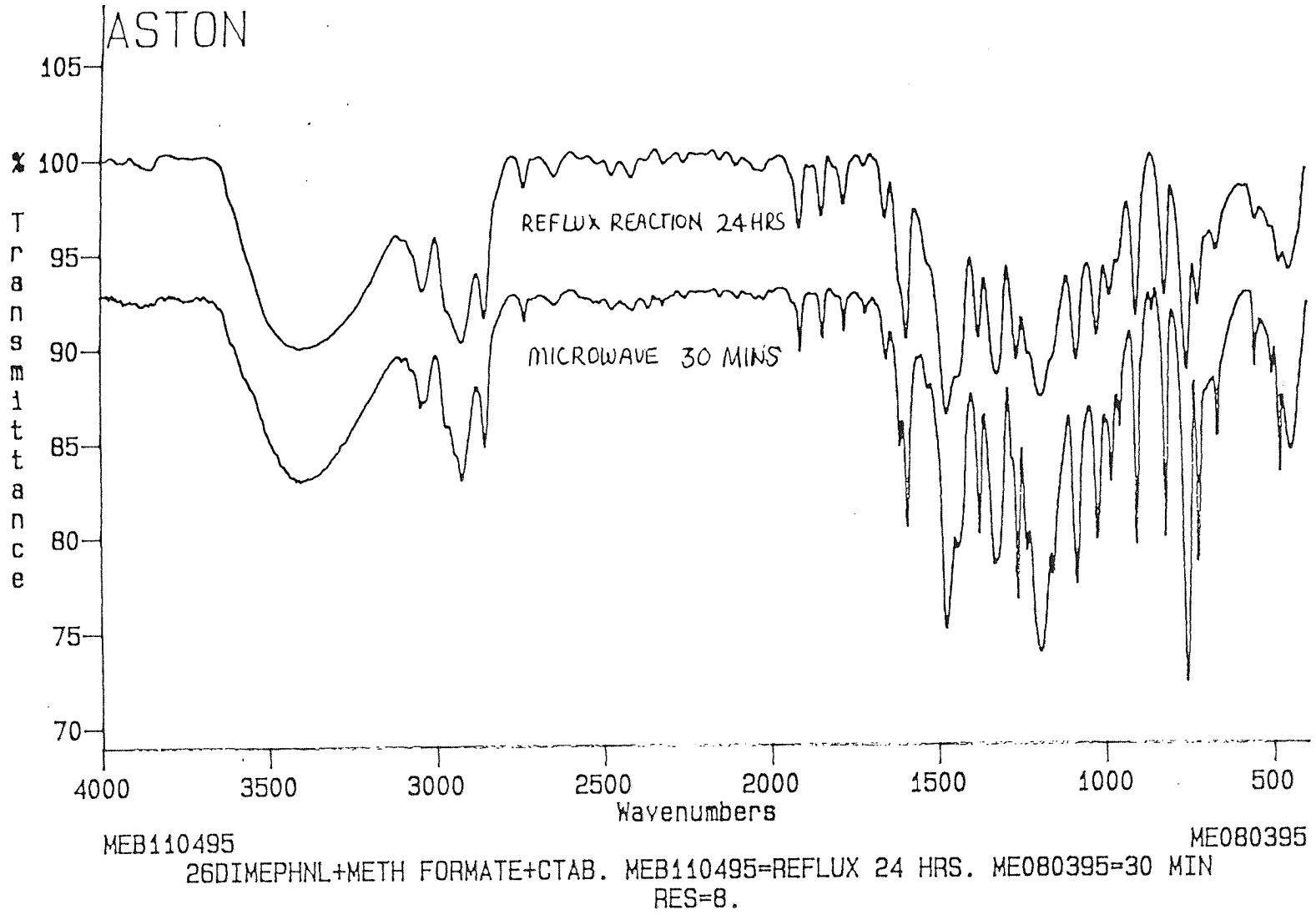

Fig6.20
IR of the methylated 2,6-dimethylphenol product after 24 hrs reflux
(methyl formate method)